

EVALUATING FORAMINIFERA AS A TOOL FOR RECREATING HISTORICAL
LANDSCAPES AND VERIFYING CARTOGRAPHIC ACCURACY AT FORT
FISHER, NORTH CAROLINA

by

Sofia Emma Di Bari

A thesis submitted to the faculty of
The University of North Carolina at Charlotte
in partial fulfillment of the requirements
for the degree of Master of Science in
Earth Sciences

Charlotte

2015

Approved by:

Dr. Scott Hippensteel

Professor Laurie Garo

Dr. Gang Chen

ABSTRACT

SOFIA EMMA DI BARI. Evaluating Foraminifera as a tool for recreating historical landscapes and verifying cartographic accuracy at Fort Fisher, North Carolina (under the direction of DR. SCOTT HIPPENSTEEL).

The research in this thesis focused on the use of Foraminifera to determine paleo-subenvironments and to quantify changes in the subenvironments through time at Fort Fisher, North Carolina. Historical maps were assessed with respect to the subenvironmental changes through time as recorded by Foraminifera.

To establish past subenvironments, eight modern surface samples were collected from various subenvironments surrounding the Fort Fisher Historical site. These modern samples were compared to 98 samples taken from five cores, which were recovered from the marshes behind the fort. These samples were transported to UNC Charlotte and were wet sieved and analyzed for Foraminifera content. The number of Foraminifera from each core, surface, and beach sample was recorded and then compiled to recreate the subenvironments through time. Geochronology was established using radiocarbon dates from buried organic matter.

The Fort Fisher Historical Site, an old Confederate military base, was chosen as the place of study due to the availability of images, aerial photographs, and hand-drawn historical maps that date back to the American Civil War. Aerial photographs and hand-drawn maps of the area were available through military atlases, the United States Geological Survey (USGS), and local and state governments. High-resolution satellite images from the 1990s to the present were accessed through Google Earth.

Maps of Fort Fisher with the location of the surface and core samples overlain were created using the suite of tools in ArcGIS, and the ArcPy module in the language script Python.

To determine the effectiveness of using Foraminifera as a tool for recreating paleo-subenvironments and past shoreline positions, the laboratory data from the core samples were compared to the maps from the chronoequivalent period. Additional emphasis was placed on maps from the Civil War, particularly maps from 1865, in order to validate historians' accounts of the battles that occurred at Fort Fisher.

ACKNOWLEDGMENTS

First, I would like to thank my advisor Dr. Scott Hippensteel and the two other members on my committee, Professor Laurie Garo, and Dr. Gang Chen for their insights and useful comments. I wish to send a special thanks to Dr. Hippensteel who collected all of the surface and core samples that were used for this study, and who assisted me in completing the lab work section of this thesis, and to Professor Garo, for her help with ArcGIS.

I would also like to thank my mother, Judy, and father, Michael, for their continuing support and encouragement through this endeavor, as well as my identical twin sister Rebecca, who, while geographically distant, has been by my side every step of the way.

I would now like to thank all the others who have assisted me when I have run into issues with my research, and those who have helped keep me focused through this process. I thank UNC Charlotte's Ph.D. student Alex Hohl who assisted me with ArcGIS and coding, Ph.D. student Adam Griffith who showed me an excellent source to download the most recent, already geo-referenced, natural-color coastal data, and master's candidate Stephen Rachide for assistance in double-checking the calculations for the sedimentation rate. My office mates in Room 410 should also get a mention for listening to all the good, the bad, and everything in-between, as well as Aiken Small (Dr. Hippensteel's other master's candidate), who kept me company while I was completing the crux of my data collection in a windowless lab. I am grateful to have met such a great group of colleagues here whom I proudly call my friends. Thank you.

TABLE OF CONTENTS

LIST OF TABLES	viii
LIST OF FIGURES	x
CHAPTER 1: INTRODUCTION	1
1.1 Morphology of North Carolina's Coast	1
1.2 Local Subenvironments	7
1.3 Foraminifera as a Tool for Reconstructing Subenvironment	8
1.4 Morphology of Fort Fisher Historical Site	12
1.5 History of Fort Fisher and Relevant Legislation	14
CHAPTER 2: HYPOTHESIS	20
CHAPTER 3: PREVIOUS STUDIES	23
CHAPTER 4: METHODS	28
4.1 Field Methods	28
4.2 Sedimentation Rates	29
4.3 Laboratory Methods	30
4.4 Georeferencing and Mapping Subenvironments	32
4.5 Comparing insights derived from Foraminiferal Data to Historical Maps	35
CHAPTER 5: RESULTS	43
5.1 Foraminiferal Results	43
5.2 Map Results	51
5.3 Foraminiferal and Map Data Results	56
5.4 Fort Fisher in 1865	64

CHAPTER 6: DISCUSSION	107
6.1 Interpretation of the Foraminiferal Data	107
6.2 Interpretation of Landscapes through Time	112
CHAPTER 7: CONCLUSIONS	123
REFERENCES	125
APPENDIX A: LEGISLATION AT KURE BEACH	131
APPENDIX B: MAPS OF THE CORE LOCATIONS THROUGH TIME	133

LIST OF TABLES

TABLE 1: Concentration of Foraminifera found from the mid-Atlantic region.	10
TABLE 2: Concentration of Foraminifera found in the Pamlico Sound.	11
TABLE 3: Summary of the most abundant species found in each subenvironment.	27
TABLE 4: The depths and years that were analyzed for Foraminifera content in each core.	41
TABLE 5: The elevation value's assigned for each subenvironment.	42
TABLE 6: The link point coordinates that were used to georeferenced the maps.	42
TABLE 7: Core 1's normalized raw data.	74
TABLE 8: Core 2's normalized raw data.	77
TABLE 9: Core 3's normalized raw data.	77
TABLE 10: Core 4's normalized raw data.	78
TABLE 11: Core 5's normalized raw data.	78
TABLE 12: Core 1's non-filtered Pearson values.	79
TABLE 13: Core 2's non-filtered Pearson values.	80
TABLE 14: Core 3's non-filtered Pearson values.	80
TABLE 15: Core 4's non-filtered Pearson values.	81
TABLE 16: Core 5's non-filtered Pearson values.	81
TABLE 17: Core 1's filtered Pearson values.	82
TABLE 18: Core 2's filtered Pearson values.	83
TABLE 19: Core 3's filtered Pearson values.	83
TABLE 20: Core 4's filtered Pearson values.	84
TABLE 21: The subenvironment of each core depth through time.	85

TABLE 22: The elevations of each core depth through time.	86
TABLE 23: The non-filtered elevation differences for each core between the Foraminifera values and Map values of each chronoequivalent year.	88
TABLE 24: The filtered elevation differences for each core between the Foraminifera values and Map values of each chronoequivalent year.	89
TABLE 25: The figure number, year, publisher, and source of each map used in this study.	133
TABLE 26: The cores change in subenvironments through time.	134

LIST OF FIGURES

FIGURE 1: The location of Fort Fisher.	2
FIGURE 2: Geologic map of North Carolina's northern and southern coastal provinces.	4
FIGURE 3: Map of Fort Fisher at 1865 with the 2014 shoreline juxtaposed on top.	15
FIGURE 4: Map of Fort Fisher (1865) highlighting the swash dam.	17
FIGURE 5: Illustration of this projects' hypothesis.	21
FIGURE 6: Map of the core and surface sample locations taken at Fort Fisher.	36
FIGURE 7: Mathematic Equations for calculating the Sedimentation Rate.	37
FIGURE 8: The location of the Tar Landing Bay, Alligator Bay, and Fort Caswell marshes.	38
FIGURE 9: Sedimentation Rates of the organic material that was ^{14}C dated.	39
FIGURE 10: The python script.	40
FIGURE 11: Graph of the Foraminifera concentration in the Estuary (Deep) subenvironment.	67
FIGURE 12: Graph of the total concentration of the agglutinated and calcareous species in the Estuary (Deep) subenvironment.	67
FIGURE 13: Graph of the Foraminifera concentration in the Estuary (Shallow) subenvironment.	68
FIGURE 14 Graph of the total concentration of the agglutinated and calcareous species in the Estuary (Shallow) subenvironment.	68
FIGURE 15: Graph of the Foraminifera concentration in the Extreme Low marsh subenvironment.	69
FIGURE 16: Graph of the total concentration of the agglutinated and calcareous species in the Extreme Low marsh subenvironment.	69
FIGURE 17: Graph of the Foraminifera concentration in the Low marsh subenvironment.	70

FIGURE 18: Graph of the total concentration of the agglutinated and calcareous species in the Low marsh subenvironment.	70
FIGURE 19: Graph of the Foraminifera concentration in the Intermediate marsh subenvironment.	71
FIGURE 20: Graph of the total concentration of the agglutinated and calcareous species in the Intermediate marsh subenvironment.	71
FIGURE 21: Graph of the Foraminifera concentration in the High marsh subenvironment.	72
FIGURE 22: Graph of the total concentration of the agglutinated and calcareous species in the High marsh subenvironment.	72
FIGURE 23: Graph of the Foraminifera concentration in the Extreme High marsh subenvironment.	73
FIGURE 24: Graph of the total concentration of the agglutinated and calcareous species in the Extreme High marsh subenvironment.	73
FIGURE 25: Graph of the Foraminifera concentration in the Beach subenvironment.	74
FIGURE 26: Graph of the total concentration of the agglutinated and calcareous species in the Beach subenvironment.	74
FIGURE 27: Pie graph of the total number of different Foraminifera species that were found in this study.	75
FIGURE 28: Graph of the change in each core's subenvironment through time.	84
FIGURE 29: Graph of Core 1's change in subenvironments through time based on both the Foraminifera data and Map data.	90
FIGURE 30: Graph of Core 2's change in subenvironments through time based on both the Foraminifera data and Map data.	91
FIGURE 31: Graph of Core 3's change in subenvironments through time based on both the Foraminifera data and Map data.	92
FIGURE 32: Graph of Core 4's change in subenvironments through time based on both the Foraminifera data and Map data.	93

FIGURE 33: Graph of Core 5's change in subenvironments through time based on both the Foraminifera data and Map data.	94
FIGURE 34: Graph of Core 1's c change in subenvironments through time based on both the Foraminifera data and Map data.	95
FIGURE 35: Graph of Core 2's change in subenvironments through time based on both the Foraminifera data and Map data.	96
FIGURE 36: Core 1's change in subenvironments through time based on both the non-filtered and filtered Foraminifera data and the Map data.	97
FIGURE 37: Core 2's change in subenvironments through time based on both the non-filtered and filtered Foraminifera data and the Map data.	98
FIGURE 38: Core 3's change in subenvironments through time based on both the non-filtered and filtered Foraminifera data and the Map data.	99
FIGURE 39: Core 4's change in subenvironments through time based on both the non-filtered and filtered Foraminifera data and the Map data.	100
FIGURE 40: Core 5's change in subenvironments through time based on both the non-filtered and filtered Foraminifera data and the Map data.	101
FIGURE 41: Graph of Core 1's shift in subenvironments between the years 1859 and 1872 based on both the Foraminifera data and Map data.	102
FIGURE 42: Graph of Core 2's shift in subenvironments between the years 1859 and 1872 based on both the Foraminifera data and Map data.	103
FIGURE 43: Graph of Core 3's shift in subenvironments between the years 1859 and 1872 based on both the Foraminifera data and Map data.	104
FIGURE 44: Graph of Core 4's shift in subenvironments between the years 1859 and 1872 based on both the Foraminifera data and Map data.	105
FIGURE 45: Graph of Core 5's shift in subenvironments between the years 1859 and 1859 based on both the Foraminifera data and Map data.	106
FIGURE 46: Map (made in ArcMap) of Fort Fisher (2015). Cartographer: Digital Globe	135
FIGURE 47: Map (made in ArcMap) of Fort Fisher (2014). Cartographer: Digital Globe	136

FIGURE 48: Map (made in ArcMap) of Fort Fisher (2013). Cartographer: Digital Globe	137
FIGURE 49: Map (made in ArcMap) of Fort Fisher (2011). Cartographer: Digital Globe	138
FIGURE 50: Map (made in ArcMap) of Fort Fisher (2010). Cartographer: Digital Globe	139
FIGURE 51: Map (made in ArcMap) of Fort Fisher (2009). Cartographer: USDA Farm Survey	140
FIGURE 52: Map (made in ArcMap) of Fort Fisher (2008). Cartographer: USDA Farm Survey	141
FIGURE 53: Map (made in ArcMap) of Fort Fisher (2007). Cartographer: USGS	142
FIGURE 54: Map (made in ArcMap) of Fort Fisher (2006). Cartographer: NASA	143
FIGURE 55: Map (made in ArcMap) of Fort Fisher (2004). Cartographer: Digital Globe	144
FIGURE 56: Map (made in ArcMap) of Fort Fisher (2002). Cartographer: New Hanover County	145
FIGURE 57: Map (made in ArcMap) of Fort Fisher (1999). Cartographer: USGS	146
FIGURE 58: Map (made in ArcMap) of Fort Fisher (1993). Cartographer: USGS	147
FIGURE 59: Map (made in ArcMap) of Fort Fisher (1980). Cartographer: USGS	148
FIGURE 60: Map (made in ArcMap) of Fort Fisher (1974). Cartographer: USGS	149
FIGURE 61: Map (made in ArcMap) of Fort Fisher (1970). Cartographer: USGS	150
FIGURE 62: Map (made in ArcMap) of Fort Fisher (1969). Cartographer: New Hanover County	151

FIGURE 63: Map (made in ArcMap) of Fort Fisher (1945). Cartographer: USGS	152
FIGURE 64: Map (made in ArcMap) of Fort Fisher (1938). Cartographer: New Hanover County Highway and Public Works Commission	153
FIGURE 65: Map (made in ArcMap) of Fort Fisher (1937). Cartographer: New Hanover County Highway and Public Works Commission	154
FIGURE 66: Map (made in ArcMap) of Fort Fisher (1930). Cartographer: Board of Education	155
FIGURE 67: Map (made in ArcMap) of Fort Fisher (1921). Cartographer: U.S Department of Commerce	156
FIGURE 68: Map (made in ArcMap) of Fort Fisher (1917). Cartographer: U.S Department of Commerce	157
FIGURE 69: Map (made in ArcMap) of Fort Fisher (1915). Cartographer: U.S Department of Commerce	158
FIGURE 70: Map (made in ArcMap) of Fort Fisher (1912). Cartographer: U.S Department of Commerce	159
FIGURE 71: Map (made in ArcMap) of Fort Fisher (1910). Cartographer: U.S Department of Commerce	160
FIGURE 72: Map (made in ArcMap) of Fort Fisher (1900). Cartographer: U.S Department of Commerce	161
FIGURE 73: Map (made in ArcMap) of Fort Fisher (1897). Cartographer: U.S Department of Commerce	162
FIGURE 74: Map (made in ArcMap) of Fort Fisher (1886). Cartographer: Moss Engraving Company	163
FIGURE 75: Map (made in ArcMap) of Fort Fisher (1882). Cartographer: O.W Gray and Son	164
FIGURE 76: Map (made in ArcMap) of Fort Fisher (1870). Cartographer: Unknown	165

FIGURE 77: Map (made in ArcMap) of Fort Fisher (1865). Cartographer: Engineer Otto Julian Schultze	166
FIGURE 78: Map (made in ArcMap) of Fort Fisher (1865). Cartographer: Engineer Otto Julian Schultze	167
FIGURE 79: Map (made in ArcMap) of Fort Fisher (1865). Cartographer: Engineer Otto Julian Schultze	168
FIGURE 80: Map (made in ArcMap) of Fort Fisher (1865) Cartographer: Engineer Otto Julian Schultze	169
FIGURE 81: Map (made in ArcMap) of Fort Fisher (1865). Cartographer: Engineer Otto Julian Schultze	170
FIGURE 82: Map (made in ArcMap) of Fort Fisher (1865). Cartographer: Engineer Otto Julian Schultze	171
FIGURE 83: Map (made in ArcMap) of Fort Fisher (1865). Cartographer: Engineer Otto Julian Schultze	172
FIGURE 84: Map (made in ArcMap) of Fort Fisher (1865). Cartographer: Engineer Otto Julian Schultze	173
FIGURE 85: Map (made in ArcMap) of Fort Fisher (1865). Cartographer: Engineer Otto Julian Schultze	174
FIGURE 86: Map (made in ArcMap) of Fort Fisher (1865). Cartographer: Robert Knox Sneden	175
FIGURE 87: Map (made in ArcMap) of Fort Fisher (1865). Cartographer: Engineering Department Bureau	176
FIGURE 88: Map (made in ArcMap) of Fort Fisher (1863). Cartographer: U.S Army Engineering Department	177
FIGURE 89: Map (made in ArcMap) of Fort Fisher (1863). Cartographer: U.S Army Engineering Department	178
FIGURE 90: Map (made in ArcMap) of Fort Fisher (1861). Cartographer: U.S Army Engineering Department	179
FIGURE 91: Map (made in ArcMap) of Fort Fisher (1833). Cartographer: Unknown	180

FIGURE 92: Map (made in ArcMap) of Fort Fisher (1821). Cartographer: U.S Navy Engineering Department	181
FIGURE 93: Map (made in ArcMap) of Fort Fisher (1770). Cartographer: Unknown	182
FIGURE 94: Map (made in ArcMap) of Fort Fisher (1749). Cartographer: Edward Hyrne	183
FIGURE 95: Map (made in ArcMap) of Fort Fisher (1733). Cartographer: Unknown	184
FIGURE 96: Map (made in ArcMap) of the boundaries between each subenvironment (2015).	185
FIGURE 97: Map (made in ArcMap) of the boundaries between each subenvironment (2013).	186
FIGURE 98: Map (made in ArcMap) of the boundaries between each subenvironment (2009).	187
FIGURE 99: Map (made in ArcMap) of the boundaries between each subenvironment (2006).	188
FIGURE 100: Map (made in ArcMap) of the boundaries between each subenvironment (2002).	189
FIGURE 101: Map (made in ArcMap) of the boundaries between each subenvironment (1999).	190
FIGURE 102: Map (made in ArcMap) of the boundaries between each subenvironment (1993).	191
FIGURE 103: Map (made in ArcMap) of the boundaries between each subenvironment (1980).	192
FIGURE 104: Map (made in ArcMap) of the boundaries between each subenvironment (1974).	193
FIGURE 105: Map (made in ArcMap) of the boundaries between each subenvironment (1970).	194
FIGURE 106: Map (made in ArcMap) of the boundaries between each subenvironment (1946).	195

FIGURE 107: Map (made in ArcMap) of the boundaries between each subenvironment (1921).	196
FIGURE 108: Map (made in ArcMap) of the boundaries between each subenvironment (1917).	197
FIGURE 109: Map (made in ArcMap) of the boundaries between each subenvironment (1915).	198
FIGURE 110: Map (made in ArcMap) of the boundaries between each subenvironment (1912).	199
FIGURE 111: Map (made in ArcMap) of the boundaries between each subenvironment 1910).	200
FIGURE 112: Map (made in ArcMap) of the boundaries between each subenvironment (1900).	201
FIGURE 113: Map (made in ArcMap) of the boundaries between each subenvironment (1897).	202
FIGURE 114: Map (made in ArcMap) of the boundaries between each subenvironment (1865).	203
FIGURE 115: Map (made in ArcMap) of the boundaries between each subenvironment (1865).	204
FIGURE 116: Map (made in ArcMap) of the boundaries between each subenvironment (1865).	205
FIGURE 117: Map (made in ArcMap) of the boundaries between each subenvironment (1865).	206
FIGURE 118: Map (made in ArcMap) of the boundaries between each subenvironment (1865).	207
FIGURE 119: Map (made in ArcMap) of the boundaries between each subenvironment (1865).	208
FIGURE 120: Map (made in ArcMap) of the boundaries between each subenvironment (1865).	209
FIGURE 121: Map (made in ArcMap) of the boundaries between each subenvironment (1865).	210

FIGURE 122: Map (made in ArcMap) of the boundaries between each subenvironment (1864).	211
FIGURE 123: Map (made in ArcMap) of the boundaries between each subenvironment (1863).	212
FIGURE 124: Map (made in ArcMap) of the boundaries between each subenvironment (1863).	213
FIGURE 125: Map (made in ArcMap) of the boundaries between each subenvironment (1781).	214

CHAPTER 1: INTRODUCTION

1.1 Morphology of North Carolina's Coast

North Carolina's coastline is unique, dynamic and has changed dramatically over the past two centuries. Understanding its geology and history is important because that provides perspective on how the Fort Fisher region formed, and how it differs from other parts of the coastline. The Fort Fisher Historical Site comprises only 1.2 kilometers of the state's 523-kilometer shoreline. Located just south of Kure Beach in New Hanover County, the Fort Fisher Historical Site is bordered by the Cape Fear River to the west and the Atlantic Ocean to the east (Figure 1).

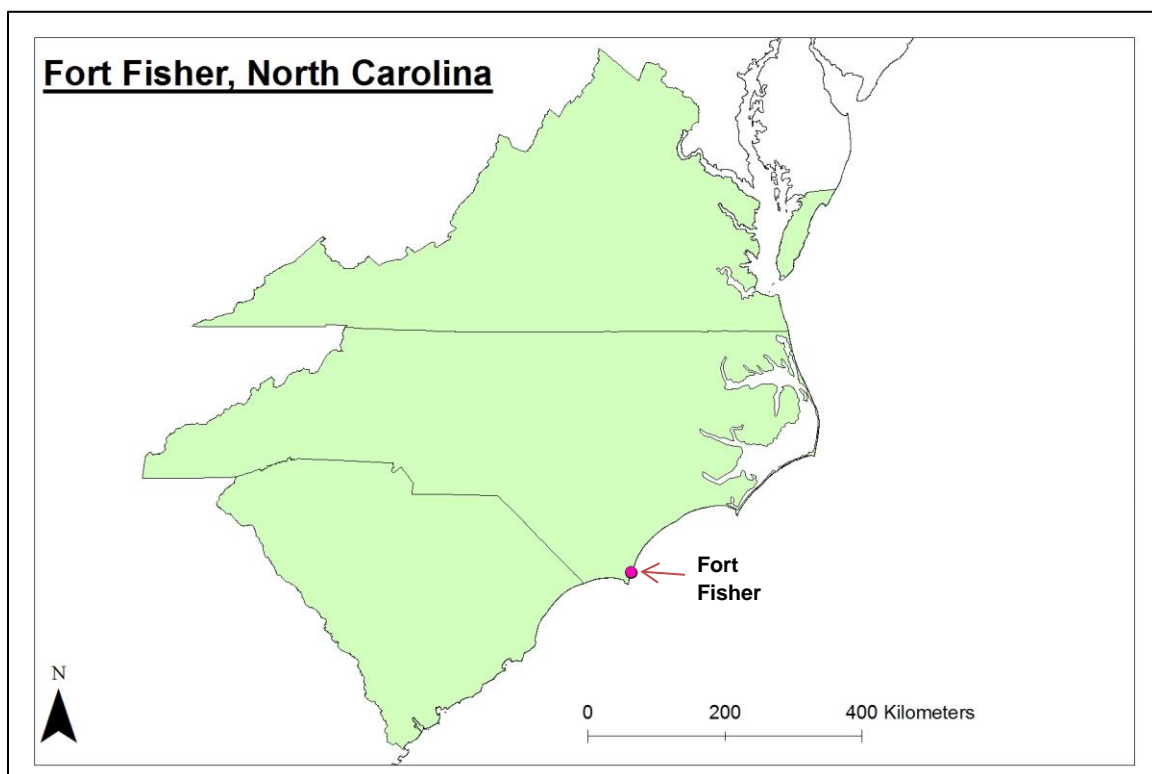


FIGURE 1: A map made in ArcGIS indicating the location of Fort Fisher (the pink dot) relative to the North Carolina coastline and surrounding states.

The elevation of North Carolina's shoreline during the end of the last glacial maximum (approximately 20,000 years ago) was roughly 120 meters below the modern shoreline, and the location of the shoreline was about 96 kilometers east of the present-day shoreline at Wilmington, and 24 km east of the present-day shoreline at Cape Hatteras. This indicates that North Carolina's coast has not evenly transgressed (the term given to the movement of the shoreline landward). Some areas such as Wilmington and points south have seen a larger shift in the position of the shoreline compared to the northern section of the coast. At Fort Fisher, the shoreline has transgressed, while the marshes that make up the area west of the fort have grown (Riggs et al., 2011).

North Carolina has two distinct coastal regions due to differences in the geometry and geological processes that occur along the shoreline. These regions are known as the northern coastal province and the southern coastal province (Figure 2). The northern coastal province includes areas from the Virginia/North Carolina border to Cape Lookout, while the southern coastal province (which contains Fort Fisher) extends south from Cape Lookout to Cape Romain in South Carolina.

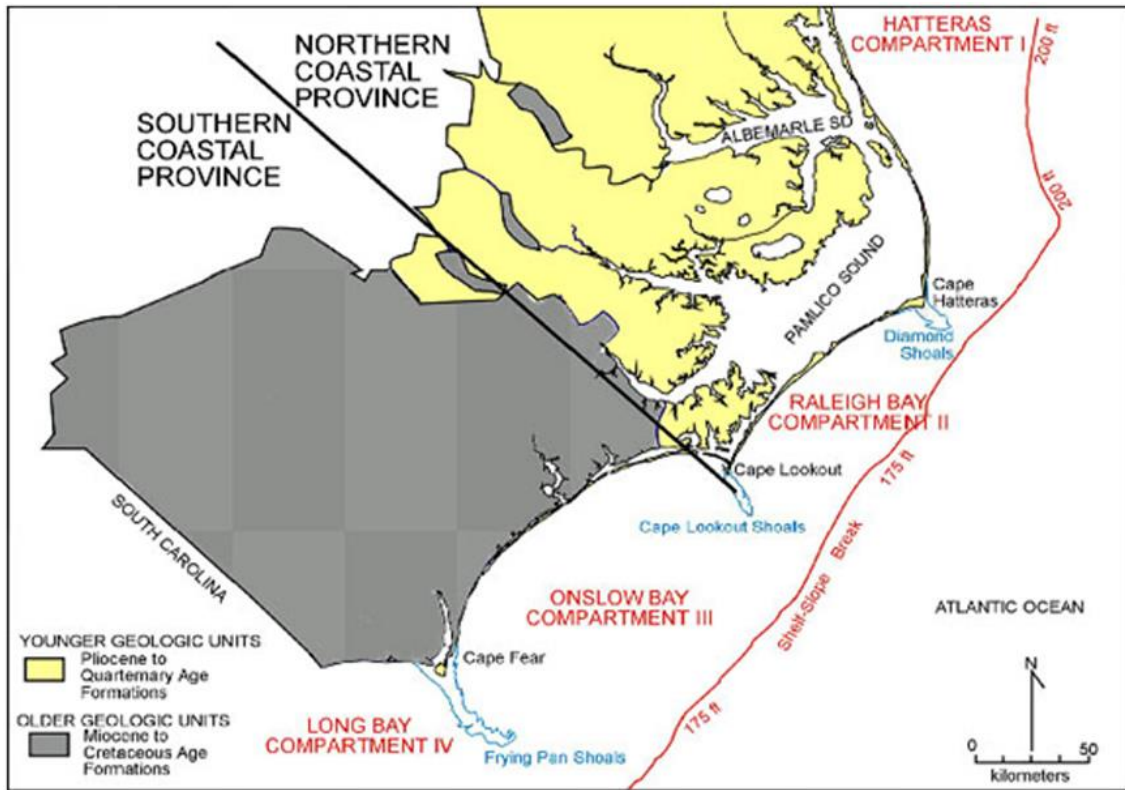


FIGURE 2: A map showing the age and the rock type that underlies the northern and the southern coastal provinces of North Carolina (Source: Riggs et al., 2011).

Other than the type and age of the rocks, the main difference between the two regions is the slope of the coastal plain. In the northern zone, a gently sloping coastal plain produces long barrier strips with an estuary or bay landward of the barrier strip, while in comparison, the southern coastal plain is steeper and thus produces short, stubbier barrier beaches that parallel the main shoreline (Riggs et al., 2011). The difference in this land morphology (long barrier strips versus short, wide beaches) can be attributed to the tidal fluctuations at each location. A steeper coastal plain allows the tidal fluctuations to be smaller than those of a more gently sloping coastal plain (Riggs et al., 2011).

Another factor that explains the difference in the slope between the northern and southern coastal provinces is tectonic activity. The southern section of the southern coastal province (where the Cape Fear River is located) has been tectonically active for centuries. This area is known as the Cape Fear Arch, and it is defined by elliptically-shaped bays and sand dunes. These are the most conspicuous features that make the Cape Fear River valley unique. Soller (1998) found that a gentle, sustained uplift to the north or northeast of the valley axis has forced the Cape Fear River to migrate southwestward over time. This explains the southward flow of the Cape Fear River. The river's tributaries currently drain to the southwest, providing evidence of continued uplift of the axis (Wright, 1991). This continual uplift is the reason why the coastal plain in this area is steeper than the coastal plain in other areas of North Carolina.

The difference in the coastal slope results in the variety of beaches along the shoreline. Headland beaches and barrier beaches are the most common types of coastlines in the United States. Headland beaches form on the mainland, whereas barrier beaches are separated from the mainland by a body of water. According to the United States Geological Survey (USGS) "barrier islands make up more than two thirds of the southeastern Atlantic shoreline," (Morton & Miller, 2005, page 17). In North Carolina, 95 percent of the coastline is classified as either a complex or simple barrier beach system, while five percent of the coast (26 kilometers of the 523 kilometers of the state's shoreline) is considered a headland beach (Riggs et al., 2011).

The Fort Fisher beach is short, wide, and parallels the mainland thus may be classified as a headland beach. Conversely, the Fort Fisher beach is separated from the mainland by the Cape Fear Estuary, so it could also be classified as a barrier beach. The

headland and barrier beach characteristics found on the Fort Fisher beach make it an interesting study site.

The current morphology of Fort Fisher was shaped after the end of the last glacial maximum approximately 20,000 years ago. When the glaciers began to melt, the deeper river valleys that once extended across the continental shelf (when the sea-level was much lower) began to flood. This resulted in the formation of a series of parallel estuaries on the landward side of the island. In response to sea-level rise, the barrier island began to laterally accrete and roll over in a landward direction (a process now happening at other unarmored coastal areas in North Carolina), creating headland areas and adjacent valleys. The rolling over of the barrier beach allowed the wide valley estuaries that were once present alongside the barrier island to turn into small inlets (Riggs et al., 2011). The formation of these small inlets caused the estuaries to narrow and fill with overwash sand deposits and inlet sediments. These events contribute to the continuing evolution of the Fort Fisher region.

The inlet sediments and barrier overwash sand deposits are comprised of mud, organic matter (peat), and plant materials. These sediments tend to build up in tidal areas because during high tide, the presence of calm water allows the mud, organic matter and halophytes to flow slowly onshore, and during low tide, the water retreats and the sediments that were brought in by the high tide. These sediments are deposited and undisturbed until the next high tide cycle. As this cycle continues over time, the collection of these sediments, particularly halophytes and algae, creates a salt marsh. A salt marsh is present on the western side of Fort Fisher because the area is inundated by

salt water and then drained due to daily tidal fluctuations, enabling the sediments to settle into the soil. During storm events, overwashes also add sediment to the salt marsh.

Sediment supply is the most important variable that controls the nature of the beach and the deposition of salt marshes. Sediment supply affects the rate at which the shoreline and marshes erode and is therefore a major factor in beach stability. Both headland beaches and barrier beaches are affected by the rate and amount (if any) of sediment available. Sources that can provide sand to the beaches include inlets and flood tide deltas, paleo-riverine channels on the continental shelf, adjacent cape shoals that extend to the continental shelf and, lastly, exposed sediments that are immediately offshore on the shoreface and continental sea bed (Pilkey et al., 2002; Riggs et al., 2011). In general, southeastern U.S. rivers do not contribute significantly to the present sand budget of the beaches because most of the rivers empty into estuaries and deposit their sediment loads far inland from the shoreline (Morton & Miller, 2005). In North Carolina, the barrier and headland beaches downstream and southwest of Cape Lookout are sediment-starved because river sediments are trapped upstream in the river system and never make it to the beach-front (Pilkey et al., 2002).

1.2 Local Subenvironments

Salt marshes protect shorelines from erosion by buffering wave action and trapping sediment. Fagherazzi (2013) found that the typical length and width of a salt marsh does not exceed a few kilometers, and can be built or destroyed within a few thousand years. Others report a similar conclusion: that the geological history of salt marshes indicates that they are continuously recycled, destroyed, and reformed in very dynamic coastal environments (Rampino & Sanders, 1981; Engelhart & Horton, 2012).

Foraminifera can be used to detect transgressions and regressions in the marginal-marine and salt-marsh strata. Transgressions and regressions are defined by the movement of the land in response to mean sea-level (MSL) through time. Transgression is a term given to the movement of the land landward, whereas regression is the term that describes the land's movement seaward. Because land elevations within a salt marsh vary, salt marshes can be divided into distinct local subenvironments: High marsh, Intermediate marsh, and Low marsh. The term "Low Marsh" characterizes the area where the land elevation is closest to MSL, while the "High marsh" refers to the land that is highest relative to MSL. Each subenvironment usually contains a different Foraminiferal assemblage thus, analyzing Foraminifera content is a useful tool for determining paleo-transgressions and or paleo-regressions.

1.3 Foraminifera as a Tool for Reconstructing Subenvironments

Foraminifera are short-lived microorganisms that are extremely sensitive to salinity, acidity, and temperature changes within marine and marginal-marine environments. They are also very abundant and easy to identify. Two types of Foraminifera are discussed in this study: agglutinated and calcareous taxa. These Foraminifera make excellent climate proxies because they are temperature-sensitive, meaning only one assemblage usually lives in a particular temperature range, and if the temperature of the environment changes, the Foraminifera present will change. Additionally, Foraminifera are elevation and water-depth dependent, therefore subenvironments can be distinguished by the Foraminifera assemblages that are present.

Foraminifera in marshes form high-abundance, low-diversity assemblages. Their distribution throughout the salt marsh is dependent upon the frequency and duration of

the tidal inundations (Scott & Medioli, 1978). Scott and Medioli have demonstrated that Foraminifera can be readily preserved in these salt marsh environments; therefore, Foraminifera are quite abundant in the areas adjacent to the Fort Fisher Historical Site. Their abundance and durability make them a useful tool in determining previous subenvironments.

Hippensteel et al. (2000) found that the five most common dead and living Foraminifera species in the Bombay Hook National Wildlife Refuge in Delaware were *Trochammina inflata*, *Jadammina macrescens*, *Pseudothurammina limnetis*, *Miliammina fusca*, and *Arenoparrella mexicana* (Table 1).

TABLE 1: The concentration (specimens/ cm³) of the most common dead and live (in parenthesis) Foraminifera found at particular depths in each subenvironment in the mid-Atlantic region. From Hippensteel et al. (2000).

Depth (cm)	<i>Arenoparrella mexicana</i>	<i>Miliammina fusca</i>	<i>Pseudothurammina limnetis</i>	<i>Trochammina inflata</i>	<i>Jadammina macrescens</i>	Total
High Marsh						
0-1	176 (70)	2 (0)	14 (1)	101 (41)	65 (25)	358 (137)
1-3	424 (149)	10 (3)	14 (0)	323 (148)	180 (79)	951 (379)
3-5	476 (176)	23 (8)	34 (3)	430 (162)	308 (151)	1271 (500)
10	459 (206)	47 (12)	63 (13)	344 (169)	442 (144)	1355 (544)
20	285 (140)	99 (40)	14 (3)	254 (120)	308 (111)	960 (414)
30	142 (52)	134 (28)	10 (0)	318 (90)	270 (79)	874 (249)
40	112 (21)	28 (5)	11 (3)	383 (143)	271 (34)	805 (206)
50	114 (10)	2 (0)	0 (0)	292 (38)	208 (24)	616 (72)
60	83 (1)	1 (0)	0 (0)	244 (7)	238 (10)	566 (18)
Intermediate Marsh						
0-1	38 (3)	0 (0)	0 (0)	67 (37)	53 (18)	158 (58)
1-3	311 (83)	22 (12)	35 (8)	662 (215)	333 (162)	1363 (480)
3-5	274 (90)	59 (21)	73 (27)	632 (242)	446 (199)	1484 (579)
10	204 (79)	18 (12)	116 (87)	350 (119)	271 (87)	959 (384)
20	224 (49)	20 (7)	27 (13)	523 (144)	327 (116)	1121 (329)
30	163 (37)	38 (3)	17 (4)	496 (88)	316 (62)	1030 (194)
40	144 (8)	4 (0)	5 (0)	464 (67)	452 (59)	1069 (134)
50	154 (15)	1 (0)	4 (0)	422 (45)	402 (57)	983 (117)
60	170 (9)	11 (0)	0 (0)	425 (17)	331 (4)	937 (30)
Low Marsh						
0-1	18 (13)	0 (0)	3 (1)	58 (24)	16 (7)	95 (45)
1-3	28 (22)	4 (1)	35 (16)	81 (36)	71 (37)	219 (112)
3-5	66 (32)	19 (12)	118 (92)	147 (56)	265 (167)	615 (359)
10	84 (22)	13 (0)	45 (11)	231 (27)	166 (32)	539 (92)
20	129 (47)	7 (0)	48 (26)	302 (58)	213 (83)	699 (214)
30	108 (78)	24 (15)	41 (22)	324 (66)	497 (110)	994 (291)
40	143 (37)	41 (14)	31 (11)	399 (53)	519 (60)	1133 (175)
50	179 (9)	6 (3)	29 (3)	430 (14)	385 (21)	1029 (50)
60	261 (4)	1 (0)	14 (1)	519 (3)	375 (4)	1170 (12)

A study completed in Pamlico Sound, North Carolina by Abbene et al. (2006) found that more agglutinated species are present in the marsh setting compared to an estuary setting, and that a marine setting is comprised mostly of calcareous species (Table 2).

TABLE 2: The number of Foraminifera found at four distinct subenvironments in the Pamlico Sound. The letter O stands for the occurrence of the species, the letter C represents the consistency, and the letters BF stand for the bioface fidelity. If a score of six or higher was found for the C and BF columns, it was inferred that the species could represent an assemblage. These are highlighted by the black boxes. From Abbene et al. (2006).

Species:	Marsh Biofacies			Estuarine Biofacies A			Estuarine Biofacies B			Marine Biofacies		
	O	C	BF	O	C	BF	O	C	BF	O	C	BF
<i>Ammonoastuta inepta</i>	2	2	10	0	0	0	0	0	0	0	0	0
<i>Ammonia parkinsoniana</i>	6	7	2	6	4	1	9	9	3	4	10	3
<i>Ammonia tepida</i>	1	1	2	1	1	1	1	1	2	1	3	5
<i>Ammotium salsum</i>	7	8	3	16	10	4	10	10	4	0	0	0
<i>Arenoparrella mexicana</i>	4	4	6	3	2	3	1	1	1	0	0	0
<i>Asterigerina carinata</i>	0	0	0	0	0	0	1	1	2	2	5	8
<i>Ammobaculites crassus</i>	3	3	4	5	3	4	1	1	1	0	0	0
<i>Ammobaculites dilatatus</i>	0	0	0	1	1	10	0	0	0	0	0	0
<i>Ammobaculites exiguus</i>	0	0	0	3	2	10	0	0	0	0	0	0
<i>Cibicides lobatulus</i>	0	0	0	0	0	0	0	0	0	3	8	10
<i>Cibicides refulgens</i>	0	0	0	0	0	0	0	0	0	1	3	10
<i>Elphidium excavatum</i>	5	6	2	11	7	2	10	10	3	4	10	3
<i>Elphidium galvestonense</i>	1	1	1	1	1	1	0	0	0	3	8	8
<i>Elphidium mexicanum</i>	0	0	0	0	0	0	0	0	0	4	10	10
<i>Elphidium cf. E. mexicanum</i>	0	0	0	0	0	0	1	1	10	0	0	0
<i>Elphidium subarcticum</i>	0	0	0	0	0	0	0	0	0	3	8	10
<i>Hanzawaia strattoni</i>	0	0	0	0	0	0	1	1	1	4	10	9
<i>Haplophragmoides bonplandi</i>	2	2	10	0	0	0	0	0	0	0	0	0
<i>Haplophragmoides wilberti</i>	5	6	6	5	3	3	1	1	1	0	0	0
<i>Jadammina macrescens</i>	4	4	7	1	1	1	1	1	2	0	0	0
<i>Miliammina fusca</i>	6	7	6	3	2	2	2	2	2	0	0	0
<i>Quinqueloculina lamarckiana</i>	0	0	0	0	0	0	0	0	0	2	5	10
<i>Quinqueloculina seminula</i>	0	0	0	0	0	0	0	0	0	3	8	10
<i>Quinqueloculina sp. C</i>	0	0	0	0	0	0	0	0	0	1	3	10
<i>Siphonotrochammina lobata</i>	4	4	9	1	1	1	0	0	0	0	0	0
<i>Textularia earlandi</i>	0	0	0	4	3	10	0	0	0	0	0	0
<i>Tiphotocha comprimata</i>	6	7	7	2	1	1	1	1	1	0	0	0
<i>Trochammina inflata</i>	6	7	6	4	3	2	2	2	2	0	0	0
Indeterminate agglutinated	1	1	10	0	0	0	0	0	0	0	0	0
Indeterminate calcareous	0	0	0	0	0	0	3	3	5	1	3	5
Organic lining	4	4	6	3	2	3	1	1	1	0	0	0

Agglutinated species *Haplophragmoides wilberti*, *Miliammina fusca*, *Trochammina inflata*, and *Tiphotocha comprimata*, were the highest scoring (i.e. species with the highest concentration) Foraminifera in the marsh environment (Table 1). For the marine

environment, three calcareous taxa: *Elphidium* spp., *Quinqueloculina seminula*, and *Cibicides lobatulus* were the highest scoring.

Additionally, cores taken at the Low and High marsh environments at Pea Island, Oregon Inlet, and Currituck Barrier Beach Island of North Carolina's Outer Banks show similar results to the Hippensteel et al. (2000) and Abbene et al. (2006) findings. Culver et al. (2005) found that the most common living species in the low marshes from all three locations include *Ammonium salsum*, *Arenoparrella mexicana*, *Trochammina inflata*, *Tiphotrocha comprimata*, *Jadammina macrescens*, *Ammobaculites subcatenulatus*, *Miliammina fusca*, *Siphotrochammina lobata*, and *Haplophragmoides wilberti* (all of which are agglutinated species). The High marsh environment was dominated by similar living Foraminifera species but the Low marsh had a much higher concentration. Additionally, the High marsh contained more loose plant material than the Low marsh (Culver et al., 2005).

1.4 Morphology of Fort Fisher Historical Site

The Fort Fisher region has a salt marsh on its western side that marks the interaction between land and the Cape Fear River. This area has a mean tidal range of 1.15 meters/year so it is classified as a "semi-tidal, wave-dominant barrier coast with mixed energy environments" (National Oceanic and Atmospheric Administration Tidal Current Data for the Coastal United States, 2007). The tidal range in this region is amplified by the Georgia embayment, about 480 kilometers south of the fort (Hayes, 1994). Because the marsh is tidal and protected by the embayment, the sediments carried by the Cape Fear River are able to settle on the westward side of the structure but not on the eastern, beach-front side.

The Fort Fisher beach, like many others in North Carolina, is in a sediment-poor region and the rate of erosion on the Fort Fisher beach is greater than the rate of deposition. One possible explanation for this sediment-poor beach-front is the littoral drift direction along this portion of the Atlantic Ocean. The littoral drift current during low-energy events flows from the north to the south, allowing the weathered sand to be eroded away from the beach-front (Moorefield, 1978).

Fort Fisher differs from the rest of the headland beaches because it is also a barrier beach. Unlike many other barrier beaches, coquina is exposed at the surface and extends onto the beach front and seaward toward the continental shelf. It is thought that the coquina present at this beach is the product of “post depositional diagenesis of carbonate shell sands where dissolution, cementation, and calcification of aragonite occurred at or near the paleowater table” (Dockal, 1996, page 9). The exposed coquina acted as a natural barrier — a natural protector — for the beach, by refracting some of the wave energy that would have normally hit the beach-front. A study completed in 1931 by the U.S. Army Corps of Engineers (USACE) indicated that the coquina was as much as "9 feet thick" in places and extended continuously throughout the area (Dockal, 1996, page 14). However, over the years, this natural barrier has been removed. A major contributor to this loss was the construction of Highway 421 around 1932, which cut into the coquina on the surface. About 6,000 cubic yards of coquina were removed during the construction of the highway which exposed the beach and the surrounding area and led to an increase in wave energy on the beach (Mabry, 2009). In 1982, another USACE report noted that "The coquina is irregular in thickness and elevation" and that it is

discontinuous in many places where it was originally exposed (Dockal, 1996, page 14).

1.5 History of Fort Fisher and Relevant Legislation

Fort Fisher was built in 1861 and served as one of the main bases for the Confederate Army during the American Civil War. Two major battles occurred at Fort Fisher (December 24, 1864 and January 13-15, 1865), with January 15, 1865 being particularly important. January 15 marked the day when this Confederate military fortification was captured via land assault by Union soldiers. This was one of the turning points in the Civil War, because this was the last major fort that Confederate forces still controlled

According to historical maps of historical accounts of both battles, the Union soldiers attacked the fort from the north and west. For this to be true, the terrain adjacent to the Fort (on the western and northern side) would have had to be land or a high marsh because unconsolidated and wet ground (as found in an estuary or low marsh) would have rendered the terrain impassable for the troops.

Even though the sand fortification fell to the Union Army, Fort Fisher remained an icon in North Carolina. Despite the many attempts to protect the fort from the sea, Fort Fisher has still dramatically changed in appearance since 1865. Fort Fisher is much closer to the ocean today than in previous years, due to the narrowing and erosion of the land beside the structure (Dockal, 1996; Riggs et al., 2011).

The strip of land containing Fort Fisher, Kure Beach, and Carolina Beach, now known as Pleasure Island (renamed from Federal Point Peninsula), was not always an island. A major storm in 1761 breached the northern part of the Federal Point Peninsula, producing the modern island and an inlet dubbed “New Inlet,” which connected the

Atlantic Ocean to the Cape Fear River. This new inlet developed into the second largest inlet system in the southeastern part of North Carolina, and made areas upstream more vulnerable to military attacks. As a result Fort Fisher was built in 1861, to guard the entrance of this inlet, (Figure 3).

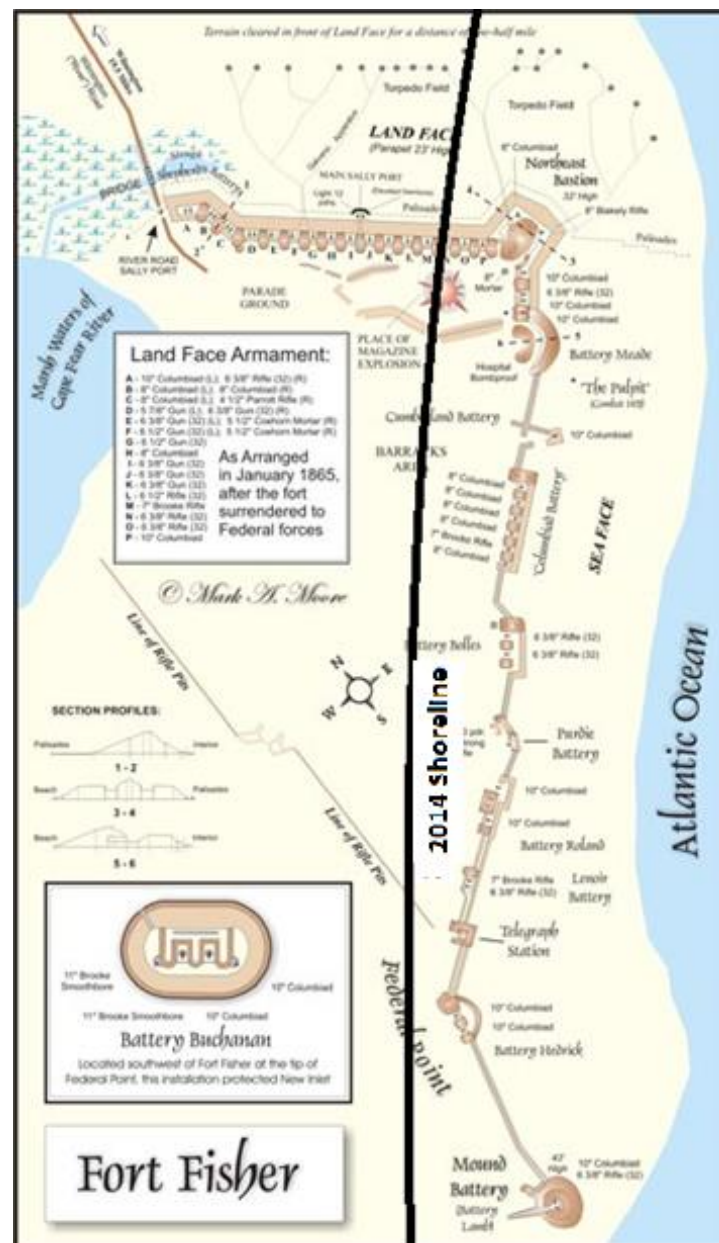


FIGURE 3: A map of Fort Fisher in 1865. The solid black line indicates the position of the 2014 shoreline, which extends much farther inland than the 1865 shoreline. This image was taken from the Fort Fisher Historical website and annotated using Microsoft Paint.

The creation of New Inlet also allowed for the shoaling of the Cape Fear River shipping channel. Shoaling is a term used to describe the process in which wave amplitude increases, enhancing wave energy and erosion due to the decrease in the coastal slope (Dennis, 1996). In 1862, the USACE began to mitigate the shoaling and continued to do so for the next two decades by installing a series of sunken blockade runners that acted as a barrier. Finally, in 1887, the USACE built the swash dam, which is now known as “The Rocks” project. The Rocks project was a 4.5-kilometer-long, 30-meter-wide, and 9-meter-high pile of rocks that successfully controlled the shoaling of the water into the Cape Fear River. Although the dam temporarily stopped shoaling in the Cape Fear River, many side effects were seen. For one, the building of the dam altered the tidal connection between the Cape Fear River and the ocean, resulting in the shift of the main tidal flow southward. This shift led to formation of the estuary known as the “Basin” (Figure 4).

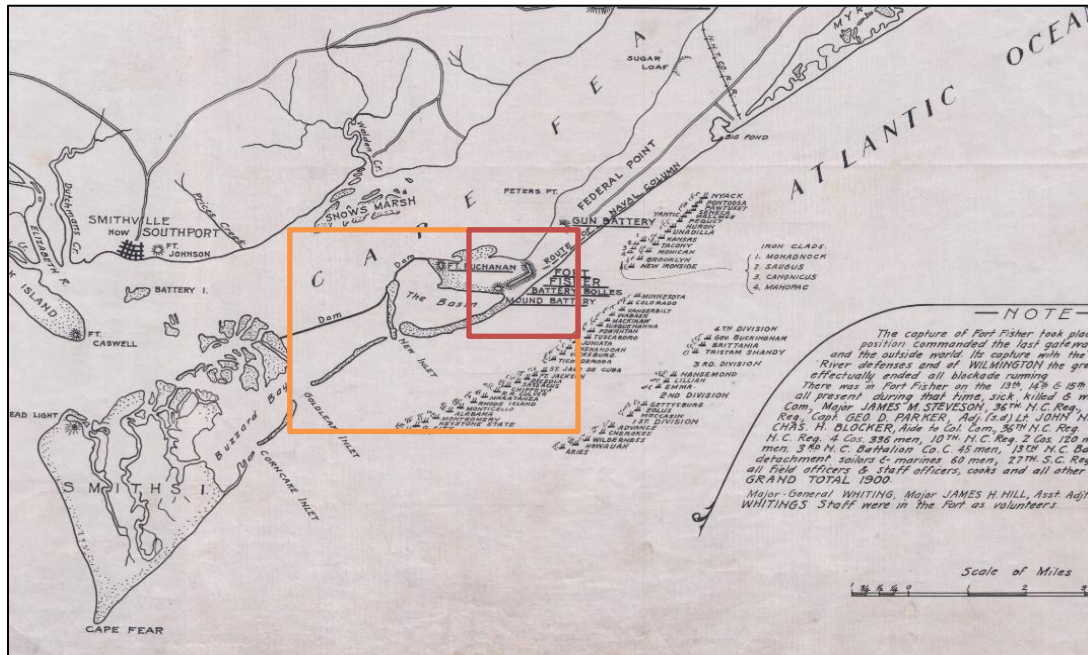


FIGURE 4: A map from 1865 showing a large scale view of Fort Fisher. The orange box outlines the swash dam and the location of the Basin relative to the fort, which is highlighted by the red box. This image was taken from the North Carolina State Archive Site.

Furthermore, the dam caused the entire New Inlet system to migrate southward and stretch seaward (Dennis, 1996) and allowed for further erosion of the shoreline south of the structure (near Cape Fear).

Battle Acre, located immediately west of Mound Battery and due south of North Carolina's Historical Visitors Center, marks the area where intense fighting took place during the Civil War. To protect this historic area from coastal storms and erosion from the sea, New Hanover County constructed two short groins east of Battle Acre in 1955. About ten years after the groins were constructed, concrete and brick rubble supplemented the groin structures and has, for the most part, been effective in minimizing the rate of erosion. Another structure, comprised of marine shell limestone, was placed a few meters offshore (extending from Battle Acre northward to the exposed coquina outcrop) to further prevent erosion along the coastline. This structure failed almost

immediately as a storm in 1976 breached the middle section, causing the entire structure to fall apart. Between 1976 and 1999 the region between Battle Acre and the exposed coquina outcrop to the north, was eroding at an average rate of 3.4 meters/year, while just south of Battle Acre, the average erosion rate was about 3.1 meters/year (Dennis, 1996, page 69).

This long history of beach erosion remediation led in part to the Coastal Area Management Act (CAMA) that was passed by the North Carolina state legislature in 1985. The act prohibited permanent erosion control devices on beaches, including the construction of sea walls, groins and revetments at all coastal locations. In 1989, the Coastal Area Management Act was amended by the Carolina Coastal Resource Committee in that “permanent erosion structures apply to all such structures, regardless of their location or date of construction” (Mabry, 2009, page 1). Nevertheless, the rule contained narrow exceptions that allowed for the construction of seawalls at Fort Fisher and at the Cape Hatteras lighthouse in later years (Mabry, 2009).

Taking advantage of this provision, in 1996, the USACE constructed a \$4.6 million, 926-meter-long, multi-layered rubble revetment composed of granite, to protect the fort and stabilize the adjacent coastline against further erosion. Although the wall stopped erosion directly at the fort, it led to increased erosion rates on the beaches just south and north of the construction area, where sediment was being lost to the littoral drift at an average rate of about 2.5 meters/year (Hashbrouck, 2007).

Evidence of this accelerated erosion due to the construction of the 1996 sea wall can be seen at Kure Beach which lies directly north of the Fort Fisher beach. See

Appendix A for more information about the recent erosion and legislative issues that have transpired regarding Kure Beach.

CHAPTER 2: HYPOTHESIS

The goal of this project was to validate the use of Foraminifera to determine previous subenvironments and past storm deposits in areas where high-resolution maps do not currently exist. This study also sought to confirm the accuracy of the military and historical maps of Fort Fisher created in the last 200 years, with a focus on the 1860s, when Civil War battles occurred at the fort.

Fort Fisher, North Carolina, was the focus of the study because numerous aerial and historical maps were available from the UNC Charlotte library collection, atlases, and the USGS site, as well as local North Carolina government websites. Thus the hypotheses for this study were as follows.

1) Foraminifera can provide information about the change in subenvironments through time (Figure 5), and information about the paleo-storm record. Foraminifera are globally abundant in marine and marginal-marine environments and are extremely sensitive to salinity and water-depth changes. Certain assemblages are only found in particular subenvironments. If disparities in the Foraminifera taxa within two salt marsh core samples were found, that was evidence that the subenvironments within the marsh have shifted. Paleo- storm deposits were identified in marsh strata if offshore-indicative taxa were present.

- 2) Historical Maps can also demonstrate the change in subenvironments through time. This was accomplished by georeferencing all of the maps and creating polygons for each marsh subenvironment.
- 3) The subenvironments derived from the Foraminifera data should be equivalent to the subenvironments from the Map data of the chronoequivalent year. If this scenario is true, Foraminifera can be used to assess paleo-subenvironments for areas either lacking maps or depicted by maps of questionable accuracy.
- 4) The Union troops attacked the fort by foot from the North and West on December 24, 1864 and January 15, 1865. The terrain would have had to be a High marsh or Land because the Union troops would have been unable to attack the fort otherwise. Using Foraminiferal assemblages present in the cores along with the historical high-resolution maps from that time, the terrain that the troops marched across will be verified.

The final product of this study illustrated the change in landscape at this well-known military site resulting from sea-level fluctuations and storms. After creating the time-series maps, further analysis of the Fort Fisher region was conducted by assessing the accuracy of the 1865 maps as well as the effectiveness of the hardened structures that were constructed to protect the fort and its surroundings. Verifying the accuracy of such maps especially during the year 1865 was quite challenging due to the inherent georeferencing inaccuracies and the high sedimentation rate in the region which resulted in a limited amount of Foraminifera data for that specific decade.

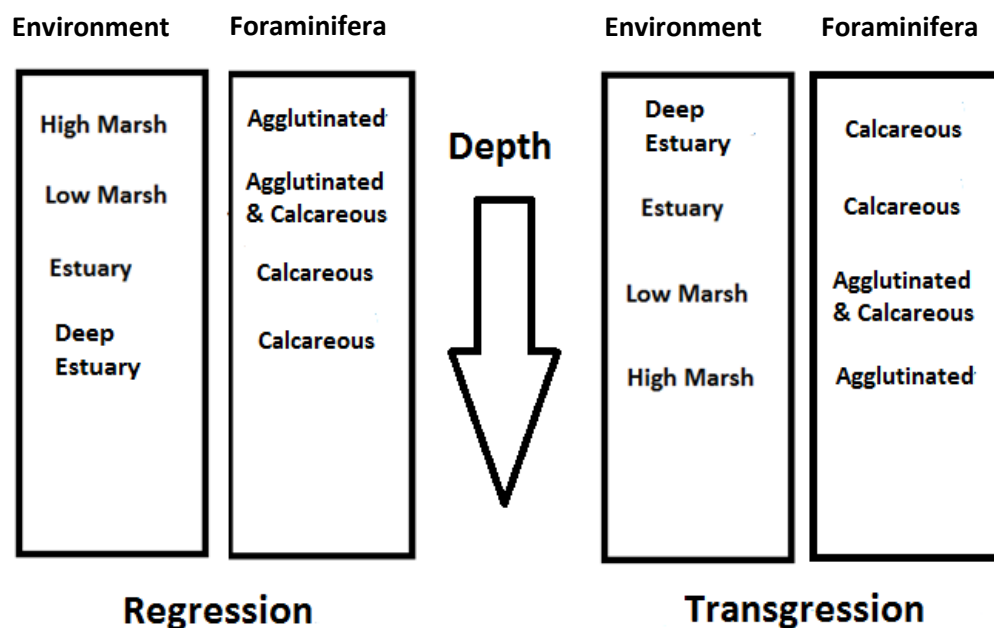


FIGURE 5: An illustration of a portion of this study's hypothesis. If the cores yield results similar to the Foraminifera assemblages and subenvironments on the left, then the results signify a regression. If the core samples produce results similar to those subenvironment and assemblages on the right, then a transgression has occurred.

CHAPTER 3: PREVIOUS STUDIES

A number of studies have validated the use of Foraminifera and other microfossils in determining changes in sea-level. One regional study completed in the Outer Banks of North Carolina looked at diatoms for the reconstruction of sea-level (Horton et al., 2006). Others have proven that Foraminifera within a salt marsh are elevation-dependent, and thus are excellent microfossils to use as proxies for previous landscape changes because the Foraminifera species are environmentally controlled. Some of these Foraminifera studies were completed on the coast of New Jersey, Canada, and in North Carolina (e.g. Scott & Medioli, 1980; Kemp et al., 2012).

Horton and Culver (2008) studied cores from three back-barrier study sites at the Outer Banks in North Carolina. They focused on areas at Pea Island, Currituck Barrier Island, and Oregon Inlet, where the tides were directly affected by irregular wind patterns rather than diurnal astronomical tides. This was the first study to address the gap in Foraminifera assemblages in this particular environment, reviewing the relationship between elevation and the Foraminifera assemblages present. The authors used Canonical Correspondence Analysis (CCA) and Partial Canonical Correspondence Analysis (PCCA) of the Foraminiferal and environmental data to determine the relationship between Foraminiferal assemblages and elevations. The study concluded that in the intertidal zone, the most important factor for the distribution of Foraminifera in each environment is the duration and frequency of tidal exposure or the inundation of the area.

They demonstrated that the distribution of Foraminifera in an intertidal zone is a direct function of elevation because different Foraminifera species were found only at certain elevations.

In a similar study Culver and Horton (2005) found that calcareous species are more abundant in mud and sand flats, while agglutinated Foraminifera are found in more vegetated areas. All samples were collected along one transect and were correlated to MSL. Two samples were taken for analysis at each site, and each sample was stored in buffered ethanol to allow analysis of both dead and living Foraminifera types. Culver and Horton (2005) also concluded that the (0 -1 cm) depth can be used for the reconstruction of paleo-subenvironments.

Another study from North Carolina focused on the Albermarle-Pamlico Estuary system, which is located about 250 kilometers north of Fort Fisher. Kemp et al. (2009) worked in the Albemarle-Pamlico estuarine system of North Carolina because the region is microtidal and has thick and continuous sequences of salt-marsh sediments. The authors took 193 surface samples from ten physiographically distinct salt marshes. They defined elevation-dependent ecological zones at individual sites using cluster analysis and detrended correspondence analysis and described the spatial distribution of the salt marsh Foraminiferal assemblages found. At each of the 10 study sites, the authors established a transect running from shallow environments to deeper environments during the late spring and early summer. The stations along each transect were positioned according to differences in vascular vegetation and elevation, to capture the full range and variety of conditions. At each station they collected a 1-cm deep surface sample for Foraminifera analysis. They used the VDatum transformation tool provided by the

National Oceanic and Atmospheric Administration for North Carolina to relate all sample elevations to local MSL and to estimate tidal ranges at each of the sites.

They found that the most abundant Foraminifera species in the high-marsh setting were *Haplophragmoides wilberti*, *Trochammina inflata*, *Arenoparrella mexicana*, and *Jadammina macrescens*. *Miliammina fusca* dominated almost all of the low marsh samples, while both *Trochammina inflata* and *Arenoparrella mexicana* were found in the intermediate marsh setting. In half of the samples collected, the near-shore, sub-tidal zones, and shallow estuaries and lagoons, were dominated by calcareous Foraminifera such as *Ammonia* spp. and *Elphidium* spp. The other half of the samples analyzed supported a different theory: in North America, many estuarine environments and sub-tidal settings were actually dominated by agglutinated species such as *Ammobaculites* spp. and *Ammotium salsum* instead of calcareous species. The authors also concluded that salt-marsh Foraminifers can be used as a tool to reconstruct the sea-level during the Holocene because eight of the ten locations studied in this experiment contained Foraminiferal assemblages that were elevation-dependent and thus could be classified and divided into different ecological zones (Kemp et al., 2009).

In a related study, Hashbrouck (2007) looked at the migration of tidal inlets in response to sea-level fluctuations and storms through time at Federal Point, North Carolina (the present-day Fort Fisher). This paper discussed the landscape changes, inlet formation, and inlet closures on Federal Point from the 1900s to 2006. Using historical maps and past aerial photographs of the site, the author was able to show when and how the landscape was altered.

Another study completed near Fort Fisher by Xia et al. (2008) focused on the Cape Fear River Estuary (CFRE) and the river's response to storm surge and ocean circulation during the passing of four hurricanes between 1996 to 2006. The hurricanes analyzed included: Bertha, a Category 2 storm that passed on July 13, 1996; Fran, a Category 3 storm on September 6, 1996; Floyd, a Category 2 on September 16, 1999; and Charley, a Category 1 storm on August 15, 2004. Among the conclusions of this study were that hurricanes that pass to the west of the CFRE (such as Hurricane Charley) tend to push water into the entrance of the river, bringing extreme storm surge into its mouth. When a hurricane passes along the axis or to the east of the CFRE, the greatest storm surge is seen along the southern coasts of Oak Island and Bald Head Island. Additionally, the study found that the lowest-lying land of the coastal plain is the most easily inundated. The northeastern part of Cape Fear (where Fort Fisher is located) is the lowest lying part of the area and would therefore be most easily flooded.

One goal of this project was to include the findings from these past studies (Table 3), and to use the research to verify the physical landscape changes and important historical events that have transpired at Fort Fisher.

TABLE 3: A table summarizing the most abundant Foraminifera species found in each subenvironment from other studies completed in and around North Carolina.

Source	Hippensteel et al. (2000)	Culver et al. (2005)	Abbene et al. (2006)	Kemp et al. (2009)
Location	Bomby Hook National Wildlife, Refuge DE	Pea Island, Oregon Inlet, Carrituck Barrier Beach, NC	Pamlico Sound, NC	Albermarle Pamlico Estuary, NC
Species Found				HIGH MARSH
				<i>Arenoparrella mexicana</i>
	MARSH	MARSH	MARSH	<i>Jadammina macrescens</i>
	<i>Arenoparrella mexicana</i>	<i>Ammonium salsum</i>	<i>Haplophragmoides wilberti</i>	<i>Haplophragmoides wilberti</i>
	<i>Jadammina macrescens</i>	<i>Ammobaculites subcatenulatus</i>	<i>Miliammina fusca</i>	<i>Trochammina inflata</i>
	<i>Miliammina fusca</i>	<i>Arenoparrella mexicana</i>	<i>Tiphotocha comprimata</i>	
	<i>Pseudothurammina limnetis</i>	<i>Haplophragmoides wilberti</i>	<i>Trochammina inflata</i>	INTERMEDIATE MARSH
	<i>Trochammina inflata</i>	<i>Jadammina macrescens</i>		<i>Arenoparrella mexicana</i>
		<i>Miliammina fusca</i>		<i>Trochammina inflata</i>
		<i>Siphotrochammina lobat</i>		
		<i>Tiphotocha comprimata</i>		LOW MARSH
		<i>Trochammina inflata</i>		<i>Miliammina fusca</i>
			MARINE	
			<i>Elphidium spp.</i>	
			<i>Quinqueloculina seminula</i>	
			<i>Cibicides lobatulus</i>	
Notes	*Low Marsh and Intermediate Marsh had higher concentrations of <i>Jadammina marescens</i> and <i>Miliammina fusca</i> than the High Marsh	*High concentration of these species were found in the Low Marsh than the High Marsh		

CHAPTER 4: METHODS

4.1 Field Methods

Eight surface samples and five core samples were taken adjacent to the fort to validate the method of using Foraminifera to determine paleo-subenvironments and to confirm the accuracy of military and historical maps showing Fort Fisher at different time periods. The surface samples were taken in a linear transect at seven different subenvironments, ranging from the Estuary (Deep) to the Extreme High marsh and one additional surface sample was taken on the beach-front. Five cores were then taken nearly perpendicularly to the transect. A map showing the exact locations of the surface and core samples can be seen on a 2015 Google Earth image (Figure 6).

All surface samples were taken to a depth of one centimeter. The core samples however, ranged in depth and are as follows: Core One was taken to a 125-centimeter depth and was divided in the field into 25-centimeter intervals: surface-to-25 centimeters; 26-to-50-centimeters; 51-to-75-centimeters; 76-to-100-centimeters and, lastly, 101-to-125-centimeters. Core Two only went to a depth of 50 centimeters and is also divided into 25-centimeter intervals, in the same manner as Core One. Cores Three, Four and Five are as follows: Core Three contains surface, 20-centimeter, 40-centimeter, and 60-centimeter samples. Core Four is comprised of surface, 40-centimeter, and 50-centimeter

samples. Core Five has surface, 20-centimeter, 40-centimeter, and 50-centimeter grab samples. For the continuous cores (Core One and Core Two), the Foraminifera content was analyzed at two centimeter intervals (Table 4).

4.2 Sedimentation Rates

To determine the year the core depths corresponded to, average sedimentation rates for the area were calculated. The sedimentation rate is important because it can provide information about when a particular layer of sediment was deposited.

At Fort Fisher, the sedimentation rate was found by radiocarbon dating organic material. *Spartina* spp. fragments were collected from cores a few meters away from core one at 45, 50, and 80-centimeters and were sent to the University of Georgia UGAMS Laboratory. Using ^{14}C radiocarbon analysis and a stable isotope ratio analysis, the age of the roots were calculated at 190 years and 500 years, respectively. The 190-year date corresponds to the root material at 45 centimeters, while the 500-year date corresponds to the 50-centimeter depth. The 80-centimeter age was disregarded because the material was reported to be “modern,” meaning it was probably either bioturbated or contaminated. Because the two depths (45 centimeters and 50 centimeters) were quite close, an average sedimentation rate was used. To find this average sedimentation rate in centimeters/years, 190 years was divided by 45 centimeters and the 500 years was divided by 50 centimeters, and then averaged (Figure 7, Equation A).

The average sedimentation rate for the Fort Fisher region was 0.17 cm/yr. Because this 0.17 cm/yr value was derived from only two dates at Fort Fisher, it was important to corroborate this rate with findings from other nearby marshes. Organic matter from five samples in three cores at Tar Landing Bay marsh, three samples in three

cores at Alligator Bay marsh, and four samples in two cores at Fort Caswell (Oak Island) marsh were also dated. The locations of these marshes relative to Fort Fisher can be seen on Figure 8.

The twelve samples were also radiocarbon dated, and sedimentation rates for each sample were derived (Figure 8). The calculations associated with finding the average sedimentation rate for all 12 samples can be seen in Figure 7, Equation B and Equation C.

These three sites (Alligator Bay marsh, Tar Landing Bay marsh and Fort Caswell marsh) had similar depositional environments, geomorphological features, and orientations to the Fort Fisher marsh. Consequently, averaging the sedimentation rates found at these three locations provided an accurate basis for comparison of sedimentation rates. The average sedimentation rate for these three locations produced a result of 1.7 mm/yr or 0.17 cm/yr, which is the same average sedimentation rate found for the Fort Fisher marsh. Therefore, 0.17 cm/yr is a valid average sedimentation rate to use for the cores taken at Fort Fisher (Figure 7, Equation C).

A sedimentation rate of 0.17 cm/yr, yields 5.88 years per centimeter (Figure 7, Equation D). Because the Foraminiferal assemblages for the continuous cores were analyzed at 2-cm intervals, every 2 cm equated to 11.76 years. See Table 4 for the years the core depths correspond to, and Figure 7, Equation E for the calculations.

4.3 Laboratory Methods

Once the sediment and core samples were collected, the samples were stored in a plastic bag and were brought to UNC Charlotte where they were prepared for analysis of Foraminifera content by the process of wet sieving. Wet sieving involves concentrating the Foraminifera in a 5-milliliter sediment sample using water. The samples were wet

sieved using a 0.71-millimeter sieve followed by a 0.177-millimeter sieve and a 63-micrometer screen. The 0.71-millimeter fraction was discarded and Foraminiferas were picked from the 0.177-millimeter and the 63-micrometer fractions, and then poured onto a sorting tray and viewed under a binocular microscope. Once in the tray, the first 100 Foraminifera, if present, were identified to genus level in each sample and recorded.

Identifying the Foraminifera taxa in each sample involved observing the foraminifer's shape, appearance, size, and thickness. Making use of previous Literature Reviews (e.g. Abbene et al., 2006), and class work (2013 Applied Paleontology Course under Dr. Hippensteel), the Foraminifera species were classified as being coarsely-agglutinated, finely-agglutinated, or calcareous. Depending on the number of Foraminifera in each sample, the volume of sediment analyzed also varied. At depths where Foraminifera were scarce, all of the sediment at that depth was analyzed. To account for differences in the volume of sediment, the data was normalized and the concentration was found by dividing the total volume used, by the total number of Foraminiferas found at each depth. For statistical analysis, the data was then filtered: Any concentration value under $30 \text{ specimens/cm}^3$ was removed because it was determined that these values would produce statistically invalid results because only finding 30 specimens/cm³ would not accurately represent the Foraminiferal assemblage of the core sample. A value of $30 \text{ specimens/cm}^3$ or lower means that not enough data was found for that samples.

The Foraminifera assemblages found from the eight surface samples (Deep and Shallow Estuary, Extreme High marsh, High marsh, Intermediate marsh, Low marsh, Extreme Low marsh, and the Beach) were the control variables because they represent

the modern analog for paleo-subenvironments. The Foraminifera found within the core samples were then compared to the Foraminifera species found in surface (control) samples by calculating Pearson values. Pearson values for the Foraminifera concentration at every depth were found for each of the surface analogs. Of the remaining Pearson values, the analog that produced the highest Pearson value was considered indicative of the paleo-subenvironment because of the similarity of the Foraminiferal assemblages. By correlating the modern analog and the core assemblages, a graph of the subenvironments at various time periods was created. Each surface subenvironment received an elevation value relative to mean sea-level to document how the subenvironments in the strata from the Foraminifera in the cores have changed through time. The elevation values given to each subenvironment can be seen in Table 5.

4.4 Georeferencing and Mapping Subenvironments

To determine if the Foraminifera data matched the historic record of the area, high-resolution aerial images, historical maps, and topographic maps were collected. Ideally, the images and maps, when combined with the core and surface locations, would show exactly what the Foraminifera data produced: each core's change in subenvironments (if any) through time.

The high-resolution aerial images were downloaded from Google Earth and the Digital Coast Data Access Viewer, while the military, historical and topographical maps came from a variety of sources and were all scanned at 1200 X 1200 dpi resolution. These sources included UNC Charlotte Library's Atlas Collection and Map Collection, the United States Geologic Survey website, North Carolina One Map website, the Fort Fisher Historical Museum, North Carolina State Archives website and, lastly, UNC

Chapel Hill Library's North Carolina Maps. See Appendix B for the maps and Table 25 for the figure number, year, publisher, and source of each map used.

All of the downloaded images and maps needed to have the same spatial reference and same spatial extent, so the georeferencing tool in ArcMap 10.1 was used. The most common georeferencing method is a first-order polynomial transformation (also known as an affine transformation), and was therefore, selected as the georeferencing transformation method for this project.

Georeferencing is the process of transforming or warping a raster image to a target image by assigning a spatial reference to the raster image. This was accomplished by identifying ground control points on a target image and matching these points to the raster file. A target image is an image that has been spatially referenced in the preferred coordinate system with the desired x and y extent. The ground control points are objects of any identifiable feature that has remained in the same coordinate location through time. The affine transformation in particular, ensures that straight lines in the georeferenced raster dataset are preserved in the final product. Thereby, the affine transformation shifts, scales and rotates the image that is being georeferenced in order to maintain straight lines.

Once the ground control points were identified, link points between the raster file (that was being georeferenced) and the target image were created, and then rectified to save the changes of the newly transformed raster file. See Table 7 for the coordinate list all of the ground control points used. In all cases, the target image was a 2013 Natural Color base image downloaded from the Digital Coast Data Access Viewer. This high-resolution image, provided by the NOAA National Geodetic Survey, contains data that is

accurate with a 95% circular error confidence level because it was taken from a Digital Sensor System (Red Green Blue) scale.

After georeferencing all of the Google Earth images, and scanning and downloading the maps, the georeferenced products were used to create subenvironmental boundaries to differentiate between the surface subenvironments (Estuary, Extreme Low, Low, Intermediate, High and Extreme High marshes, Land, and Beach) through time. A fort boundary was also created to indicate the position of the fort relative to these subenvironments through time. To ensure all of the georeferenced products showed exactly the same boundary extent, the footprint of the 2015 georeferenced Google Earth image was created and then used as the outline for all of the other images. Using the “math algebra” tool under the spatial statistics tab in ArcGIS 10.1, the 2015 raster file was transformed so that the pixels that comprised the image were of identical resolution. After that, the image was converted from a raster file to a polygon shapefile, which, when added to the data frame, contained only the outline of the 2015 image. Using the cut polygon feature in the editor tool in ArcGIS 10.1, other polygons were created from the initial outline by drawing on the perimeter of the specific boundaries. Depending upon the resolution of the images, the number and name of the polygons differed. In some instances, the High marsh and Low marsh were distinguishable and were therefore shown by two different polygons. However, in other images, the High and Low marshes were indistinguishable, and were therefore represented by the same polygon called Marsh.

4.5 Comparing insights derived from Foraminiferal Data to Historical Maps

To compare the results from the Foraminifera data to that of the Map data, a Python script was written using the arcpy module. The idea was to display the map data in a way that enabled the comparison between the two methods.

The first step was to create new shapefiles by intersecting the surface and core locations with all of the boundaries that were created from each georeferenced product. This was done to determine the subenvironment for all of the surface and core samples at a specific time period.

Once that step was complete, the new shapefiles were then joined to create one master shapefile. Using the “Add Join” function, the master shapefile was created and the associated attribute table was exported as an Excel file. See Figure 10 for the Python script that automated this process.

The process of creating all graphs and maps is explained in the Results and Discussion sections. To compare the Map data to the Foraminifera data, the surface subenvironments were assigned similar elevation values (Table 5).

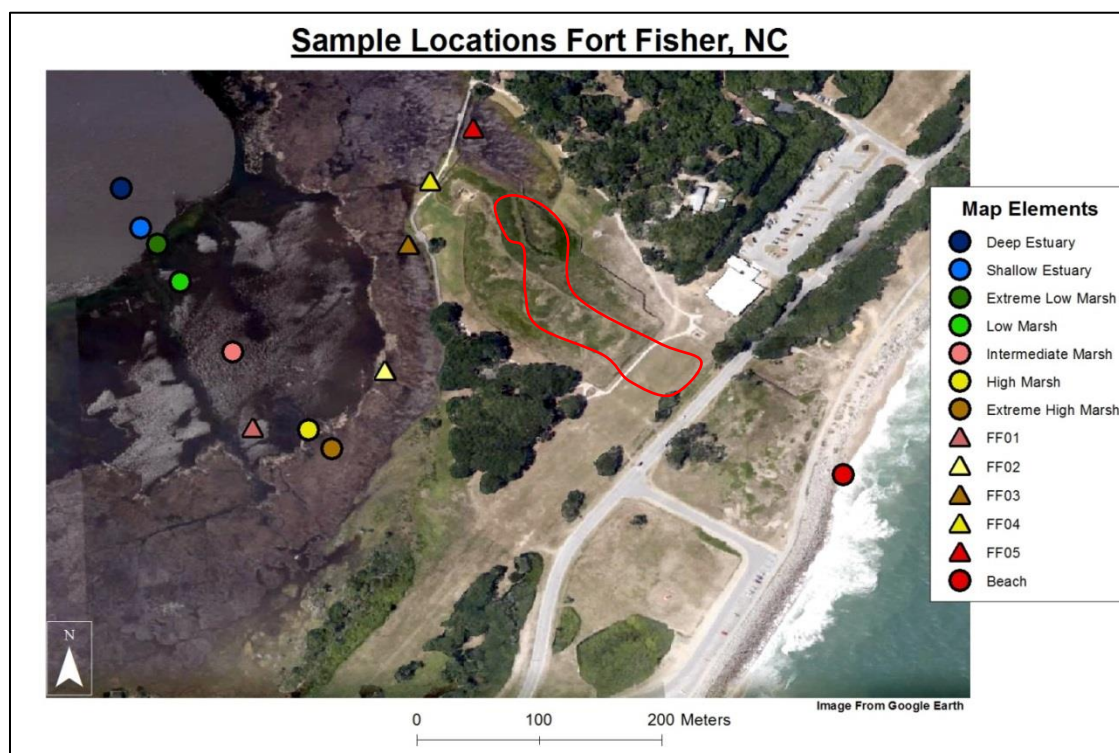


FIGURE 6: A map of the core and surface sample locations that were taken at Fort Fisher, North Carolina. The points are overlaid on a georeferenced 2015 Google Earth image. The red outline, just east of Core 4, outlines the remnants of the fort that remains today. Note: All samples and cores were recovered outside of the Fort Fisher Historical Site state property.

Equation A: Fort Fisher's Average Sedimentation Rate

$$\frac{45\text{cm}}{190\text{yr}} = \frac{0.24\text{cm}}{\text{yr}}; \frac{50\text{cm}}{500\text{yr}} = \frac{0.1\text{cm}}{\text{yr}}; \frac{\frac{0.24\text{cm}}{\text{yr}} + \frac{0.1\text{cm}}{\text{yr}}}{2} = \frac{0.17\text{cm}}{\text{yr}}$$

Equation B: Sedimentation Rates for Tar Landing Bar Marsh (TLB), Alligator Bay Marsh (AB) and Fort Caswell Marsh (FC)

$$\frac{\frac{2.6\text{mm}}{\text{yr}} + \frac{1.9\text{mm}}{\text{yr}} + \frac{3.3\text{mm}}{\text{yr}} + \frac{2.2\text{mm}}{\text{yr}} + \frac{1.4\text{mm}}{\text{yr}}}{5} = \frac{2.28\text{mm}}{\text{yr}}$$

$$\frac{\frac{1.3\text{mm}}{\text{yr}} + \frac{1.9\text{mm}}{\text{yr}} + \frac{1.3\text{mm}}{\text{yr}}}{3} = \frac{1.50\text{mm}}{\text{yr}}$$

$$\frac{\frac{1\text{mm}}{\text{yr}} + \frac{1.2\text{mm}}{\text{yr}} + \frac{1\text{mm}}{\text{yr}} + \frac{1.9\text{mm}}{\text{yr}}}{4} = \frac{1.275\text{mm}}{\text{yr}}$$

Equation C: The Average Sedimentation Rate of the three TLB, AB and FC rates

$$\frac{\frac{2.28\text{mm}}{\text{yr}} + \frac{1.50\text{mm}}{\text{yr}} + \frac{1.275\text{mm}}{\text{yr}}}{3} = \frac{1.68\text{mm}}{\text{yr}} = \frac{0.168\text{cm}}{\text{yr}}$$

Equation D: The Inverse

$$\frac{\frac{0.168\text{cm}}{\text{yr}} + \frac{0.17\text{cm}}{\text{yr}}}{2} = \frac{0.169\text{cm}}{\text{yr}}; \frac{1}{\frac{0.169\text{cm}}{\text{yr}}} = \frac{5.88\text{yr}}{\text{cm}}$$

Equation E: Every two centimeters

$$\frac{5.88\text{yr}}{\text{cm}} \times 2 = \frac{11.76\text{yr}}{2\text{cm}}$$

FIGURE 7: Mathematic Equations for calculating the Sedimentation Rate

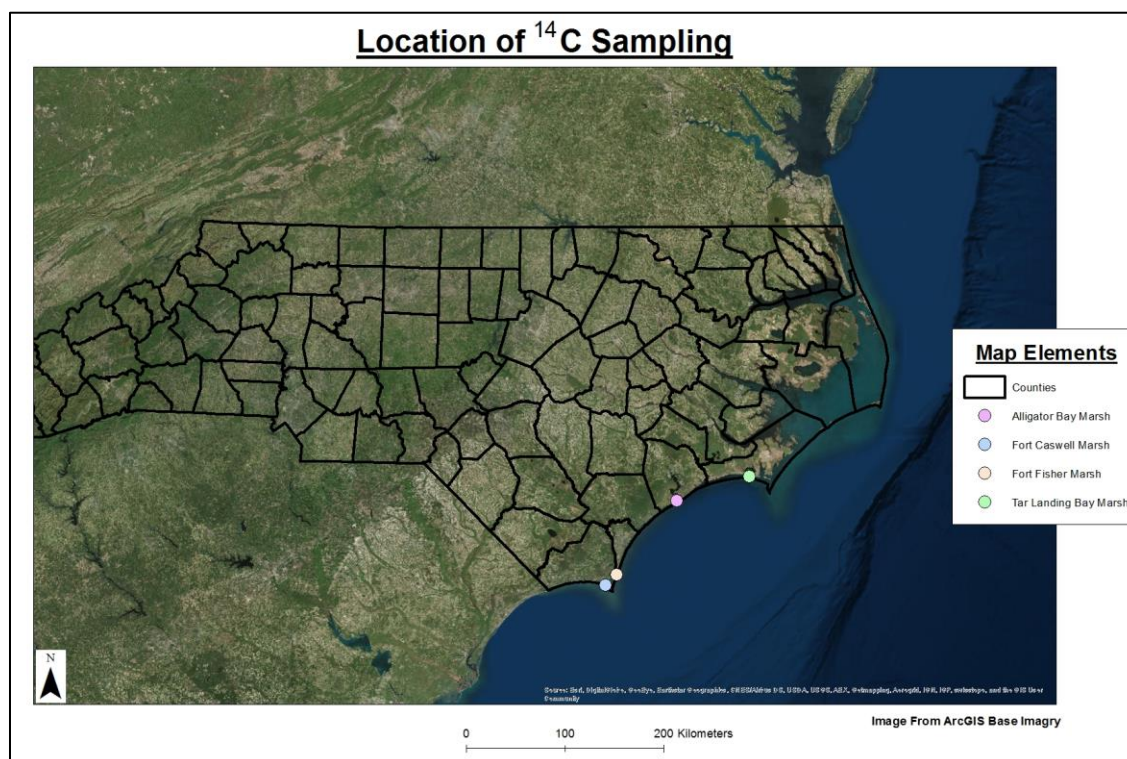


FIGURE 8: A map (created in ArcGIS 10.1 with the ArcGIS Base Imagery) showing the location of Tar Landing Bay Marsh, Alligator Bay Marsh, and Fort Caswell Marsh relative to the Fort Fisher marsh. These were the sedimentation rate sampling locations used in this study. The North Carolina counties are also shown on this image which was downloaded from the 2010 Census Bureau.

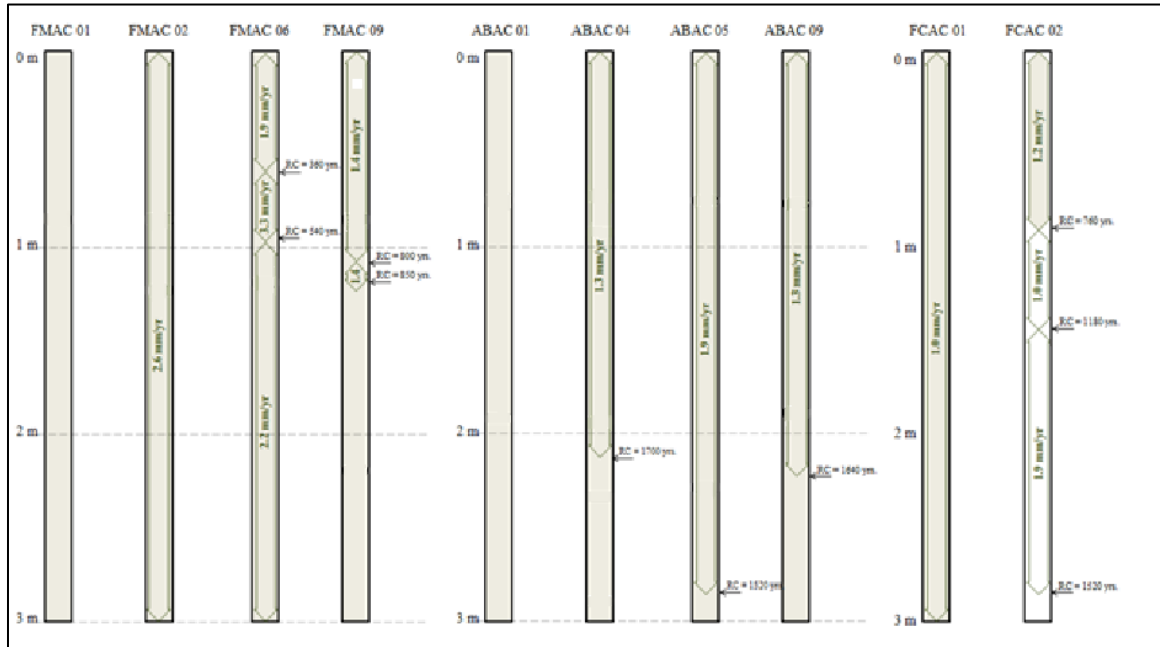


FIGURE 9: Sedimentation rates based on the organic material that was ^{14}C dated from Tar Landing Bay Marsh, Alligator Bay Marsh and Fort Caswell Marsh (modified from Hippensteel et al., 2014). The organic material was sent to University of Georgia Accelerator Mass Spectrometry Laboratory where uncalibrated dates for the material before 1950 were produced. The sedimentation rates were then derived based on the years, and are in mm/yr.

```

#Imports necessary libraries
import arcpy
from arcpy import env
import os

# Defines the workspace and reads the boundary shapefiles
env.workspace = r"E:\Shapefiles\Boundaries"

# Allows the files (when the script runs) to be overwritten
arcpy.env.overwriteOutput = True

# Uses the ListFeatureClass function to return a list of shapefiles
fcList = arcpy.ListFeatureClasses()

# Reads the shapefiles in the SampleLocations folder
samplePoints = r'E:\Shapefiles\SampleLocations\AllSamples.shp'

# Creates a loop to instect all of the boudary shapefiles with the sample locations
# and then joins all of the shapefiles together
for fc in fcList:
    inFeatures= [samplePoints,fc]
    output= r"E:\Shapefiles\Python"+os.sep+fc.split(".")[0]
    arcpy.Intersect_analysis(inFeatures,output)
    arcpy.JoinField_management(r"E:\Shapefiles\lu1781to2015.shp", "FID", output+".shp", "FID", ["LandUse"])

# Checks the output
print(output)

```

FIGURE 10: Script from python that was written to create an excel table that contained all of the mapping information; year and the location's environment. The number sign followed by the red lettering in the script are comments that describe each stage of the code. Using the arcpy module, the arcpy.Intersect, and the arcpy.JoinField functions, the script successfully ran and the master excel file was created.

TABLE 4: The five cores, the depths, and the associated years that were analyzed for Foraminifera content.

Year	Core 1 Depths (cm)	Year	Core 2 Depths (cm)	Year	Core 3 Depths (cm)	Year	Core 4 Depths (cm)	Year	Core 5 Depths (cm)
2013	Surface	2013	Surface	2013	Surface	1778	40	1895	20
2001	2	2007	2	1895	20	1719	50	1778	40
1989	4	2001	4	1778	40			1719	50
1978	6	1995	6	1766	60				
1966	8	1989	8						
1954	10	1983	10						
1942	12	1977	12						
1931	14	1971	14						
1919	16	1965	16						
1907	18	1959	18						
1895	20	1953	20						
1884	22	1947	22						
1872	24	1941	24						
1860	26	1935	26						
1848	28	1929	28						
1837	30	1923	30						
1825	32	1917	32						
1813	34	1911	34						
1801	36	1905	36						
1790	38	1899	38						
1778	40	1893	40						
1766	42	1887	42						
1754	44	1881	44						
1743	46	1875	46						
1731	48	1869	48						
1719	50	1863	50						
1707	52								
1695	54								
1684	56								
1672	58								
1660	60								
1648	62								
1637	64								
1625	66								
1613	68								
1601	70								
1590	72								
1578	74								
1566	76								
1554	78								
1543	80								
1531	82								
1519	84								
1507	86								
1496	88								
1484	90								
1472	92								
1460	94								
1449	96								
1437	98								
1425	100								
1413	102								
1401	104								
1390	106								
1378	108								
1366	110								
1354	112								
1343	114								
1331	116								
1319	118								
1307	120								
1296	122								
1284	124								

TABLE 5: Elevation values assigned for each method's subenvironment shows the elevation values that were given to all the subenvironments. The top column corresponds to the environments that the Map data yielded, while the bottom column corresponds to the environments that the Foraminifera data produced. All the elevation values are in meters. The negative value indicates that the elevation is below the mean sea-level whereas the positive numbers indicate that the land is above the mean sea-level. For all purposes, the ocean was at mean sea-level.

		Subenvironments											
		Deep Estuary	Estuary	Shallow Estuary	Extreme Low Marsh	Low Marsh	Marsh	Intermediate Marsh	High Marsh	Extreme High Mash	Land	Ocean	Fort
Method Type	Map Boundaries	N/A	-1	N/A	N/A	0.5	0.75	N/A	1	N/A	2	0	1.5
	Foram Boundaries	-1	N/A	-0.5	0.25	0.5	N/A	0.75	1	1.25	N/A	N/A	N/A

TABLE 6: Georeferenced coordinates (link points) in decimal degrees that were used to transform/warp the scanned, downloaded maps, and the google earth images to the target image.

Old Ycoord	Old Xcoord	Xcoord	Ycoord
491.792019	-90.233734	-77.9197	33.97289
787.053702	-317.521376	-77.9177	33.97159
670.800597	-581.732429	-77.9185	33.97013
925.693611	-112.445169	-77.9168	33.97275
507.295937	-45.136943	-77.9196	33.97313
712.5388	-717.613864	-77.9182	33.96936
487.179625	-286.426825	282.08	33.9724
248.278308	-427.332875	282.059	33.96007
494.93159	-340.940761	282.08	33.9684
506.69862	-308.791397	282.081	33.9714
404.556373	-163.642157	282.083	33.97087
152.149265	-166.012092	282.08	33.97235
422.959125	-869.81076	282.077	33.96232
353.059801	-717.670566	282.078	33.96427
407.735941	-258.067228	282.082	33.96936

CHAPTER 5: RESULTS

The results section was divided into three parts. The first part discussed the findings of the Foraminiferal analysis. The second part presented the results of the map data analysis and the third section compared the findings of the two methods.

5.1 Foraminiferal Results

Eight surface samples (modern analogs), and five core samples were analyzed for Foraminifera content to determine which subenvironments the depths in Cores 1- 5 corresponded to. The taxa that were found within each modern subenvironment can be seen in Figures 11-26. The taxa within the core samples can be seen in Table 7 and Table 8. Figures 11-26 will be discussed first.

A. beccarii was the most common species in the Estuary (Deep) subenvironment (Figure 11). In this subenvironment, three times as many *A. beccarii* were found compared with other species. In conjunction with the calcareous species, *M. fusca*, an agglutinated species, was the second most abundant, with a concentration value near 20 specimens/cm³. The other abundant species found in the Estuary (Deep) subenvironment, were *A. parkinsoniana* and *E. excavatum*.

Figure 12 shows the total number of calcareous and agglutinated taxa that were found in the Estuary (Deep) subenvironment. Calcareous, rather than agglutinated taxa, were dominant in this subenvironment. The overall concentration of calcareous Foraminifera totaled a value near 90 specimens/cm³ compared to agglutinated taxa at 15 specimens/cm³. The Estuary (Shallow) subenvironment yielded similar results.

In the Estuary (Shallow) subenvironment, *A. beccarii* was the most dominant species because it had the highest abundance (55 specimens/cm³). However in this environment, *Elphidium* spp. was much more prevalent than in the Estuary (Deep) subenvironment, with *E. excavatum* and *Elphidium* spp. totaling 40 specimens/cm³. The overall concentration of calcareous and agglutinated taxa can be seen in Figure 13.

Calcareous taxa were more dominant in the Estuary (Shallow) subenvironment than the agglutinated taxa, with a total concentration of around 90 specimens/cm³. The agglutinated taxa totaled 15 specimens/cm³ (Figure 14).

The next subenvironments from the Estuary to the east towards the fort, are the marshes, with the Extreme Low Marsh being the lowest in elevation compared to the other marsh subenvironments (Figure 6).

The Foraminifera species that were found in the Extreme Low marsh were much different than those found in the Estuaries. Figure 15 illustrated that the agglutinated species, *M. fusca* is the most abundant, with a concentration value near 40 specimens/cm³. The Foraminifera species with the second highest abundance was *T. inflata*, with a value near 15 specimens/cm³. Additionally, the coarsely agglutinated Foraminifera species were more prevalent here than in the estuaries. The abundance of

Ammobaculities sp. and *Ammotium salsum* in the Extreme Low marsh subenvironment, was about 15 specimens/cm³, the same as *T. inflata*.

Figure 16 shows that the agglutinated taxa were most dominant in the Extreme Low marsh subenvironment compared to the calcareous species. The total concentration of agglutinated Foraminifera totaled nearly 80 specimens/cm³ compared to calcareous taxa, which totaled fewer than 10 specimens/cm³. All subenvironments were distinguished by their elevation relative to the mean sea-level (MSL). As subenvironments shift east from the Cape Fear River to the fort, the elevation of the land relative to MSL increases. Along this transect, the Extreme Low marsh subenvironment eventually changes to the Low marsh subenvironment.

The Low marsh yielded similar results to the Extreme Low marsh subenvironment (Figure 17). The agglutinated species, *M. fusca*, was still the most abundant, with a concentration value near 40 specimens/cm³. The second most abundant Foraminifera species was *T. inflata*, with a value of 15 specimens/cm³. Additionally, the abundance of the coarsely-agglutinated Foraminifera species; *Ammobaculities* sp. and the *Ammotium salsum*, remained constant from the Extreme Low marsh subenvironment to the Low marsh. The concentration values of both *Ammobaculities* sp. and *Ammotium salsum* totaled 15 specimens/cm³, which is similar to *T. inflata* concentration value. The Low marsh differs slightly from the Extreme Low marsh subenvironment, as evidenced by the appearance of some calcareous species such as *A. beccarii*, *A. parkinsoniana* and *E. subarticum*. Conversely, trace amounts of these species were found within the Extreme Low marsh subenvironment.

Within in the Low marsh subenvironment, the total concentration of agglutinated Foraminifera was nearly 70 specimens/cm³, compared to calcareous taxa, which totaled a concentration value fewer than 20 specimens/cm³ (Figure 18). These calcareous species were more prevalent in this environment compared to the Extreme Low marsh (Figure 16).

The next environment (to the east), was the Intermediate marsh. The Intermediate marsh produced results that were both similar and different (Figure 19) to the Extreme Low and Low marshes. The most abundant species in the Intermediate Marsh was *T. inflata*, with a value of 25 specimens/cm³ (instead of the *M. fusca* species). The species with the second highest concentration value was *M. fusca*, with about 15 specimens/cm³. It became apparent that the two Foraminifera species (*T. inflata* and *M. fusca*) had switched in abundance from the Low marsh to the Intermediate marsh. In contrast, the coarsely-agglutinated species, *Ammobaculites* sp. and *Ammotium salsum*, maintained their concentration levels, with an abundance value near 15 specimens/cm³. Thus, the primary difference between the low marshes and the Intermediate marsh was the third most abundant species, *J. macrescens* with a total concentration value also near 15 specimens/cm³.

Another difference between the Intermediate Marsh and the Extreme Low and Low marsh subenvironments was the concentration of agglutinated taxa compared to calcareous taxa (Figure 20). Agglutinated taxa were the most dominant in the Intermediate marsh subenvironment, with a total Foraminifera value over 110 specimens/cm³. Subsequently, calcareous taxa totaled a concentration near 2

specimens/cm³. Clearly, the number of calcareous species between the Low and Intermediate marshes dwindled.

The Foraminifera species found in the High marsh were similar to those found in the Intermediate marsh, and were both similar and different from the Foraminifera species that were present in the Extreme Low and Low marshes (Figure 21). As with the Intermediate marsh, *T. inflata*, with a concentration value above 50 specimens/cm³, was the most dominant species in the High marsh. The species with the second highest concentration value was *M. fusca* (25 specimens/cm³). *J. macrescens* was the third most abundant species, with a concentration value also near 15 specimens/cm³.

However, differences existed between this subenvironment and the other subenvironments. The first difference is that *A. mexicana* was present, with a concentration value near 15 specimens/cm³. This concentration value (15 specimens/cm³) was three times the concentration value of *A. mexicana* species in the other subenvironments. Second, the coarsely agglutinated Foraminiferal taxa decreased in abundance as both *Ammobaculites* sp. and *Ammotium salsum* concentration levels dropped by 50%. Lastly, no calcareous taxa were found in this subenvironment. Only agglutinated taxa were present (Figure 22).

Figure 22 illustrates that agglutinated taxa were undoubtedly the most dominant taxa in the High marsh subenvironment. The total concentration of agglutinated taxa neared 110 specimens/cm³, a value quite similar to the number of agglutinated taxa that were recorded in the Intermediate marsh. In contrast, no calcareous species were found.

The Extreme High marsh produced similar results to the High marsh subenvironment (Figure 23). Again, *T. inflata*, with a concentration near 60 specimens/cm³, was the most dominant species in the Extreme High marsh subenvironment. However, the species with the second highest concentration was *J. macrescens*, instead of *M. fusca*, which was the case in the High marsh. The concentration of *J. macrescens* in the Extreme High Marsh environment neared 15 specimens/cm³. *A. mexicana* was the third most abundant species, followed by *M. fusca*. As in the High marsh, the Extreme High marsh was dominated by agglutinated taxa (Figure 24). Agglutinated taxa had a concentration value near 110 specimens/cm³. In contrast, the concentration of the calcareous species that were found in the Extreme High marsh subenvironment yielded only 1 specimen/cm³.

The Beach subenvironment, as shown in Figure 25, was unlike any of the estuary or marsh subenvironments. The main difference between the Beach environment and all of the other subenvironments was that the most dominant Foraminifera species was *Quinqueloculina* sp. with a concentration value near 10 specimens/cm³. No other subenvironment contained that particular genus. Also notable was the trace amounts of agglutinated taxa were found, and while calcareous taxa were present, the overall concentrations of Foraminifera were quite low (Figure 26).

Figure 26 illustrates that in the Beach subenvironment, calcareous taxa were more abundant compared to agglutinated taxa. The overall concentration of the calcareous taxa totaled 10 specimens/cm³. When compared to the other subenvironments, the abundance of Foraminifera in the Beach was five times lower than the abundance of the

Foraminiferas in the other environments. In all other subenvironments, the concentration of agglutinated or calcareous taxa was close to or above 50 specimens/cm³.

Figures 11-26 present the concentrations of the Foraminifera species that were found in the surface samples (0 to 1-cm deep). Figures 27 and 28 and Tables 7-11 describe Foraminifera species that were found in the cores. A total of 6,178 specimens were found within the core samples. This 6,178-value was normalized to account for the differences in the volume of sediment used during the data collection. Figure 27 shows the breakdown of the species that comprise this total. Figure 27 displays that *T. inflata*, an agglutinated taxa, was the most dominant species present. *T. inflata* was found 34% of the time. It was assumed that higher percentages meant that the particular Foraminifera species was most prevalent. Other species that were commonly found within the core samples were *J. macrescens* and *M. fusca*, also agglutinated taxa, with respective values of 19% and 13%.

The normalized data for the Foraminifera species that were found in the cores can be seen in Tables 7- 11. Each table shows the normalized data for every core. These normalized concentration values were then transformed into Pearson values by comparing each depth to the subenvironments from the surface analogs. Subsequently, each depth was matched to the year in which it was deposited, in order to see how each core changed subenvironments through time. This can be seen in Tables 12-16. The sedimentation rate for this area was 0.17 cm/yr.

After the Pearson values were calculated, the data was filtered to remove any Pearson values that were between 0.5 and -0.5, as well as concentrations that were less than 30 specimens/cm³. This yielded 15 data points for Core 1 (from 63 points), 17 data

points for Core 2 (from 26 points), and all the data points (4 and 2) for Cores 3 and 4, for analysis. Unlike the other cores, when the data was filtered, the values (in Core 5) became insignificant and therefore were not used in subsequent analysis. Additionally, the subenvironments for each Pearson value were assigned an elevation value relative to MSL, in meters (Tables 17-20).

After data filtering, the highest Pearson values for each depth were changed to the particular subenvironment to which the depth corresponded (Table 21). Table 22 shows the same information, but with the elevation (in meters) of each subenvironment. No core sample was most like the Low marsh, Estuary or Beach subenvironments, so they do not appear in Table 21.

Lastly, the information in Table 22 was graphed on an x-y scatter plot (Figure 28) in order to illustrate how the cores have changed location through time. Figure 28 shows the migration of subenvironments in each core through time. Ideally, each core should have produced similar results; either a transgression or regression through time. In actuality, this was not the case.

In 2013, the location of Core 1 started in the High marsh. From 1970-1990, the subenvironment of Core 1 changed from the High marsh to the Extreme High marsh, and then shifted to the Intermediate marsh subenvironment in the 1960s. Core 1 stayed in the Intermediate marsh environment from 1880-1960, when the subenvironment changed yet again. The figure indicates that Core 1's subenvironment changed to the Extreme Low marsh at 1880 and stayed as an Intermediate marsh to the year 1330, which was the oldest year recorded. This progression, a High marsh transforming to an Extreme Low marsh, indicates a regression. In other words, the estuary has retreated in recent years.

Core 3 exhibited similar changes to those of Core 1. In 2013, the location of Core 3, as with Core 1, began in the High marsh subenvironment. Around 1880, the subenvironment shifted to the Extreme Low marsh subenvironment and stayed in the Extreme Low marsh subenvironment from 1660-1880, which was the oldest point recorded for this depth. The movement from the High marsh on the surface to the Extreme Low marsh subenvironment indicates a regression.

Core 2 and Core 4 produced different results than Core 1 and Core 3. Through the years, Core 2 stayed in the Extreme High marsh subenvironment, with two extremes at the years 1840 and 1990. In those two years, the subenvironment shifted to the Intermediate marsh. Two depths were associated with Core 4. From the year 1710-1780, Core 4 was located in the Extreme High marsh subenvironment. No extrapolations can be made with this data, so no further results were obtained for this core.

5.2 Map Results

To validate the method of using Foraminifera to recreate paleo-subenvironments, images from Google Earth, maps from military atlases, and state and local government archives were used. These images and maps were downloaded, georeferenced and then overlaid with the surface and core samples that were taken adjacent to Fort Fisher (Figures 46-95).

Two different approaches were used to present maps. When the images and maps were clear and not pixelated, one data frame was used to show the location of each core (Figure 46-58 and 77-89). When the images and maps were of poor quality, meaning the features on the map were difficult to distinguish, two data frames were used (Figures 59-76 and 90-95). One data frame showed the location of the cores while the other data

frame displayed the area surrounding the cores. Prior to 1865, the resolution of the maps was extremely poor, resulting in blurry images. Therefore, they were represented using dual data frames.

All of the images were georeferenced (utilizing the suite of tools in ArcGIS) to a target image that was downloaded from the digital coast access viewer. Boundaries were created (depending upon the quality of the map) for each subenvironment to show how the subenvironments have changed through time. In other words, boundaries were only created for the maps where enough detail was displayed. The boundaries that were created (if distinguishable) were the Estuary, Extreme Low/ Low/ Intermediate/High/and Extreme High marshes, Fort, Land, and Ocean. In some cases, the differences in the marsh subenvironments were unidentifiable, and were therefore described as “the Marsh.” These boundary maps (Figures 96-125) were not made for all the figure numbers from 46-95.

Each image and map used in this study was created by a cartographer or from a satellite. Table 25 lists the cartographers responsible for creating each image and map. Table 26 displays the change in the subenvironments for all the cores through time. This table was produced using a Python script (Figure 10), which automated the process of intersecting the sample locations to the boundaries of each year and then joining the tables (see Chapter 3 for details regarding the technique).

The remaining portion of this Results section is spilt into subsections discussing the change in subenvironments of each core through time. The surface samples are shown on the maps as well, but can be disregarded because the surface samples were taken from a 0-to-1 cm depth, and therefore represent the environments from the year 2013. From

1970-2013, Core 1 contained sediments deposited in an Extreme Low, Low, and Intermediate marsh subenvironments (Figures 48-61 and 97-105). The boundaries between these three subenvironments were indistinguishable and therefore not separated. The one exception was the map showing the year 1974 (Figure 60 and Figure 104). This map was not as detailed as the more recent maps. Consequently, boundaries for this year only included the Marsh, Land, Ocean and Fort. Core 1, according to the 1974 map, remained in the Marsh subenvironment. From 1865 to 1946, the maps revealed that the subenvironment of Core 1 was Land (Figures 63-87 and 106-120). Prior to 1865, the subenvironment of Core 1 differed depending upon the map. According to the map from 1864, the location of Core 1 was in a High marsh subenvironment, while in 1863, Core 1 was either on Land or in an Estuary subenvironment. Two values at 1863 (of the same map) were shown to represent the error in georeferencing a historic hand-drawn map (Figures 88- 89 and 123-124). The technique used to georeference the map and images directly impacted the position of the cores on the map. From 1781-1863, the maps depicted that the subenvironment of Core 1 was Land and stayed on Land. From 1733-1770 (Figures 93 -95) the subenvironment of Core 1 was located in the Marsh.

The maps for the subenvironment of Core 2 through time produced identical results to those of Core 1. Two exceptions were from the years 1980-2013 (Figures 48-59 and 97- 103) and the year 1970 (Figures 60 and 104), where the subenvironment of Core 2 was located in the High to Extreme-High marsh instead of the Extreme-Low, Low and Intermediate marsh subenvironments. The boundaries between the High and Extreme High marsh were indistinguishable and therefore, not separated. The last difference between Core 2 and Core 1 was in the year 1863 (Figures 88 and 89 and 123 to 124).

Both maps from this time period indicated that the subenvironment of Core 2 was the Estuary, rather than Land.

From 1970-2013, the location of Core 3, as with Core 2, remained in the Extreme High and High marsh subenvironments (Figures 48-61 and 97 to 105). The one exception was from the year 1974. This map indicated that the subenvironment of Core 2 was the Marsh, because the boundaries between the Marsh subenvironments were indistinguishable, and therefore not separated (Figure 60). From 1865-1946, the maps revealed that subenvironment of Core 3 was Land (Figures 63-77 and Figures 106-114). For 1865, different maps depicting the same environment at the same time disagreed on the subenvironment of Core 3. A total of eight maps from the year 1865 were analyzed. January 15, 1865, was an extremely important day in North Carolina's history making this year central to the analysis. January 15, 1865 marked the fall of Fort Fisher as Confederate forces ceded control to the advancing Union army (Figures 77-87 and 114-121). Of the eight 1865 maps that were analyzed, three of them indicated that the subenvironment of Core 3 was the Estuary (Figures 114, 119, and 121) while the other five indicated that the subenvironment of Core 3 was Land (Figures 115-118 and 120). According to the map from 1864, Core 3 was in a Low marsh, and in 1863, Core 3 was in the Estuary, (Figures 88-89 and 123-124). The map from 1781 indicated that the subenvironment of Core 3 was Land (Figure 125), whereas the maps from 1733-1770 indicated that the subenvironment of Core 3 was in the Marsh (Figures 93-95).

From 1870-2013, the maps indicated that Core 4's subenvironment was Land, which was different than the other cores' locations, especially in 2013 (Figures 48-76 and 78-94). The only exception of Core 4's subenvironment comes from the 1974 map, which

showed that Core 4 in the Marsh subenvironment (Figure 60 and Figure 104). In 1865, different maps of the same time, depicting the same environment, did not concur on the location of Core 4. Of the eight 1865 maps that were analyzed, one indicated that Core 4 was in the Estuary subenvironment (Figure 114), another indicated Core 4 was in the Marsh subenvironment (Figure 121), while the rest indicated that the subenvironment of Core 4 was on Land (Figures 115-120). According to the map from 1864, the subenvironment of Core 4 was in a Low Marsh (Figure 122), while in 1863, Core 4 was either located in the Estuary subenvironment or Land subenvironment (Figures 88-89 and 123-124). In 1781, the subenvironment of Core 4 was depicted to be on Land (Figure 125), then returned to a Marsh subenvironment from 1733 to 1770 (Figures 93-95).

The maps indicated that the subenvironments of Core 5 through time were identical to the subenvironments of Core 4 through time. Only two exceptions exist, and they are in years 1863 and 1865. Of the eight maps that were analyzed for 1865, one of the maps indicated that Core 5 was in the Estuary subenvironment (Figure 121), four were in the Marsh subenvironment (Figures 114, and 116-118), and three maps showed that the subenvironment of Core 5 was Land (Figures 77-87, 115, 119 and 120). According to the maps from 1863, the subenvironment of Core 5 was Land (Figures 88, 89 and 123, 124).

5.3 Foraminiferal and Map Data Results

The previous two result subsections described what the Foraminifera data revealed and what the Map data revealed. In this segment, the results from both sections are compared. While the depths in the core samples were analyzed for Foraminifera content in small increments, the amount of time between each depth (sample) was still quite large. Every two centimeters corresponded to nearly twelve years. Therefore, when comparing the chronoequivalent change in subenvironments that the Foraminifera data produced, to the change in subenvironments that the Map data produced, through time, it was necessary to correct for the small discrepancies that appeared between the map and Foraminiferal sample intervals.

Maps were not produced for each year, so maps from every decade were analyzed. As the depths in the cores represented earlier time periods, maps were not as plentiful. Therefore, maps from every other decade (where possible) were assessed before the year 1900. Additionally, because the oldest map that was used in this study was from 1730, there was no basis for comparison with Foraminifera data before this time. In many cases, due to the high sedimentation rate, the resolution in the cores, and the inaccessibility of maps, the Foraminifera data represented a year where no map existed. To account for this difference, running averages were calculated for the Foraminifera data to obtain an average environment for three decades. The average was rounded to the nearest whole number, and then the average value was compared to the environment of the map that was closest in age. The elevation depicted from the maps was then subtracted from the Foraminifera environment in order to see the difference in environments from the two methods (if any difference existed: Tables 25 and 26). Table

25 is the difference from the nonfiltered Foraminifera and Map data, while Table 26 is the difference between the filtered Foraminifera data and Map data. The contrasting environments are shown by the elevation differences in meters. Any elevation difference greater than 1 or less than -1 are highlighted, because values greater than those thresholds indicated two dissimilar environments with respect to elevation. For example, if one method showed that the subenvironment of a core at a certain time was an Estuary (-1 meters relative to MSL: Table 5), while the other method showed the subenvironment was an Extreme High marsh (1.25 meters above sea-level: Table 5), then the difference in elevation would be -2.25 meters.

For the non-filtered Foraminifera data, 49 of the 90 elevation differences (54%), were greater than 1 or -1, indicating that more than half of the environments from the Foraminifera data did not match results from the Map data (Table 25). In Table 26, the filtered Foraminifera data, only 16 of the 47 elevation differences (34%), were greater than 1 or -1. In this case, less than half of the subenvironments depicted by the Foraminifera analysis were significantly different than the subenvironments yielded from the Map data. There are two additional ways to portray this data (Figures 29-39). Figures 29-33 are graphs that depict the location of each core's subenvironment through time, using the non-filtered Foraminifera data and the Map data, while Figures 34 and 35 show the same information as Figures 29-33, but with the filtered Foraminifera data. In some cases, the non-filtered and filtered data (as in Cores 3, 4 and 5) yielded the same map for each core, and are therefore only shown once (Figures 31-33). Figures 36-40 incorporate both the maps with the boundaries, and the Foraminifera data.

In 2013, the subenvironment of Core 1 started in the High marsh subenvironment (Figure 29, 34, and 36). From 1970-1990, Core 1 changed subenvironment from the High marsh to the Extreme High marsh, and then shifted to the Intermediate marsh subenvironment in the 1960s. Core 1 stayed in the Intermediate marsh subenvironment until about 1880. From 1730-1880, the Foraminifera data showed that the subenvironment for Core 1 was either an Extreme High marsh, an Intermediate marsh, the Extreme Low marsh.

In contrast, the maps indicated a different change in Core 1's subenvironments through time. The map from 2013 indicated that Core 1 was located in a Low marsh subenvironment, which already differed from what the Foraminifera data revealed. Around 1970, the subenvironment of Core 1 shifted to Land and remained on Land from 1770-1970, with one inconsistency. At 1865, one map revealed that the subenvironment of Core 1 was a High marsh. From 1730-1780 the subenvironment of Core 1 was an Intermediate marsh. The map depicting Fort Fisher at 1730 was the oldest map that was analyzed, and therefore was the last year the Foraminifera data and Map data were compared.

Figures 30, 35, and 37 illustrated that in 2013, the subenvironment of Core 2 was located in the High marsh. Through the years, Core 2 mainly stayed in the Extreme High marsh subenvironment, however there are four exceptions. According to the Foraminifera data, Core 2's subenvironment shifted from the Extreme High marsh to the Intermediate marsh at the years 1750, 1800, 1850, and 1990-2000.

The Map data for Core 2 (Figures 30, 35 and 37) indicated that the subenvironment of Core 2 in 2013 was located in the High marsh subenvironment, which

matched the Foraminifera data. From 1975-2013, the subenvironment of Core 2 stayed as a High marsh. At 1975 the subenvironment of Core 1 shifted to the Intermediate marsh. From 1865-1950, the maps revealed that the subenvironment of Core 2 was Land. Prior to 1865, depending upon the map, the subenvironment of Core 2 was either Land, a Low marsh or an Estuary. During this time (1865-1950), the Foraminifera method showed that the subenvironment of Core 2 was an Intermediate marsh. After 1865, the Map method revealed that the subenvironment Core 2 was Land from 1780 to 1864, when the subenvironment of Core 2 changed to an Intermediate marsh. From 1730-1780, the subenvironment of Core 2 remained as an Intermediate marsh, which is consistent with the Foraminifera data.

Core 3 (Figure 31 and Figure 38), showed the non-filtered Pearson values and the filtered Pearson values for the Foraminifera data because the filtered data produced the same results as the non-filtered Foraminifera data. Only four depths were analyzed for Foraminifera content in Core 3, so only four data points are shown for this method. Core 3 exhibited similar changes in subenvironments as observed in Core 1. In 2013, Core 3 started in the High marsh subenvironment, and at about 1895, the subenvironment of Core 3 shifted to the Extreme Low marsh subenvironment. The year of 1895 was the oldest year recorded for Core 3.

The Map method revealed similar yet differing results to the Foraminifera data for Core 3. In 2013, according to the Map data, the subenvironment of Core 3 was the High marsh. At about 1970, the maps revealed that Core 3 shifted subenvironments, indicating the area was Land, which differed from the Foraminifera data. The maps indicated that the subenvironment of Core 3 was Land from 1870-1950. At 1865, the maps (depending

on which map) indicated that the subenvironment of Core 3 was either the Estuary (Deep) (Figures 114, 119 and 121), or Land (Figures 115-118 and 120). From 1780-1865, the maps revealed that Core 3's subenvironment was on Land. From 1730-1780, the subenvironment of Core 3 remained in an Intermediate marsh, which differed from the results of the Foraminifera method. The Foraminifera method indicated that in the 1770s, the subenvironment of Core 3 was an Extreme Low marsh (Figures 31 and 37).

Only two depths were analyzed for Foraminifera content in Core 4 (Figures 32 and 39), and only one data point was shown, because the other data point corresponded to a year that was older than the oldest map. Additionally, as with Core 3, the non-filtered Pearson values and the filtered Pearson values for the Foraminifera data produced the same results, and therefore, only one figure for Core 4 was created (Figure 32).

According to this single point, in 1780, the subenvironment of Core 4 was the Extreme High marsh. No extrapolations can be made based on this data point, so no further results can be obtained for this core using this method.

The Map data of 1780 indicated that the subenvironment of Core 4 was Land rather than the High marsh subenvironment. The map indicated that for Core 4 the subenvironment in 2013 was Land and remained on land from 1865-2013. The only shift in Core 4's subenvironment during 1865-2013 was in the year 1975, when the Land subenvironment shifted to the Intermediate marsh. The maps during the year 1865 produced differing results for the subenvironments of Core 4. Figures 115-120 indicated that the subenvironment of Core 4 was Land. On the other hand, Figure 114 showed the subenvironment of Core 4 was in the Estuary and Figure 121 showed that the subenvironment of Core 4 was Marsh. From 1780-1865, the maps revealed that the

subenvironment of Core 4 was Land. At 1780, the map showed that the subenvironment of Core 4 changed to an Intermediate marsh. Core 4 remained in an Intermediate marsh subenvironment from 1730-1780.

Only three depths were analyzed for Foraminifera content in Core 5 (Figure 33 and Figure 40). However, only two data points are shown for this method, because the third data point corresponded to a year that was older than the year of the oldest map. Additionally, as with Cores 3 and 4, one figure was created for Core 5 (Figure 33). According to the Foraminifera data (the two points), the subenvironment of Core 5 was located in the Extreme Low marsh between the years 1780-1900. No extrapolations can be made based on these data points, so no further results can be obtained for this core using this method.

The Map data at year the 1780 indicated that the subenvironment of Core 5 was Land rather than High marsh. Comprehensively comparing the subenvironmental shifts indicated by the maps, the shift of subenvironments through time of Core 5 is extremely similar to the changes in subenvironments seen in Core 4. In 2013, the subenvironment of Core 5 was depicted as Land and remained on Land from 1865-2013, with one exception. The one exception was the shift in subenvironments of Core 5 at 1975, where the subenvironment shifted from Land to the Intermediate marsh. The maps indicated that the subenvironment of Core 5 during 1865 (depending upon the map) was either the Estuary (Figure 121), Marsh (Figures 114 and 116-118), or Land (Figures 115 and 119-120). Prior to 1865 (from 1770-1860), the maps revealed that the subenvironment of Core 5 was Land. From 1733-1770, the subenvironments of Core 5 shifted to an Intermediate marsh. Core 5 remained in an Intermediate marsh back to the year 1730.

An interesting pattern emerged for all of the cores. From 1733 to 1770, the subenvironments for each of the cores were identical. In all cases, the subenvironments of the cores before 1770 shifted to the Intermediate marsh. Additionally, it is important to mention that only three of the eight 1865 subenvironment values that were created from georeferencing were plotted on the graphs in Figures 29-35. These three values depict Fort Fisher at different times of the year and correspond to Figure 115, Figure 120, and Figures 114, 116-119 and 121. Figure 120 was of January 14, 1865; Figure 115 depicted Fort Fisher at February, 1865; Figures 114, 116-119 and 121, depicted Fort Fisher at January 15, 1865. The maps that depicted Fort Fisher on January 15, 1865 were averaged to create one value (the last of the three) that was plotted on the graph in Figures 29-35.

These next two paragraphs will discuss the filtered Foraminifera results (Figure 34 and Figure 35). In 2013, the location of Core 1 was in the High marsh (Figure 34). From 1970-1990, the subenvironment of Core 1 changed from the High marsh to the Extreme High marsh, and then shifted again to the Intermediate marsh subenvironment in the 1960s. From 1880-1960, Core 1 stayed in the Intermediate marsh subenvironment. The year 1880 was the last data point for the filtered Pearson values analyzed for Core 1. This progression, a High Marsh transforming to an Extreme Low marsh down core, is indicative of a regression.

The Map data yielded a dissimilar set of results compared to the Foraminifera data. According to the maps, in 2013, Core 1 was located in a Low marsh subenvironment, and then around 1970, the subenvironment of Core 1 shifted to Land. Core 1 was on the land from 1970-1865, when a shift back to the High marsh subenvironment can be seen. From 1780-1865, the subenvironment of Core 1 was Land,

and from 1730-1780, according to the maps, Core 1 shifted subenvironments to an Intermediate marsh. In 2013, Core 2 was located in the High marsh subenvironment (Figure 35). Through the years, Core 2 mainly stayed in the Extreme High marsh subenvironment, with two exceptions. According to the Foraminifera data, the subenvironment of Core 2 changed from the Extreme High marsh subenvironment to an Intermediate marsh subenvironment in 1850 and 1990.

Relating the subenvironmental shifts indicated by the Foraminifera, in 2013, the Map data indicated that the area of Core 2 was in the High marsh subenvironment (Figure 35). From 1975-2013, Core 2 was depicted as being a High marsh subenvironment, when it shifted to the Intermediate marsh at 1975. In 1950 the map method revealed that the subenvironment of Core 2 was Land, and remained on land from 1865-1950. At the depth representing 1865, the maps revealed that the subenvironment of Core 2 was also Land (Figures 114-121). In comparison, during this time (1865-1950), the Foraminifera method showed that the subenvironment of Core 2 was located in an Intermediate marsh. From 1780-1865, the maps revealed that the subenvironment of Core 2 was Land. In 1780, the subenvironment of Core 2 changed to an Intermediate marsh, and remained in an Intermediate marsh subenvironment from 1730 to 1770. This agrees with the results of the Foraminifera data.

5.4 Fort Fisher in 1865

The year 1865 is extremely important in North Carolina's history because it marked the end of the Civil War. Fort Fisher, which was built in 1861, was a Confederate base until January 15, 1865 when the fort was captured by Union forces. This marked a turning point in the war, as this was one of the last major forts that Confederate forces controlled.

Thus, to validate historians' accounts of the battles that occurred before and on that day, multiple maps depicting Fort Fisher in 1865 were analyzed and compared to the Foraminifera data (Figures 41-45). Two graphs with different y-axes can be seen in these figures. On the first graph, the left-hand side of the figure shows the core's subenvironment between the years 1860 and 1872. Two values at 1863 are shown on these graphs to represent the error arising from georeferencing a hand-drawn map from 150+ years ago. The link points and the order of the link points that were used to georeference the image/map directly impacted the location of the cores on the map (Figures 88-89 and 123-124). The second graph, on the right-hand side of the figure, is of January 15, 1865 with the hour of day on the y-axis. In Figures 42, 43 and 45, the two 1863 maps produced identical results for the subenvironments for the cores each figure depicts and therefore do not show conflicting information. In Figure 41 and Figure 44 this is not case.

Figure 41 showed that for Core 1, the Foraminifera data differs from the Map data. According the graph on the right in Figure 41, the Foraminifera data indicated that the subenvironment of Core 1 shifted to the High marsh in 1860, from the Extreme Low marsh subenvironment in 1872. This shift in subenvironments signifies a transgression.

On the other hand, the Map data indicated that the subenvironment of Core 1 shifted from Land to the High marsh subenvironment prior to 1865, which signifies the opposite trend, a regression. The graph on the right of Figure 41 focused on January 15, 1865 because of its significance during the battle. All the maps from that day indicated that the subenvironment of Core 1 was land.

Figure 42 showed that for Core 2, the Foraminifera data again differs from the Map data. According the graph on the right in Figure 42, the Foraminifera data indicated that the subenvironment of Core 2 remained in the Extreme High marsh from 1860-1872. On the other hand, the Map data revealed a shift in subenvironments from 1863-1865 from the Land to the High marsh to the Estuary subenvironment, which signifies a regression. The graph on the right in Figure 42 also focuses on January 15, 1865. All the maps from that day indicated that the subenvironment of Core 2, as with Core 1, was Land.

Figure 43 showed that no Foraminifera data existed for Core 3 between the years 1860-1872 because no samples taken in Core 3 corresponded to those years. The Map data however, revealed that Core 3's subenvironment was Land from 1865-1870. During 1865, depending upon the maps, the subenvironment of Core 3 was either Land or Marsh. The subenvironment shifted from the Land to the Low marsh subenvironment in 1865 to the Estuary subenvironment in 1863. This trend signifies a regression.

The graph on the right of Figure 43 focused on January 15, 1865. The maps from that day depicted different subenvironments for Core 3. Maps portraying battles at 3 P.M., 6 P.M., and 9 P.M. showed that the subenvironment of Core 3 was Land (Figures

116-118), while the other maps depicting Fort Fisher at midnight and noon respectively, showed that Core 3 was in the Estuary (Deep) subenvironment (Figure 114 and 121).

As in Figure 123, no Foraminifera data existed for Core 4 (Figure 44) between the years 1860-1872, for the exact reason as before. No samples that were taken in Core 4 corresponded to those years. The map data revealed that from 1865-1970, the subenvironment shifted from the Land to the Low marsh subenvironment to the Estuary (Deep) subenvironment. This signifies a regression.

The maps of January 15, 1865, depicted different subenvironments for the location of Core 4. The maps indicating battles at 3 P.M., 6 P.M., and 9 P.M. show that the subenvironment of Core 4 was Land (Figures 116-118), while the two other maps depicting Fort Fisher at midnight, show that the subenvironment of Core 4 was Estuary (Deep) subenvironment (Figure 114).

Core 5 (Figure 45), is similar to Core 3 and Core 4 in that the samples that were analyzed for Foraminifera content in Core 5 did not correspond to the 1860-1872 time period. Therefore, only the Map data is shown. From 1865-1870, the subenvironment of Core 5 was Land. During 1865, depending upon the map, the subenvironment of Core 5 was either Land, Estuary, or Low marsh.

The graph to the right in Figure 45 also focused on January 15, 1865. Maps from that day again depict different subenvironments for Core 5. Maps indicating the battles at 3 P.M., 6 P.M. and 9 P.M. showed that the subenvironment of Core 5 was an Intermediate marsh (Figures 114 and 116-118) while the other maps showing Fort Fisher at midnight and noon respectively, showed that the subenvironment of Core 5 was either Land (Figures 115 and 119), or Estuary (Deep) (Figure 121).

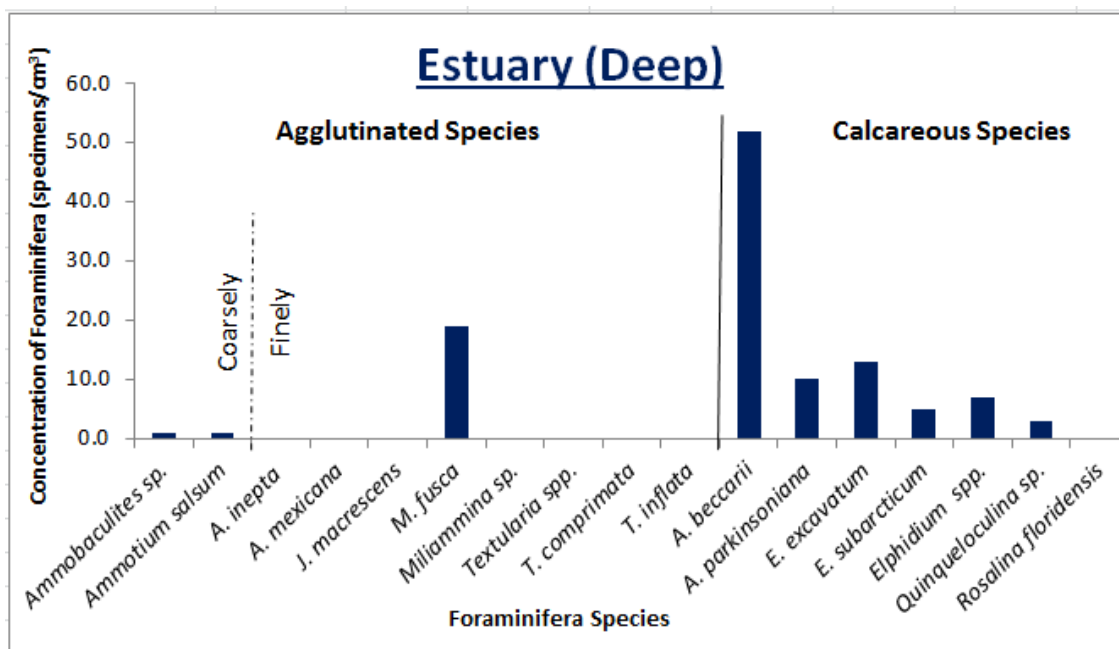


FIGURE 11: The concentration of the Foraminifera species that were found in the Estuary (Deep) subenvironment. The name of the Foraminifera species is shown on the x-axis, while the Foraminifera concentration is on the y-axis. The figure is divided into two categories: calcareous species and agglutinated species with the agglutinated species being subcategorized into coarsely-agglutinated and finely-agglutinated taxa.

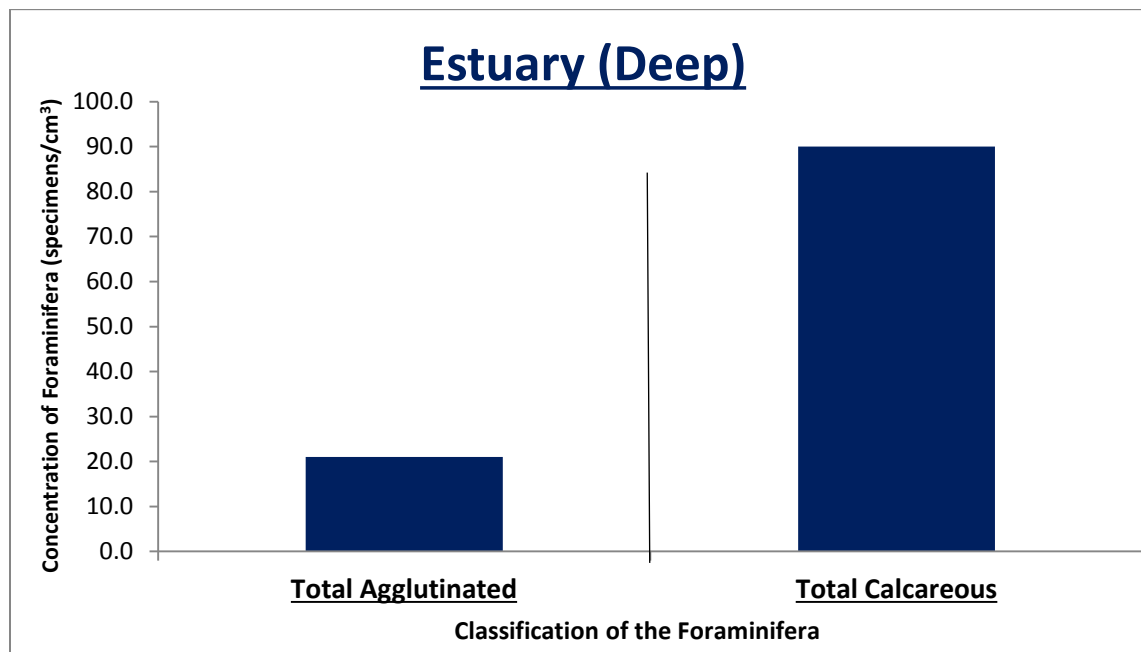


FIGURE 12: The total concentration of the agglutinated and calcareous species that were present in the Estuary (Deep) subenvironment. The Foraminifera taxa are shown on the x-axis, while the Foraminifera concentration is on the y-axis.

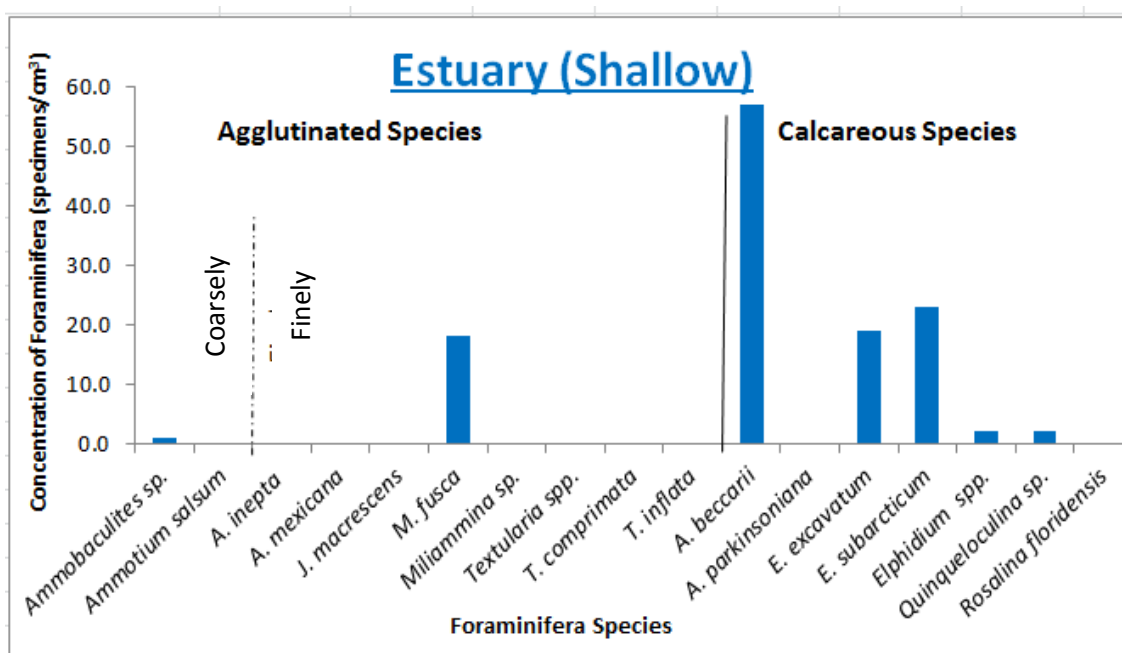


FIGURE 13: The concentration of the Foraminifera species that were found in the Estuary (Shallow) subenvironment. The name of the Foraminifera species is shown on the x-axis, while the Foraminifera concentration is on the y-axis. The figure is divided into two categories: calcareous species and agglutinated species, with the agglutinated species being subcategorized into coarsely-agglutinated and finely-agglutinated taxa.

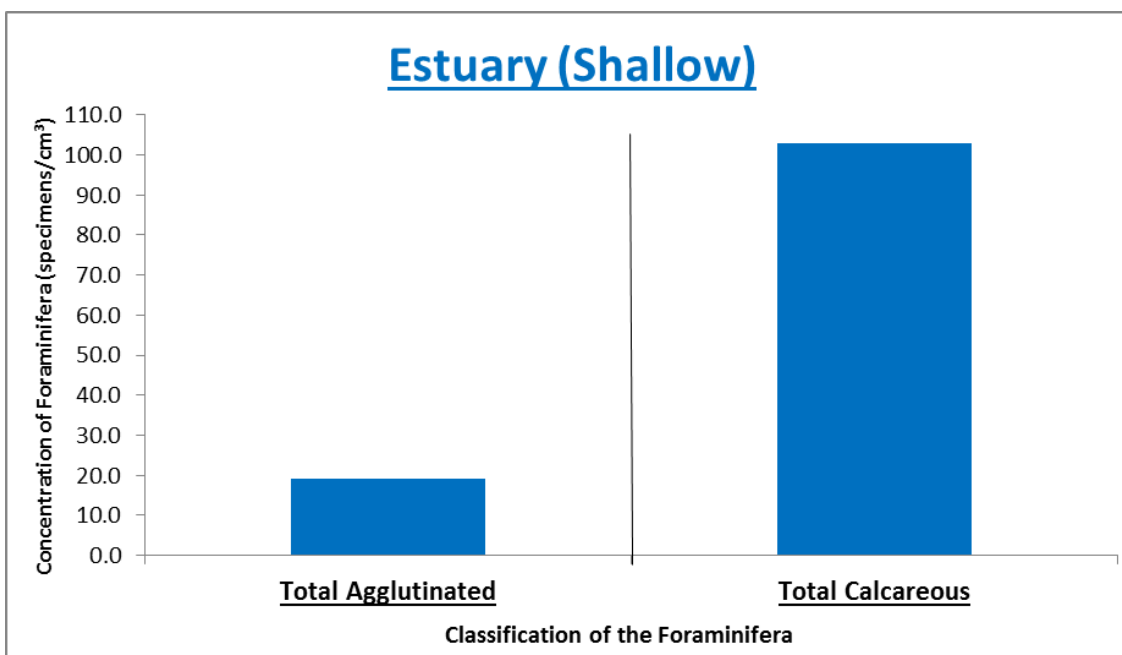


FIGURE 14: The total concentration of the agglutinated and calcareous species that were present in the Estuary Shallow subenvironment. The Foraminifera taxa are shown on the x-axis, while the Foraminifera concentration is on the y-axis.

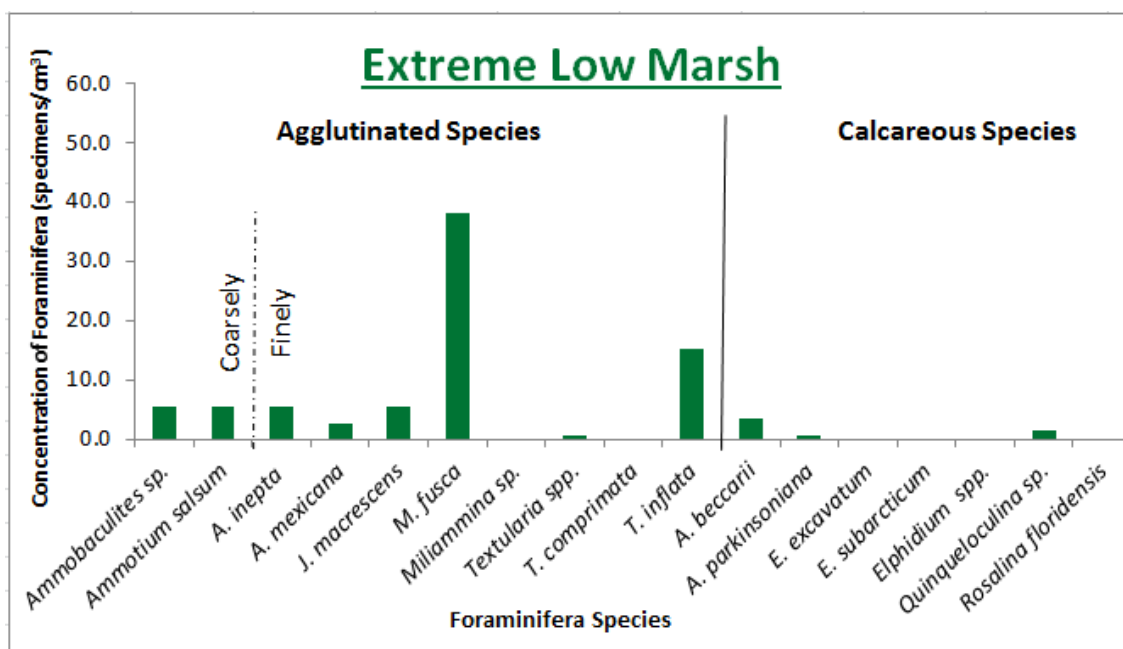


FIGURE 15: The concentrations of the Foraminifera species that were found in the Extreme Low Marsh subenvironment. The name of the Foraminifera species is shown on the x-axis, while the Foraminifera concentration is on the y-axis. The figure is broken into two categories: calcareous species and agglutinated species with the agglutinated species being subcategorized into coarsely-agglutinated and finely-agglutinated taxa.

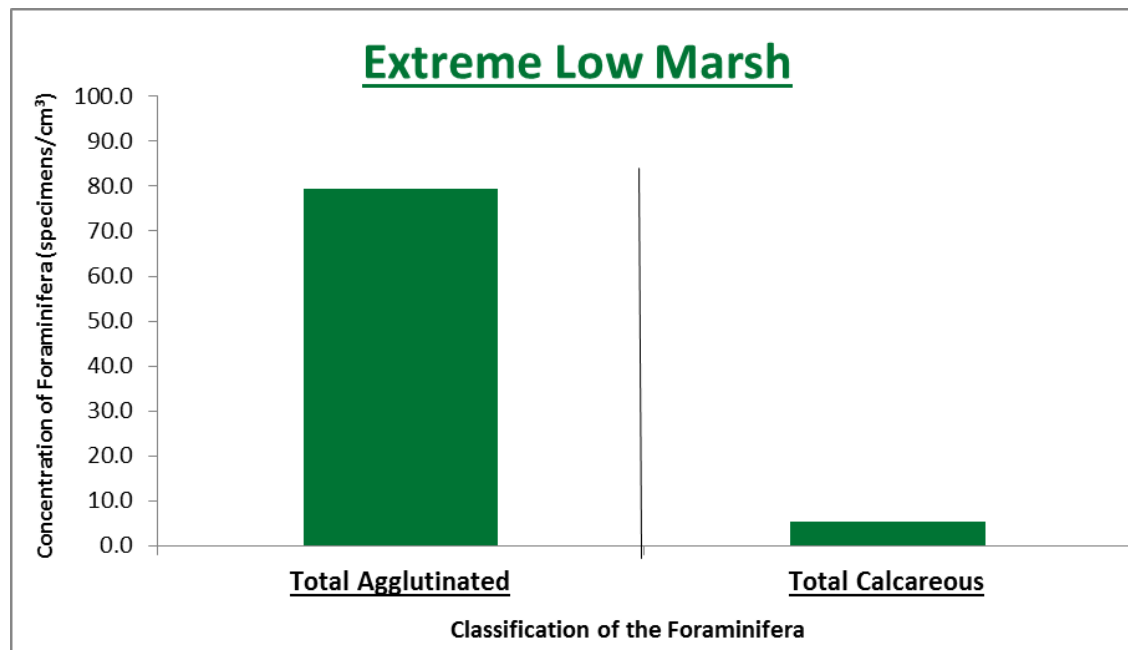


FIGURE 16: The total concentration of the agglutinated and calcareous species that were present in the Extreme Low Marsh subenvironment. The Foraminifera taxa are shown on the x-axis, while the Foraminifera concentration is on the y-axis.

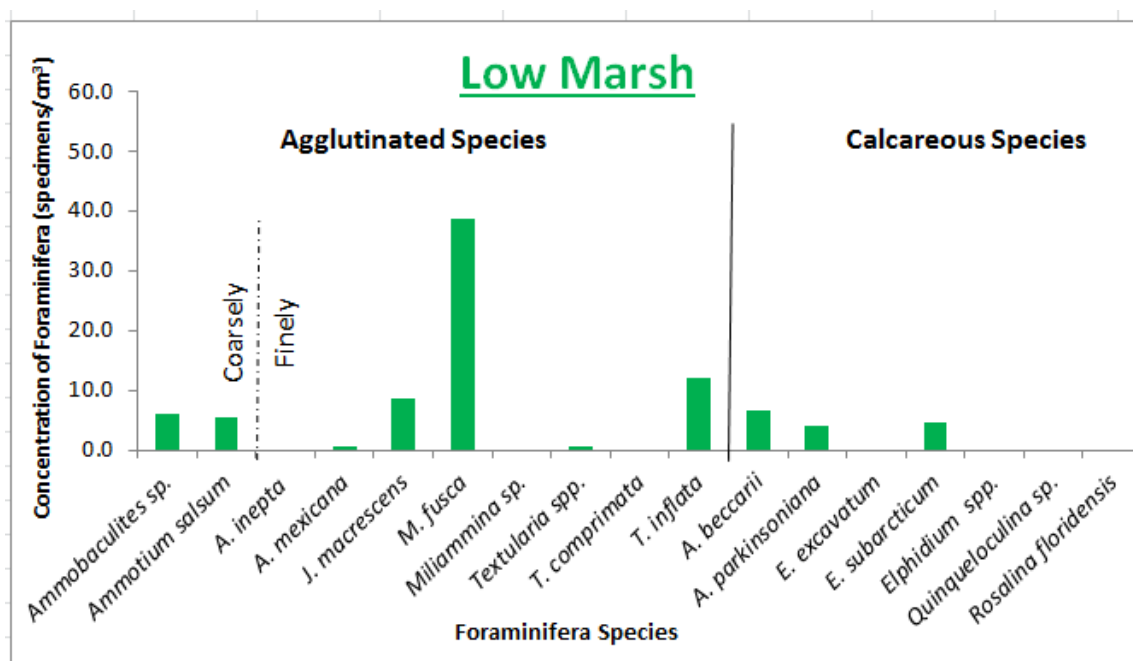


FIGURE 17: The concentration of the Foraminifera species that were found in the Low Marsh subenvironment. The name of the Foraminifera species is shown on the x-axis, while the Foraminifera concentration is on the y-axis. The figure is broken into two categories: calcareous species and agglutinated species with the agglutinated species being subcategorized into coarsely-agglutinated and finely-agglutinated taxa.

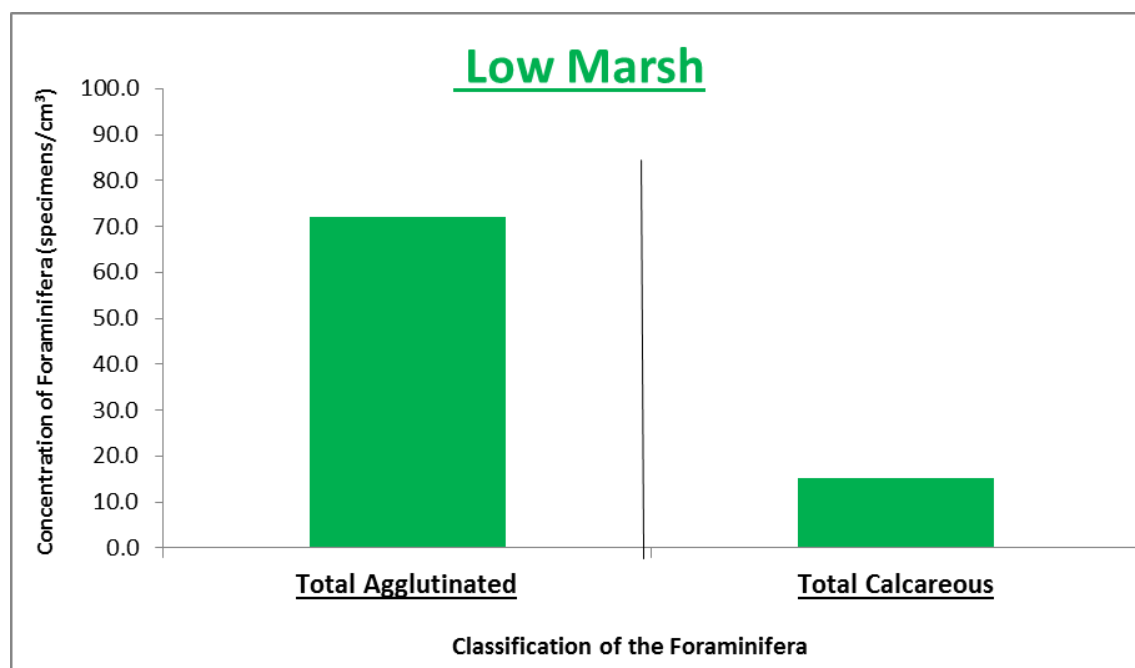


FIGURE 18: The total concentration of the agglutinated and calcareous species that were present in the Low Marsh subenvironment. The Foraminifera taxa are shown on the x-axis, while the Foraminifera concentration is on the y-axis.

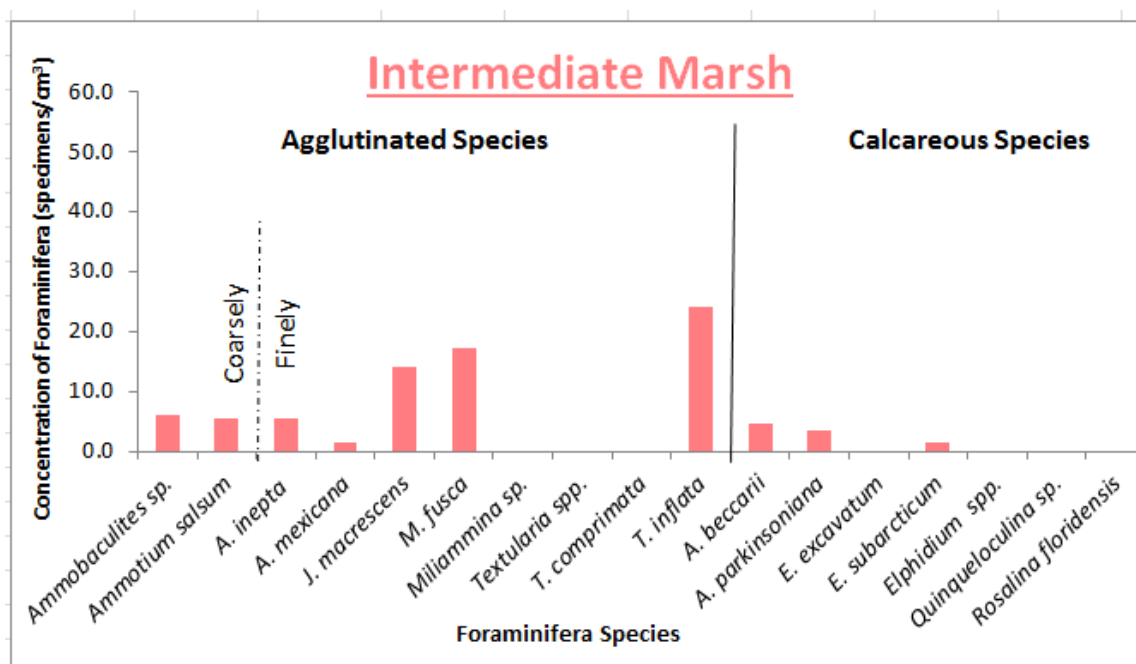


FIGURE 19: The concentration of the Foraminifera species that were found in the Intermediate Marsh subenvironment. The name of the Foraminifera species is shown on the x-axis, while the Foraminifera concentration is on the y-axis. The figure is broken into two categories: calcareous species and agglutinated species with the agglutinated species being subcategorized into coarsely-agglutinated and finely-agglutinated taxa.

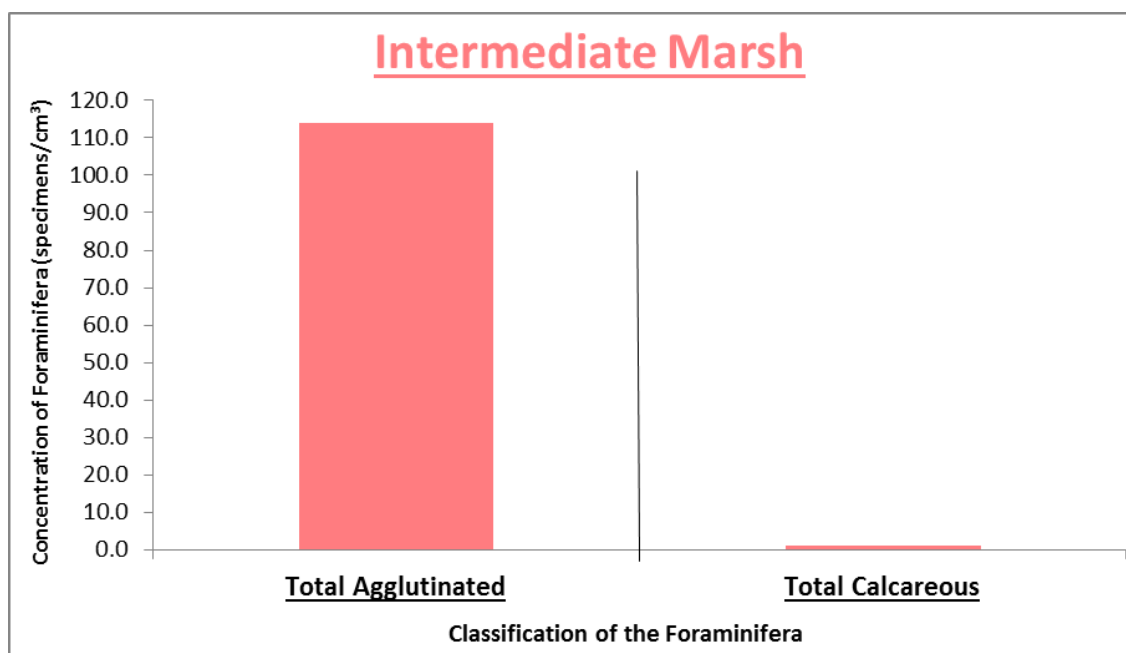


FIGURE 20: The total concentration of the agglutinated and calcareous species that were present in the Intermediate Marsh subenvironment. The Foraminifera taxa are shown on the x-axis, while the Foraminifera concentration is on the y-axis.

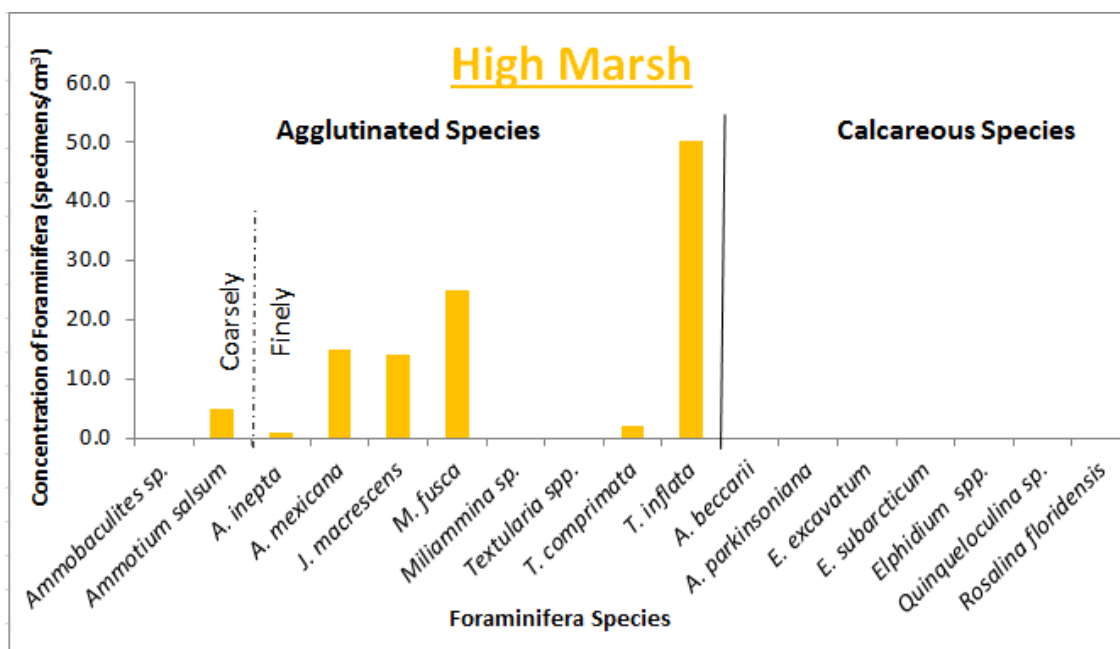


FIGURE 21: The concentration of the Foraminifera species that were found in the High Marsh subenvironment. The name of the Foraminifera species is shown on the x-axis, while the Foraminifera concentration is on the y-axis. The figure is broken into two categories: calcareous species and agglutinated species with agglutinated species being subcategorized into coarsely-agglutinated and finely-agglutinated taxa.

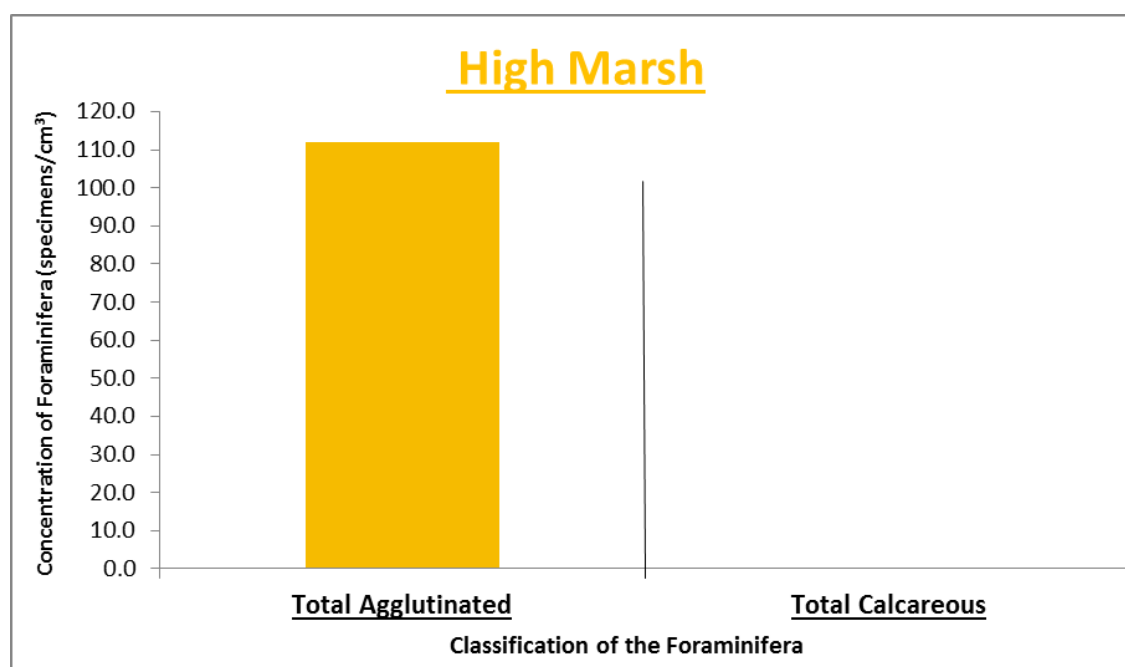


FIGURE 22: The total concentration of the agglutinated and calcareous species that were present in the High Marsh subenvironment. The Foraminifera taxa are shown on the x-axis and the Foraminifera concentration on the y-axis.

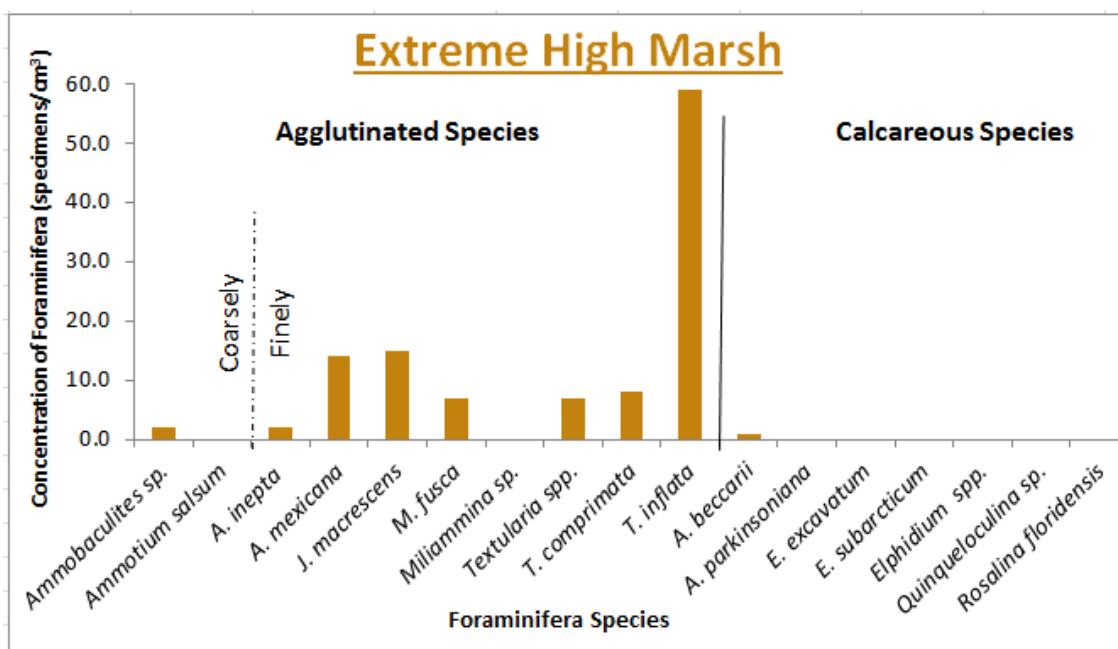


FIGURE 23: The concentration of the Foraminifera species that were found in the Extreme High Marsh subenvironment. The name of the Foraminifera species is shown on the x-axis, while the Foraminifera concentration is on the y-axis. The figure is broken into two categories: calcareous species and agglutinated species with agglutinated species being subcategorized into coarsely-agglutinated and finely-agglutinated taxa.

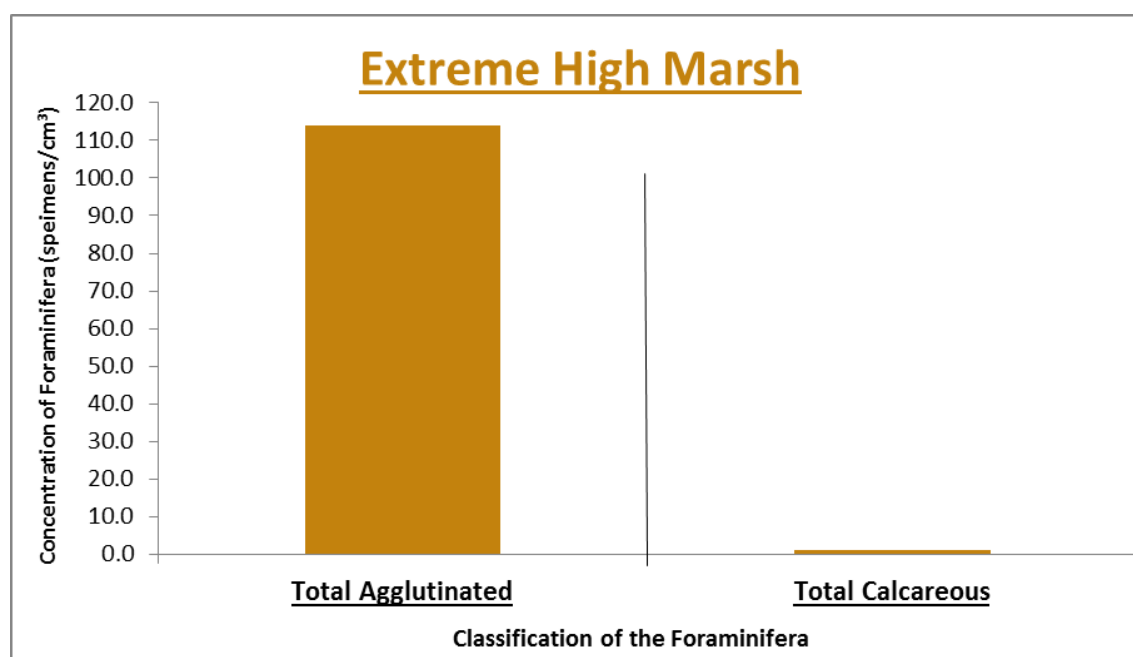


FIGURE 24: The total concentration of the agglutinated and calcareous species that were present in the Extreme High Marsh subenvironment. The Foraminifera taxa are shown on the x-axis and the Foraminifera concentration on the y-axis.

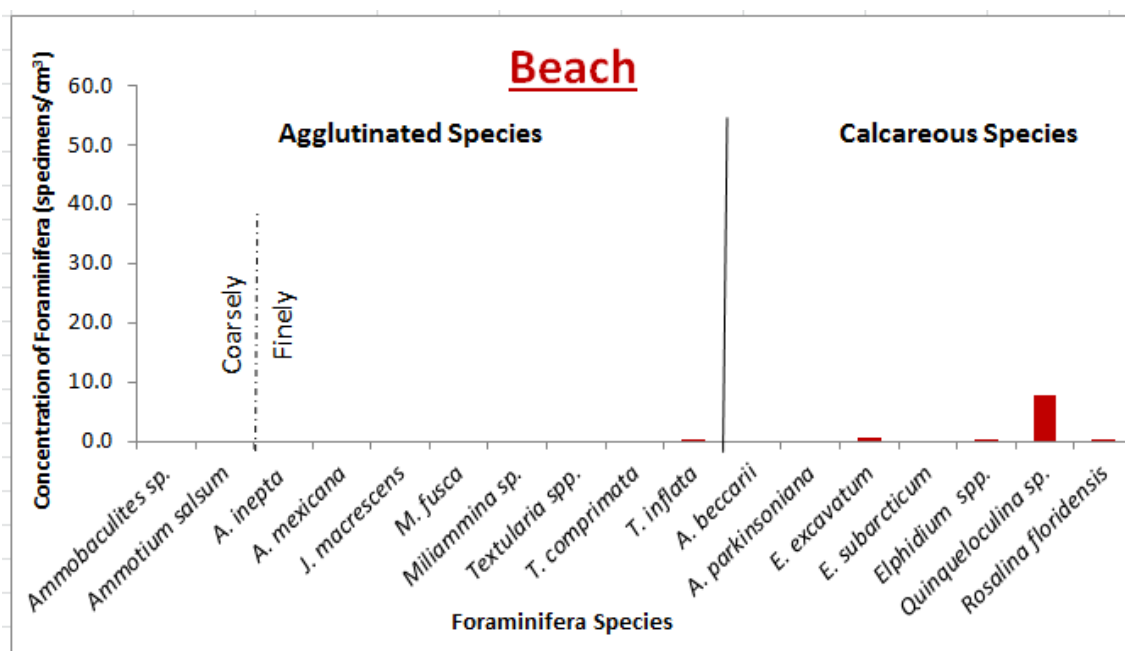


FIGURE 25: The concentration of the Foraminifera species that were found in the Beach subenvironment. The name of the Foraminifera species is shown on the x-axis, while the Foraminifera concentration is on the y-axis. The figure is broken into two categories: calcareous species and agglutinated species with agglutinated species being subcategorized into coarsely- agglutinated and finely- agglutinated taxa.

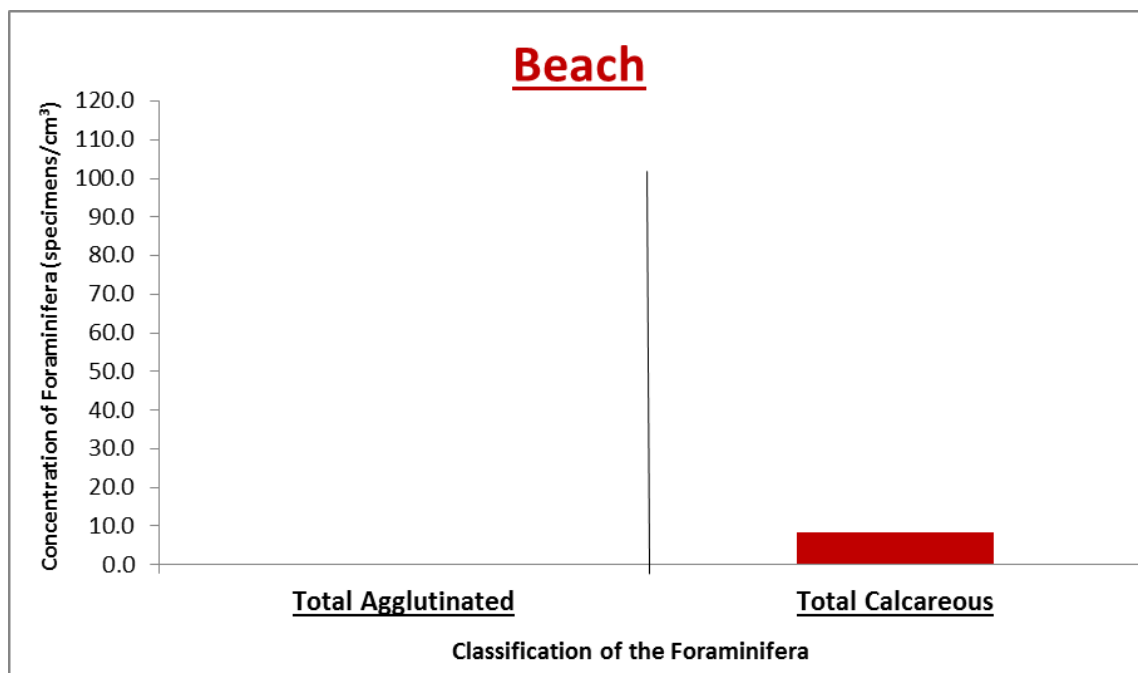


FIGURE 26: The total concentration of the agglutinated and calcareous species that were present in the Beach subenvironment. The Foraminifera taxa are shown on the x-axis and the Foraminifera concentration on the y-axis.

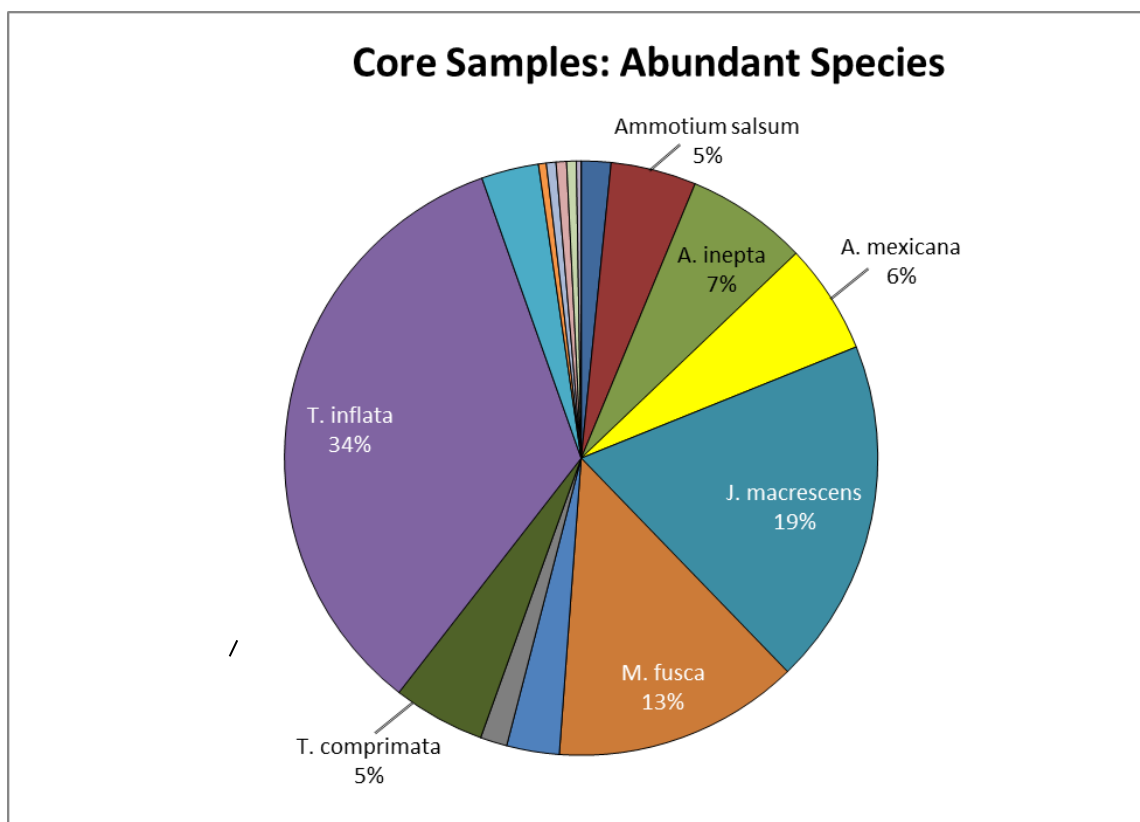


FIGURE 27: A Pie chart showing the total percentage of the different Foraminifera species that were found in the all of the core samples. Seventeen different species were found within the core samples. The data shown in this pie chart was normalized first in order to account for the differences in the volume of sediment used.

TABLE 7: Normalized data for Core 1 shows the Foraminifera species and the total number of Foraminifera species that were found while completing the lab work. The values under the Composite data column are depths below the surface and are in centimeters. The bolded values at the bottom and right side are composite totals.

Depth (cm)	Agglutinated Species									Calcareous Species						Totals				
Composite data	<i>Ammobaculites</i> sp.	<i>Ammobaculum salinarum</i>	<i>A. inepta</i>	<i>A. mexicana</i>	<i>A. macrescens</i>	<i>A. fovei</i>	<i>Miliammina</i> sp.	<i>Tertularia</i>	<i>T. compressa</i>	<i>T. inflata</i>	<i>A. beccarii</i>	<i>A. parkinsoniana</i>	<i>E. excavatum</i>	<i>E. subarcticum</i>	<i>Elphidium</i> spp.	<i>Quinqueloculina</i> sp.	<i>Rosalina floridensis</i>	Total Agglutinated	Total Calcareous	Total Foraminifers
Surface		1.0	8.0	31.0	25.0	18.0			5.0	53.0								141.0	0.0	141.0
2	0.5		0.5	6.5	1.5	3.0			1.5	34.5								60.0	0.0	60.0
4			3.0	24.0	3.0	12.0				71.0								119.0	0.0	119.0
6			7.0	32.0	4.0	14.0			3.0	58.0								118.0	0.0	118.0
8			6.0	17.0	4.0	8.0			2.0	26.0								63.0	0.0	63.0
10			4.0	5.0	27.0				1.0	13.0								50.0	0.0	50.0
12			15.3	2.7	12.0	10.0			1.3	25.3								66.7	0.0	66.7
14	1.5		20.5	7.0	13.0	6.5			2.5	12.0	1.0		0.5					63.0	1.5	64.5
16			27.0	15.0	30.0	10.0			7.0	13.0								102.0	0.0	102.0
18			36.7	0.7	22.7	3.3			1.3	3.3								68.0	0.0	68.0
20			11.5	1.0	21.5	8.5			0.5	6.0								43.0	0.0	43.0
22	1.3		8.7	3.3	14.0	4.0			3.3	3.3								38.0	0.0	38.0
24			3.3		2.0	5.3				1.3								12.0	0.0	12.0
26	4.7		2.7	6.0	2.0	4.0			0.7	6.0								26.0	0.0	26.0
28			0.7	0.7	0.7	2.0				0.7								4.7	0.0	4.7
30			1.0	1.0		1.5												3.5	0.0	3.5
32	0.5	2.0				1.5				0.5				0.5				4.5	0.5	5.0
34			0.5	0.5	0.5	2.0				4.0								7.5	0.0	7.5
36	0.5	1.0	0.5		2.0	4.0				3.5								11.5	0.0	11.5
38			0.7		0.7	1.3				1.3								4.0	0.0	4.0
40			1.0		0.3	1.3				0.7								3.3	0.0	3.3
42					0.4	0.8				4.0								5.2	0.0	5.2
44			3.0	1.0	0.5	1.0				0.5								6.0	0.0	6.0
46			0.5		2.0	2.0				1.0								5.5	0.0	5.5
48			0.7		0.7	3.3												4.7	0.0	4.7
50			1.0															1.0	0.0	1.0
52		1.5	4.0	2.0		3.0				1.0					1.0			11.5	1.0	12.5
54		0.5	2.0	0.5	0.5	2.0				0.5								6.0	0.0	6.0
56			3.0			3.0												12.0	0.0	12.0
58		4.0			1.0	3.0			0.5									14.5	0.0	14.5
60	3.0	8.0	3.0		3.0	4.0												21.0	0.0	21.0
62	1.0	4.7	12.7		1.0	2.3		0.7	0.3						0.3			22.7	0.3	23.0
64	0.5	5.0	13.5		0.5	2.5		2.5	1.0									25.5	0.0	25.5
66	1.0	15.0	14.0					5.0										35.0	0.0	35.0
68	2.0	10.0	8.7		0.7	8.7		3.3							1.3			33.3	1.3	34.7
70	1.3	10.7	2.0	0.7		7.3	1.3	2.0		1.3	0.7							26.7	0.7	27.3
72	6.0	10.0	5.3		0.7	14.7		0.7										37.3	0.0	37.3
74	1.0	26.0			1.0	5.0					1.0	1.0			1.0			33.0	2.0	35.0
76		1.0				2.0					1.0							3.0	1.0	4.0
78					4.0	2.0	2.0											8.0	0.0	8.0
80		4.0	1.0	1.0		2.0	1.0					1.0				3.0		3.0	4.0	13.0
82	6.0	10.0				4.0		2.0				2.0						22.0	2.0	24.0
84										1.0								1.0	0.0	1.0
86	1.0	2.0	2.0			5.0				1.0	4.0					2.0		11.0	6.0	17.0
88			1.0	1.0		1.0				2.0		1.0						5.0	1.0	6.0
90			2.0			1.0				2.0								5.0	0.0	5.0
92	2.0	5.0	1.0			7.0						1.0						15.0	1.0	16.0
94	2.0	3.0	1.0		1.0	1.0						1.0				2.0		8.0	3.0	11.0
96	1.0	7.0	3.0	1.0		5.0	1.0		1.0		2.0							19.0	2.0	21.0
98	3.0	5.0	1.0			2.0												11.0	0.0	11.0
100		6.7	3.3	1.3	2.0	8.0				1.3								22.7	0.0	22.7
102		4.0	6.0		4.0	6.0												20.0	0.0	20.0
104	8.0	6.0	8.0			6.0												30.0	0.0	30.0
106	4.0	2.0		2.0		4.0		2.0		2.0								16.0	0.0	16.0
108	2.0	6.0	2.0		2.0	12.0	2.0	2.0							6.0			28.0	6.0	34.0
110		8.0	6.0		4.0	6.0		2.0							2.0			26.0	2.0	28.0
112	2.0	16.0				4.0		2.0		2.0								26.0	0.0	26.0
114		12.0			2.0	8.0		2.0										24.0	0.0	24.0
116		14.0			2.0	10.0	4.0											30.0	0.0	30.0
118		8.0				4.0									2.0			12.0	2.0	14.0
120		6.0			1.0	5.0		1.0							1.0			13.0	1.0	14.0
122	4.0	16.0				4.0												24.0	0.0	24.0
124	1.0	2.0		1.0		3.0												7.0	0.0	7.0
	60.8	243.0	275.2	164.8	221.7	315.0	11.3	31.2	32.0	356.2	8.7	7.0		1.0	13.7	2.0		1711.2	38.3	1749.5

TABLE 8: Normalized data for Core 2 shows the Foraminifera species and the total number of Foraminifera species that were found while completing the lab work. The values under the Composite data column are depths below the surface and are in centimeters. The bolded values at the bottom and right side are composite totals.

Depth (cm)	Agglutinated Species										Calcareous Species						Totals			
Composite data	<i>Ammonoculites</i> sp.	<i>Ammonotium salinum</i>	<i>A. hepta</i>	<i>A. mexicana</i>	<i>J. macrescens</i>	<i>M. fusca</i>	<i>Millammina</i> sp.	<i>Textularia</i>	<i>T. comprimata</i>	<i>T. inflata</i>	<i>A. beccarii</i>	<i>A. parkinsoniana</i>	<i>E. excavatum</i>	<i>E. subarcticum</i>	<i>Elphidium</i> spp.	<i>Quinqueloculina</i> sp.	<i>Rosalina floridensis</i>	Total Agglutinated	Total Calcareous	Total Foraminifers
Surface			4.0	12.0	86.0	10.0	4.0	2.0	12.0	96.0					4.0			226.0	4.0	230.0
2		2.0		12.0	58.0	2.0	6.0	4.0		42.0								126.0	0.0	126.0
4	4.0		20.0	32.0	164.0	88.0	8.0		8.0	244.0	52.0							568.0	52.0	620.0
6		2.0		8.0	24.0	10.0	10.0		16.0	30.0	2.0							100.0	2.0	102.0
8			2.0	10.0	30.0	4.0	14.0	2.0	24.0	76.0								162.0	0.0	162.0
10				16.0	66.0	6.0	18.0		34.0	106.0								246.0	0.0	246.0
12		2.0	6.0	8.0	50.0	6.0	16.0	4.0	24.0	110.0								226.0	0.0	226.0
14			4.0	8.0	48.0	8.0	8.0		20.0	148.0								244.0	0.0	244.0
16			6.0	6.0	58.0	4.0	4.0	2.0	30.0	100.0								210.0	0.0	210.0
18			4.0	2.0	32.0		4.0	2.0	14.0	60.0								118.0	0.0	118.0
20		2.0	4.0	6.0	34.0	4.0	4.0		16.0	64.0								134.0	0.0	134.0
22		4.0	2.0	12.0	56.0	12.0	14.0	6.0	18.0	72.0								198.0	0.0	198.0
24		0.8	6.4	1.2	12.8	3.2	4.0	0.8	5.2	24.0								58.4	0.0	58.4
26			4.6	2.3	17	2.3	3.4		17	30.3								46.3	0.0	46.3
28			4.0		20.0		0.0			8.0								32.0	0.0	32.0
30			10.0	2.0	16.0	2.0	4.0	2.0	2.0	52.0								90.0	0.0	90.0
32			14.7	1.3	16.7	12.0	6.7		12.7	44.7								108.7	0.0	108.7
34			8.0	4.0			2.0		2.0	10.0								26.0	0.0	26.0
36		0.7	2.7	2.7	9.3	2.7	1.3			2.0								21.3	0.0	21.3
38					12.0	2.0				2.0								16.0	0.0	16.0
40			2.0		4.0					6.0								12.0	0.0	12.0
42										2.0								2.0	0.0	2.0
44					6.0					6.0								6.0	0.0	6.0
46					2.0					2.0								2.0	0.0	2.0
48										0.0								0.0	0.0	0.0
50					0.7					0.7								1.3	0.0	1.3
	6.0	13.5	104.3	145.5	807.2	178.2	131.4	24.8	239.6	1329.6	54.0				4.0			2980.0	58.0	3038.0

TABLE 9: Normalized data for Core 3 shows the Foraminifera species and the total number of Foraminifera species that were found while completing the lab work. The values under the Composite data column are depths below the surface and are in centimeters. The bolded values at the bottom and right side are composite totals.

Depth (cm)	Agglutinated Species										Calcareous Species						Totals			
Composite data	<i>Ammonoculites</i> sp.	<i>Ammonotium salinum</i>	<i>A. hepta</i>	<i>A. mexicana</i>	<i>J. macrescens</i>	<i>M. fusca</i>	<i>Millammina</i> sp.	<i>Textularia</i>	<i>T. comprimata</i>	<i>T. inflata</i>	<i>A. beccarii</i>	<i>A. parkinsoniana</i>	<i>E. excavatum</i>	<i>E. subarcticum</i>	<i>Elphidium</i> spp.	<i>Quinqueloculina</i> sp.	<i>Rosalina floridensis</i>	Total Agglutinated	Total Calcareous	Total Foraminifers
	Surface	3.0	3.0	1.0	4.0	21.0	27.0	2.0	1.0	5.0	52.0							119.0	0.0	119.0
	20	2.0		1.0	3.0	18.0	27.0	21.0	1.0	6.0	49.0							128.0	0.0	128.0
	40	3.0	3.0	8.0	6.0	21.0	49.0	8.0	2.0	7.0	32.0							139.0	0.0	139.0
	60		0.8	2.4	1.2	4.4	26.0	1.2		0.4	6.4							42.8	0.0	42.8
	8.0	6.8	12.4	14.2	64.4	129.0	32.2	4.0	18.4	139.4								428.8	0.0	428.8

TABLE 10: Normalized data for Core 4 shows the Foraminifera species and the total number of Foraminifera species that were found while completing the lab work. The values under the Composite data column are depths below the surface and are in centimeters. The bolded values at the bottom and right side are composite totals.

Depth (cm)	Agglutinated Species										Calcareous Species						Totals				
Composite data	<i>Ammobaculites</i> sp.		<i>Ammotium salinum</i>	<i>A. inepta</i>	<i>A. mexicana</i>	<i>J. macrescens</i>	<i>M. fusca</i>	<i>Milammina</i> sp.	<i>Textularia</i>	<i>T. comprimata</i>	<i>T. inflata</i>	<i>A. beccarii</i>	<i>A. parkinsoniana</i>	<i>E. excavatum</i>	<i>E. subarcticum</i>	<i>Elphidium</i> spp.	<i>Quinqueloculina</i> sp.	<i>Rosalina floridensis</i>	Total Agglutinated	Total Calcareous	Total Foraminifers
	40			0.7	4.0	2.0	8.0	1.3		1.3	53.3	3.3	1.3						70.7	4.7	75.3
	50	2.0	1.0	1.0	6.0	8.0	12.0		22.0	8.0	50.0	2.0							110.0	2.0	112.0
		2.0	1.0	1.7	10.0	10.0	20.0	1.3	22.0	9.3	103.3	5.3	1.3						180.7	6.7	187.3

TABLE 11: Normalized data for Core 5 shows the Foraminifera species and the total number of Foraminifera species that were found while completing the lab work. The values under the Composite data column are depths below the surface and are in centimeters. The bolded values at the bottom and right side are composite total

Depth (cm)	Agglutinated Species										Calcareous Species							Totals		
Composite data	<i>Ammobaculites</i> sp.	<i>Ammotium salinum</i>	<i>A. inepta</i>	<i>A. mexicana</i>	<i>J. macrescens</i>	<i>M. fusca</i>	<i>Milammina</i> sp.	<i>Textularia</i>	<i>T. comprimata</i>	<i>T. inflata</i>	<i>A. beccarii</i>	<i>A. parkinsoniana</i>	<i>E. excavatum</i>	<i>E. subarcticum</i>	<i>Elphidium</i> spp.	<i>Quinqueloculina</i> sp.	<i>Rosalina floridensis</i>	Total Agglutinated	Total Calcareous	Total Foraminifers
20	0.4	0.7		0.4	2.2	12.7			0.2	4.9	0.4							21.6	0.4	22.0
40	0.3		0.8	0.3	2.0	4.5	0.5		0.5	2.0								10.8	0.0	10.8
50	1.0		0.5	2.0	0.8	7.0	0.3		0.8	6.3								18.5	0.0	18.5
	1.4	0.9	1.3	2.7	5.0	24.2	0.8	0.0	1.5	13.1	0.4							50.8	0.4	51.3

TABLE 12: Pearson values comparing all the depths analyzed in Core 1 to the surface subenvironments. The Pearson values that are highest for each row are highlighted in yellow. Of those, the Pearson values that are significant (greater than 0.8 and -0.8) are bolded. The depths are in centimeters and the year that each depth corresponds to is also shown. TABLE 12: Pearson values comparing all the depths analyzed in Core 1 to the surface subenvironments. The Pearson values that are highest for each row are highlighted in yellow. Of those, the Pearson values that are significant (greater than 0.8 and -0.8) are bolded. The depths are in centimeters and the year that each depth corresponds to is also shown

Year	Depth	Estuary Deep	Estuary Shallow	Extreme Low Marsh	Low Marsh	Intermediate Marsh	High Marsh	Extreme High Marsh	Beach	Total Marsh
2013	Surface	-0.184	-0.190	0.470	0.375	0.784	0.936	0.914	-0.146	141.0
2001	2	-0.125	-0.131	0.437	0.411	0.842	0.370	0.977	-0.106	60.0
1989	4	-0.143	-0.150	0.409	0.280	0.726	0.321	0.951	-0.101	119.0
1978	6	-0.157	-0.160	0.423	0.295	0.683	0.315	0.919	-0.117	118.0
1966	8	-0.171	-0.176	0.443	0.313	0.687	0.904	0.883	-0.134	63.0
1954	10	-0.223	-0.212	0.125	0.129	0.596	0.520	0.569	-0.113	50.0
1942	12	-0.160	-0.169	0.542	0.410	0.853	0.830	0.811	-0.142	66.0
1931	14	-0.192	-0.189	0.365	0.218	0.585	0.503	0.484	-0.172	64.5
1919	16	-0.232	-0.233	0.292	0.194	0.513	0.434	0.404	-0.169	102.0
1907	18	-0.183	-0.178	0.121	0.011	0.283	0.079	0.084	-0.112	68.0
1895	20	-0.129	-0.140	0.401	0.377	0.621	0.410	0.327	-0.135	43.0
1884	22	-0.214	-0.216	0.271	0.226	0.503	0.338	0.306	-0.162	38.0
1872	24	0.073	0.027	0.852	0.779	0.652	0.471	0.205	-0.130	12.0
1860	26	-0.190	-0.203	0.537	0.420	0.646	0.729	0.656	-0.185	26.0
1848	28	0.068	0.020	0.909	0.848	0.696	0.643	0.349	-0.144	4.7
1837	30	0.058	0.017	0.684	0.576	0.295	0.304	0.026	-0.125	3.5
1825	32	0.007	0.022	0.617	0.614	0.421	0.316	0.053	-0.140	5.0
1813	34	-0.051	-0.071	0.683	0.583	0.885	0.969	0.896	-0.109	7.5
1801	36	0.009	-0.033	0.839	0.852	0.947	0.857	0.645	-0.143	11.5
1790	38	-0.008	-0.042	0.837	0.750	0.917	0.839	0.673	-0.135	4.0
1778	40	0.042	0.001	0.848	0.736	0.711	0.578	0.352	-0.132	3.3
1766	42	-0.093	-0.098	0.465	0.380	0.818	0.921	0.949	-0.078	5.2
1754	44	-0.127	-0.136	0.340	0.164	0.283	0.217	0.133	-0.129	6.0
1743	46	0.015	-0.021	0.757	0.763	0.810	0.634	0.426	-0.130	5.5
1731	48	0.193	0.135	0.904	0.899	0.518	0.359	0.016	-0.095	4.7
1719	50	-0.130	-0.123	0.028	-0.141	0.017	-0.108	-0.086	-0.069	1.0
1707	52	-0.063	-0.015	0.573	0.397	0.340	0.322	0.112	-0.166	12.5
1695	54	-0.005	-0.045	0.740	0.607	0.519	0.390	0.142	-0.151	6.0
1684	56	0.198	0.140	0.886	0.844	0.445	0.310	-0.023	-0.089	12.0
1672	58	0.167	0.104	0.860	0.871	0.461	0.333	-0.030	-0.105	14.5
1660	60	-0.107	-0.140	0.431	0.394	0.337	0.097	-0.110	-0.156	21.0
1648	62	-0.143	-0.160	0.189	0.025	0.115	-0.063	-0.124	-0.122	23.0
1637	64	-0.162	-0.169	0.169	0.003	0.073	-0.080	-0.121	-0.126	25.5
1625	66	-0.211	-0.215	0.041	-0.124	-0.017	-0.137	-0.155	-0.121	35.0
1613	68	-0.055	-0.105	0.542	0.437	0.258	0.075	-0.148	-0.164	34.7
1601	70	0.012	-0.035	0.571	0.522	0.319	0.216	-0.036	-0.154	27.3
1590	72	0.057	0.002	0.771	0.725	0.409	0.201	-0.113	-0.144	

TABLE 13: Pearson values comparing all the depths analyzed in Core 2 to the surface subenvironments. The Pearson values that are highest for each row are highlighted in yellow. Of those, the Pearson values that are significant (greater than 0.8 and -0.8) are bolded. The depths are in centimeters and the year that each depth corresponds to is also shown.

[illegible]

TABLE 14: Pearson values comparing all the depths analyzed in Core 3 to the surface subenvironments. The Pearson values that are highest for each row are highlighted in yellow. Of those, the Pearson values that are significant (greater than 0.8 and -0.8) are bolded. The depths are in centimeters and the year that each depth corresponds to is also shown.

[illegible]

TABLE 15: Pearson values comparing all the depths analyzed in Core 4 to the surface subenvironments. The Pearson values that are highest for each row are highlighted in yellow. Of those, the Pearson values that are significant (greater than 0.8 and -0.8) are bolded. The depths are in centimeters and the year that each depth corresponds to is also shown.

[illegible]

TABLE 16: Pearson values comparing all the depths analyzed in Core 5 to the surface subenvironments. The Pearson values that are highest for each row are highlighted in yellow. Of those, the Pearson values that are significant (greater than 0.8 and -0.8) are bolded. The depths are in centimeters and the year that each depth corresponds to is also shown.

[illegible]

TABLE 18: Filtered Pearson values comparing all the depths analyzed in Core 2 to the surface subenvironments. The Pearson values shown are all those that were greater than .5 or negative .5, and contained N values greater than 30. The Pearson values that are highest for each row are highlighted in yellow. Of those, the Pearson values that are significant (greater than 0.8 and -0.8) are bolded. The depths are in centimeters and the year that each depth corresponds to is also shown. Additionally, the elevations that were given to each subenvironment are in meters and are directly below the subenvironment names.

		Estuary Deep	Estuary Shallow	Extreme Low Marsh	Low Marsh	Intermediate Marsh	High Marsh	Extreme High Marsh	
Year	Depth	-1	-0.5	0.25	0.5	0.75	1	1.25	Total N
2013	Surface	-0.209	-0.207	0.276	0.250	0.779	0.786	0.849	230.0
2001	2	-0.227	-0.218	0.180	0.184	0.676	0.657	0.711	126.0
1989	4	0.023	0.006	0.510	0.479	0.909	0.895	0.879	620.0
1978	6	-0.191	-0.196	0.357	0.328	0.724	0.793	0.818	102.0
1966	8	-0.244	-0.234	0.244	0.172	0.706	0.835	0.946	162.0
1954	10	-0.245	-0.235	0.232	0.186	0.721	0.809	0.907	246.0
1942	12	-0.234	-0.225	0.268	0.200	0.756	0.844	0.947	226.0
1931	14	-0.190	-0.184	0.303	0.228	0.777	0.878	0.971	244.0
1919	16	-0.230	-0.220	0.246	0.192	0.749	0.810	0.919	210.0
1907	18	-0.234	-0.222	0.224	0.165	0.744	0.807	0.927	118.0
1895	20	-0.228	-0.220	0.277	0.215	0.771	0.844	0.938	134.0
1884	22	-0.246	-0.242	0.307	0.270	0.775	0.819	0.881	198.0
1872	24	-0.244	-0.239	0.332	0.241	0.794	0.828	0.906	58.4
1860	26	-0.172	-0.167	0.334	0.211	0.723	0.863	0.944	46.3
1848	28	-0.196	-0.187	0.122	0.136	0.583	0.434	0.479	32.0
1837	30	-0.207	-0.199	0.301	0.198	0.778	0.853	0.951	90.0
1825	32	-0.200	-0.203	0.449	0.337	0.813	0.856	0.897	108.7
									2951.4

TABLE 19: Filtered Pearson values comparing all the depths analyzed in Core 3 to the surface subenvironments. The Pearson values shown are all those that were greater than .5 or negative .5, and contained N values greater than 30. The Pearson values that are highest for each row are highlighted in yellow. Of those, the Pearson values that are significant (greater than 0.8 and -0.8) are bolded. The depths are in centimeters and the year that each depth corresponds to is also shown. Additionally, the elevations that were given to each subenvironment are in meters and are directly below the subenvironment names.

[illegible]

TABLE 20: Filtered Pearson values comparing all the depths analyzed in Core 4 to the surface subenvironments. The Pearson values shown are all those that were greater than .5 or negative .5, and contained N values greater than 30. The Pearson values that are highest for each row are highlighted in yellow. Of those, the Pearson values that are significant (greater than 0.8 and -0.8) are bolded. The depths are in centimeters and the year that each depth corresponds to is also shown. Additionally, the elevations that were given to each subenvironment are in meters and are directly below the subenvironment names.

[illegible]

TABLE 21: The subenvironment of each depth in the cores through time. Each subenvironment is abbreviated and are as follows; EHI = Extreme High Marsh; HI = High Marsh; INT = Intermediate Marsh and ELO= Extreme Low Marsh

Time (years)	Core 1	Core 2	Core 3	Core 4
2013	HI	EHI	HI	
2001	EHI	EHI		
1989	EHI	INT		
1978	EHI	EHI		
1954	INT	EHI		
1931	INT	EHI		
1919	INT	EHI		
1907	INT	EHI		
1895	INT	EHI	HI	
1884	INT	EHI		
1872		EHI		
1860		EHI		
1848		INT		
1837		EHI		
1825		EHI		
1778			ELO	EHI
1719				EHI
1660			ELO	
1613	ELO			
1590	ELO			
1378	ELO			
1331	ELO			

TABLE 22: The elevation of each depth in the cores through time. The elevations are in meters and are the same values that were in Table 18

Time (years)	Core 1	Core 2	Core 3	Core 4
2013	1	1.25	1	
2001	1.25	1.25		
1989	1.25	0.75		
1978	1.25	1.25		
1966	1	1.25		
1954	0.75	1.25		
1942	0.75	1.25		
1931	0.75	1.25		
1919	0.75	1.25		
1907		1.25		
1895	0.75	1.25	1	
1884	0.75	1.25		
1872		1.25		
1860		1.25		
1848		0.75		
1837		1.25		
1825		1.25		
1778			0.25	1.25
1719				1.25
1660			0.25	
1613	0.25			
1590	0.25			
1378	0.25			
1331	0.25			

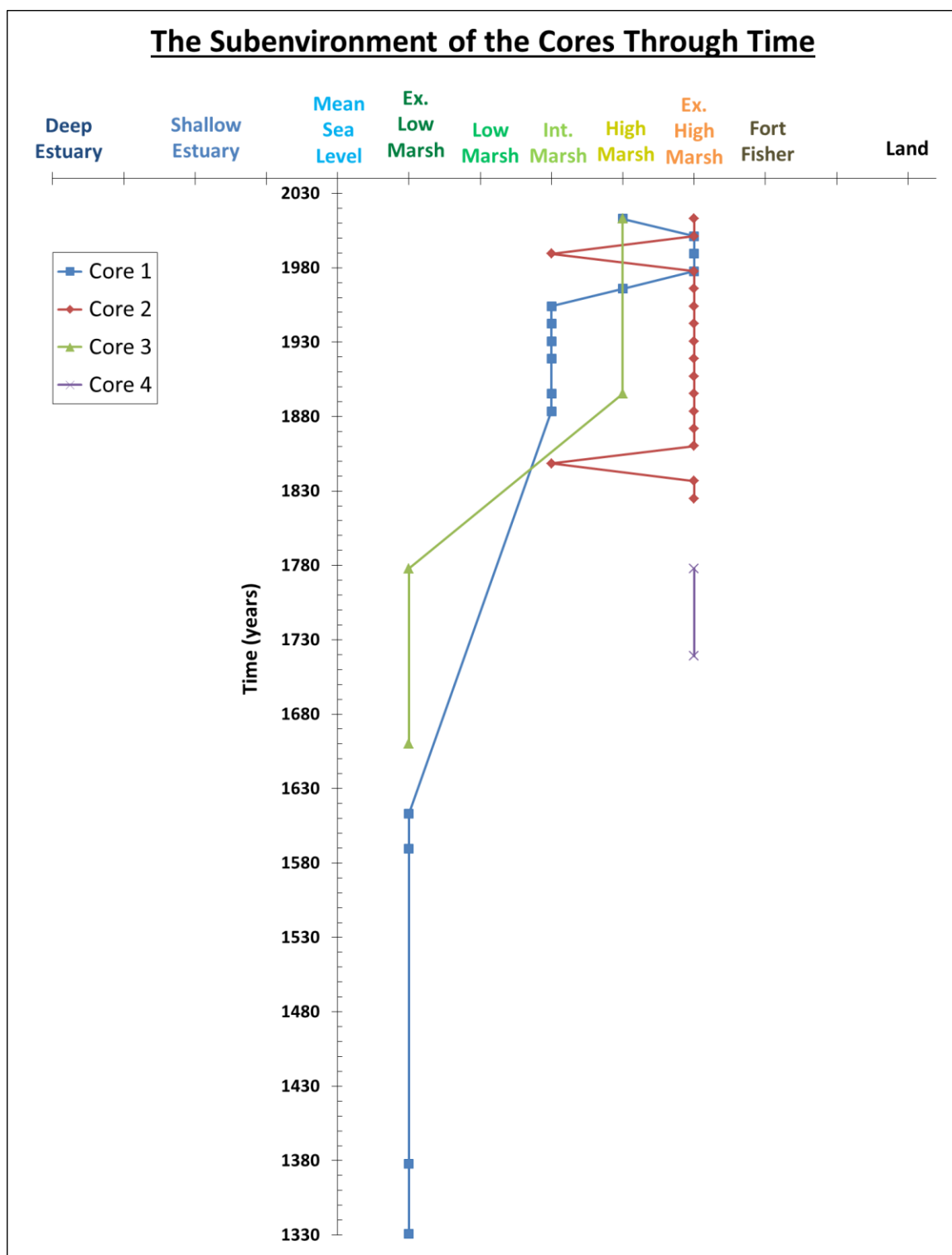


FIGURE 28: The change in each core's subenvironment through time. The values shown in this figure are the filtered Pearson values for each core (values greater than 0.5 and negative 0.5, and concentration values greater than 30 specimens/cm³). The subenvironments are shown on the x-axis, while the years are shown on the y-axis.

TABLE 23: Non-filtered differences between the elevations that the Foraminifera values yielded, and the elevations that the Map data yielded for each year. The elevation values are in meters. Any value greater than 1 or negative 1 represents years where the Foraminifera data and the Map data conflicted; they are highlighted in yellow.

Nonfiltered Difference		Core1	Core2	Core3	Core4	Core5
ForamYear	MapYear					
2001	2002	0.67	-0.08	0		
1989	1993	0.67	-0.08			
1978	1980	0.5	0.08			
1966	1970	0.33	0.25			
1954	1946	-1.25	-0.75			
1942	1946	-1.25	-0.75			
1931	1921	-1.25	-0.75			
1919	1917	-1.25	-0.75			
1907	1910	-1.25	-0.75	-1		-1.75
1895	1897	-1.25	-0.75	-1		-1.75
1884	1897	-1.42	-0.75	-1		-1.75
1872	1870	-1.33	-0.75			
1860	Jan 15 1865	-1.5	-0.92			
1860	Feb 1865	-1.5	-0.92			
1860	3PM Jan 15 1865	-1.5	-0.92			
1860	6PM Jan 15 1865	-1.5	-0.92			
1860	3PM Jan 15, 1985	-1.5	-0.92			
1860	1865 Atlas	-1.5	-0.92			
1860	1865	-1.5	-0.92			
1860	1865	-1.5	-0.92			
1860	1864	-0.5	0.08			
1860	1863	1.5	2.08			
1860	1863	-1.5	2.08			
1848	1863	1.5	2.08			
1848	1863	-1.5	2.08			
1837	1863	1.25	2.08			
1837	1863	-1.75	2.08			
1825	1781	-1.5	-0.75			
1813	1781	-1.33	-0.92			
1801	1781	-1.17	-1.08			
1790	1781	-1.42	-1.08	-1.75	-0.75	-1.75
1778	1770	0	-0.92	-0.5	0.5	-0.5
1766	1770	-0.17	0.33	-0.5	0.5	-0.5
1754	1770	0	0.17			
1743	1749	-0.33	0			
1731	1733	-0.33	0.25	-0.75	0.5	0.5

TABLE 24: Filtered differences between the elevation that the Foraminifera values yielded, and the elevations that the Map data yielded for each year. The elevation values are in meters. Any value greater than 1 or negative 1 represents years where the Foraminifera data and the Map data conflicted; they are highlighted in yellow.

Filtered Difference				
Foram Year to Map Year	Core 1	Core 2	Core 3	Core 4
2001 to 2002	0.67	0.08	0	
1989 to 1993	0.75	0.08		
1978 to 1980	0.67	0.08		
1966 to 1970	0.5	0.25		
1954 to 1946	-1.17	-0.75		
1942 to 1946	-1.25	-0.75		
1931 to 1921	-1.25	-0.75		
1919 to 1917	-1.25	-0.75		
1907 to 1910	-1.25	-0.75	-1	
1895 to 1897	-1.25	-0.75	-1	
1884 to 1897	-1.25	-0.75	-1	
1872 to 1870	-1.25	-0.75		
1860 to Jan 15 1865		-0.92		
1860 to Feb 1865		-0.92		
1860 to 9PM Jan 15 1865		-0.92		
1860 to 6PM Jan 15 1865		-0.92		
1860 to 3PM Jan 15,1865		-0.92		
1860 to 1865 Atlas		-0.92		
1860 to 1865		-0.92		
1860 to 1865		-0.92		
1860 to 1864		0.08		
1860 to 1863		2.08		
1860 to 1863		2.08		
1848 to 1863		2.08		
1837 to 1863		2.08		
1813 to 1781		-0.75	-1.75	-0.75
1774 to 1770		0.5	-0.5	0.5

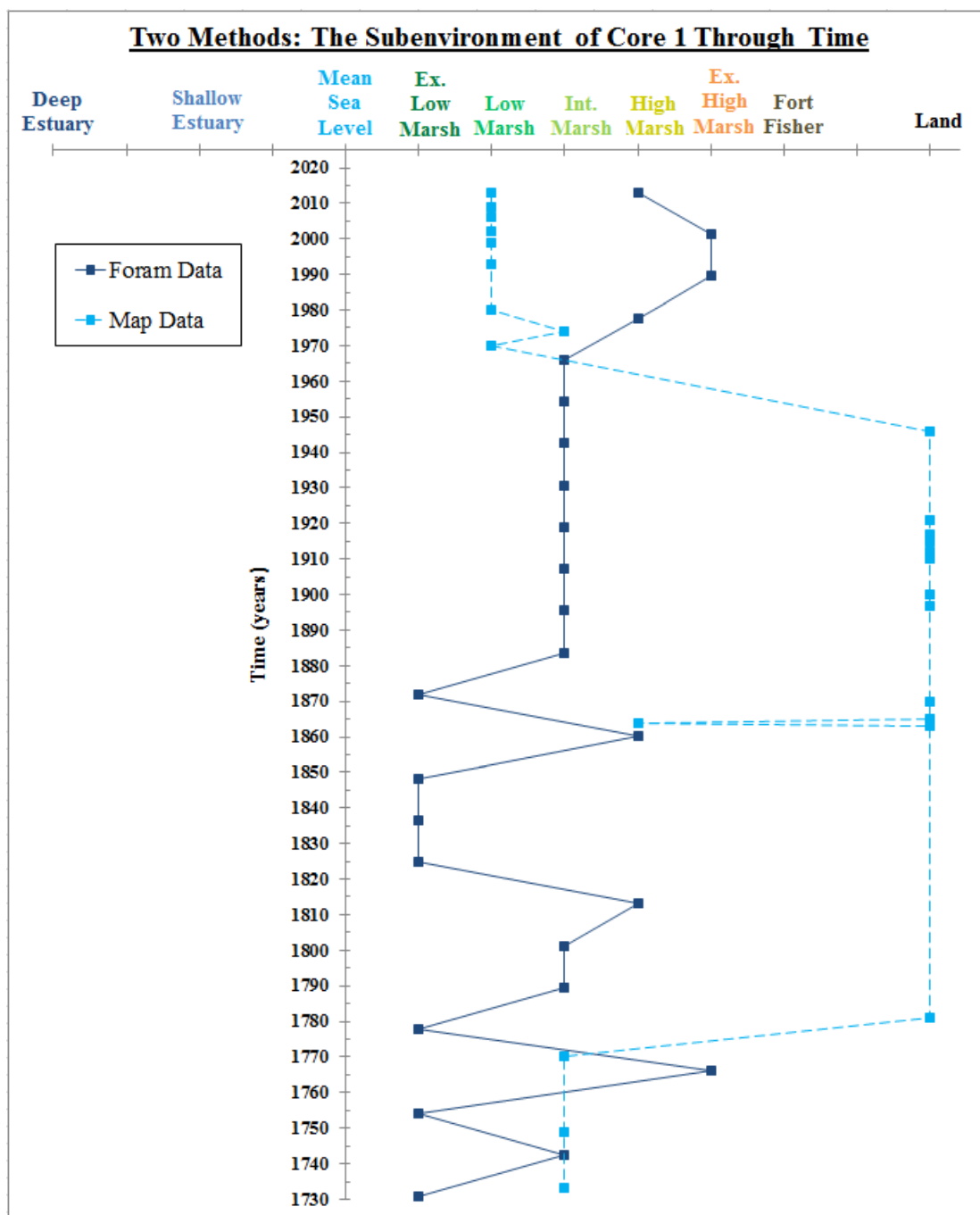


FIGURE 29: The change in Core 1's subenvironment through time based on two methods, the Foraminifera data (solid line), and the Map data (dashed line). The subenvironments are shown on the x-axis, while the years are shown on the y-axis. The values shown in this figure are the non-filtered Pearson values for the Foraminifera data.

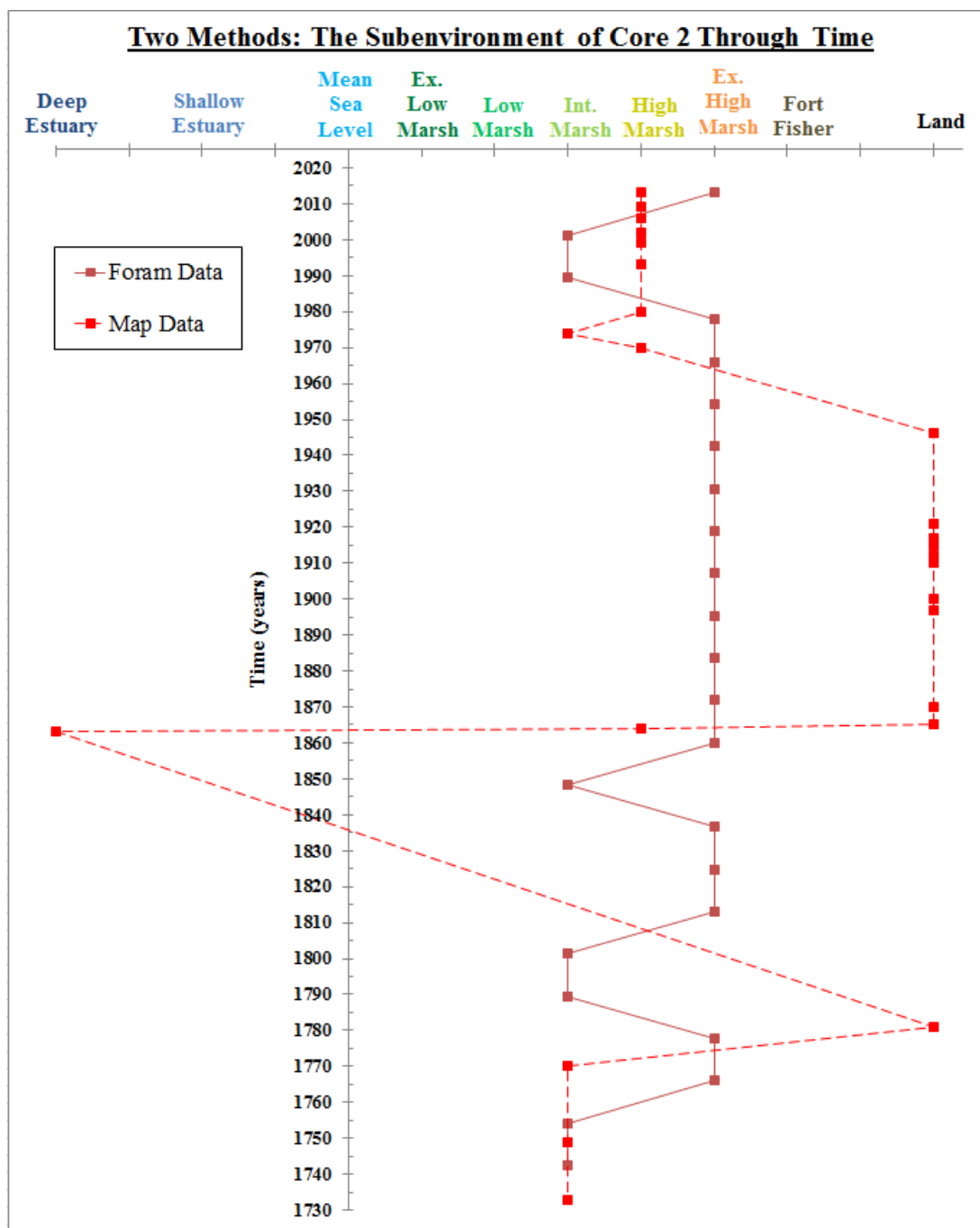


FIGURE 30: The change in Core 2's subenvironment through time based on two methods, the Foraminifera data (solid line), and the Map data (dashed line). The subenvironments are shown on the x-axis, while the years are shown on the y-axis. The values shown in this figure are the non-filtered Pearson values for the Foraminifera data.

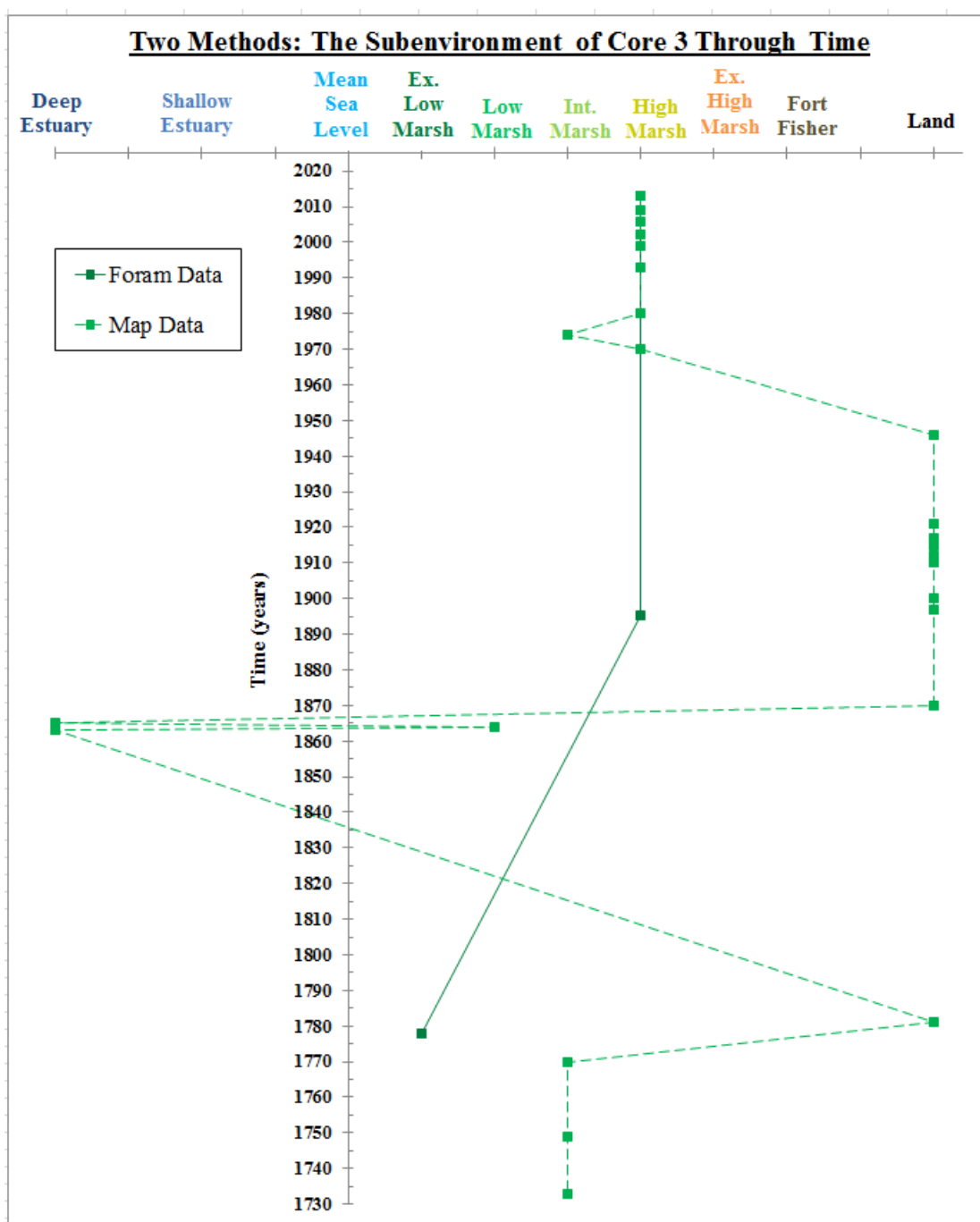


FIGURE 31: The change in Core 3's subenvironment through time based on two methods, the Foraminifera data (solid line), and the Map data (dashed line). The subenvironments are shown on the x-axis, while the years are shown on the y-axis. The values shown in this figure are the non-filtered Pearson values and the filtered Pearson values for the Foraminifera data.

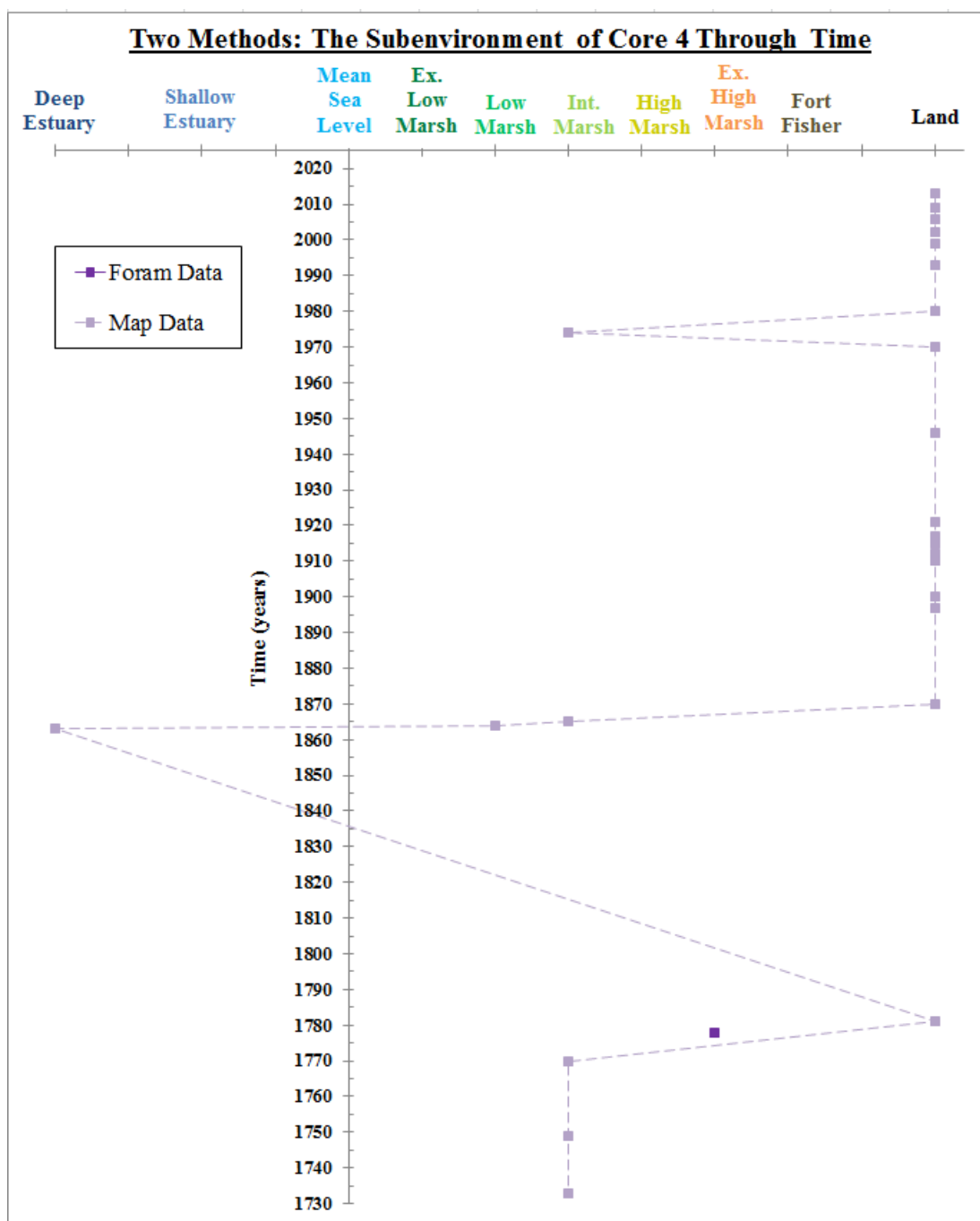


FIGURE 32: The change in Core 4's subenvironment through time based on two methods, the Foraminifera data (solid line), and the Map data (dashed line). The subenvironments are shown on the x-axis, while the years are shown on the y-axis. The values shown in this figure are the non-filtered Pearson values and the filtered Pearson values for the Foraminifera data.

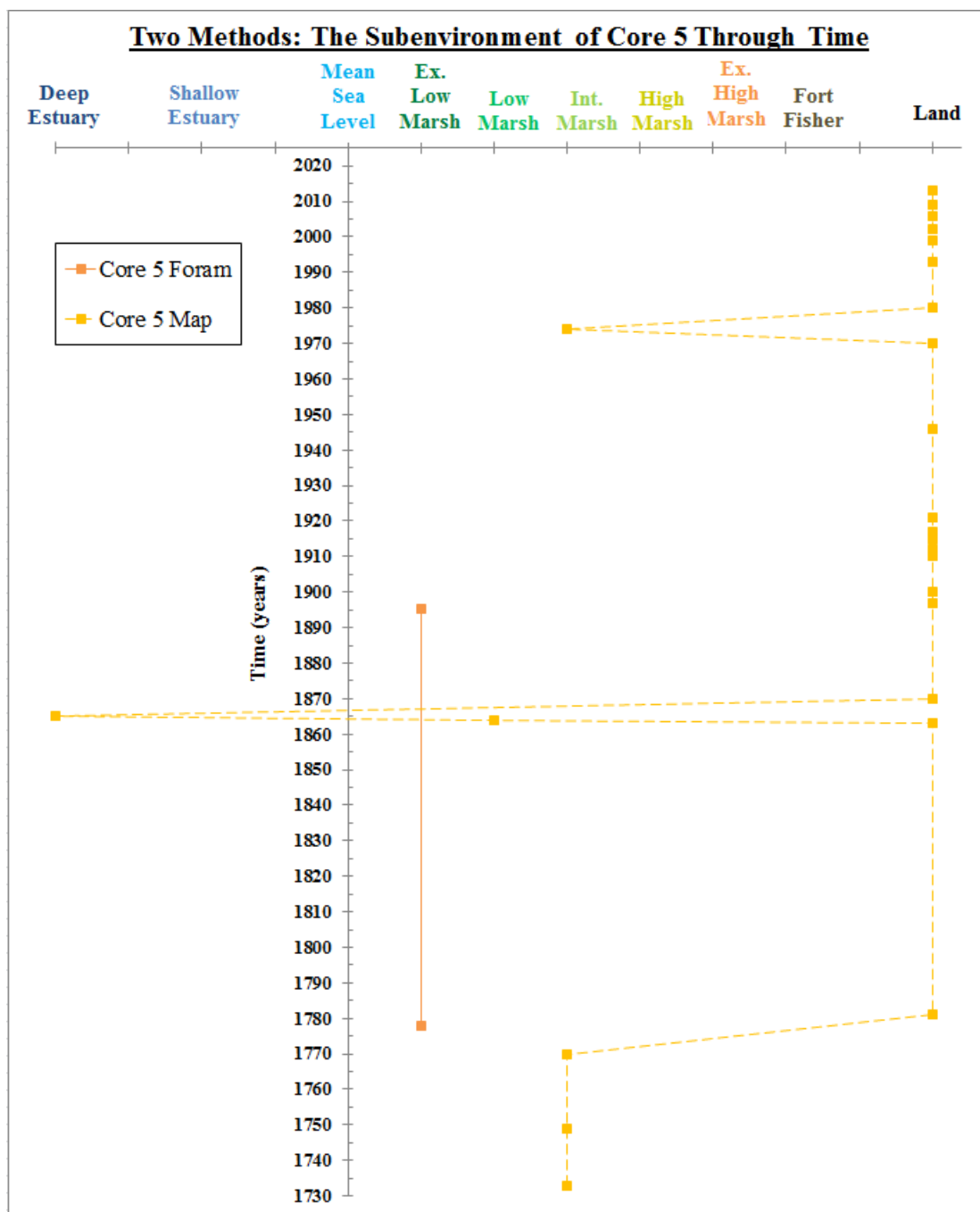


FIGURE 33: The change in Core 5's subenvironment through time based on two methods, the Foraminifera data (solid line), and the Map data (dashed line). The subenvironments are shown on the x-axis, while the years are shown on the y-axis. The values shown in this figure are the non-filtered Pearson values for the Foraminifera data.

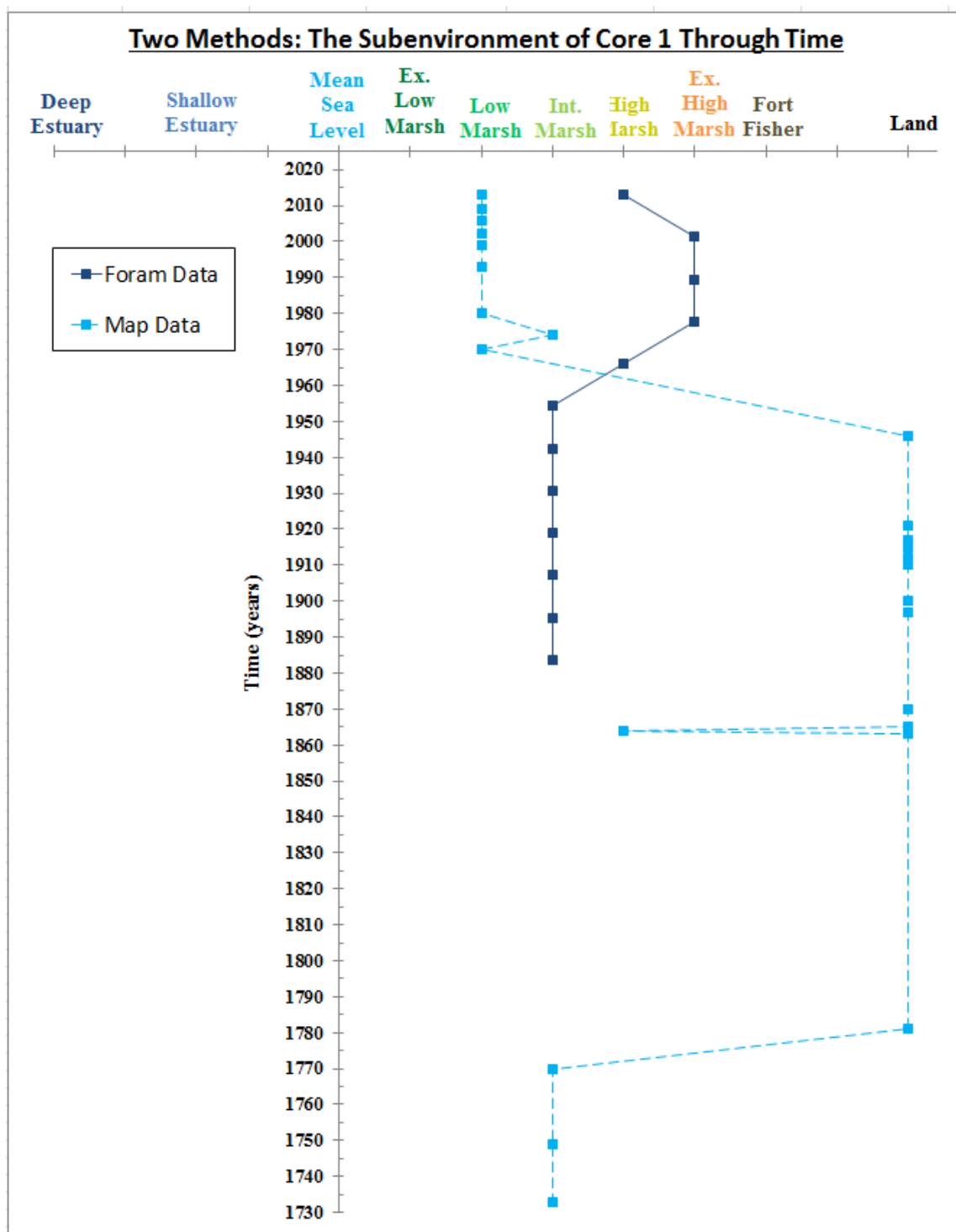


FIGURE 34: : The change in Core 1's environment through time based on both the Foraminifera data (solid line), and the Map data (dashed line). The subenvironments are shown on the x-axis, while the years are shown on the y-axis. The values shown in this figure are the filtered Pearson values for the Foraminifera data.

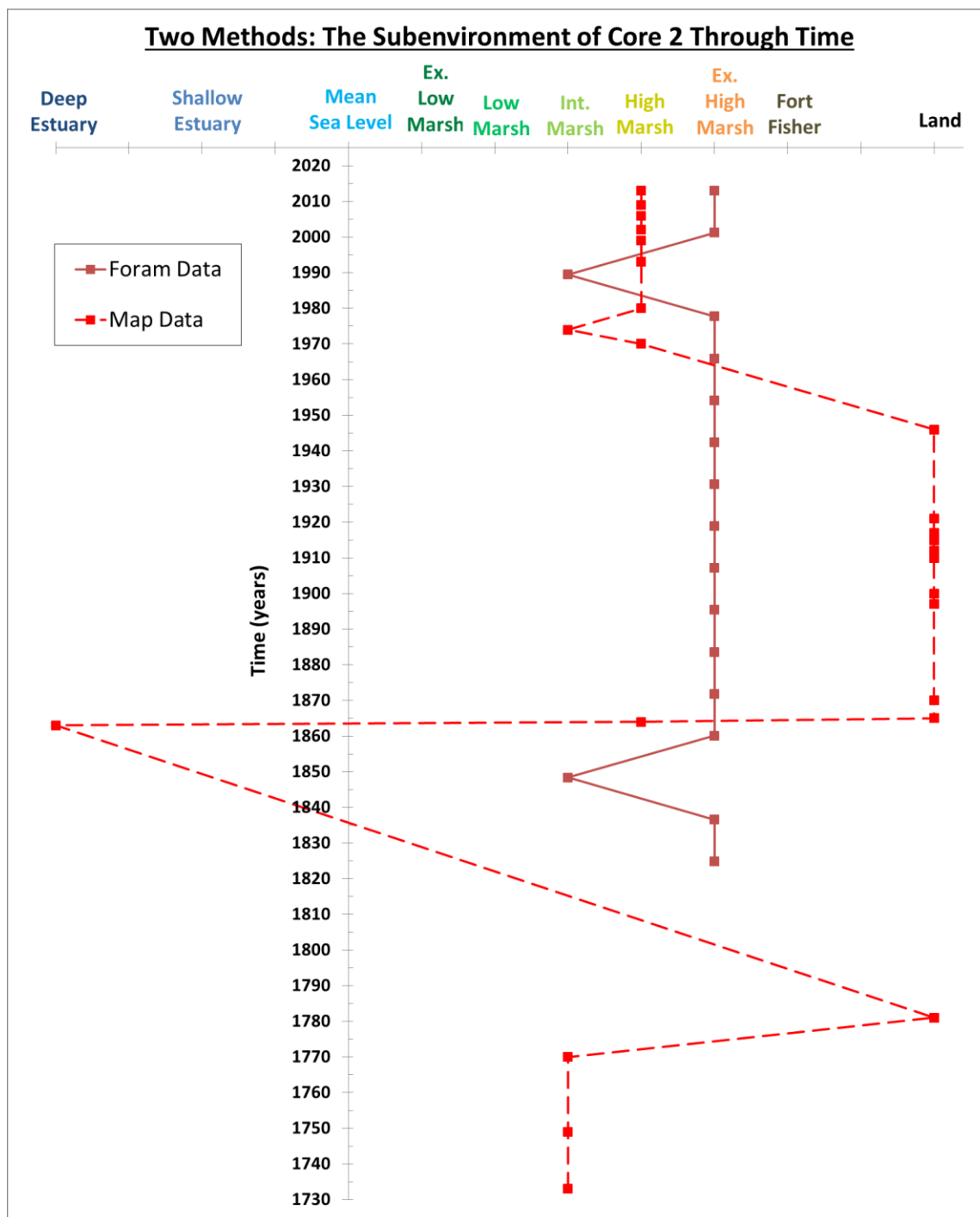


FIGURE 35: The change in Core 2's environment through time based on both the Foraminifera data (solid line), and the Map data (dashed line). The subenvironments are shown on the x-axis, while the years are shown on the y-axis. The values shown in this figure are the filtered Pearson values for the Foraminifera data.

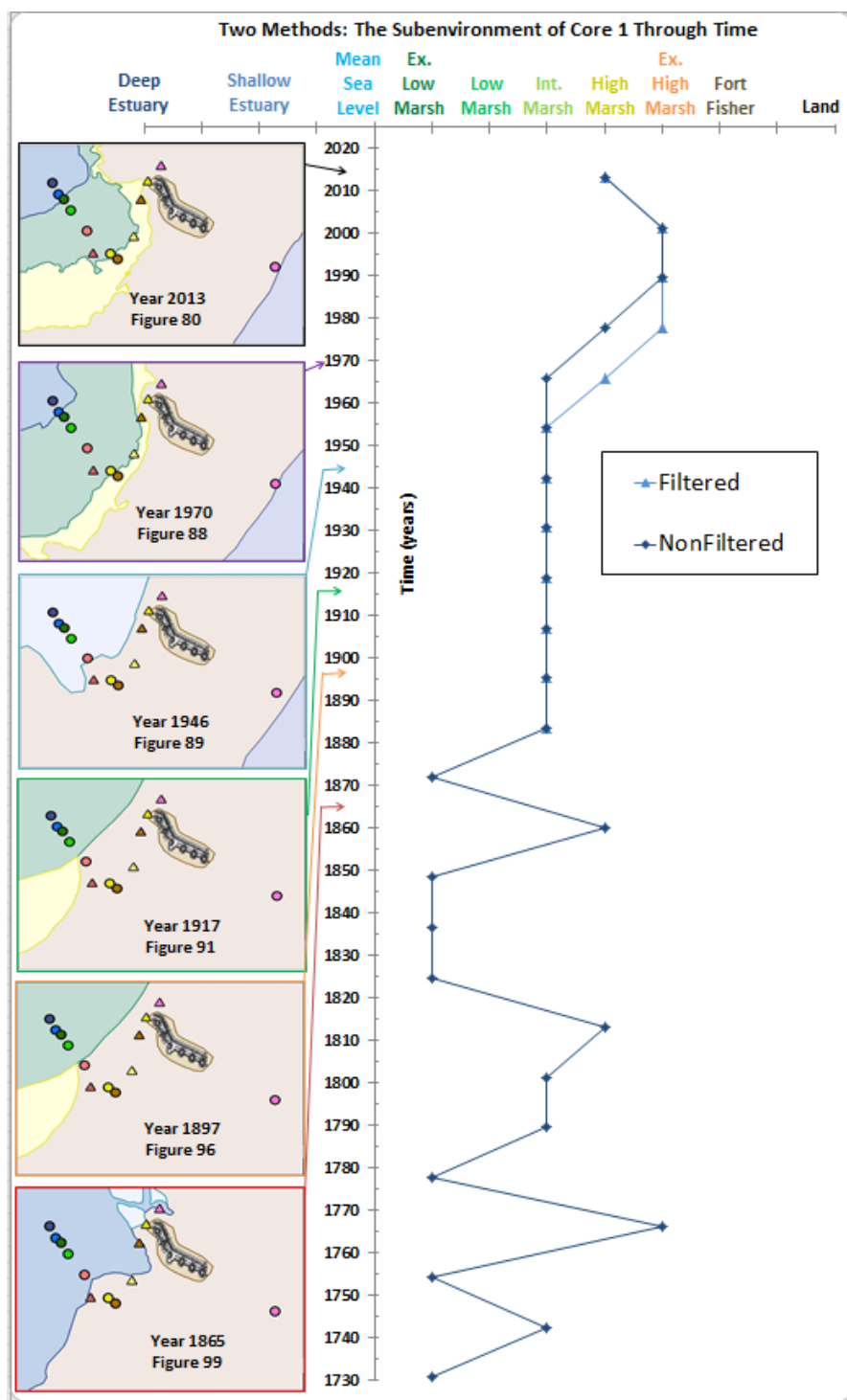


FIGURE 36: The change in Core 1's environment through time based on both the non-filtered and filtered Foraminifera data and the Map data. The subenvironments are on the x-axis, while the years are on the y-axis. The Map data at selected years are shown on the left-hand side of the figure. The arrow indicates the time period that the map represents. The remnant of Fort Fisher is also displayed on the map. The color and symbols on the maps are the same as the figures in section 6.2. The figure that each map corresponds to is in black under the year the map depicts.

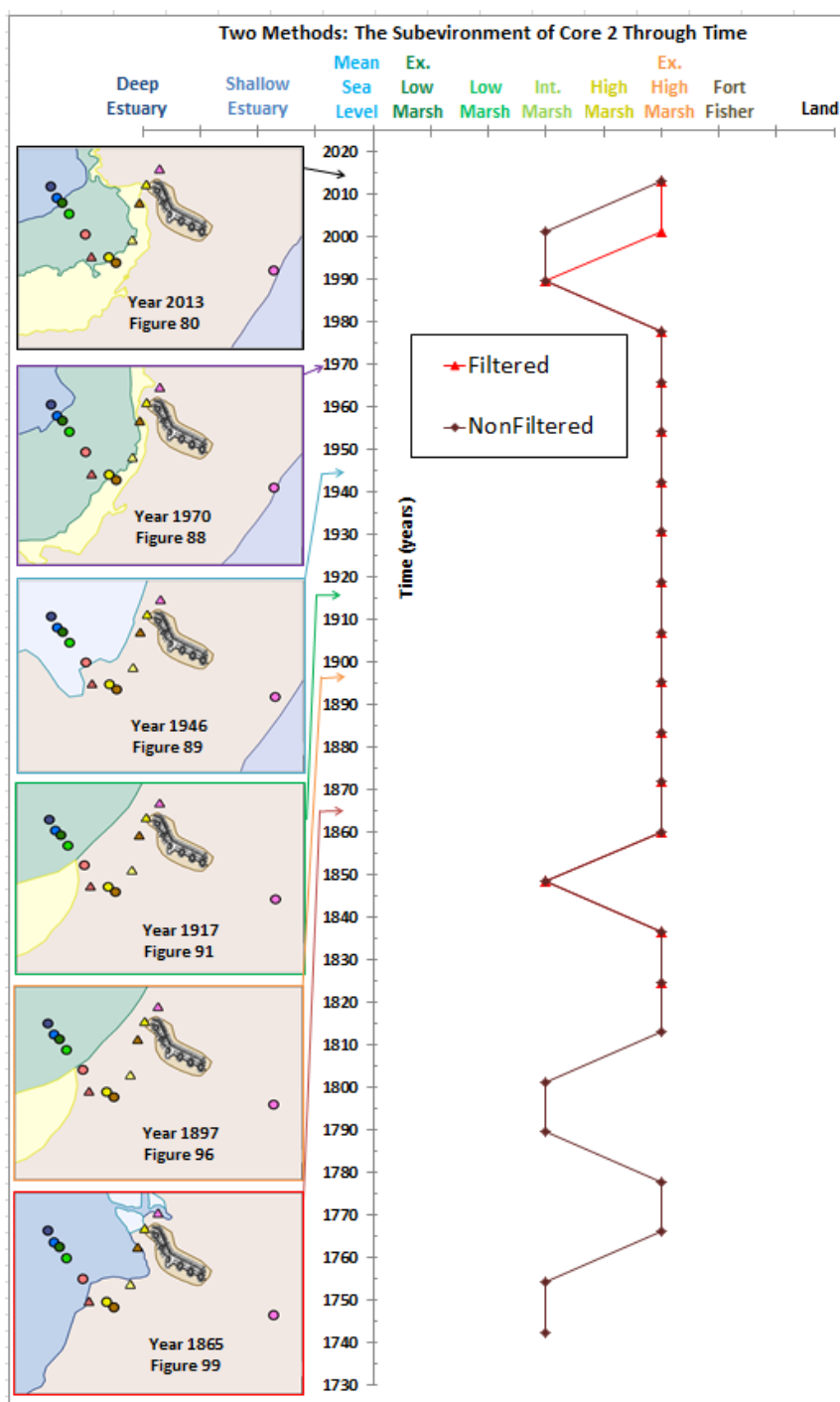


FIGURE 37: The change in Core 2's environment through time based on both the non-filtered and filtered Foraminifera data and the Map data. The subenvironments are on the x-axis, while the years are on the y-axis. The Map data at selected years are shown on the left-hand side of the figure. The arrow indicates the time period that the map represents. The remnant of Fort Fisher is also displayed on the map. The color and symbols on the maps are the same as the figures in section 6.2. The figure that each map corresponds to is in black under the year the map depicts.

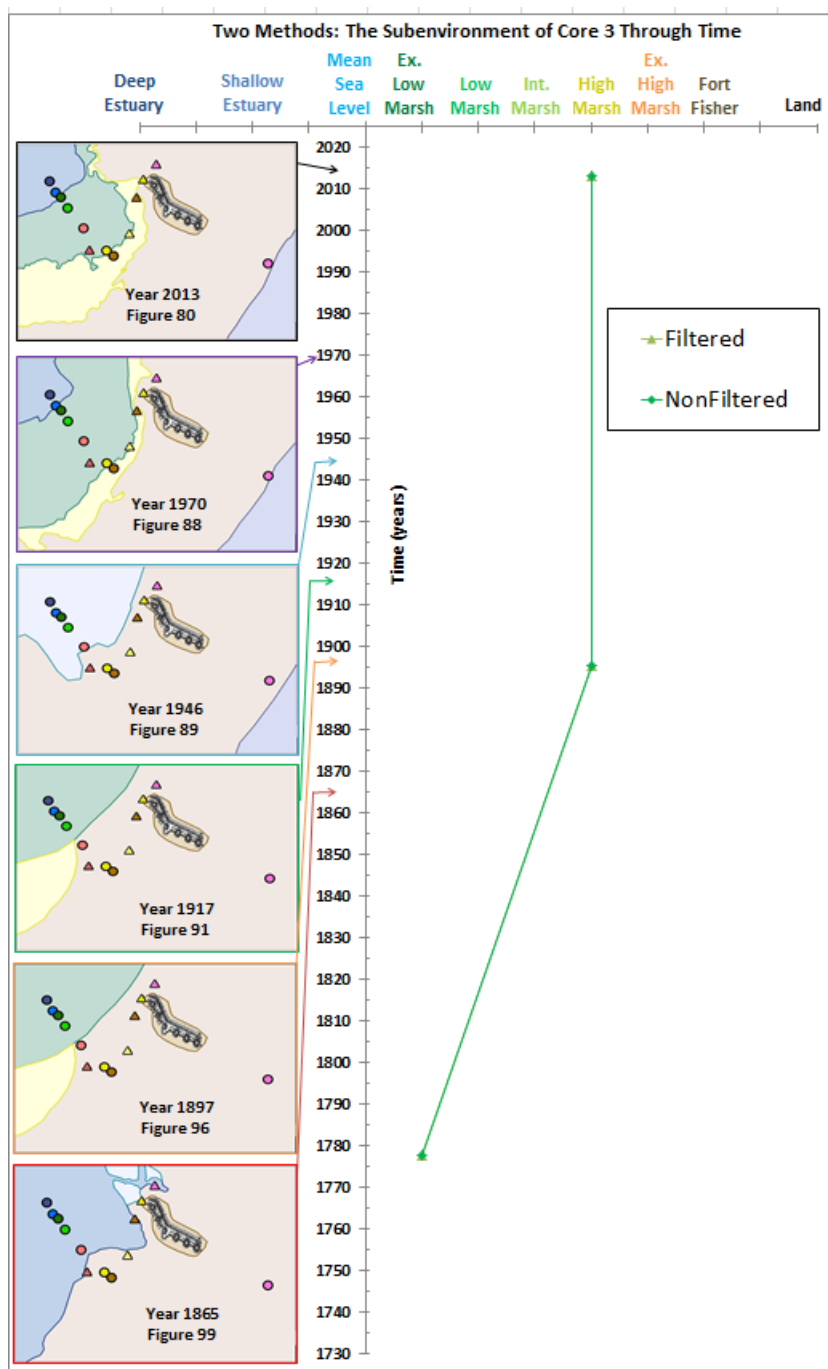


FIGURE 38: The change in Core 3's environment through time based on both the non-filtered and filtered Foraminifera data and the Map data. The subenvironments are on the x-axis, while the years are on the y-axis. The Map data at selected years are shown on the left-hand side of the figure. The arrow indicates the time period that the map represents. The remnant of Fort Fisher is also displayed on the map. The color and symbols on the maps are the same as the figures in section 6.2. The figure that each map corresponds to is in black under the year the map depicts.

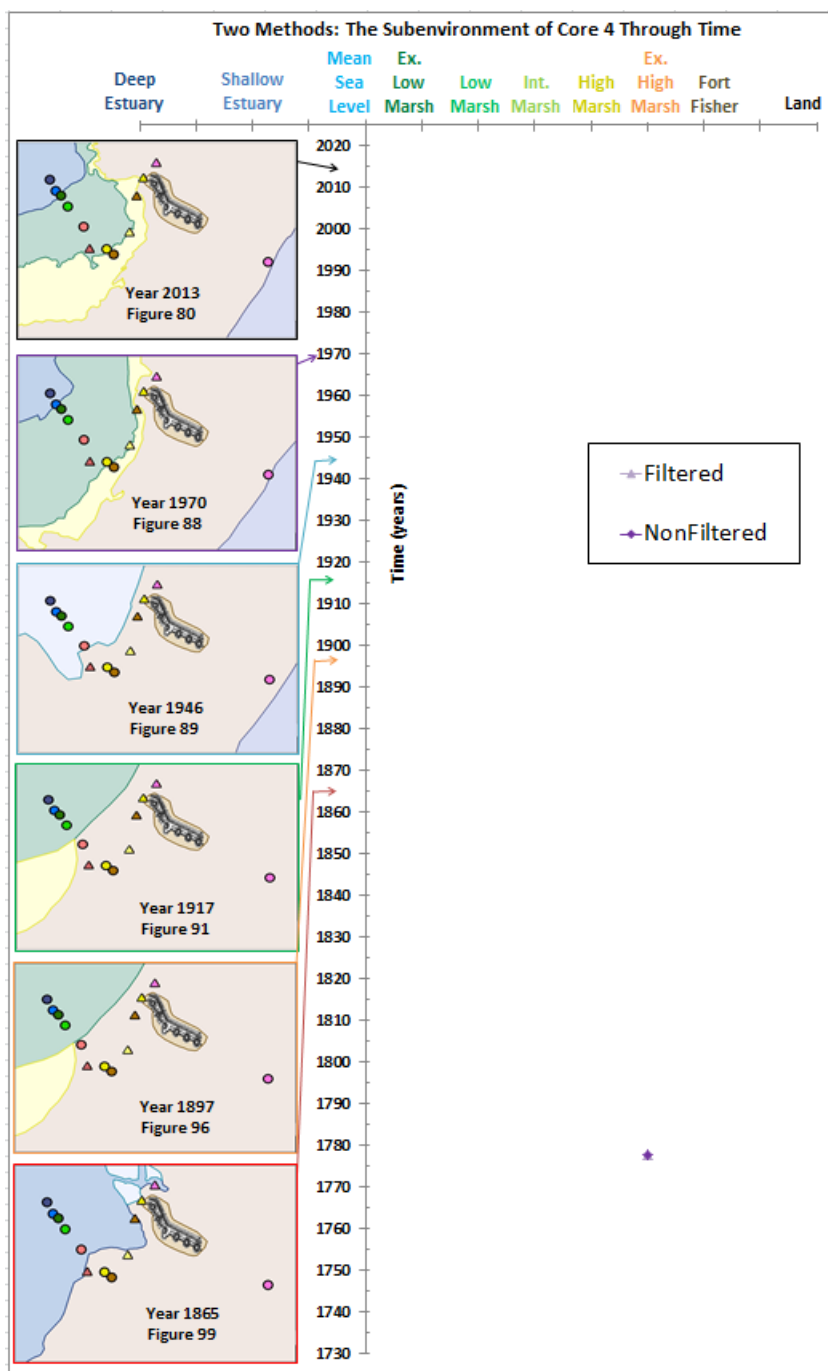


FIGURE 39: The change in Core 4's environment through time based on both the non-filtered and filtered Foraminifera data and the Map data. The subenvironments are on the x-axis, while the years are on the y-axis. The Map data at selected years are shown on the left-hand side of the figure. The arrow indicates the time period that the map represents. The remnant of Fort Fisher is also displayed on the map. The color and symbols on the maps are the same as the figures in section 6.2. The figure that each map corresponds to is in black under the year the map depicts.

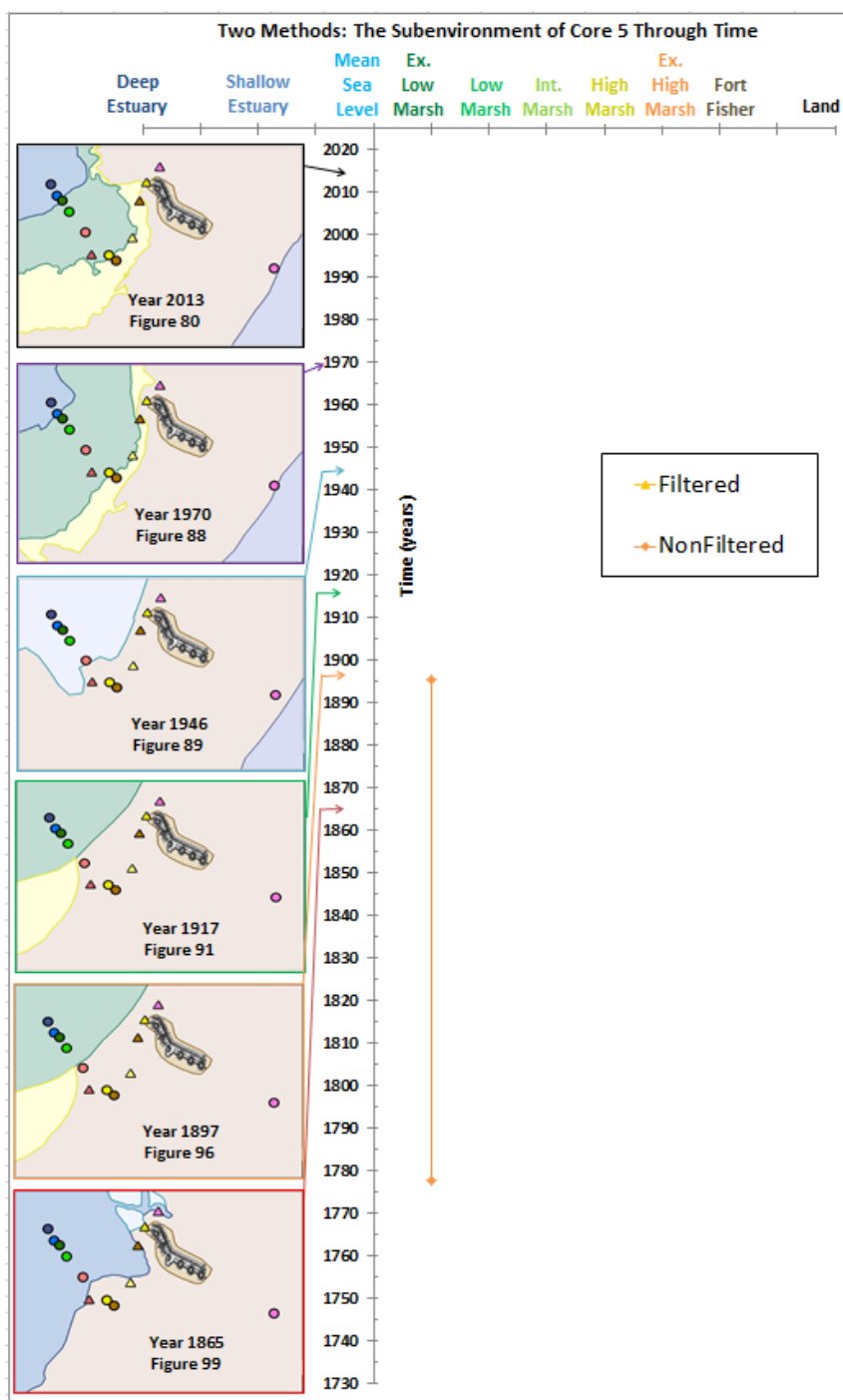


FIGURE 40: The change in Core 5's environment through time based on both the non-filtered and filtered Foraminifera data and the Map data. The subenvironments are on the x-axis, while the years are on the y-axis. The Map data at selected years are shown on the left-hand side of the figure. The arrow indicates the time period that the map represents. The remnant of Fort Fisher is also displayed on the map. The color and symbols on the maps are the same as the figures in section 6.2. The figure that each map corresponds to is in black under the year the map depicts.

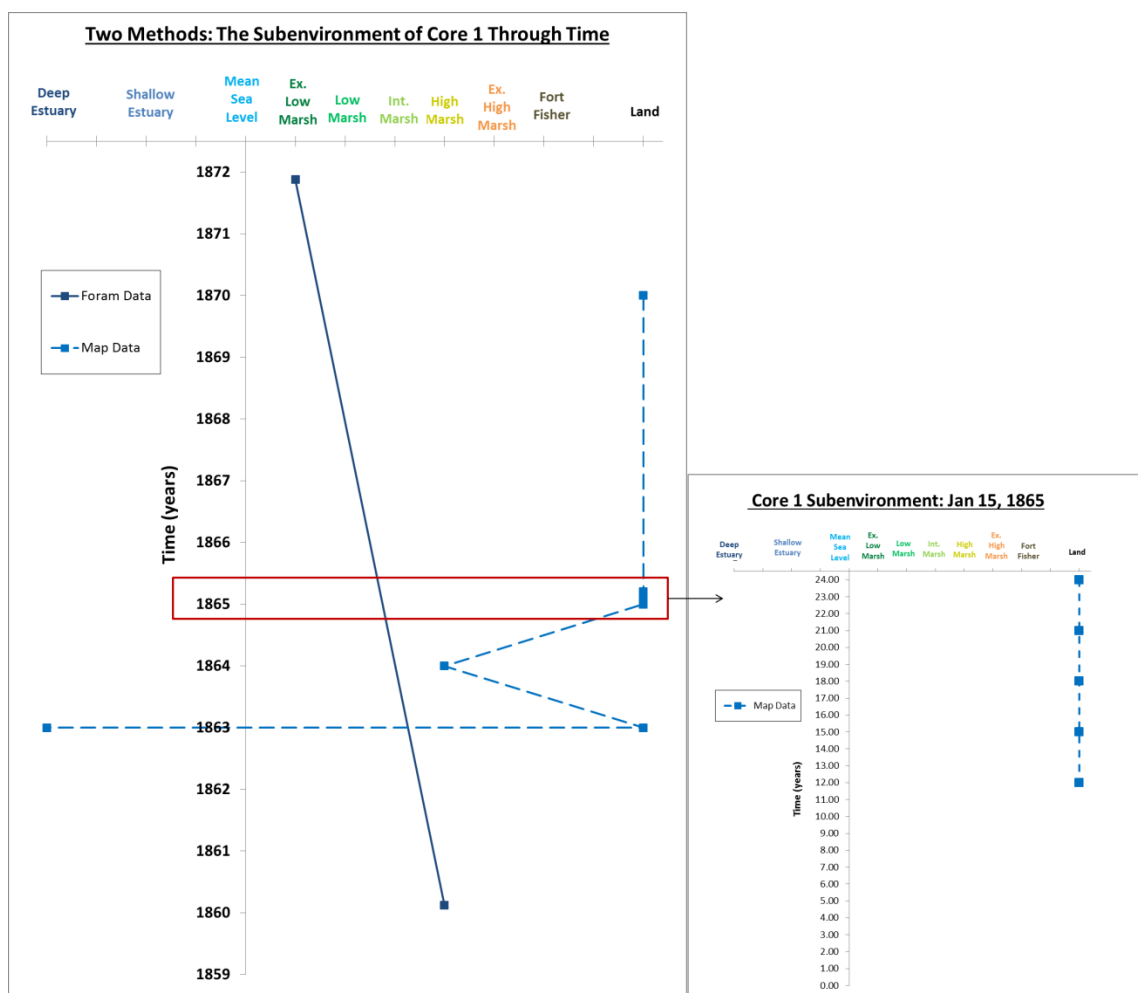


FIGURE 41: Core 1's shift in subenvironment between the years 1859-1872 based on two different methods: Foraminifera data (solid line), and Map data (dashed line). The subenvironments are shown on the x-axis, while the years are shown on the y-axis. A red box is shown on the left graph to indicate the time period that the graph on the right portrays. The graph on the right shows the subenvironments of the various maps that depict Fort Fisher on January 15, 1865. The subenvironments are shown on the x-axis, while the time of day (in military time) is displayed on the y-axis.

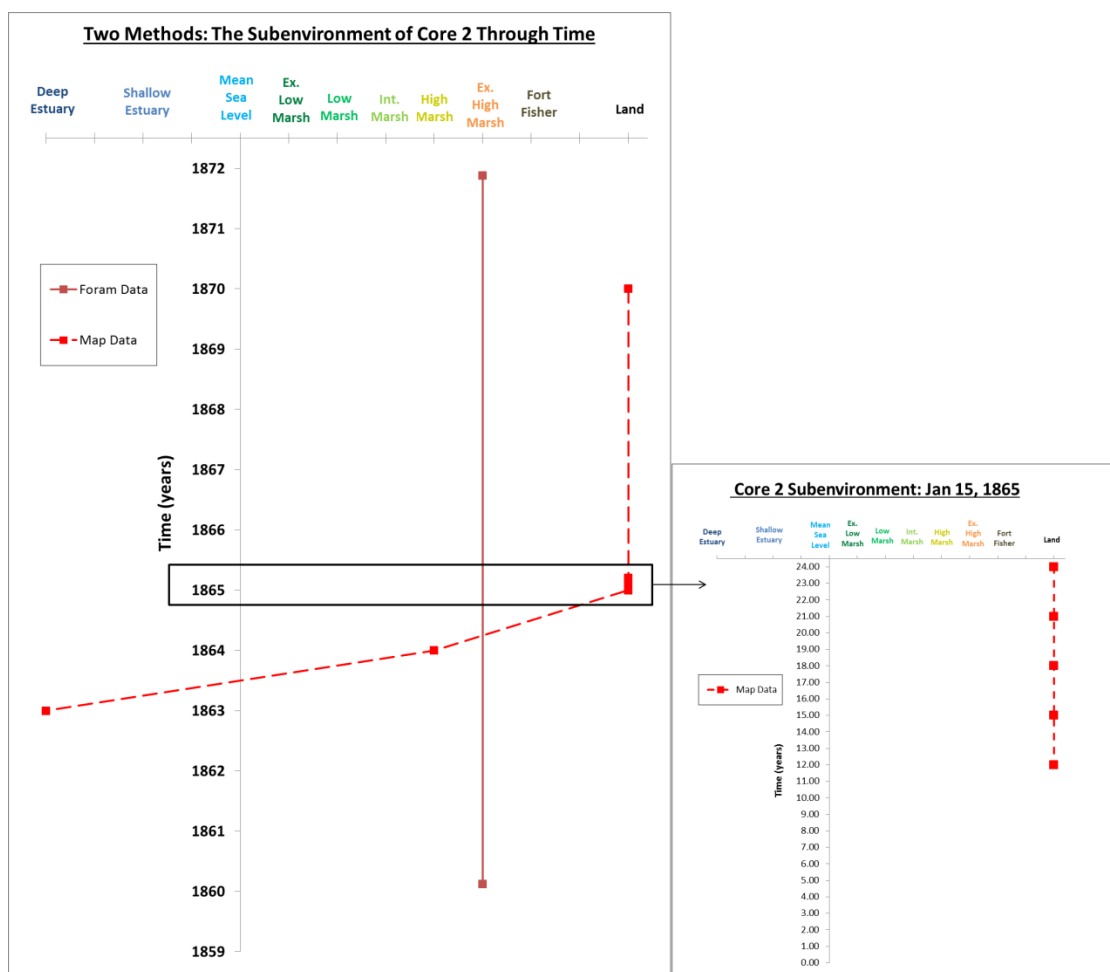


FIGURE 42: Core 2's shift in subenvironment between the years 1859-1872 based on two different methods: Foraminifera data (solid line), and Map data (dashed line). The subenvironments are shown on the x-axis, while the years are shown on the y-axis. A black box is shown on the left graph to indicate the time period that the graph on the right portrays. The graph on the right shows the subenvironments of the various maps that depict Fort Fisher on January 15, 1865. The subenvironments are shown on the x-axis, while the time of day (in military time) is displayed on the y-axis.

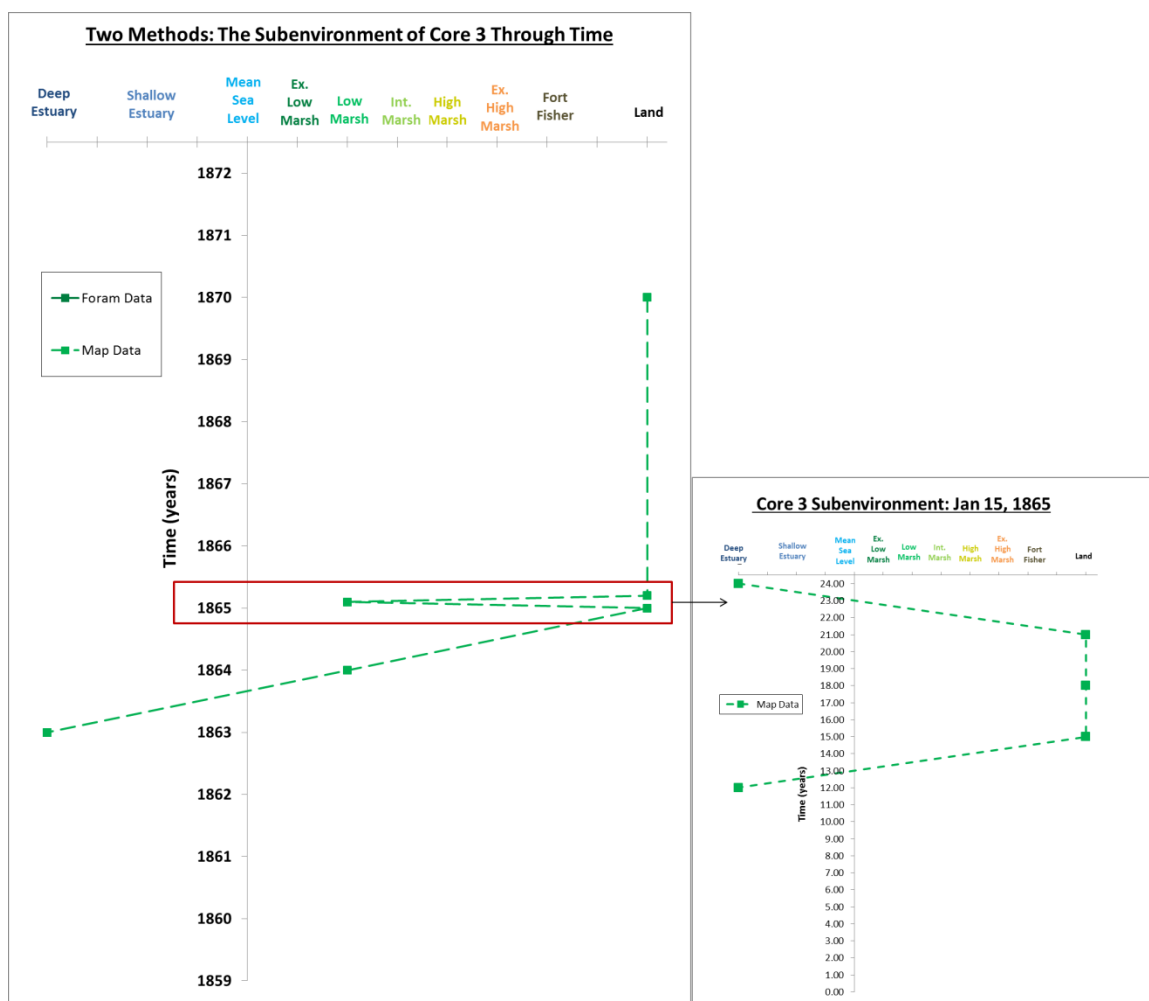


FIGURE 43: Core 3's shift in subenvironment between the years 1859-1872 based on two different methods: Foraminifera data (solid line), and Map data (dashed line). The subenvironments are shown on the x- axis, while the years are shown on the y-axis. A red box is shown on the left graph to indicate the time period that the graph on the right portrays. The graph on the right shows the subenvironments of the various maps that depict Fort Fisher on January 15, 1865. The subenvironments are shown on the x- axis, while the time of day (in military time) is displayed on the y-axis.

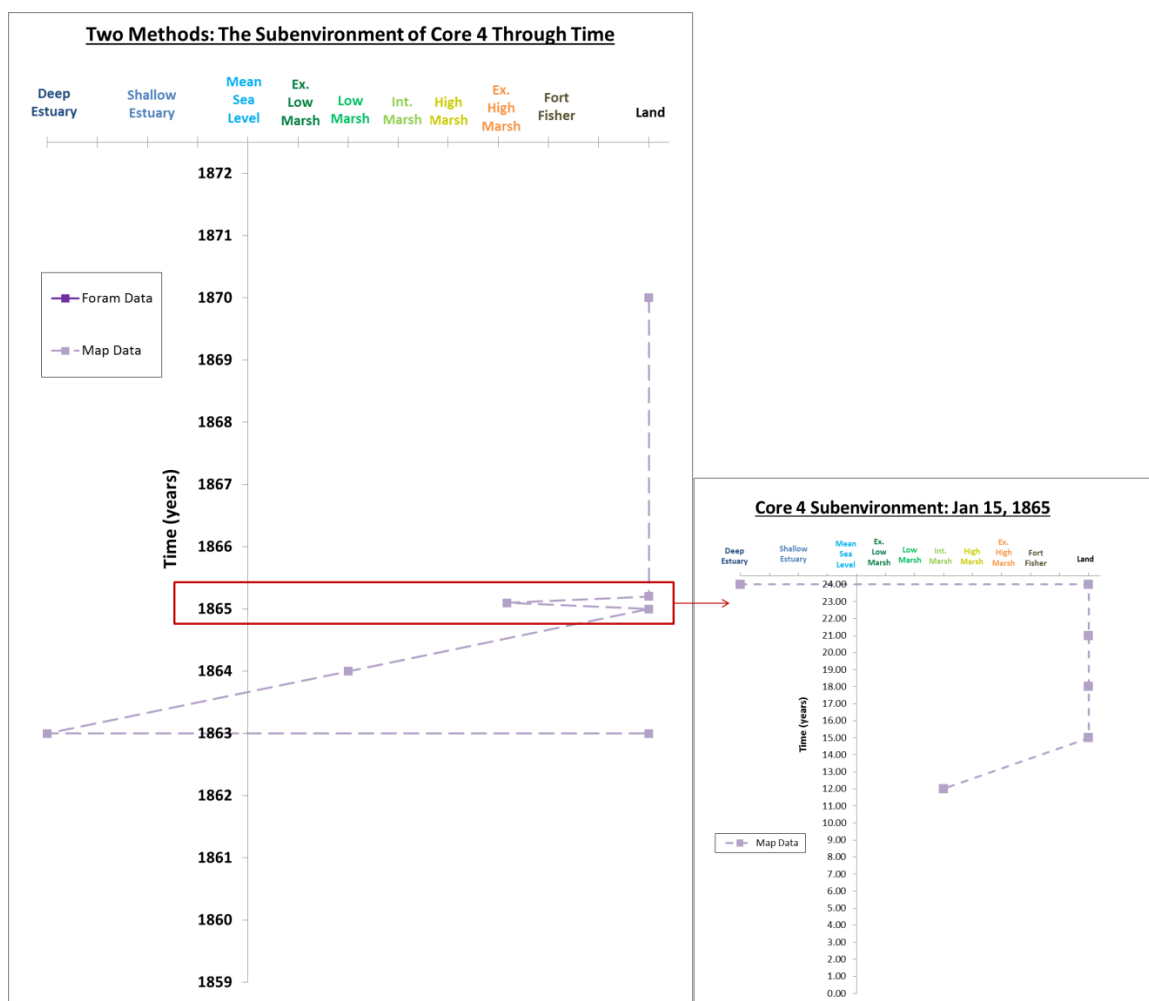


FIGURE 44: Core 4's shift in subenvironment between the years 1859-1872 based on two different methods: Foraminifera data (solid line), and Map data (dashed line). The subenvironments are shown on the x- axis, while the years are shown on the y-axis. A red box is shown on the left graph to indicate the time period that the graph on the right portrays. The graph on the right shows the subenvironments of the various maps that depict Fort Fisher on January 15, 1865. The subenvironments are shown on the x- axis, while the time of day (in military time) is displayed on the y-axis.

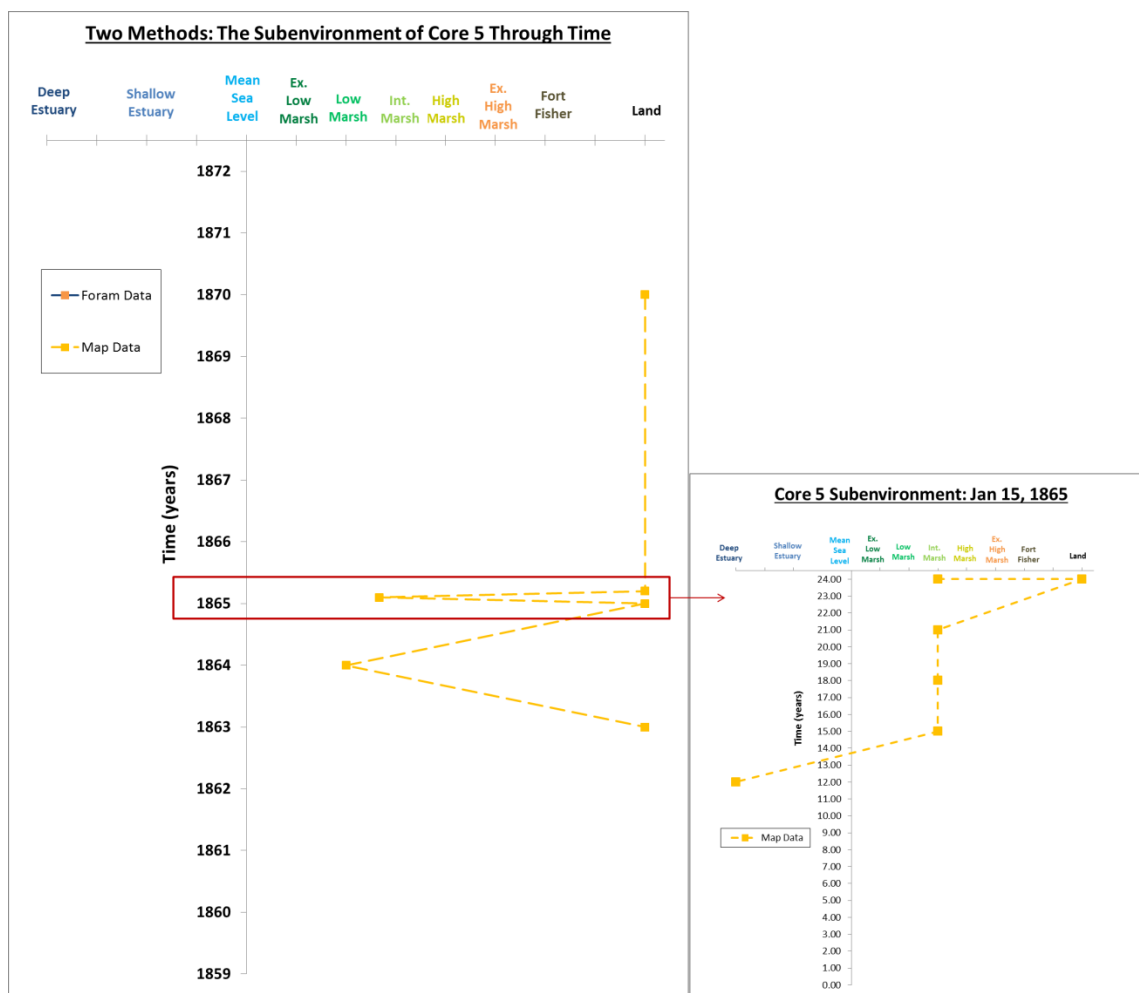


FIGURE 45: Core 5's shift in subenvironment between the years 1859-1872 based on two different methods: Foraminifera data (solid line), and Map data (dashed line). The subenvironments are shown on the x-axis, while the years are shown on the y-axis. A red box is shown on the left graph to indicate the time period that the graph on the right portrays. The graph on the right shows the subenvironments of the various maps that depict Fort Fisher on January 15, 1865. The subenvironments are shown on the x-axis, while the time of day (in military time) is displayed on the y-axis.

CHAPTER 6: DISCUSSION

6.1 Interpretation of the Foraminiferal Data

Previous studies have found conflicting results regarding the distribution of Foraminifera across marsh subenvironments (Scott and Medioli, 1980; Hippensteel et al., 2000; Kemp et al., 2009). There is general agreement among the studies that the agglutinated taxa are most common in the marsh subenvironments and calcareous taxa are more abundant in the lower elevation estuarine subenvironments. A particular taxa may (Scott and Medioli, 1980) or may not (Hippensteel et al., 2000; Kemp et al., 2009) dominate a specific subenvironment.

In the surface samples from this study, a trend regarding agglutinated versus calcareous taxa distribution was observed. Calcareous taxa were primarily found in the Estuary, both taxa were found in the low marshes, and only agglutinated taxa were found in the high marshes. Other studies found that the most abundant species present in the marsh subenvironments were agglutinated species such as *M. fusca*, *T. inflata*, *J. macrescens*, *A. mexicana* and *A. inepta* (Hippensteel et al., 2000; Culver et al., 2005, Abbene et al., 2006; and Kemp et al., 2009; Table 3).

In contrast, other species such as *Pseudothurammia limnetis*, *Siphotrochammina lobata*, and *Haplophragmoides wilberti*, recorded in Hippensteel et al. (2000); Culver et al. (2005); Abbene et al. (2006); and Kemp et al. (2009), were not found in this study. In the Estuary subenvironment, *A. beccarii* was the most dominant species, followed by *M. fusca*, *E. excavatum* and *Elphidium* spp. These results match what other researchers have previously reported for similar subenvironments.

While the majority of results held true to the agglutinated/calcareous trend, there were some outliers. The first outlier was the concentration of *M. fusca* in both Estuary subenvironments. This was unexpected, as it was predicted that only calcareous taxa would be found within the Estuary subenvironments. Instead, *M. fusca* was the second most abundant species in the estuaries. *M. fusca* species was also fairly abundant in the Intermediate and High marshes. Therefore, because *M. fusca* can be found in almost all subenvironments, it alone was not a good indicator for distinguishing subenvironments, unless it was extremely abundant.

Another example of an abundant species that was not a distinctive taxon was *T. inflata*. *T. inflata* was most abundant in the High marsh subenvironment. However, it was also found in moderate frequency in the Intermediate and Low marsh subenvironments. While these two species were too cosmopolitan to be indicative of subenvironments, other species were. *A. mexicana*, for example, was only found in the High marsh subenvironments. Additionally, *Textularia* sp. was only found in the Low marsh subenvironments, making it indicative of those subenvironments. The Intermediate marsh was unlike of the other subenvironments, in that no taxon was dominant. Instead, a variety of species were found in small numbers. On the contrary, the beach

subenvironment was unique because it was the only environment where *Quinqueloculina* sp. was found, indicating that this taxa was also representative of a particular subenvironment.

The core samples yielded a variety of results. For one, it was expected that the core samples would have shown a transgression through time (Figure 5) and that storm deposits (washover sediments) within the cores could have been identified, because sea-level since the last glacial maximum has risen at Fort Fisher at an average rate of 1.8 meters/year (Riggs et al., 2003). Coincidentally, the average sedimentation rate of Fort Fisher was also 1.8 meters/year, which means that the rate of sediment accumulation within the salt-marsh was dependent upon the global sea-level rise.

Paleotempestology is the study and use of historical and geological records to interpret past cyclonic activity. It was thought that if a cyclone had made landfall at Fort Fisher, the storm surge and wind generated from the storm would have created a breach, enabling sediment to transfer across the marsh between the ocean and the river. The sediment from the ocean (carrying displaced Foraminifera species) would settle in the marshes and be preserved through time. As seen in Tables 4-9, no displaced offshore Foraminifera species were found, and no hurricane deposits were found in the marsh strata.

Furthermore, it was also hypothesized that the five cores would have shown a similar change in subenvironments through time because of their proximity to one another. However, this did not hold true. Based on the analyzed Foraminiferal assemblages, the location of Core 1 and Core 3 produced a change in subenvironments through time that indicated a regression had occurred while the location of Core 2 did not

change subenvironments much through time. Its location largely remained in an Extreme High marsh subenvironment. Not enough data was available to present any conclusive results for how the subenvironments changed through time for Core 4 and Core 5.

Three reasons exist for why Cores 1 and 3 showed a regression instead of a transgression through time. First, the regression could be extremely localized. Other sections of the island may have experienced a different trend. The localized regression could indicate that the barrier island has been rolling over in response to a transgressive coastline due to rising seas, thus allowing sediment to accumulate in just those locations. The term island roll-over explains the process of a barrier beach migrating landward. Usually, islands roll-over in response to either sea-level changes (a transgressive coastline), overwash events from major storms, or both. Because no offshore Foraminifera species were found within the cores, the most likely explanation for this event would be the rise in sea-level during the late Holocene. Sediment accumulates on the back-side of the island during island roll-overs in response to sea-level rise or washover events, to maintain stability (Tanski, 2012). Cores 1 and 3 were taken on the estuary side of Pleasant Island adjacent to the fort, so sand would have accumulated in those areas. Interestingly, Core 2 does not follow this regression. Core 2 was taken closer to the mainland than Core 1, so it is possible that that area was more protected from the currents, and therefore did not exhibit much of a change in environments through time.

Another plausible explanation for a regression is the numerous armoring structures that have been built in the area throughout the years. These structures may have altered the water currents and allowed sediment to be carried and deposited to those two locations multiple times. The structures that were placed or built since the year 1860

include, sunken ships from blockades in the 1860's, a swash dam erected in 1887, and the series of groins that were installed in 1955. A sea wall, which was built by the Army Corps of Engineers in 1996, was placed on the seaward side of the island, and therefore may not have had a direct effect on the marsh (see Appendix A for details on how Kure Beach, located just north of Fort Fisher, has been affected by the building of the sea wall).

The third possible explanation for this regression is that it may be attributed to beach replenishment projects that have been completed in the area. This would only explain why sand has accumulated in these locations after 1955, the earliest year that beach replenishment projects were recorded. Carolina and Kure beaches are the two closest beaches to the north of Fort Fisher. According to the Western Carolina's Beach Nourishment Viewer, 30 beach nourishment projects have been completed at Carolina beach since 1955, and seven beach nourishment projects have been completed at Kure Beach (<http://beachnourishment.wcu.edu/visualization.php?state=NC&beach=Carolina%20Beach>). Additionally, a study completed by Magliocca et al. (2011) found that if artificial dunes were created during beach nourishment projects, when the dunes were overtopped (during a storm event), sediment would more likely have been redistributed unevenly, compared to overwash events in a more natural environment. Sediments from overwash events accumulate on the back-side of barrier islands, where the marshes are located. Subsequently, due to the number of beach replenishment projects that have occurred just north of the fort, and the occurrence of storms in the area, there could be an elevated amount of replenished sediment in the marshes. This replenished sand would not contain

offshore Foraminifera, and therefore, may explain why the cores lack such taxa. Because the Cape Fear River flows to the south, sediment in those marshes could have been eroded and deposited in the marshes adjacent to Fort Fisher, explaining the shift in subenvironments from a Low marsh to a High marsh through time.

6.2 Interpretation of Landscapes through Time

Maps created by analyzing the core samples with modern analogs were anticipated to be identical to chronoequivalent historical maps and aerial photographs. This hypothesis proved to be false. When the Map data, showing the change in the cores' environments through time were compared to the Foraminifera data, the two methods yielded conflicting results. In many cases, the quality of the maps which were available for this study were quite poor, and contained multiple points of inaccuracy.

One inaccuracy had to do with latitude and longitude—which were merely educated estimates on maps dating from before the advent of Global Positioning System (GPS) technology. While these estimates improved over time, any map created before 1984 had a high probability of containing imprecise latitudes and longitudes, with 1984 maps still being less accurate than 2013 maps. The year 1984 is specifically noted because the United States Geologic Survey released a datum in that year standardizing latitudes and longitudes. This 1984 datum replaced the North American Datum of 1927 with more accurate measurements, according to the National Geospatial- Intelligence Agency et al. (2005).

Before the USGS World Geodetic System (WGS) 1984 datum and the North American Datum of 1927 (NAD) were released, calculating latitude was difficult. Latitude was calculated by finding the degree at which the normal of the

ellipsoid, also known as the surface of the earth, crosses the equatorial plane. However, knowledge of the earth's surface has been changing over the last few centuries.

Understanding the surface of the earth is dependent upon knowing the length of the polar axis (the distance between the center of the earth and the North Pole). Scientists' determination of the length of the polar axis has changed by hundreds of meters in the last few centuries, thereby significantly changing measured on degree of latitude (Stern, 2004).

Limitations exist in this calculation of latitude. For one, the surface of the earth is calculated using mean sea-level. Areas of the earth that are above or below the Mean Sea-level impact the normal line needed to calculate latitude, thereby affecting the measurement of the degree. Second, in some cases, the location of the ellipsoid was unknown, and therefore cartographers were unable to determine a normal line to use to find the degree of intersection. In this case, cartographers would use the distance between their location and the North Star to calculate latitude. At the equator, the distance between the North Star and the equator, also known as the horizon, is 0 degrees, while at the North Pole, it is 90 degrees. Weather patterns and the time of the year affect the visibility of the North Star, making this method unreliable. Any map created before 1927 carries these latitudinal inaccuracies with it, according to the Polaris Project of the Physics and Astronomy Department, Iowa State (2000; http://www.polaris.iastate.edu/NorthStar/Unit7/unit7_sub1.htm).

Longitude also proved to be somewhat difficult to calculate. Longitude is calculated from the sun's position at noon to the sun's position at the reference time. It has been deduced that the earth rotates 15 degrees per hour (360 degree rotation/ 24 hours

and 1 degree = 60 minutes), which has its own fixed errors. Accuracy in clocks is especially important because knowing the local time was essential in determining longitude (Stern, 2004).

Two other inaccuracies come into play when using a hand-drawn map instead of a satellite image. Sources of hand-drawn maps for this research included atlases, military files, and files from state archives. Such drawings tended to be a common way to depict the landscape in the early-to-mid 20th century, which in this case, comprise the majority of this dataset. In addition to coordinate inaccuracies, the problem that occurs with these hand-drawn maps has to do with scale and the mapping method. These unknowns inherently insert inaccuracies into the image. Furthermore, the drawings were not consistent between cartographers. Each drawing was specifically constructed, thus adding to the inaccuracies.

Excellent examples of cartographers' differing perspectives of one location at one time can be seen in maps from the Civil War, particularly in maps from January 15, 1865. Fort Fisher was an active Confederate military base until January 15, 1865, when Union forces overran the Confederate Army and captured the fort. Many maps depict the battles that occurred at the fort on and before that day, and therefore, were analyzed closely in an attempt to determine if they provide an accurate representation of the area's landscape. If the land west and north of the fort was an Estuary, Low marsh, or an Intermediate marsh, soldiers approaching the fort from those directions would not have been able to attack. Union tactics were dictated by the understanding that this terrain was passable by a large body of infantry.

Two battles occurred at Fort Fisher, and their accounts seem to be consistent with

most of the contemporary maps. The first attack of infantry occurred over Christmas in 1864. The battle began on December 24, 1864 when Union ships bombarded Fort Fisher from the sea. The next day, Union troops made landfall on Federal Point, somewhere between Sugar Loaf and Fort Fisher. After an initial firefight, Union troops proceeded on land southward toward Fort Fisher. Union troops made their way to Howard's Hill where they were able to establish a command post at Battery Holland and get within 68 meters of Shepherd's Battery, opposite the fort's western salient. Union troops stopped progression there under Confederate artillery bombardment, forcing them to retreat back north to the Federal Point landing zone (Fort Fisher Civil War Site- National Historic Landmark- Fort Fisher Engagement Chronology, 2015).

The second attack occurred in mid-January 1865. On January 13, 1865, Union forces struck again. This time they began bombing the peninsula about four miles north of Fort Fisher and eventually made landfall on the beach of Federal Point. This landing point was described as a "narrow sand spit near Myrtle Sound about one mile north of the previous landing zone of December, 1864" (Fort Fisher Civil War Site- National Historic Landmark- Fort Fisher Engagement Chronology, 2015). By the morning of January 14 (Figures 83 and 119), Union troops had dug a line of entrenchments between Battery Anderson and the Cape Fear River. These entrenchments spanned the width of the peninsula. Union soldiers then proceeded southward. In the afternoon of January 15, the battle began (Figures 79-81 and 116-118). As Union Naval forces bombarded the fort from the sea, the Union Army reached the fort and entered through Shepherd Battery, crowding the fort from the north and west adjacent to the Estuary. Hours later, Confederate soldiers found themselves "battling behind walls" (Edling et al., 2005) and

were forced to retreat. As with the first attack, the soldiers advanced from the north, a seemingly viable way to approach, as shown by most of the maps (Figures 60 -70 and Figures 114 -121),

According to the maps and historians' accounts of the battles, it can be deduced that standing water or low marsh subenvironments were slowing or blocking the troops as they approached Fort Fisher from the north. This unconsolidated and wet ground would have rendered the terrain impassable for the troops.

However, not all of the maps showed that the location to the west and north of the fort was land (where Cores 4 and 5 were taken). Figures 78, 85, and 87 depict the landscape in this area as either an Estuary or Marsh. One reason for the conflicting information from the maps of that time period might be attributable to the cartographer. The accuracy of the maps could depend upon the cartographer's profession and position (possibly an engineer or a soldier from either the Confederate or Union side). Confederate forces tended to generate maps that were more accurate than the maps created by Union soldiers (Figure 87) because they were more familiar with the area and held the terrain at the time the fort was constructed. Because many of the maps from 1865 used in this study were created by one engineer, it was difficult to identify inaccuracies potentially introduced by maps created by other cartographers.

Another issue that arose with using old drawings was that they contained no associated spatial information; this may have contributed to the conflicting data yielded from the maps. To define spatial information, the initial maps and images had to be georeferenced. This process introduced additional inaccuracies to the already-inaccurate maps. Georeferencing, described in more detail in the Methods section of this thesis, is

the process of linking one image to a target image. This process is accomplished by defining “link points,” in which a point in the image matches a specific point in the target image. The first-order polynomial transformation, also known as an “affine” transformation, was selected as the georeferencing transformation method for this project (Environment Systems Research Institute et al., 2011).

An affine transformation shifts, scales, and rotates the image that is being georeferenced. Typically, the transformation ensures that straight lines in the georeferenced raster dataset are preserved in the final product. Consequentially, georeferencing with this affine transformation ignores other shapes such as squares, rectangles, and circles in the raster dataset. Therefore, during transformation, these shapes are changed into parallelograms using an arbitrary scale and preset angle orientation values. This slightly skews the resulting image. Depending upon the skew, the arbitrary values may have an adverse effect in determining the precise boundaries of a specific area in the map. Furthermore, an affine transformation does not assure local accuracy, as it is optimized to fit the image to a global scale (Environment Systems Research Institute et al., 2011).

Any given area of the map, especially if it was far from the defined link points, may have had a higher error-rate compared to the error-rate of the entire map. Moreover, if the control points that were used during the transformation were only defined in one section of the image, the resulting image was most likely skewed. The georeferenced links that were chosen in this study were extremely close to each other due to the limited number of points that could be used. The Fort Fisher region was a dynamic environment with a high sedimentation rate. Because much of the fort has now been eroded by

shoreline retreat, and the area west of the fort was marsh, it was extremely difficult to find static features to georeference. The points that were georeferenced were mostly structures that were built on Federal Point, including the corner of the Fort Fisher museum roof, Highway 421, the swash dam, and the gun parapets that remain. Each of these features was within a range of 3.2 kilometers, potentially rendering the georeferencing process inaccurate.

When the Foraminifera data was compared to these map results, to corroborate historians' accounts of these battles, issues arose regarding the comparison. Even though the Foraminifera content was analyzed for the core samples at every 2 centimeters, no depth that was analyzed corresponded exactly to the year 1865. The two analyzed depths that were closest to 1865 were the years 1858 and 1872. When comparing those years to the maps of 1865, data existed for Core 1 and Core 2 only. Consequently, the Foraminifera data was not helpful in validating the location of the battles that occurred at the fort, because Cores 4 and 5 were the most relevant cores because of their GPS coordinate locations (Figure 3). In both battles (as previously mentioned), Union forces attacked from the north, and would have had to pass over the areas of where Cores 4 and 5 were recovered.

Another explanation for why maps representing the same time period were mismatched with the microfossil findings, was that the core layers had been altered by some event (possibly a major storm or bioturbation), so the sediments found in the core layers do not accurately represent the environment that was present. This can be seen by the low numbers of Foraminifera that were observed down core in Core 1 and in Core 5. When the data was filtered, half of the depths in Core 1 and all of depths in Core 5 were

eliminated because an insufficient number of Foraminifera specimens were found.

Additionally, no storm deposits were found within the cores, and this most probably can be attributed to either bioturbation or the replenished sand.

While the Map data and Foraminifera data did not quite match, especially for the year 1865, the overall hypothesis and goal of this project was partially validated. Using Foraminifera to recreate paleo-subenvironments proved to be a viable method to determine historical landscapes through time, especially in areas and for time periods where maps did not exist. By analyzing the core samples for Foraminifera content in small increments, the subenvironments were distinguishable. Conversely, with the Map data, in many cases the subenvironments that were distinguishable included only the Land, Marsh, Fort and Estuary (Tables 5, 21, 22 and Figures 96-125). Therefore, the Foraminifera analysis, when enough data was found, provided more detailed results than the map analysis.

On the other hand, the second part of the hypothesis was not totally proven. Due to the limitations of the core samples that were analyzed for Foraminifera content, and the maps that were available for the study, the comparison of the two methods yielded inconclusive results. In many cases, the Foraminifera data (if available) did not correspond to the years of the maps that were used in the study. One example where this mismatch can be seen is in the year 1865. It was extremely difficult to match the maps that depicted Fort Fisher to the results of the Foraminifera data of the chronoequivalent period, because the Foraminifera content for that year and even that decade, did not exist (Tables 4-5, 7-11, and Figures 118-122). Consequently a precise comparison between the two methods could not be completed for 1865, so the map that most accurately

represented the environment of Fort Fisher during the Civil War could not be validated based solely on a comparison with the Foraminifera data. Nevertheless, the maps of 1865 that were created by an engineer in the Confederate Army, with the highest resolution, appeared to depict Fort Fisher most accurately (Figures 114-121). These maps tended to match the historians' accounts of the progression of the attacks that occurred at Fort Fisher more thoroughly (Figures 77, 79-82, 85, 87 and 114-121) compared to the other figures (78, 83, 84, 86) because they were easier to georeference.

Analyzing the subenvironments of Cores 4 and 5 were most important because they were taken from areas the Union soldiers would have had to pass over to begin attacking the fort by land. The high-resolution maps revealed that the subenvironment for the location of Core 4 during 1865 was either a Marsh (Table 26 and Figure 121), Estuary (Table 26 and Figure 114) or Land (Table 26 and Figures 115-120). As for Core 5, the maps demonstrated that the subenvironment was either a Marsh (Table 26 and Figures 114, 116-118), an Estuary (Table 26 and Figure 121) or Land (Table 26 and Figures 115, 119, 121). However, for both cores, these conclusions cannot be verified due to the lack of Foraminifera data from that time.

Thus, the most probable locations for Cores 4 and 5 came from computing the average subenvironments (Table 26 and in Figures 114-121) because the resulting average value accounted for all of the maps' conflicting data. The average value indicated that the subenvironment of Core 4 was in the Extreme High marsh, while the average value for Core 5 revealed that the subenvironment was High marsh, similar to Core 4. Therefore, based on the maps, the soldiers would have been able to attack on January 15, 1865 because the terrain would have been passable. Again, these results cannot be

validated by the Foraminifera method because the sedimentation rate was too high.

Analyzing the Foraminifera content by every centimeter instead of every two centimeters might have produced more conclusive results.

To counter this claim, while the Foraminifera content for that year and decade were missing for Cores 4 and 5, the trend in Cores 1 and 3 suggest that the region at that time was a Low/Extreme Low marsh subenvironment. Because the Fort Fisher marsh is in a tidal area, Union soldiers might have waited for low tide and then crossed the region and attacked. At low tide, the Extreme Low and Low marsh terrain might have been passable, especially if the moon was new. When reading the historians' account of the attacks, this scenario was not described, and can therefore be discarded. Additionally, due to the differences in the sediment movement within a marsh, the assumption that Cores 4 and 5 would demonstrate similar trends through time as those of Cores 1 and 3 cannot be supported.

Another time period where the Map and Foraminifera data conflicted (with more than a 1-meter difference in interpreted elevation) was in Core 1, from the years 1870-1984, and 1780-1860 (Tables 23 and 24). The most logical explanation for these differences is in the quality of the maps that were analyzed from those times. Core 1 was most likely subjected to more disturbances than the other cores due to its position, as it was the most western core taken (Figure 6). Therefore, access to high-resolution maps would be the only way to accurately track the change of Core 1's subenvironments through time. Unfortunately, many of the maps used for this analysis were of low-resolution, and therefore, it was difficult to distinguish between subenvironments (Figures 60, 62-66, 76-78, 83 and 90-95)

On the other hand, the two methods agreed the most regarding Core 3 from 1970-2013 (Figure 31), and in Core 2 from the same time period (Figure 30, 35,38). The Foraminifera data indicated that Core 2 was located in the High marsh while the Map data indicated that the location of Core 2 was on land. Because the elevation difference between those two subenvironments is minor, it can be assumed that the subenvironment of Core 2 through time did not fluctuate much. The most reasonable explanation for Core 2's lack of subenvironment fluctuation through time was that the area was protected by the hardened structures that were built to shield the fort. Core 2 was closest to the mainland (Figure 6), so the sediment was most likely accumulating more rapidly in that area than in the others, allowing the elevation of land to stay constant. In addition, other maps that most supported the microfossil interpretations were high-resolution satellite images taken after the year 2000, because that was when the technology to obtain these photographs became more widely available (Figures 46-58).

Overall, the Foraminifera method yielded more accurate data than the maps. However, when analyzing the core samples for Foraminifera content, smaller sampling increments would have been more useful to totally validate this study's hypothesis. Due to the lack of Foraminifera content for Cores 4 and 5, the hypotheses and goals of this study were only partially verified.

CONCLUSION

The research in this thesis focused on the use of Foraminifera to determine paleo-subenvironments and to quantify changes in the subenvironments through time at Fort Fisher, North Carolina (a Confederate military fortification south of Wilmington). Eight modern surface samples were collected from various subenvironments surrounding the Fort Fisher Historical site. These modern samples were compared to 98 samples taken from five cores from the marsh fringe west of Fort Fisher. Historical maps were assessed with respect to the subenvironmental changes through time. These maps were then compared to the Foraminifera taxa found in the 98 samples to verify historians' accounts of battles that occurred at Fort Fisher during the American Civil War (1861- 1865), and the indicated change in subenvironments in the cores through time.

Evidence from the study suggests that analyzing Foraminiferal assemblages was a viable method to determine paleo-subenvironments of each core through time. This method proved to be more accurate than using historical maps to depict the change in subenvironments through time. Old maps were merely educated estimates of the landscape's appearance. Additionally, georeferencing these maps added to these inaccuracies because the number of link points that were available to use were limited, and geographically close together. Therefore, analyzing Foraminifera enhanced the accuracy of maps and aided in historical interpretations of the landscape.

Furthermore, the study generated inconclusive results for validating the battles that occurred during the years 1864 and 1865. Cores 4 and 5 were the most important cores to analyze for this validation because they were taken from the area where the Union soldiers would have had to cross to begin attacking the fort by land. Foraminiferal assemblages that were analyzed in Cores 4 and 5 were not perfectly chronoequivalent to the maps depicting Fort Fisher during the year 1864 and 1865. Therefore, no analysis could be made because no data existed for these cores at those years.

On the other hand, the maps of 1865 disagreed on the terrain north and west of the fort. To account for these differences, the subenvironments that were shown on the maps were averaged yielding the Extreme High marsh subenvironment for Core 4 and the High marsh subenvironment for Core 5. Therefore, based on the maps, the soldiers would have been able to attack the fort on December 24, 1864 and January 15, 1865 because the terrain would have been passable. This conclusion however, could not be verified.

In summary, the hypothesis and goals of this study were only half validated. Better quality maps and more samples (analyzing the cores for Foraminifera content at every centimeter instead of every two centimeters) would have generated more convincing results.

REFERENCES

- Abbene, I., Culver, S., Corbett, R., Tully, L., & Buzas, M. (April 2006). Distribution of Foraminifera in Pamlico Sound, North Carolina over the Past Century. *Journal of Foraminifera Research*, Volume 36 Number 2. pages 135-151.
- Agency, N. G. (2005). Word Geodetic System 1984 (WGS84). Retrieved from Word Geodetic System 1984: www.unoosa.org/pdf/icg/2012/template/WGS_84.pdf.
- Board of Education. (1930). Fort Fisher, North Carolina [map]. Fort Fisher, North Carolina [map]. Retrieved from North Carolina State Archive. <http://www.ncdcr.gov/archives/Public/DigitalCollectionsandPublications.aspx>.
- Brew, J., & Row, Paternoster. (1781). Fort Fisher [map]. North Carolina. Retrieved from UNC Chapel Hill Library Collection. <http://www2.lib.unc.edu/dc/ncmaps>.
- Culver, S. J., & Horton, B. (2005). Infaunal marsh Foraminifera from the Outer Banks, North Carolina, USA. . *The Journal of Foraminiferal Research*, Volume 35 number 2 pages 148 - 170.
- Davis, G. M., Perry, L. C., & Kirkley, J. C. (1978). *The Official Military Atlas of the Civil War*. New York: Arno Press, Inc. and Crown Publishers Inc.
- Dennis, W. A. (1996). Fort Fisher Revetment Project. Wilmington, NC: US Army Corps of Engineers, Coastal, Hydrology and Hydraulics Section.
- Digital Globe. (2015). Fort Fisher, North Carolina [satellite].Retrieved from Google Earth.
- Digital Globe. (2014). Fort Fisher, North Carolina [satellite].Retrieved from Google Earth.
- Digital Globe. (2013). Fort Fisher, North Carolina [satellite].Retrieved from Google Earth.
- Digital Globe. (2011). Fort Fisher, North Carolina [satellite].Retrieved from Google Earth.
- Digital Globe. (2004). Fort Fisher, North Carolina [satellite].Retrieved from Google Earth.
- Dockal, J. A. (1996). The Coquinas of the Neuse Formation, New Hanover County, North Carolina. *Carolina Geological Society; Guidebook for 1996 Annual Meeting*, pages 9 - 18.

Engineering Department Bureau. (1865). Fort Fisher, North Carolina [map]. The Official Military Atlas of the Civil War.

ESRI. (September 22, 2008). ArcGIS 9.2 Desktop Help. Retrieved from http://webhelp.esri.com/arcgisdesktop/9.2/?TopicName=Georeferencing_a_raster_dataset

Hashbrouck, E. G. (2007). The Influence of Tidal Inlet Migration and Closure on Barrier Platform Changes: Federal Beach, North Carolina. Wilmington, North Carolina: Department of Geography and Geology, University of North Carolina at Wilmington.

Hayes, M. O. (1994). The Georgia Bight Barrier System. In R. Davis, *Geology of the Holocene Barrier Island Systems*. Springer Berlin Heidelberg. Pages 233-304.

Hippensteel, S., Martin, R., Nikitina, D., & Pizzuto, J. (October, 2000). The Formation of Holocene Marsh Foraminiferal Assemblages, Middle Atlantic Coast, U.S.A: Implications for Holocene Sea-level Change. *Journal of Foraminifera Research*, Volume 30, Number 4 pages 272- 293.

Horton, B. P., & Culver, S. J. (2008). Modern Intertidal Foraminifera of the Outer Banks, North Carolina, U.S.A., and their Applicability for Sea-Level Studies. *Journal of Coastal Research*: , Volume 24, Issue 5: pages 1110 – 1125.

Horton, B. P., Corbett, R., Culver, S. J., Edwards, R. J., & Hillier, C. (2006). Modern saltmarsh diatom distributions of the Outer Banks, North Carolina, and the development of a transfer function for high resolution reconstructions of sea-level. *Estuarine, Coastal and Shelf Science* , pages 381 -394.

Hyrne, Edward. (1749). Fort Fisher, North Carolina [map]. Retrieved from UNC Chapel Hill Library Collection. <http://www2.lib.unc.edu/dc/ncmaps>.

Iowa State University, Dept. of Physics and Astronomy. (2000 to 2001). Polaris Project. Retrieved from http://www.polaris.iastate.edu/NorthStar/Unit7/unit7_sub1.htm.

Kemp, A. C., Horton, B. P., & Culver, S. J. (2009). Distribution of modern salt-marsh foraminifera in the Albemarle-Pamlico estuarine system of North Carolina, USA: Implications for sea-level research. *Marine Micropaleontology*, Volume 72, pages 222 - 238.

Kemp, A., Horton, B., Vann, D., & Engelhart, S. (2012). Quantitative Vertical Zonation of Salt-Marsh Foraminifera for Reconstructing Former Sea-level; an example from New Jersey, USA. *Quaternary Science Reviews* 54, pages 26-39.

Mabry, J. (2009). Legal Tides. Retrieved from The North Carolina Coastal Resources Law, Planning and Policy Center: http://www.nccoastallaw.org/legaltides/lt_summer_09.pdf.

Magliocca, Nicholas R., McNamara, Dylan E., & A. Brad Murray (2011) Long-Term, Large-Scale Morphodynamic Effects of Artificial Dune Construction along a Barrier Island Coastline. (2011). *Journal of Coastal Research*: Volume 27, Issue 5: pages 918 – 930.

Moorefeild, T. (1978). *Geologic Processes and History of the Fort Fisher Coastal Area, North Carolina*. Greenville, NC: Department of Geological Sciences, East Carolina University.

Morton, R. A., & Miller, T. L. (2005). *National Assessment Of Shoreline Change: Part 2 Historical Shoreline Changes And Associated Coastal Land Loss Along The U.S. Southeast Atlantic Coast*. Charleston, SC; Petersburg, FL: Open-file Report- 140. U.S. Department of the Interior.

Moss Engraving Company. (1886). Fort Fisher, North Carolina [map]. Retrieved from UNC Chapel Hill Library Collection. <http://www2.lib.unc.edu/dc/ncmaps>.

National Aeronautics and Space Administration. (2006). Fort Fisher, North Carolina [satellite]. Retrieved from Google Earth.

National Oceanic Service. (2007). Nantional Oceanic and Atmospherical Administration Tidal Current Data for the Coastal United. Retrieved from National Oceanic and Atmospheric Administration:
<http://nosdataexplorer.noaa.gov/nosdataexplorer/explorer.jsp?goTo=search&north=90&s>.

New Hanover County. (2002). Fort Fisher, North Carolina [satellite].Retrieved from Google Earth.

New Hanover County. (1969). Fort Fisher, North Carolina [map].Retrieved from United States Geologic Survey. <http://www.usgs.gov/pubprod/>.

New Hanover County State Highway and Public Works Commission. (1938). Fort Fisher, North Carolina [map].Retrieved from North Carolina State Archive.
<http://www.ncdcr.gov/archives/Public/DigitalCollectionsandPublications.aspx>

New Hanover County State Highway and Public Works Commission. (1937). Fort Fisher, North Carolina [map].Retrieved from North Carolina State Archive.
<http://www.ncdcr.gov/archives/Public/DigitalCollectionsandPublications.aspx>

North Carolina State Archives, t. O.-C. (2007). North Carolina Maps. Retrieved from <http://www2.lib.unc.edu/dc/ncmaps/>.

O.W Gray & Son. (1882). Fort Fisher, North Carolina [map]. Retrieved from UNC Chapel Hill Library Collection. <http://www2.lib.unc.edu/dc/ncmaps>.

Pilkey, O. H., Neal, W. J., Riggs, S. R., Webb, C. A., & Bush, D. M. (2002). *The North Carolina Shore and Its Barrier Islands: Restless Ribbons of Sand*. Chapel Hill, NC: 1998 Duke University Publishing Press. Pages 100-344.

Riggs, S. R., Ames, V. D., Culver, S. J., & Mallinson, D. J. (2011). *The Battle For North Carolina's Coast*. University of North Carolina Press. 160 pages.

Riggs, S. R., & Ames, V.D. (December, 2003). *Drowning the North Carolina Coast: Sea Level Rise and Estuarine Dynamics*. North Carolina Sea Grant. North Carolina State University. Raleigh, North Carolina. 156 pages.
<http://core.ecu.edu/geology/riggs/DROWNING%20The%20NC%20Coast.pdf>.

Schulze, B. (June 29, 1998). Fort Fisher Site Photos. Retrieved from Civil War Album: http://www.civilwaralbum.com/misc8/fort_fisher_info.htm.

Scott, D. B., & Medioli, F. S. (1980). *Quantitative Studies of Marsh Foraminiferal Distributions in Nova Scotia; Implications for Sea-level Studies*. Special Publications-Cushman Foundation for Foraminiferal Research.

Scott, D., & Medioli, F. (1978). Vertical zonations of marsh foraminifera as accurate indicators of former sea-levels. *Nature* 272, pages 528 -531.

Schultze, Julian Otto. Private 15th N.Y.V. Federal Survey Engineer. (1865). *Battles at Fort Fisher, North Carolina* [maps]. Retrieved from UNC Chapel Hill Library Collection. <http://www2.lib.unc.edu/dc/ncmaps>.

Schultze, Julian Otto. Private 15th N.Y.V. Federal Survey Engineer. (1865). *Fort Fisher, North Carolina* [map]. Retrieved from CW Atlas.

Snedden, Robert Knox. *Union Force Solidier*. (1865). *Fort Fisher, North Carolina* [map]. Retrieved from UNC School of Education. <http://www.learnnc.org/lp/multimedia/12418>.

Soller, D. R. (1988). *Geology and Tectonic History of the Lower Cape Fear River Valley, Southeastern North Carolina*. Washington D.C. United States Government Printing Office.

Stern, D. P. (2004). *Latitude and Longitude History*. Web page, NASA, Goddard Space Flight Center, Greenbelt, Maryland.

Survey, U. S. Geology. (January 13, 2014). *Maps, Imagery, and Publications*.

Tanski, J. (2012: revised). *Long Island's Dynamic South Shore — A Primer on the Forces and Trends Shaping Our Coast*. New York Sea Grant. pages 1-27.

United States Army Engineering Department. (1863). Fort Fisher, North Carolina [map]. Retrieved from UNC Chapel Hill Library Collection.
<http://www2.lib.unc.edu/dc/ncmaps>.

United States Department of Agriculture. (2009). Fort Fisher, North Carolina [satellite]. Retrieved from Google Earth.

United States Department of Agriculture. (2008). Fort Fisher, North Carolina [satellite]. Retrieved from Google Earth.

United States Department of Commerce. (1921). Fort Fisher, North Carolina [map]. Retrieved from North Carolina State Archive.
<http://www.ncdcr.gov/archives/Public/DigitalCollectionsandPublications.aspx>

United States Department of Commerce. (1917). Fort Fisher, North Carolina [map]. Retrieved from North Carolina State Archive.
<http://www.ncdcr.gov/archives/Public/DigitalCollectionsandPublications.aspx>

United States Department of Commerce. (1915). Fort Fisher, North Carolina [map]. Retrieved from North Carolina State Archive.
<http://www.ncdcr.gov/archives/Public/DigitalCollectionsandPublications.aspx>

United States Department of Commerce. (1912). Fort Fisher, North Carolina [map]. Retrieved from North Carolina State Archive.
<http://www.ncdcr.gov/archives/Public/DigitalCollectionsandPublications.aspx>

United States Department of Commerce. (1910). Fort Fisher, North Carolina [map]. Retrieved from North Carolina State Archive.
<http://www.ncdcr.gov/archives/Public/DigitalCollectionsandPublications.aspx>

United States Department of Commerce. (1900). Fort Fisher, North Carolina [map]. Retrieved from North Carolina State Archive.
<http://www.ncdcr.gov/archives/Public/DigitalCollectionsandPublications.aspx>

United States Department of Commerce. (1897). Fort Fisher, North Carolina [map]. Retrieved from North Carolina State Archive.
<http://www.ncdcr.gov/archives/Public/DigitalCollectionsandPublications.aspx>.

United States Geological Survey. (2007). Fort Fisher, North Carolina [satellite]. Retrieved from Google Earth.

United States Geological Survey. (1999). Fort Fisher, North Carolina [satellite]. Retrieved from Google Earth.

United States Geological Survey. (1993). Fort Fisher, North Carolina [satellite]. Retrieved from Google Earth.

United States Geological Survey. (1980). Fort Fisher, North Carolina [map]. Retrieved from University of North Carolina Charlotte's Library Map Collection.

United States Geological Survey. (1974). Fort Fisher, North Carolina [map]. Retrieved from North Carolina State Archive.
<http://www.ncdcr.gov/archives/Public/DigitalCollectionsandPublications.aspx>.

United States Geological Survey. (1970). Fort Fisher, North Carolina [map]. Retrieved from University of North Carolina Charlotte's Library Map Collection.

United States Geological Survey. (1946). Fort Fisher, North Carolina [map]. Retrieved from United States Geologic Survey. <http://www.usgs.gov/pubprod/>.

United States Navy Department. (1861). Fort Fisher, North Carolina [map]. Retrieved from University of North Carolina Charlotte's Library Map Collection.

United States Navy Department. (1821). Fort Fisher, North Carolina [map]. Retrieved from University of North Carolina Charlotte's Library Map Collection.

Unknown Author. (1870). Fort Fisher, North Carolina [map]. Retrieved from North Carolina State Archive.
<http://www.ncdcr.gov/archives/Public/DigitalCollectionsandPublications.aspx>.

Unknown Author. (1833). Fort Fisher, North Carolina [map]. Retrieved from University of North Carolina Charlotte's Library Map Collection.

Unknown Author. (1770). Fort Fisher, North Carolina [map]. Retrieved from University of North Carolina Charlotte's Library Map Collection.

Unknown Author. (1733). Fort Fisher, North Carolina [map]. Retrieved from University of North Carolina Charlotte's Library Map Collection.

Xia, M., Xie, L., Peng, M., & Pietrafesa, L. J. (2008). A Numerical Study of Storm Surge in Cape Fear River Estuary and Adjacent Coast. *Journal of Coastal Research*, pages 159 - 167.

APPENDIX A: LEGISLATIVE ISSUES REGARDING KURE BEACH

Kure Beach, which lies just north of the Fort Fisher beach, is more prone to erosion than any other beach in the area because of legislative rulings and human anthropogenic structures that have been built on and near it during the last two decades. This Appendix will explain why erosion on this beach has accelerated, and why it is relevant.

Kure Beach, only 2 square kilometers, is home to a set of condominiums that were built by a private company called Riggings, in 1985. The beach had been subject to typical erosion from storms and sea-level rise like the other beaches in the surrounding area, but began to see an accelerated increase in erosion rates in the late 1990s compared to nearby beaches. The Riggings condominium complex, located north of the 1996 sea wall at Fort Fisher (built when the CAMA act passed) and just south of the once-exposed coquina outcrop, began to experience an increase in wave energy due to the sea wall construction and the missing natural protective rocks. A second reason why the condominium complex on Kure Beach was experiencing accelerated erosion was because a beach nourishment project completed by the USACE in 2000 actually stopped about 1,500 feet away from the condominiums. (Another beach nourishment project, completed in 2003, also stopped just feet from the condominium complex.) This was the only part of Kure Beach that had not been artificially fortified to protect the land against the sea. When the Riggings company questioned why the USACE did not extend the beach nourishment projects to the condominiums, USACE responded by saying that any exposed coquina rock is an area of “natural heritage” in North Carolina. Consequently, exposed coquina just off shore of the condos’ location caused USACE to deem that

burying the rock under sand would be an "unacceptable alternative." Therefore, the two beach nourishment projects were not extended further along Kure Beach.

Later in 2003, the North Carolina General Assembly reiterated the ban on permanent, hardened structures by allowing the use of temporary sandbags to reduce the erosion rate near imminently threatened structures. The rule deemed that a structure is "imminently threatened" if the erosion scarp is as close as 20 feet away from the structure, or if the structure is in danger due to conditions in the vicinity. In order to place sandbags around an "imminently threatened" structure, a permit is required.

So the Riggings company, in dire need of erosion control, purchased a permit allowing approximately 300 sandbags to be placed on Kure Beach to control erosion and to protect their apartment complexes from the sea (Mabry, 2009). The Fort Fisher beach was not in dire need of sandbags because the sea wall construction in 1996 had more or less stabilized erosion rates in that area.

This 2003 sandbags law contained distinct rules about the size, placement, and the length of time the sandbags were supposed to be placed on the beach (Mabry, 2009). These strict rulings, especially a five-year sandbag lifespan caveat, eventually led to the big Riggings court case between the company and the North Carolina Coastal Resource Commission.

With the exception of the Riggings case, this rule has not been consistently enforced. To date, 369 temporary sandbags remain on North Carolina's coastline, where about 123 of them have been in place for more than five years (Mabry, 2009).

APPENDIX B: TABLES AND MAPS FOR RESULT SECTION 5.1

TABLE 25: A table indicating the figure number, year, publisher, and source of each that was used in this study.

Figure #	Year	Cartographer	Source	Figure #	Year	Cartographer	Source	Figure #	Year	Cartographer	Source
29	2015	Digital Globe	Google Earth	58	1882	O.W. Gray & Son	UNC Chapel Hill Library Collection	79	2015	Digital Globe	Google Earth
30	2014	Digital Globe	Google Earth	59	1870	Unknown	NC State Archive	80	2013	Digital Globe	Google Earth
31	2013	Digital Globe	Google Earth	60	1865	Federal Survey Engineer Otto Julian Schultze Private 15th N.Y.V	UNC Chapel Hill Library Collection	81	2009	USDA Farm Survey	Google Earth
32	2011	Digital Globe	Google Earth	61	1865	Federal Survey Engineer Otto Julian Schultze Private 15th N.Y.V	UNC Chapel Hill Library Collection	82	2006	NASA	Google Earth
33	2010	Digital Globe	Google Earth	62	1865	Federal Survey Engineer Otto Julian Schultze Private 15th N.Y.V	UNC Chapel Hill Library Collection	83	2002	New Hanover County	Google Earth
34	2009	USDA Farm Survey	Google Earth	63	1865	Federal Survey Engineer Otto Julian Schultze Private 15th N.Y.V	UNC Chapel Hill Library Collection	84	1999	USGS	Google Earth
35	2008	USDA Farm Survey	Google Earth	64	1865	Federal Survey Engineer Otto Julian Schultze Private 15th N.Y.V	UNC Chapel Hill Library Collection	85	1993	USGS	Google Earth
36	2007	USGS	Google Earth	65	1865	Federal Survey Engineer Otto Julian Schultze Private 15th N.Y.V	UNC Chapel Hill Library Collection	86	1980	USGS	USGS
37	2006	NASA	Google Earth	66	1865	Federal Survey Engineer Otto Julian Schultze Private 15th N.Y.V	UNC Chapel Hill Library Collection	87	1974	USGS	NC State Archive
38	2004	Digital Globe	Google Earth	67	1865	Federal Survey Engineer Otto Julian Schultze Private 15th N.Y.V	UNC Chapel Hill Library Collection	88	1970	USGS	UNCC Library Collection
39	2002	New Hanover County	Google Earth	68	1865	Federal Survey Engineer Otto Julian Schultze Private 15th N.Y.V	UNC Chapel Hill Library Collection	89	1946	USGS	USGS
40	1999	USGS	Google Earth	68	1865	Federal Survey Engineer Otto Julian Schultze Private 15th N.Y.V	CW Atlas	90	1921	Department of Commerce	NC State Archive
41	1993	USGS	Google Earth	69	1865	Robert Knox Sneden	UNC School of Education	91	1917	Department of Commerce	NC State Archive
42	1980	USGS	UNCC Library Collection	70	1865	Engineering Department Bureau	The Official Military Atlas of the Civil War	92	1915	Department of Commerce	NC State Archive
43	1974	USGS	NC State Archive	71	1863	US Army Engineering Department	UNC Chapel Hill Library Collection	93	1912	Department of Commerce	NC State Archive
44	1970	USGS	UNCC Library Collection	72	1863	US Army Engineering Department	UNC Chapel Hill Library Collection	94	1910	Department of Commerce	NC State Archive
45	1969	New Hanover County	USGS	73	1861	US Navy Department	UNCC Library Collection	95	1900	Department of Commerce	NC State Archive
46	1946	USGS	USGS	74	1833	Unknown	UNCC Library Collection	96	1897	Department of Commerce	NC State Archive
47	1938	New Hanover County State Highway and Public Works Commission	UNC Chapel Hill Library Collection	75	1821	US Navy Engineering Department	NC State Archive	97	1865	Federal Survey Engineer Otto Julian Schultze Private 15th N.Y.V	UNC Chapel Hill Library Collection
48	1937	New Hanover County State Highway and Public Works Commission	NC State Archive	76	1770	Unknown	UNCC Library Collection	98	1865	Federal Survey Engineer Otto Julian Schultze Private 15th N.Y.V	UNC Chapel Hill Library Collection
49	1930	Board of Education	NC State Archive	77	1749	Edward Hyne	UNC Chapel Hill Library Collection	99	1865	Federal Survey Engineer Otto Julian Schultze Private 15th N.Y.V	UNC Chapel Hill Library Collection
50	1921	Department of Commerce	NC State Archive	78	1733	Unknown	UNCC Library Collection	100	1865	Federal Survey Engineer Otto Julian Schultze Private 15th N.Y.V	UNC Chapel Hill Library Collection
51	1917	Department of Commerce	NC State Archive					101	1865	Federal Survey Engineer Otto Julian Schultze Private 15th N.Y.V	UNC Chapel Hill Library Collection
52	1915	Department of Commerce	NC State Archive					102	1865	Federal Survey Engineer Otto Julian Schultze Private 15th N.Y.V	UNC Chapel Hill Library Collection
53	1912	Department of Commerce	NC State Archive					103	1865	Engineering Department Bureau	CW Atlas
54	1910	Department of Commerce	NC State Archive					104	1865	Federal Survey Engineer Otto Julian Schultze Private 15th N.Y.V	UNC Chapel Hill Library Collection
55	1900	Department of Commerce	NC State Archive					105	1864	US Navy Department	The Official Military Atlas of the Civil War
56	1897	Department of Commerce	NC State Archive					106	1863	US Army Engineering Department	UNC Chapel Hill Library Collection
57	1886	Moss Engraving Co.	UNC Chapel Hill Library Collection					107	1863	US Army Engineering Department	UNC Chapel Hill Library Collection
								108	1781	J. Bew, Paternoster Row	UNC Chapel Hill Library Collection

TABLE 26: A table indicating the change in the subenvironments for all the cores through time. This table was produced using a Python script, which automated the process of intersecting the sample locations to the boundaries of each year and then joining the tables.

Year	FF01	FF02	FF03	FF04	FF05
2015	Ex Low, Low, Int Marsh	High, Ex High Marsh	High, Ex High Marsh	Land	Land
2013	Ex Low, Low, Int Marsh	High, Ex High Marsh	High, Ex High Marsh	Land	Land
2009	Ex Low, Low, Int Marsh	High, Ex High Marsh	High, Ex High Marsh	Land	Land
2006	Ex Low, Low, Int Marsh	High, Ex High Marsh	High, Ex High Marsh	Land	Land
2002	Ex Low, Low, Int Marsh	High, Ex High Marsh	High, Ex High Marsh	Land	Land
1999	Ex Low, Low, Int Marsh	High, Ex High Marsh	High, Ex High Marsh	Land	Land
1993	Ex Low, Low, Int Marsh	High, Ex High Marsh	High, Ex High Marsh	Land	Land
1980	Ex Low, Low, Int Marsh	High, Ex High Marsh	High, Ex High Marsh	Land	Land
1974	Marsh	Marsh	Marsh	Marsh	Marsh
1970	Ex Low, Low, Int Marsh	High, Ex High Marsh	High, Ex High Marsh	Land	Land
1946	Land	Land	Land	Land	Land
1921	Land	Land	Land	Land	Land
1917	Land	Land	Land	Land	Land
1915	Land	Land	Land	Land	Land
1912	Land	Land	Land	Land	Land
1910	Land	Land	Land	Land	Land
1900	Land	Land	Land	Land	Land
1897	Land	Land	Land	Land	Land
1870	Land	Land	Land	Land	Land
Jan 15 1865	Land	Land	Estuary	Estuary	Marsh
Feb 1865	Land	Land	Land	Land	Land
9PM Jan 15 1865	Land	Land	Land	Land	Marsh
6PM Jan 15 1865	Land	Land	Land	Land	Marsh
3PM Jan 15,1985	Land	Land	Land	Land	Marsh
1865 Atlas	Land	Land	Estuary	Land	Land
1865	Land	Land	Land	Land	Land
1865	Land	Land	Estuary	Marsh	Estuary
1864	High Marsh	High Marsh	Low Marsh	Low Marsh	Low Marsh
1863	Estuary	Estuary	Estuary	Land	Land
1863	Land	Estuary	Estuary	Estuary	Land
1781	Land	Land	Land	Land	Land
1770	Marsh	Marsh	Marsh	Marsh	Marsh
1749	Marsh	Marsh	Marsh	Marsh	Marsh
1733	Marsh	Marsh	Marsh	Marsh	Marsh

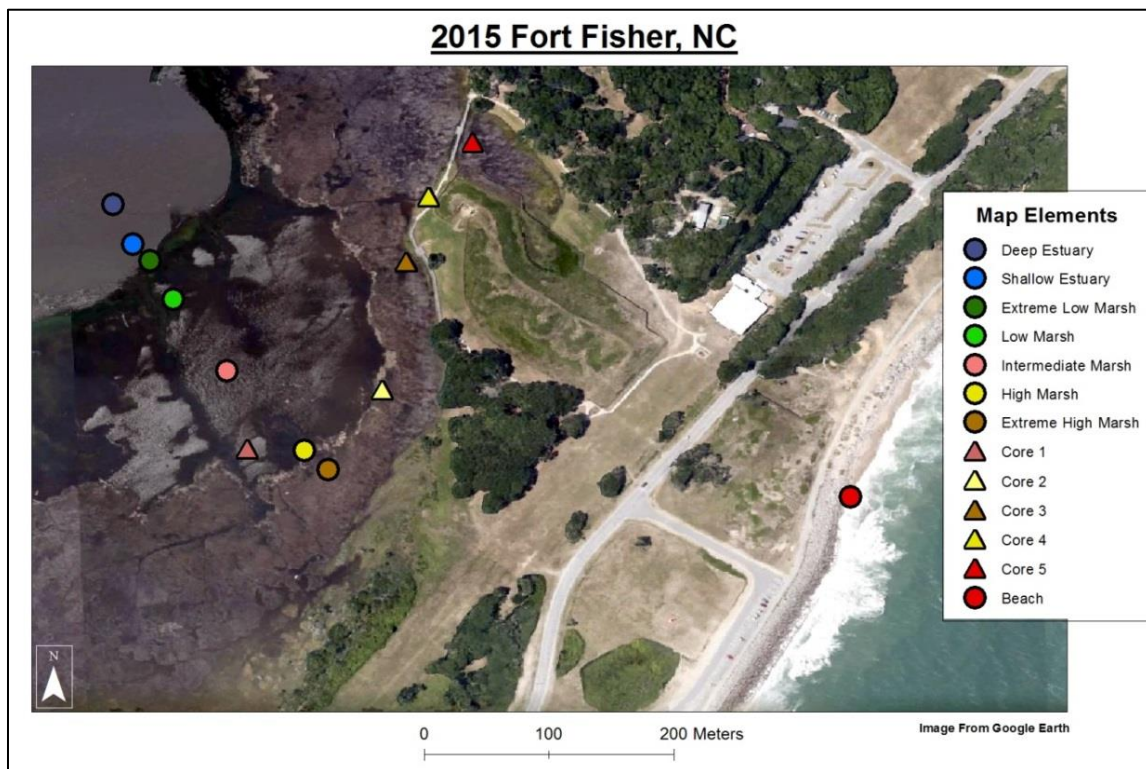


FIGURE 46: A map from 2015 showing the locations of the five core and eight surface samples that were taken adjacent to Fort Fisher. The core samples are shown by triangles and are color-coded to match the subenvironments of the surface samples that are represented by circles. Note: All samples and cores were recovered outside of the Fort Fisher Historical Site state property.

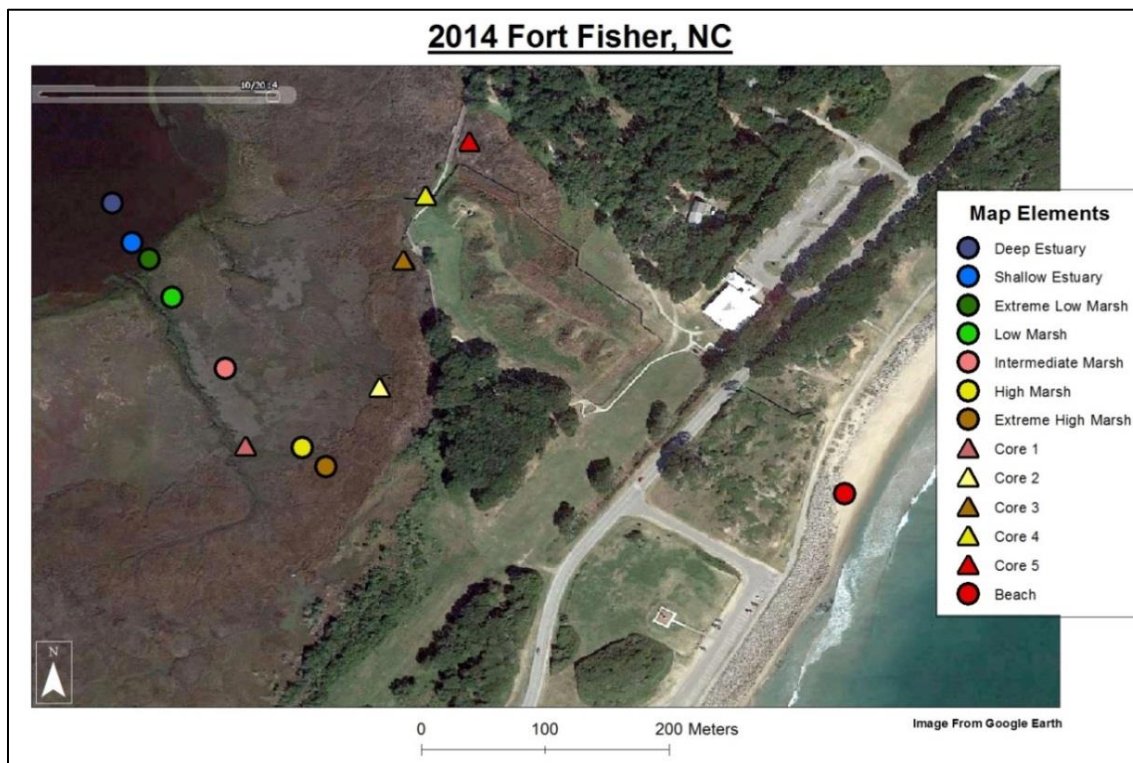


FIGURE 47: A map of 2014 showing the locations of the five core and eight surface samples that were taken adjacent to Fort Fisher. The core samples are shown as triangles and are color-coded to match the subenvironments of the surface samples that are represented by circles. Note: All samples and cores were recovered outside of the Fort Fisher Historical Site state property.

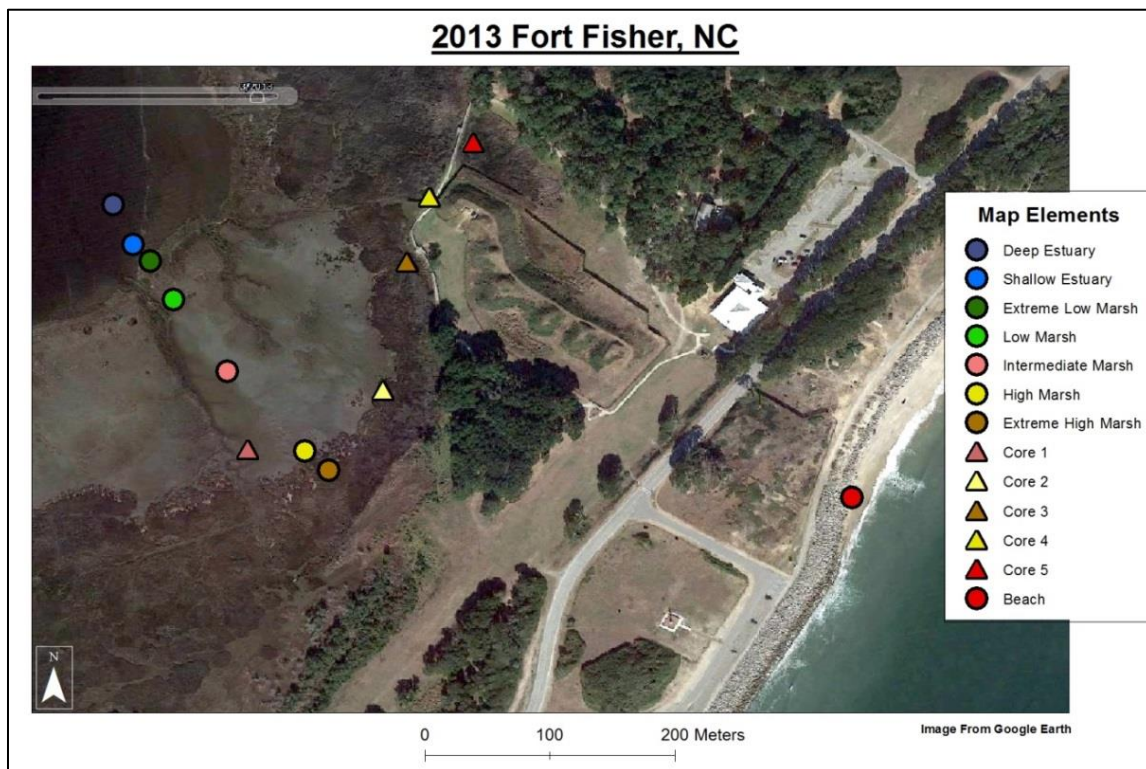


FIGURE 48: A map of 2013 showing the locations of the five core and eight surface samples that were taken adjacent to Fort Fisher. The core samples are shown by triangles and are color-coded to match the subenvironments of the surface samples that are represented by circles. Note: All samples and cores were recovered outside of the Fort Fisher Historical Site state property.

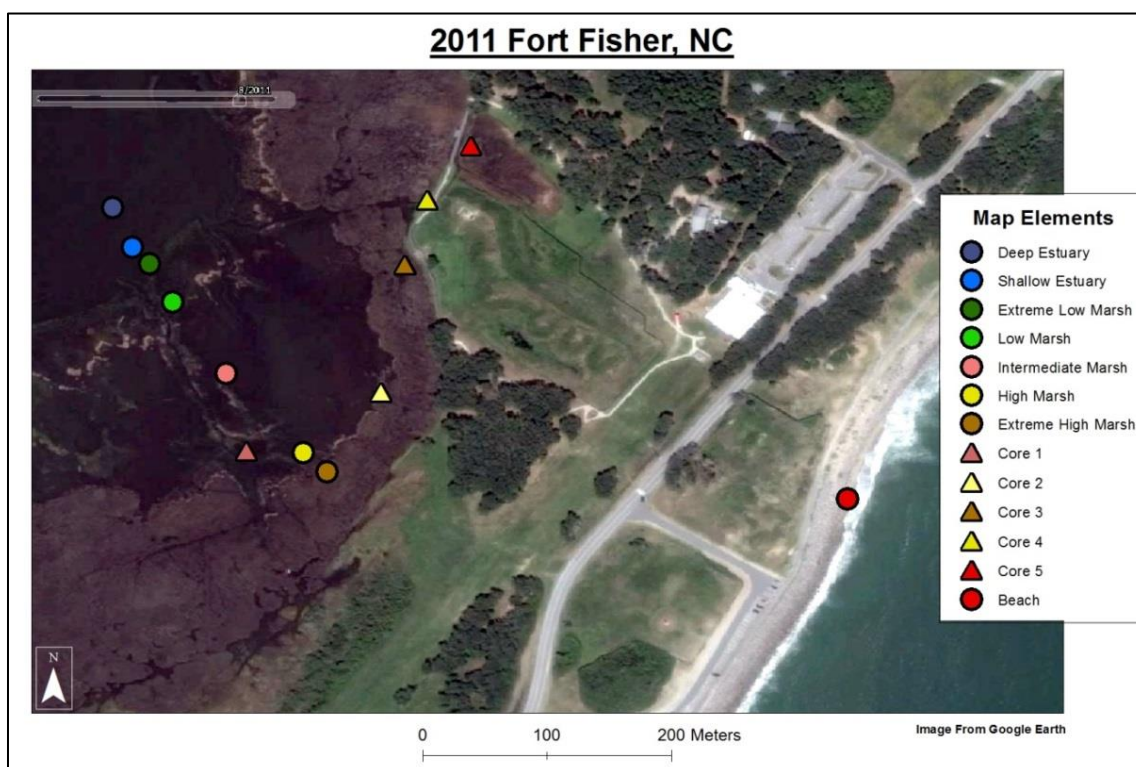


FIGURE 49: A map of 2011 showing the locations of the five core and eight surface samples that were taken adjacent to Fort Fisher. The core samples are shown by triangles and are color-coded to match the subenvironments of the surface samples that are represented by circles. Note: All samples and cores were recovered outside of the Fort Fisher Historical Site state property.

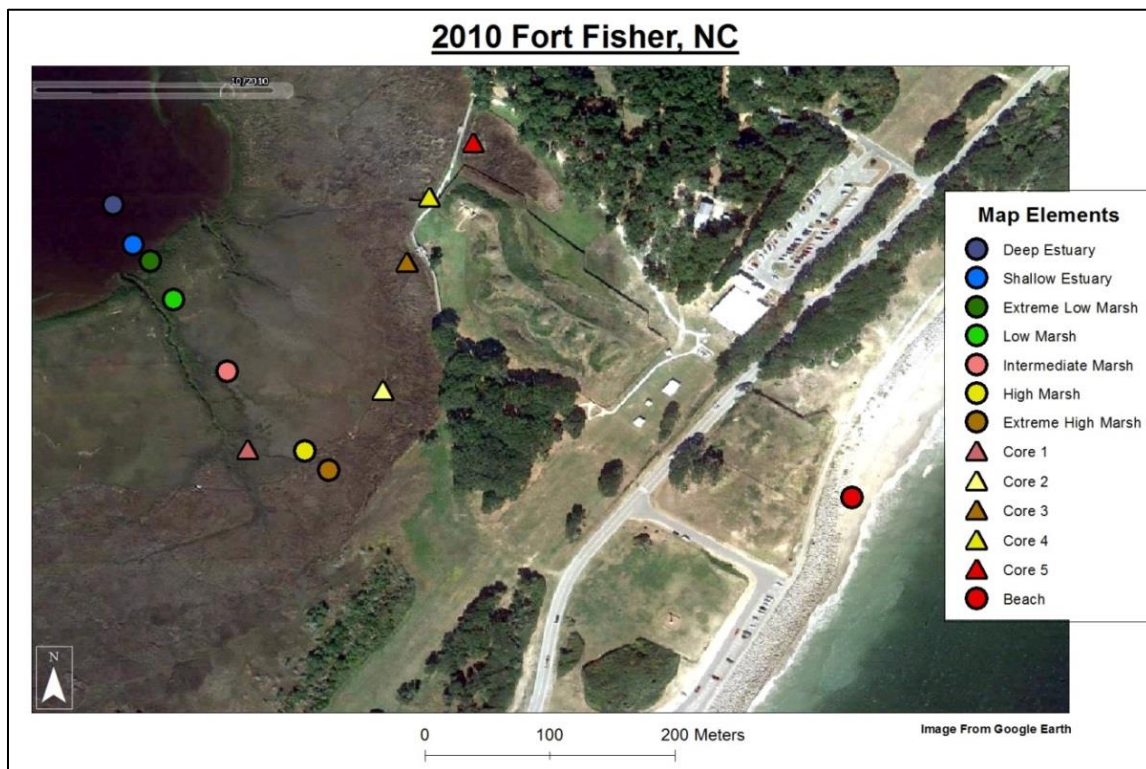


FIGURE 50: A map of 2010 showing the locations of the five core and eight surface samples that were taken adjacent to Fort Fisher. The core samples are shown by triangles and are color-coded to match the subenvironments of the surface samples that are represented by circles. Note: All samples and cores were recovered outside of the Fort Fisher Historical Site state property.

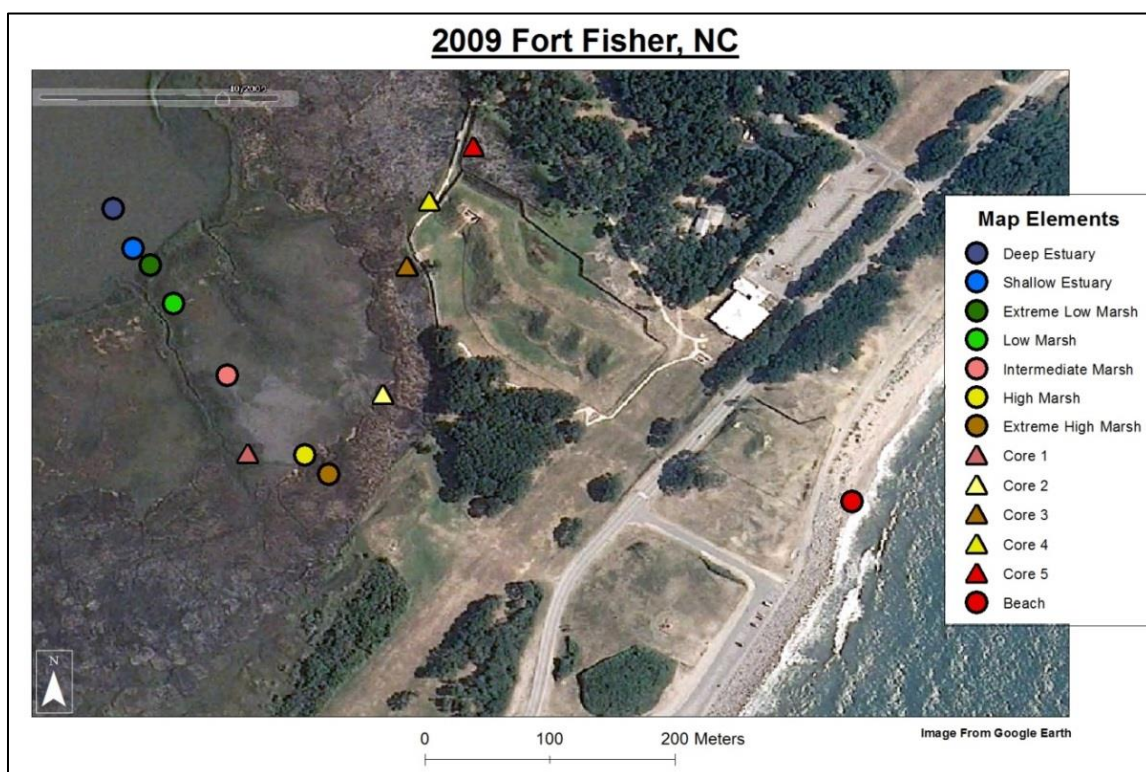


FIGURE 51: A map of 2009 showing the locations of the five core and eight surface samples that were taken adjacent to Fort Fisher. The core samples are shown by triangles and are color-coded to match the subenvironments of the surface samples that are represented by circles. Note: All samples and cores were recovered outside of the Fort Fisher Historical Site state property.

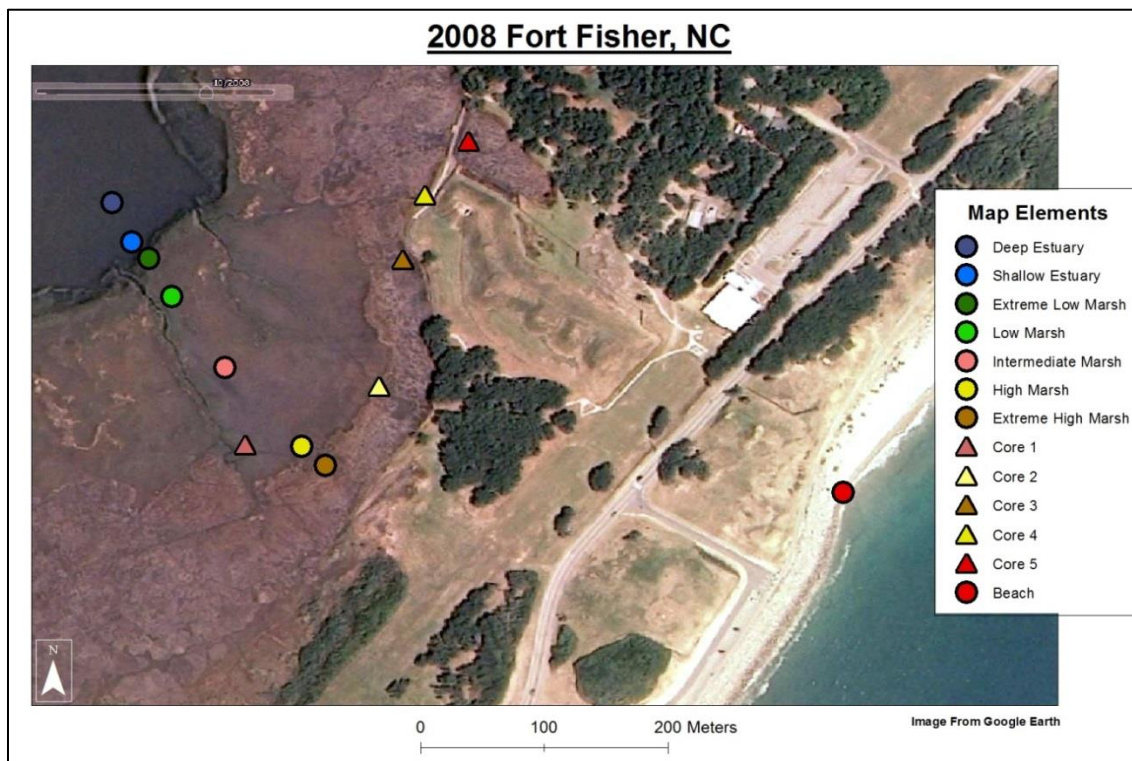


FIGURE 52: A map of 2008 showing the locations of the five core and eight surface samples that were taken adjacent to Fort Fisher. The core samples are shown by triangles and are color-coded to match the subenvironments of the surface samples that are represented by circles. Note: All samples and cores were recovered outside of the Fort Fisher Historical Site state property.

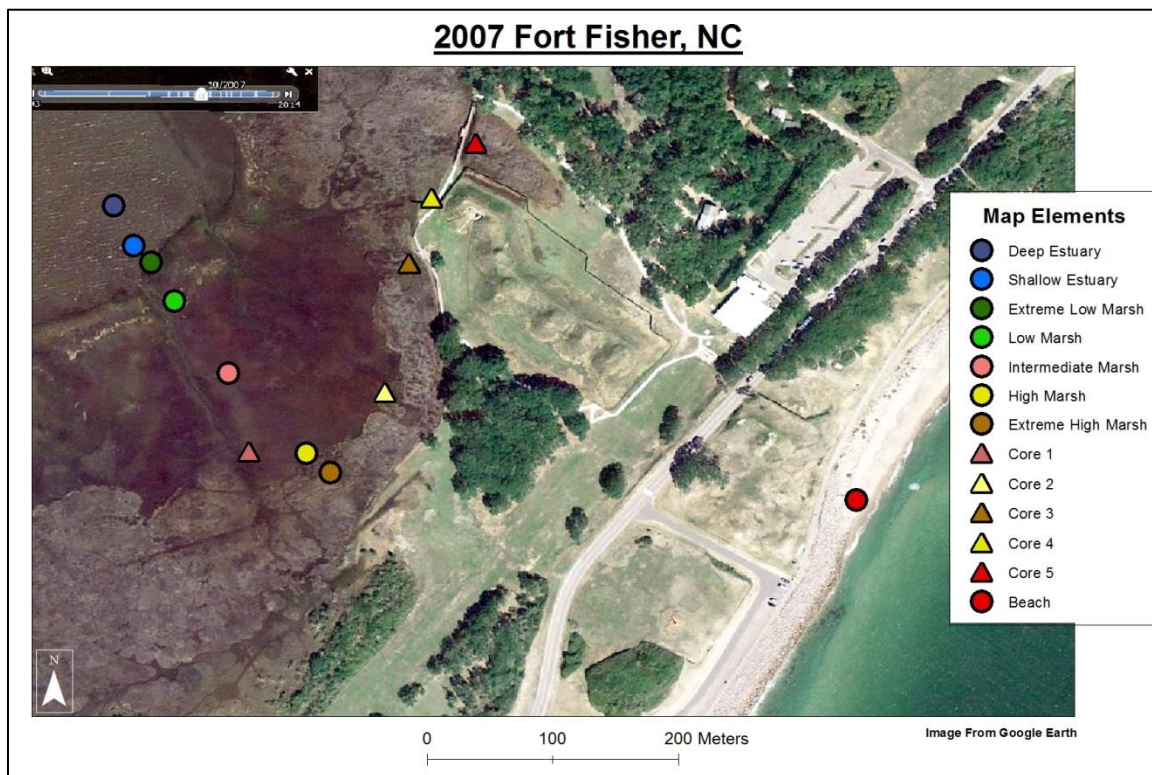


FIGURE 53: A map of 2007 showing the locations of the five core and eight surface samples that were taken adjacent to Fort Fisher. The core samples are shown by triangles and are color coded to match the subenvironments of the surface samples that are represented by circles. Note: All samples and cores were recovered outside of the Fort Fisher Historical Site state property.

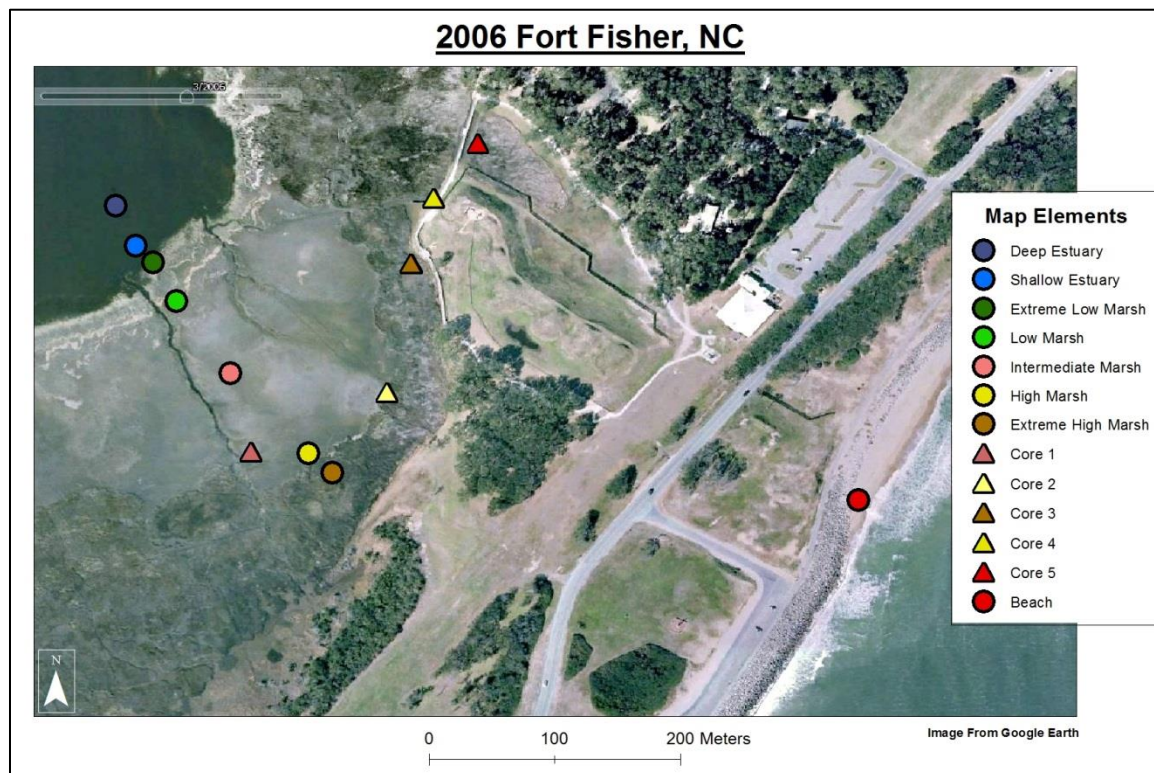


FIGURE 54: A map of 2006 showing the locations of the five core and eight surface samples that were taken adjacent to Fort Fisher. The core samples are shown by triangles and are color-coded to match the subenvironments of the surface samples that are represented by circles. Note: All samples and cores were recovered outside of the Fort Fisher Historical Site state property.

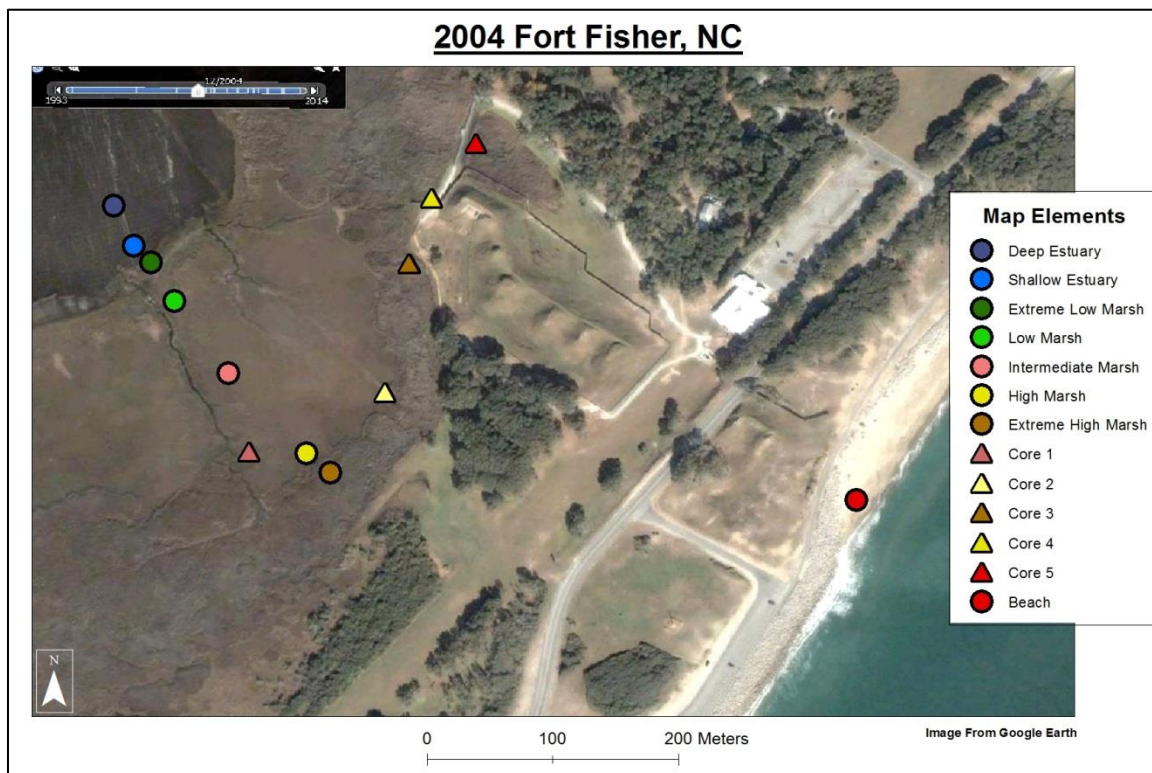


FIGURE 55: A map of 2004 showing the locations of the five core and eight surface samples that were taken adjacent to Fort Fisher. The core samples are shown by triangles and are color-coded to match the subenvironments of the surface samples that are represented by circles. Note: All samples and cores were recovered outside of the Fort Fisher Historical Site state property.

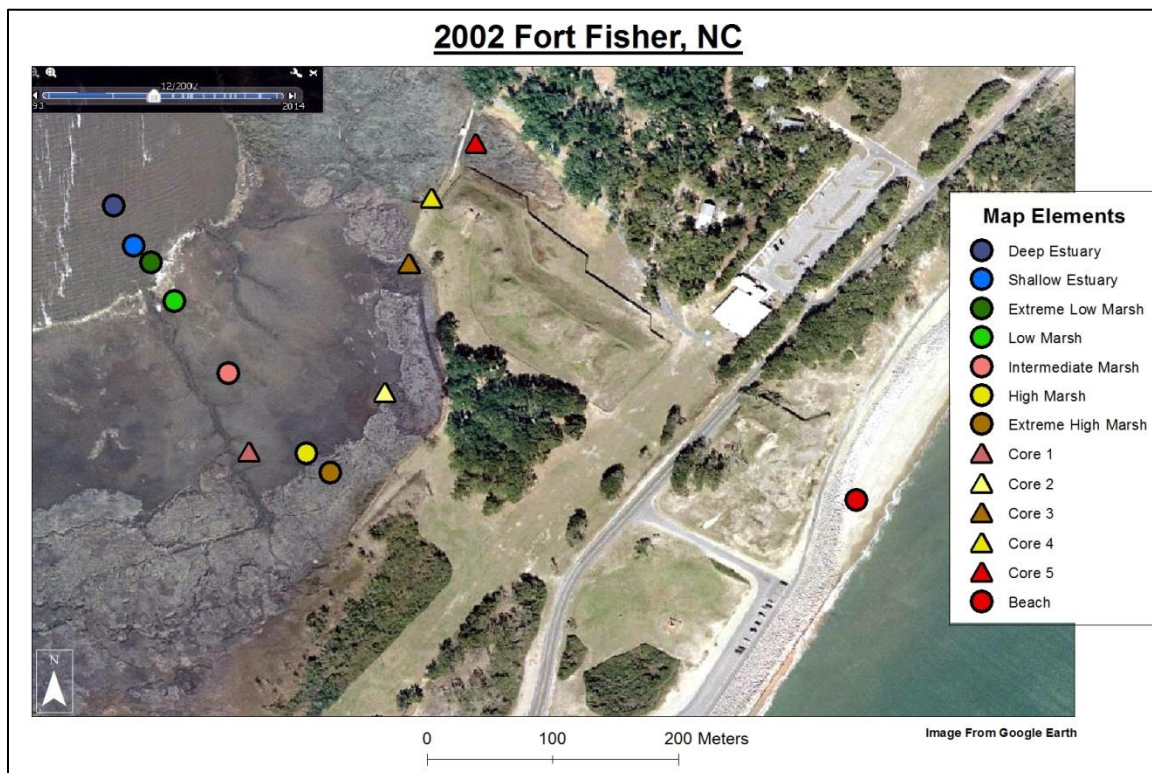


FIGURE 56: A map of 2002 showing the locations of the five core and eight surface samples that were taken adjacent to Fort Fisher. The core samples are shown by triangles and are color-coded to match the subenvironments of the surface samples that are represented by circles. Note: All samples and cores were recovered outside of the Fort Fisher Historical Site state property.

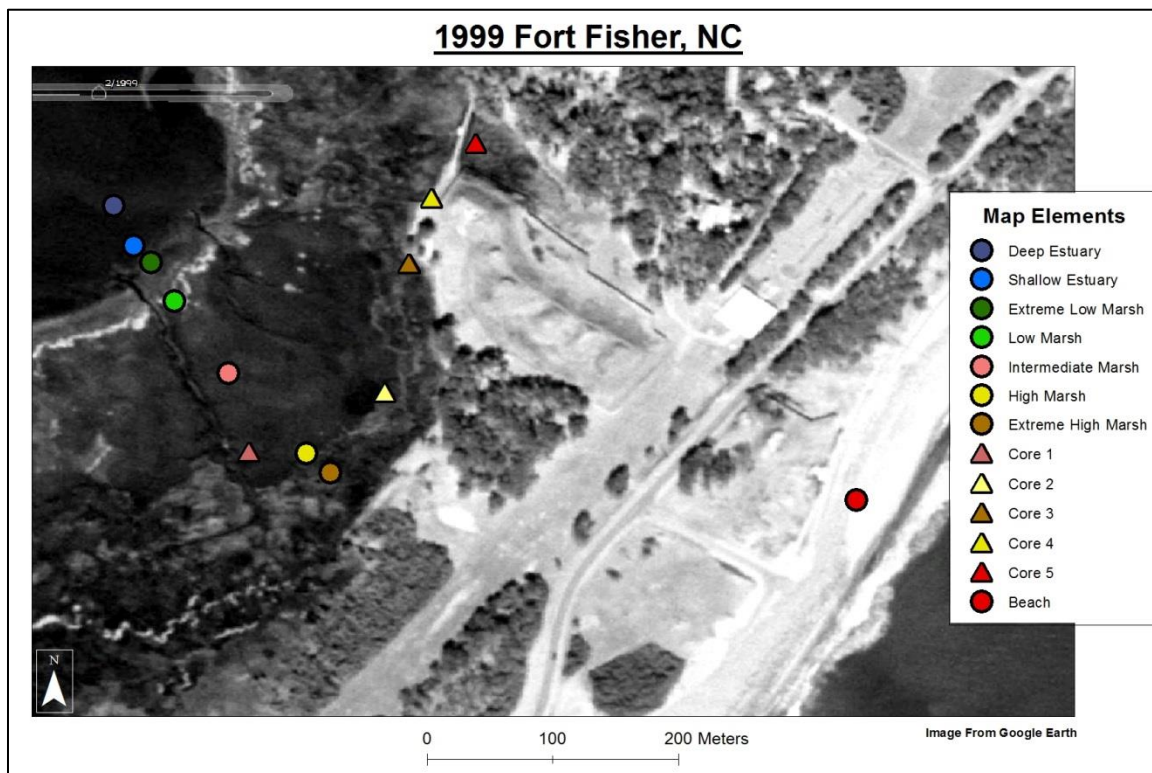


FIGURE 57: A map of 1999 showing the locations of the five core and eight surface samples that were taken adjacent to Fort Fisher. The core samples are shown by triangles and are color-coded to match the subenvironments of the surface samples that are represented by circles. Note: All samples and cores were recovered outside of the Fort Fisher Historical Site state property.

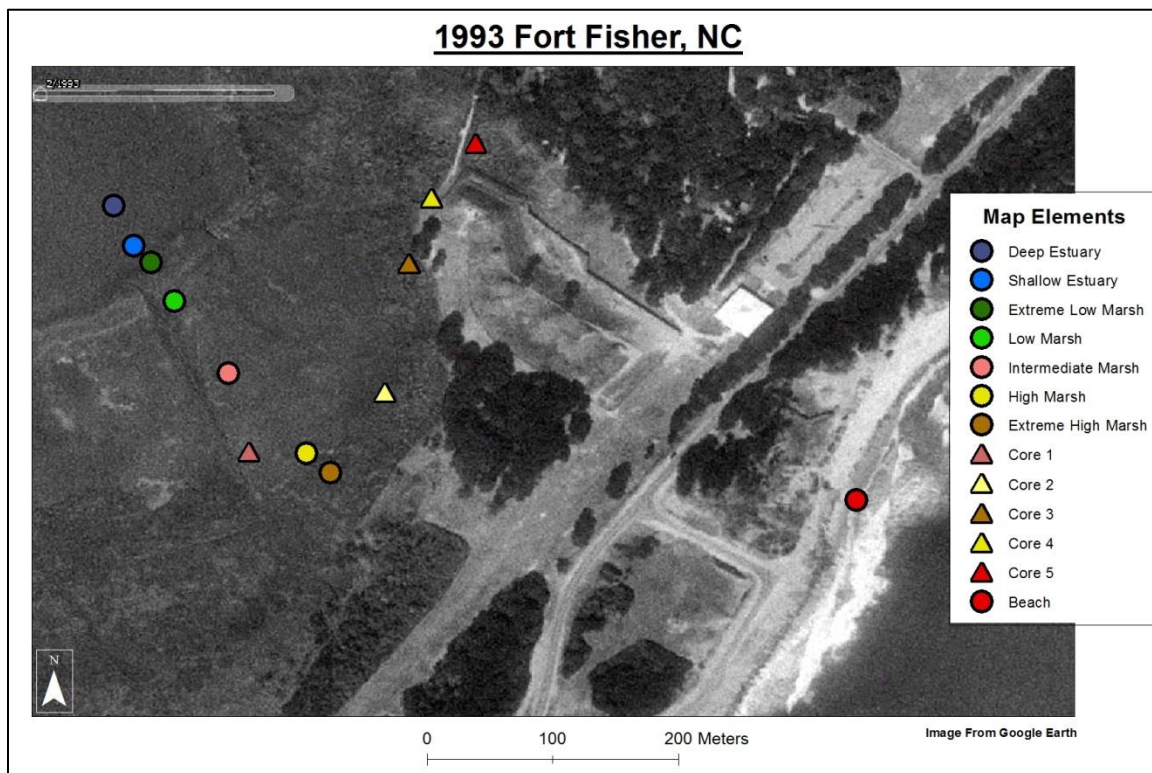


FIGURE 58: A map of 1993 showing the locations of the five core and eight surface samples that were taken adjacent to Fort Fisher. The core samples are shown by triangles and are color-coded to match the subenvironments of the surface samples that are represented by circles. Note: All samples and cores were recovered outside of the Fort Fisher Historical Site state property.

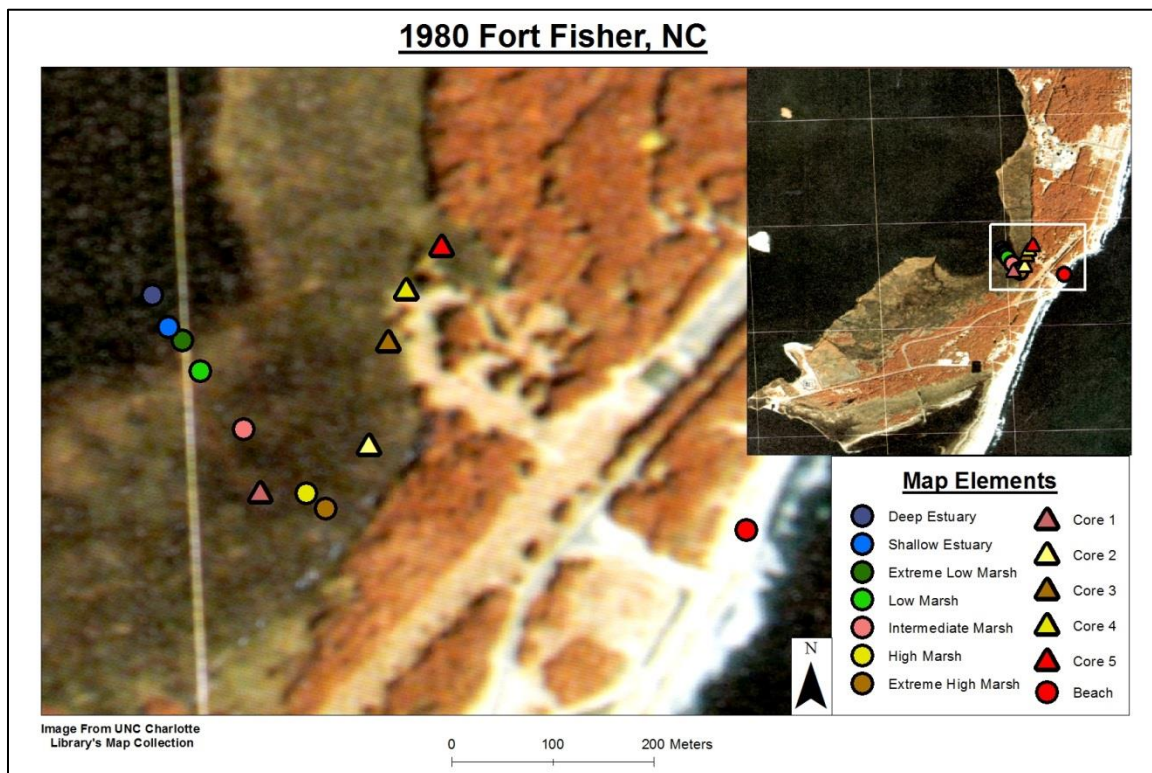


FIGURE 59: A map of 1980 showing the locations of the five core and eight surface samples that were taken adjacent to Fort Fisher. The core samples are shown by triangles and are color-coded to match the subenvironments of the surface samples that are represented by circles. Note: All samples and cores were recovered outside of the Fort Fisher Historical Site state property.

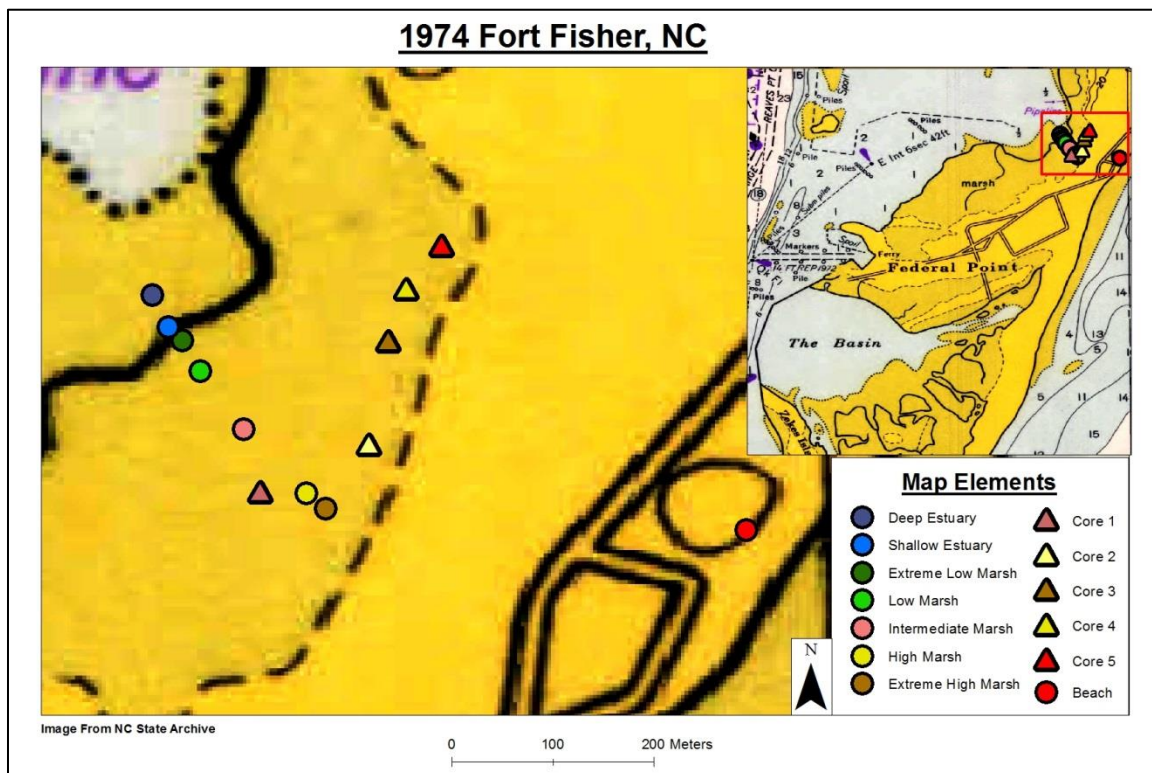


FIGURE 60: A map of 1974 showing the locations of the five core and eight surface samples that were taken adjacent to Fort Fisher. The core samples are shown by triangles and are color-coded to match the subenvironments of the surface samples that are represented by circles. Note: All samples and cores were recovered outside of the Fort Fisher Historical Site state property.

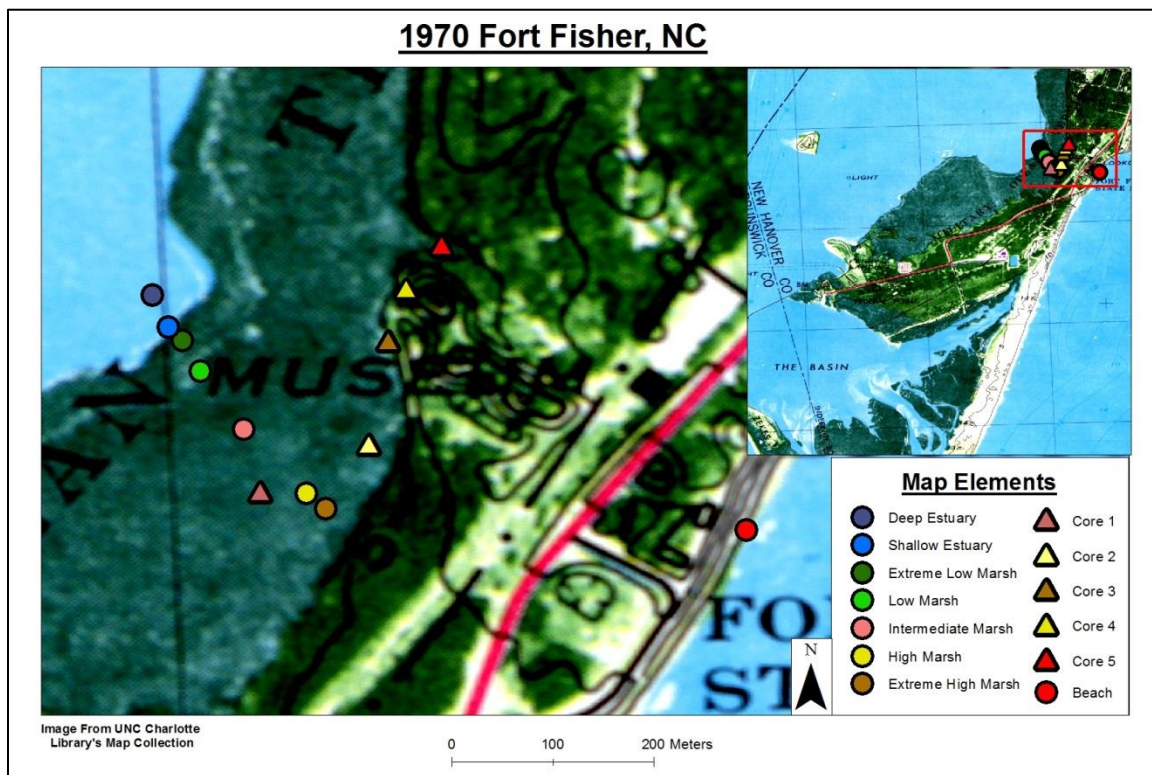


FIGURE 61: A map of 1970 showing the locations of the five core and eight surface samples that were taken adjacent to Fort Fisher. The core samples are shown by triangles and are color-coded to match the subenvironments of the surface samples that are represented by circles. Note: All samples and cores were recovered outside of the Fort Fisher Historical Site state property.

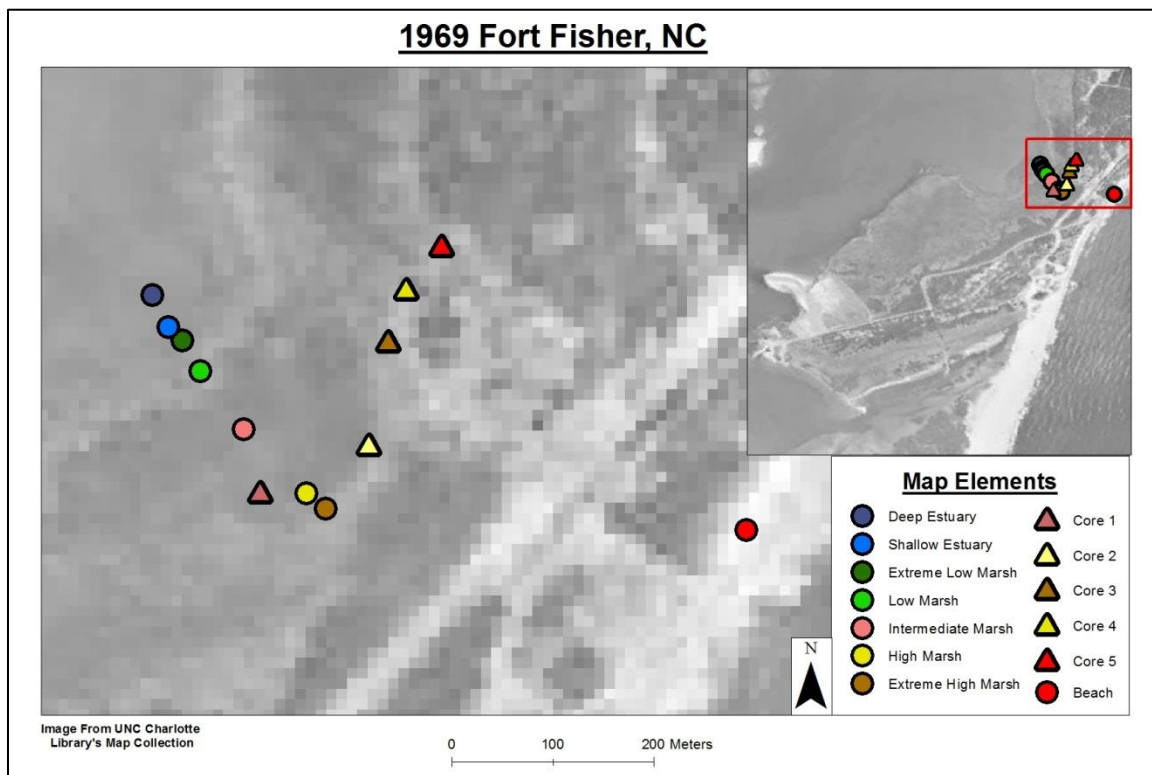


FIGURE 62: A map of 1969 showing the locations of the five core and eight surface samples that were taken adjacent to Fort Fisher. The core samples are shown by triangles and are color-coded to match the subenvironments of the surface samples that are represented by circles. Note: All samples and cores were recovered outside of the Fort Fisher Historical Site state property.

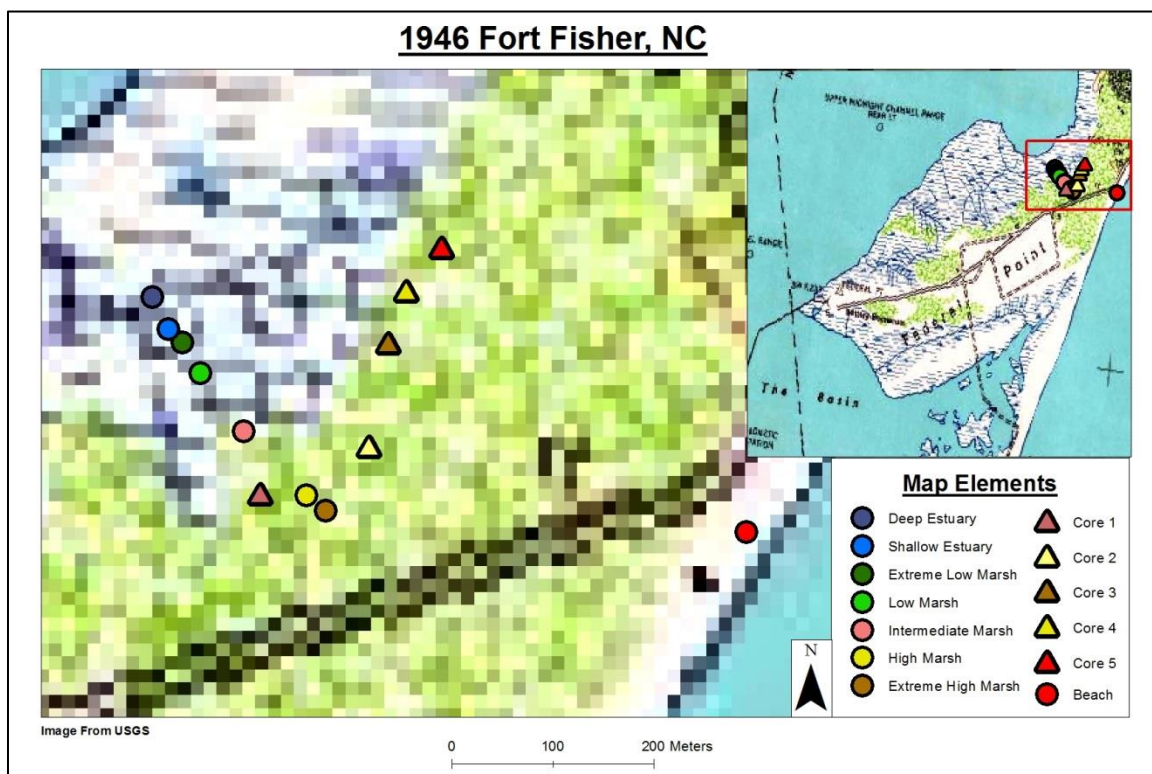


FIGURE 63: A map of 1946 showing the locations of the five core and eight surface samples that were taken adjacent to Fort Fisher. The core samples are shown by triangles and are color-coded to match the subenvironments of the surface samples that are represented by circles. Note: All samples and cores were recovered outside of the Fort Fisher Historical Site state property.

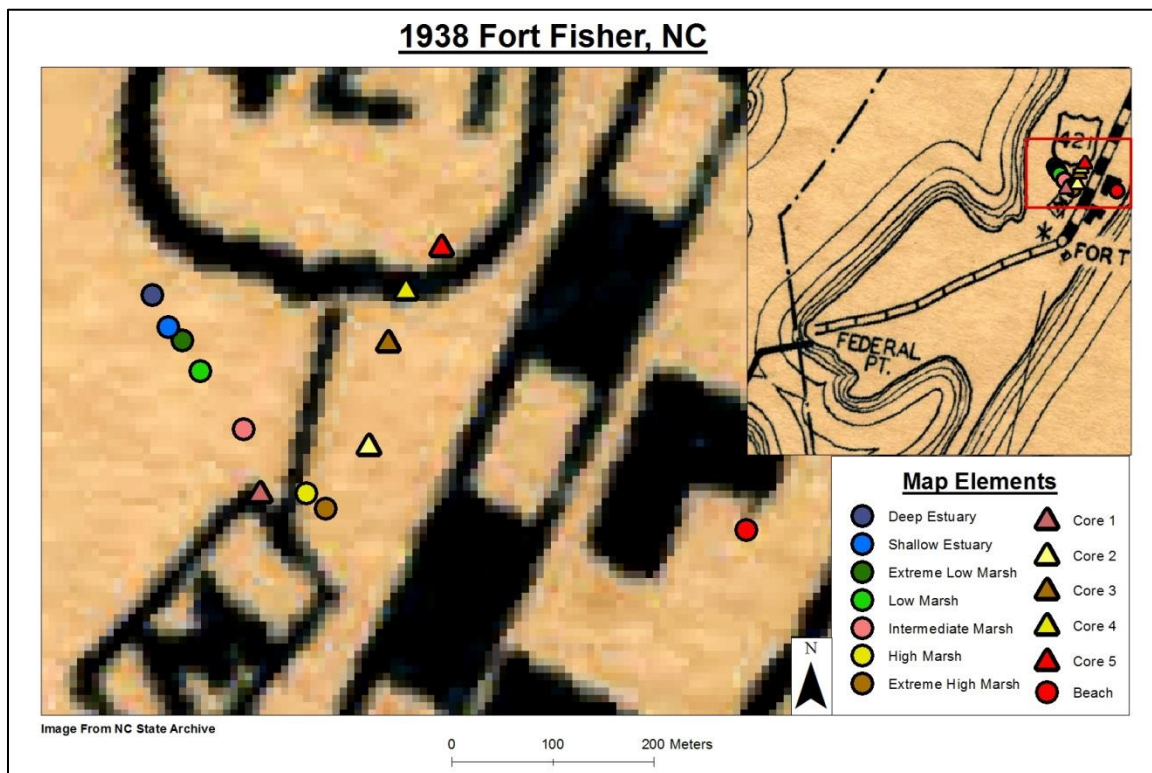


FIGURE 64: A map of 1938 showing the locations of the five core and eight surface samples that were taken adjacent to Fort Fisher. The core samples are shown by triangles and are color-coded to match the subenvironments of the surface samples that are represented by circles. Note: All samples and cores were recovered outside of the Fort Fisher Historical Site state property.

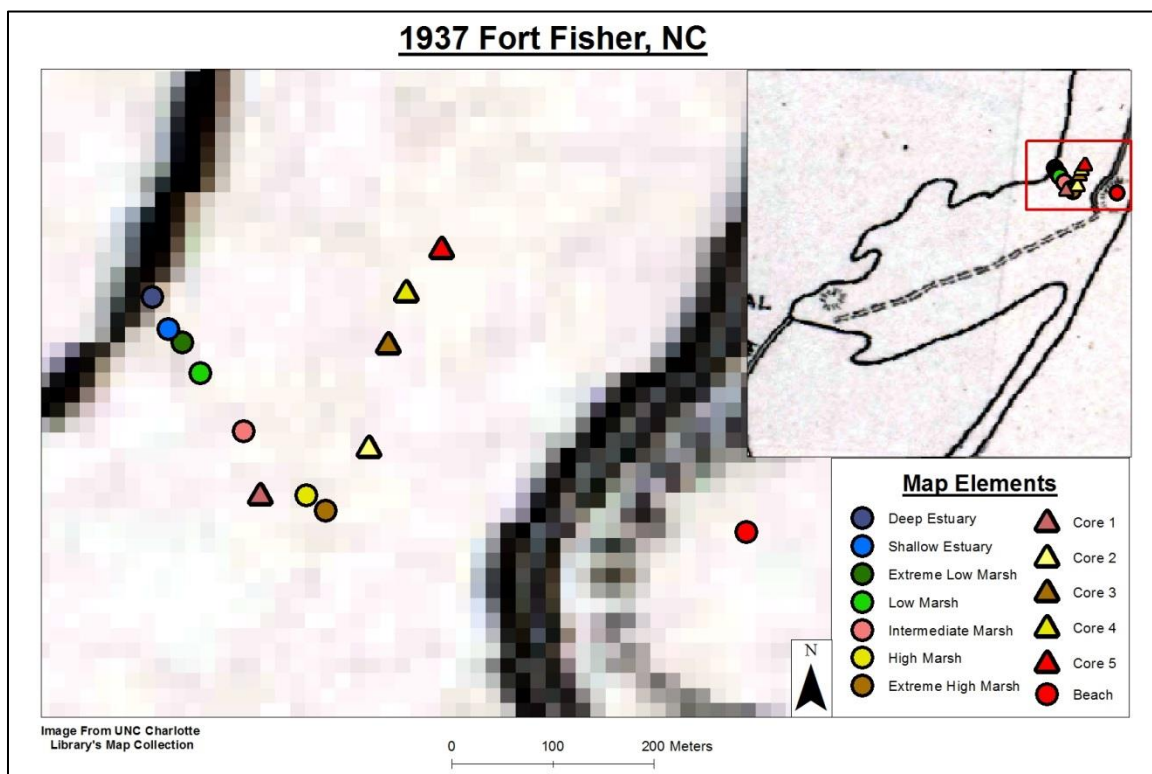


FIGURE 65: A map of 1937 showing the locations of the five core and eight surface samples that were taken adjacent to Fort Fisher. The core samples are shown by triangles and are color-coded to match the subenvironments of the surface samples that are represented by circles. Note: All samples and cores were recovered outside of the Fort Fisher Historical Site state property.

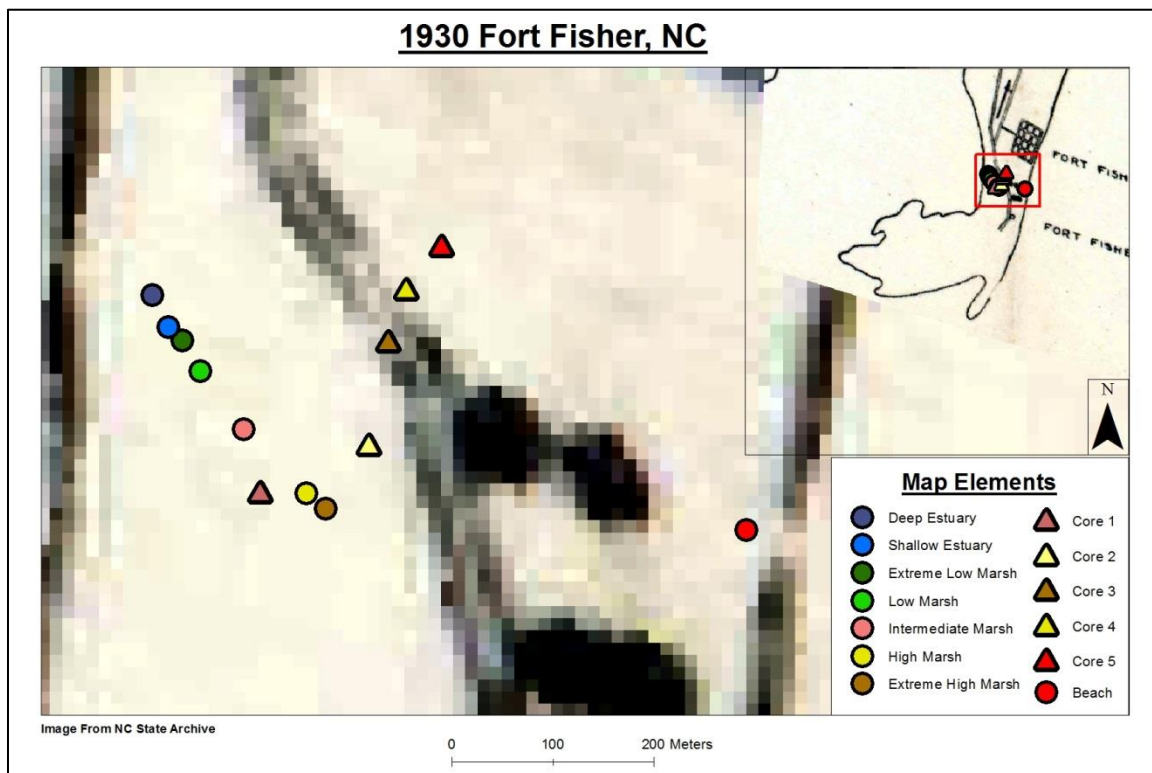


FIGURE 66: A map of 1930 showing the locations of the five core and eight surface samples that were taken adjacent to Fort Fisher. The core samples are shown by triangles and are color-coded to match the subenvironments of the surface samples that are represented by circles. Note: All samples and cores were recovered outside of the Fort Fisher Historical Site state property.

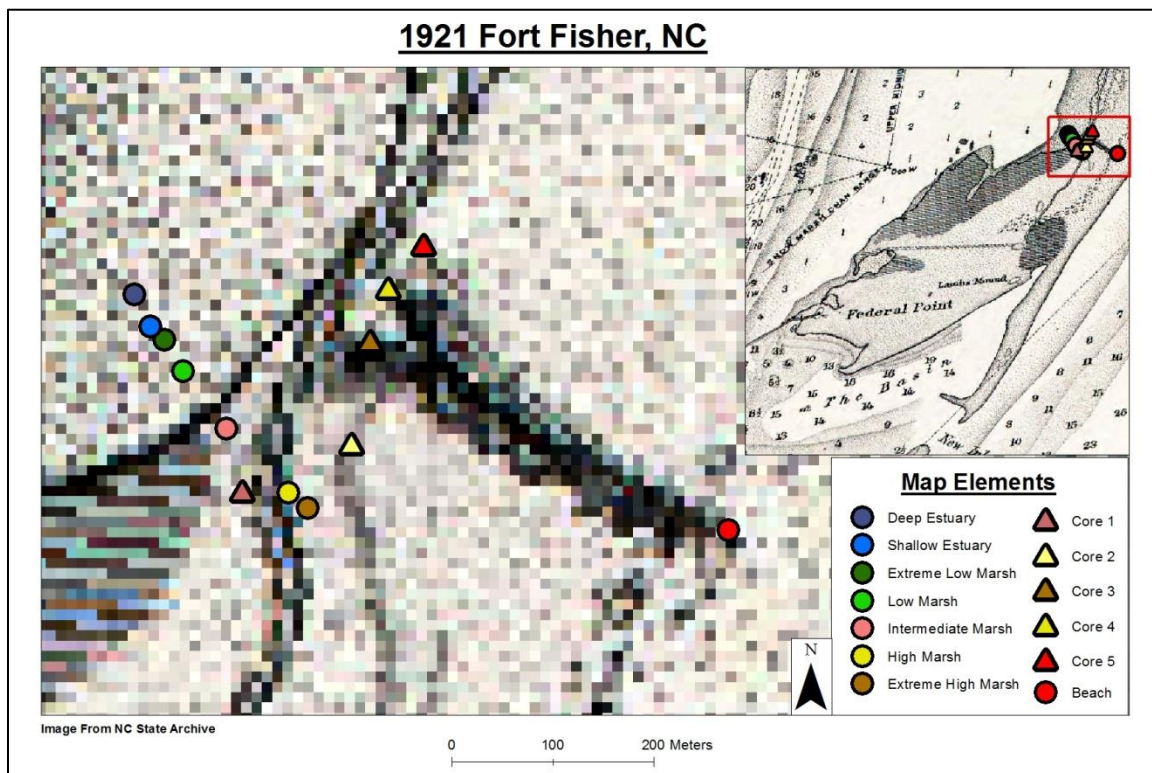


FIGURE 67: A map of 1921 showing the locations of the five core and eight surface samples that were taken adjacent to Fort Fisher. The core samples are shown by triangles and are color-coded to match the subenvironments of the surface samples that are represented by circles. Note: All samples and cores were recovered outside of the Fort Fisher Historical Site state property.

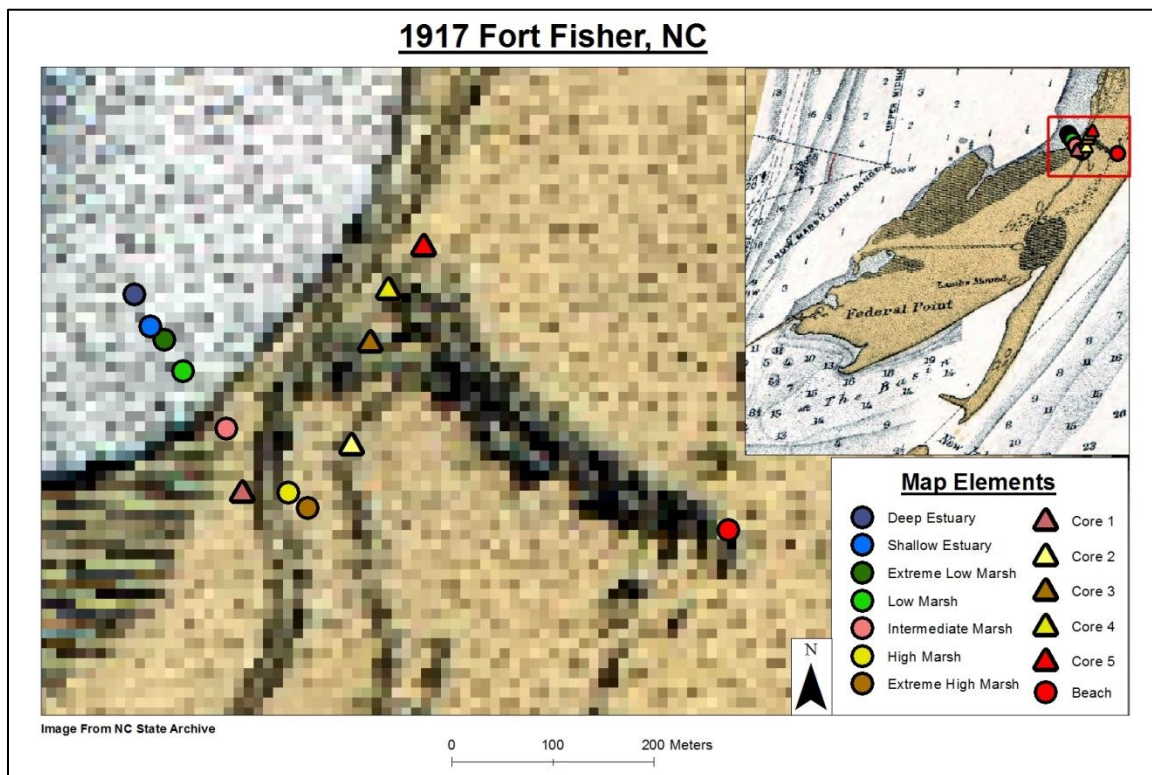


FIGURE 68: A map of 1917 showing the locations of the five core and eight surface samples that were taken adjacent to Fort Fisher. The core samples are shown by triangles and are color-coded to match the subenvironments of the surface samples that are represented by circles. Note: All samples and cores were recovered outside of the Fort Fisher Historical Site state property.

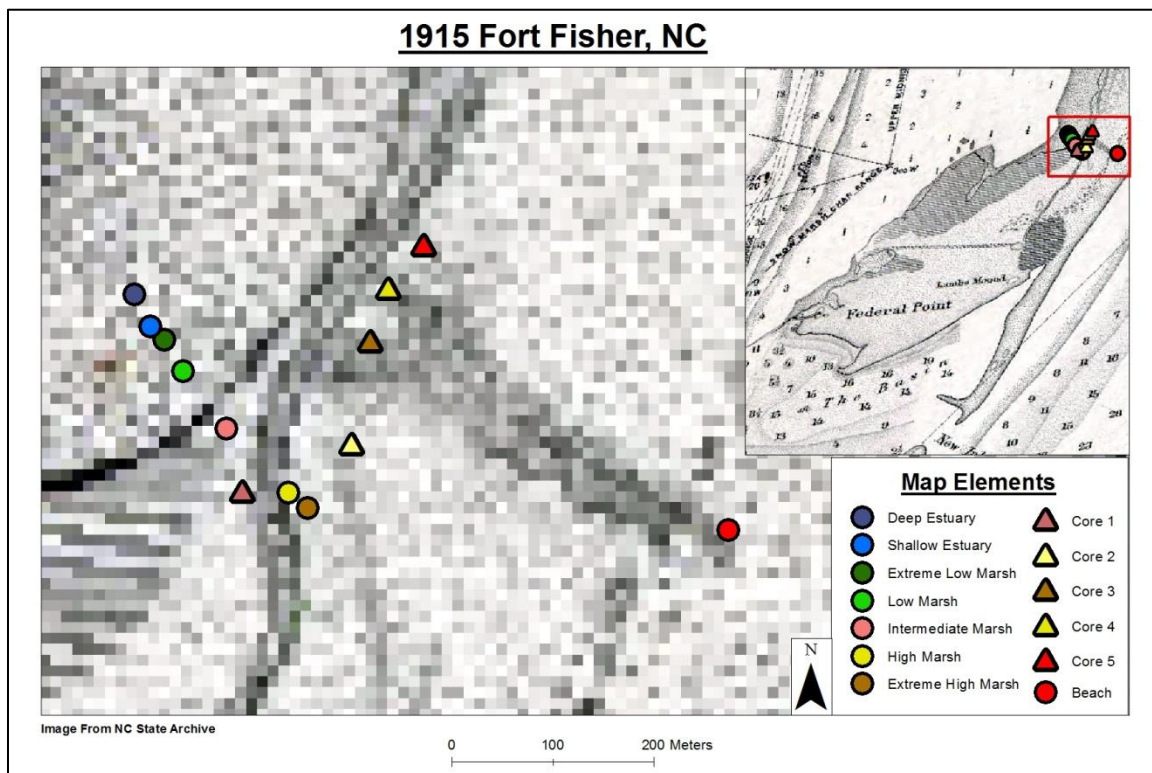


FIGURE 69: A map of 1915 showing the locations of the five core and eight surface samples that were taken adjacent to Fort Fisher. The core samples are shown by triangles and are color-coded to match the subenvironments of the surface samples that are represented by circles. Note: All samples and cores were recovered outside of the Fort Fisher Historical Site state property.

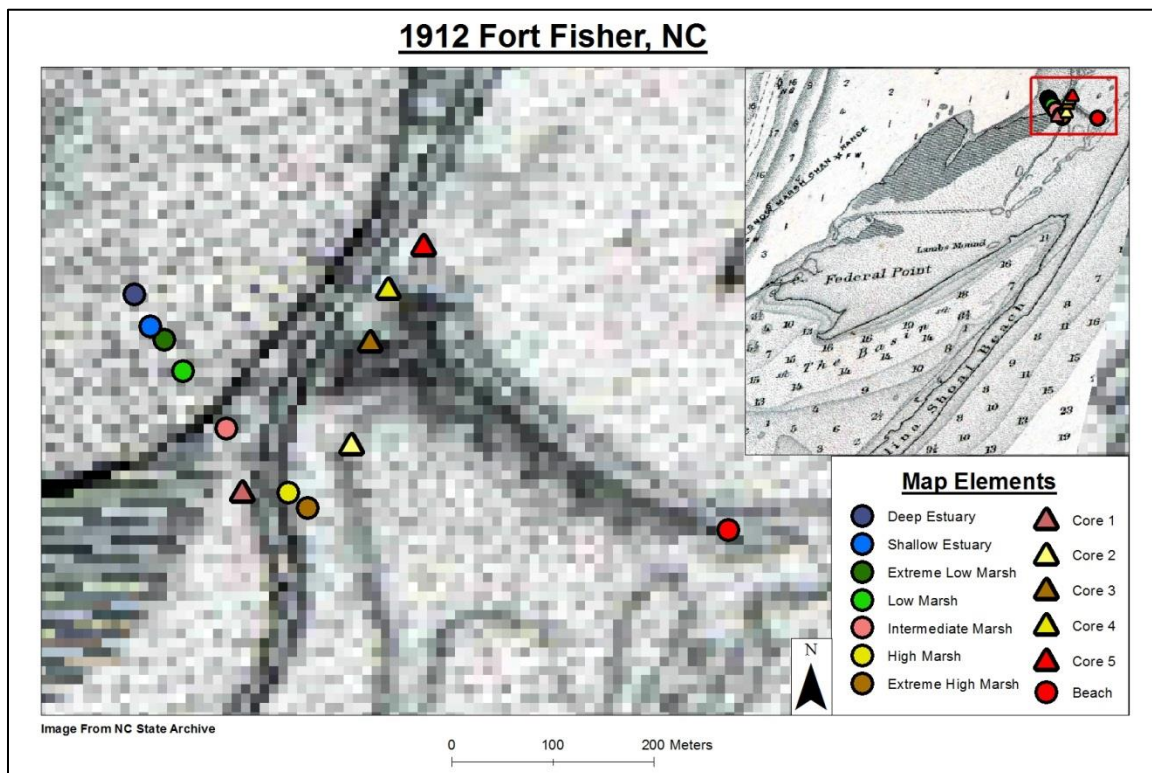


FIGURE 70: A map of 1912 showing the locations of the five core and eight surface samples that were taken adjacent to Fort Fisher. The core samples are shown by triangles and are color-coded to match the subenvironments of the surface samples that are represented by circles. Note: All samples and cores were recovered outside of the Fort Fisher Historical Site state property.

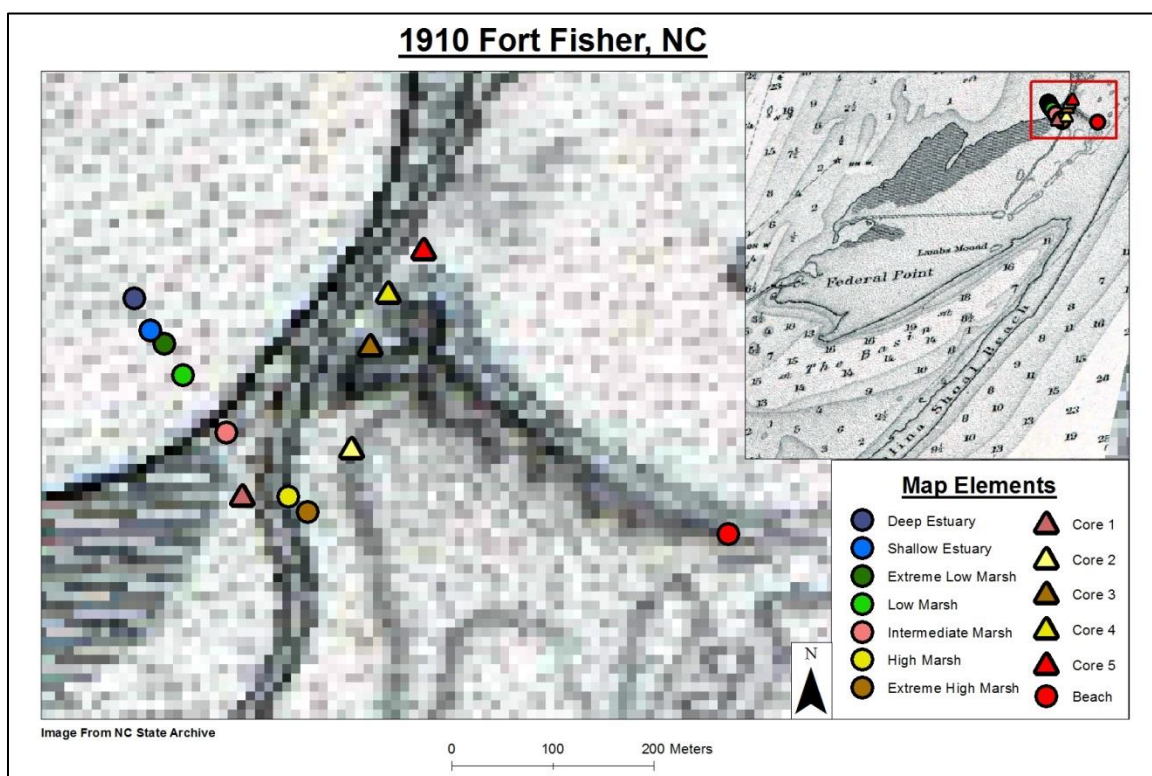


FIGURE 71: A map of 1910 showing the locations of the five core and eight surface samples that were taken adjacent to Fort Fisher. The core samples are shown by triangles and are color-coded to match the subenvironments of the surface samples that are represented by circles. Note: All samples and cores were recovered outside of the Fort Fisher Historical Site state property.

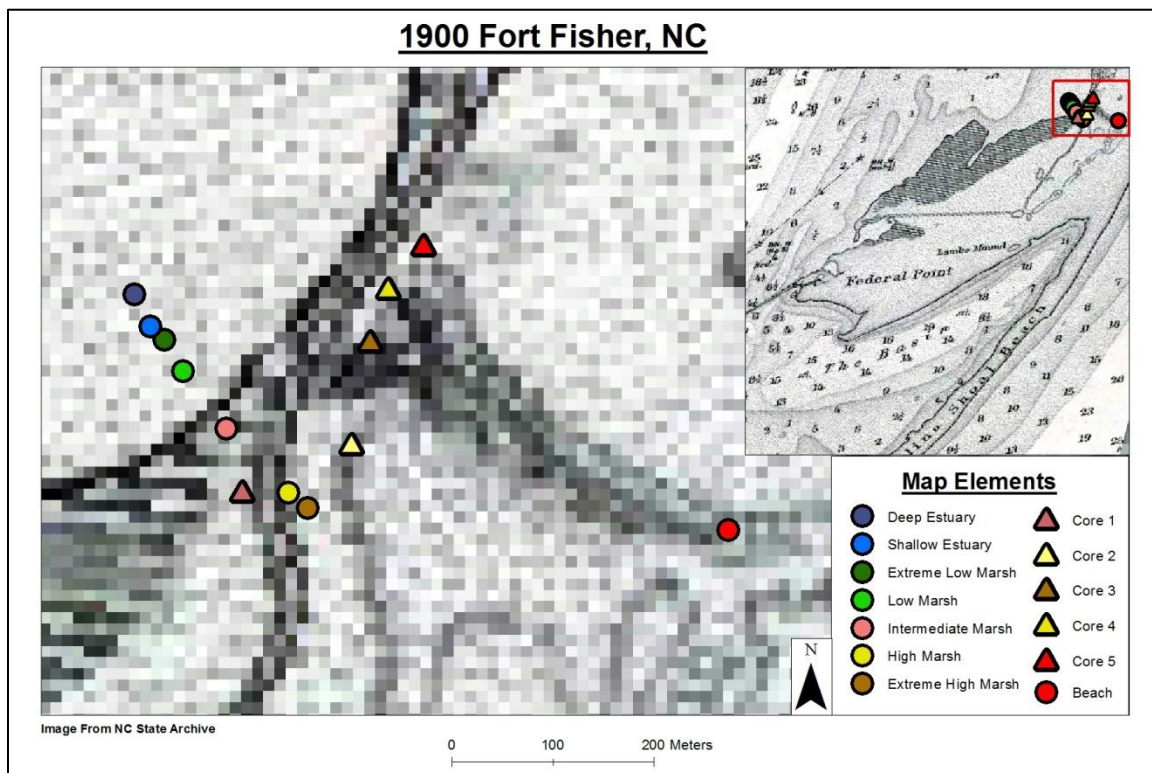


FIGURE 72: A map of 1900 showing the locations of the five core and eight surface samples that were taken adjacent to Fort Fisher. The core samples are shown by triangles and are color-coded to match the subenvironments of the surface samples that are represented by circles. Note: All samples and cores were recovered outside of the Fort Fisher Historical Site state property.

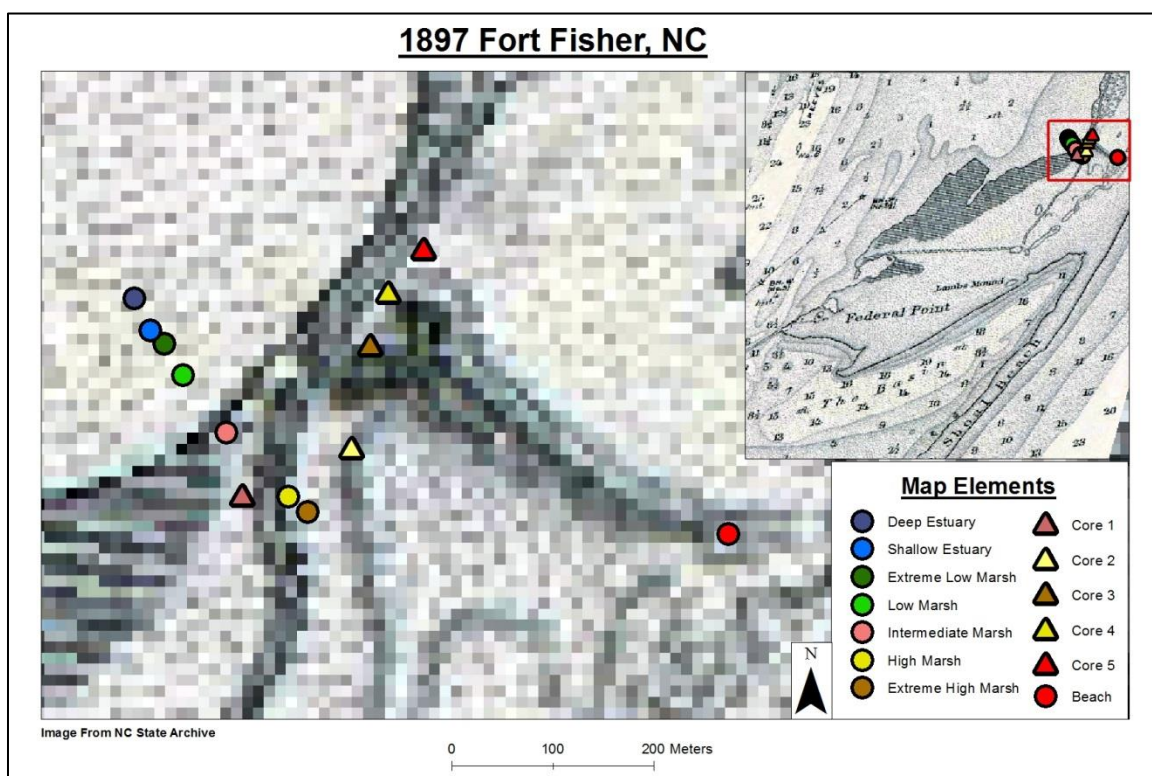


FIGURE 73: A map of 1897 showing the locations of the five core and eight surface samples that were taken adjacent to Fort Fisher. The core samples are shown by triangles and are color-coded to match the subenvironments of the surface samples that are represented by circles. Note: All samples and cores were recovered outside of the Fort Fisher Historical Site state property.

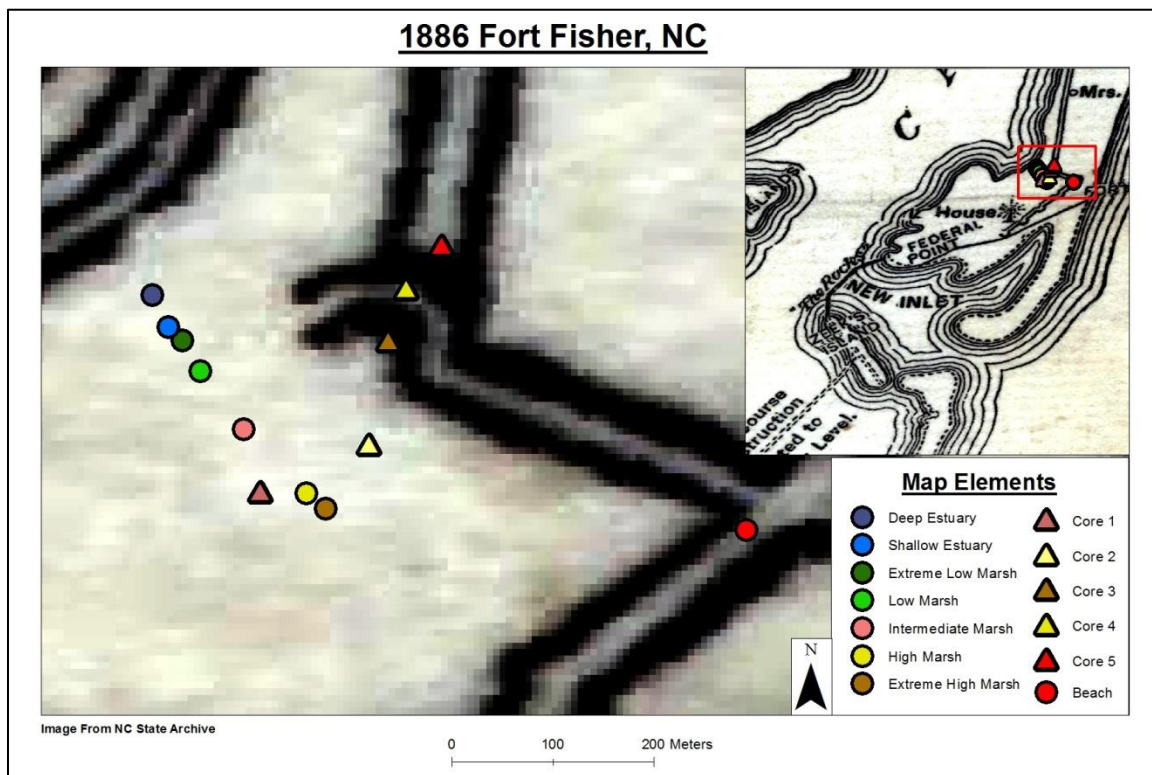


FIGURE 74: A map of 1886 showing the locations of the five core and eight surface samples that were taken adjacent to Fort Fisher. The core samples are shown by triangles and are color-coded to match the subenvironments of the surface samples that are represented by circles. Note: All samples and cores were recovered outside of the Fort Fisher Historical Site state property.

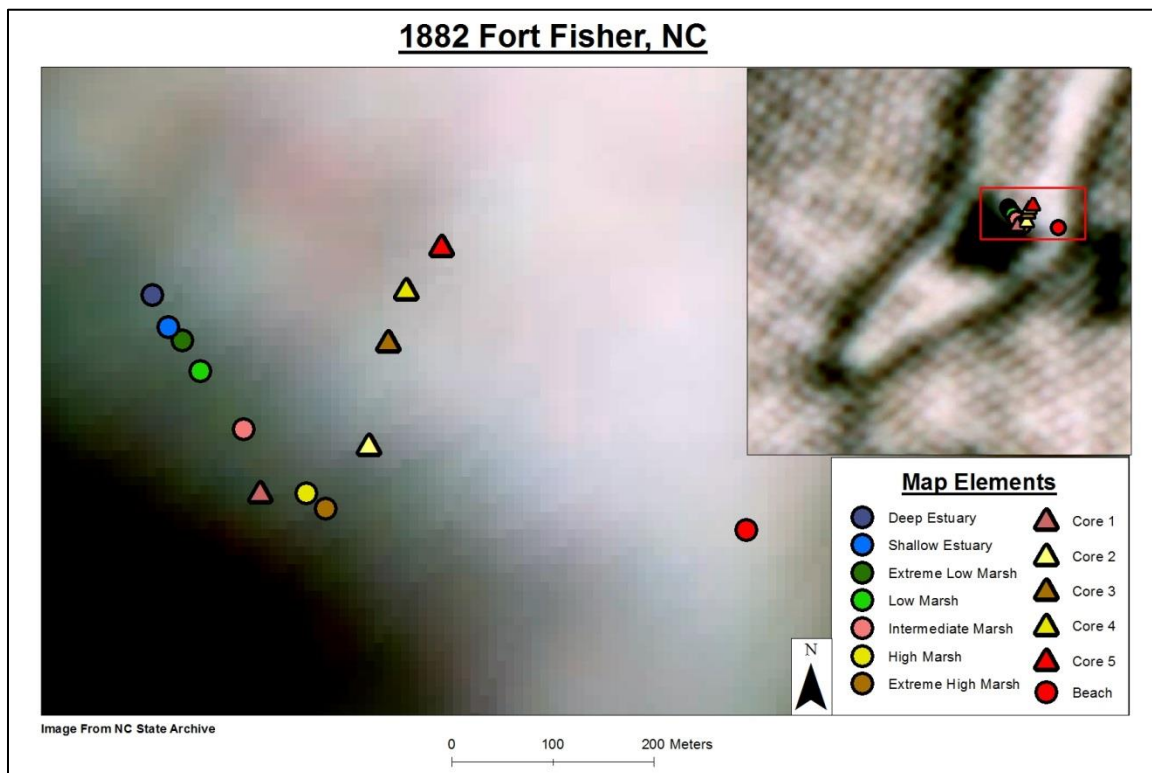


FIGURE 75: A map of 1882 showing the locations of the five core and eight surface samples that were taken adjacent to Fort Fisher. The core samples are shown by triangles and are color-coded to match the subenvironments of the surface samples that are represented by circles. Note: All samples and cores were recovered outside of the Fort Fisher Historical Site state property.

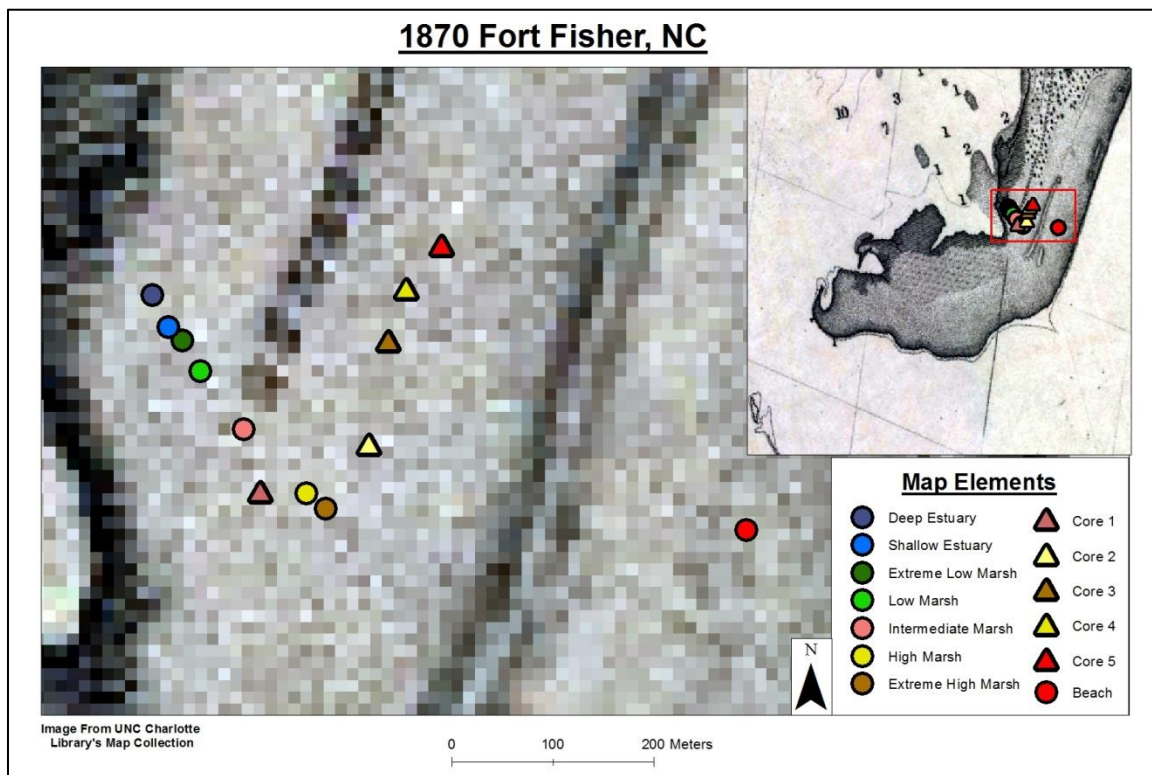


FIGURE 76: A map of 1870 showing the locations of the five core and eight surface samples that were taken adjacent to Fort Fisher. The core samples are shown by triangles and are color-coded to match the subenvironments of the surface samples that are represented by circles. Note: All samples and cores were recovered outside of the Fort Fisher Historical Site state property.

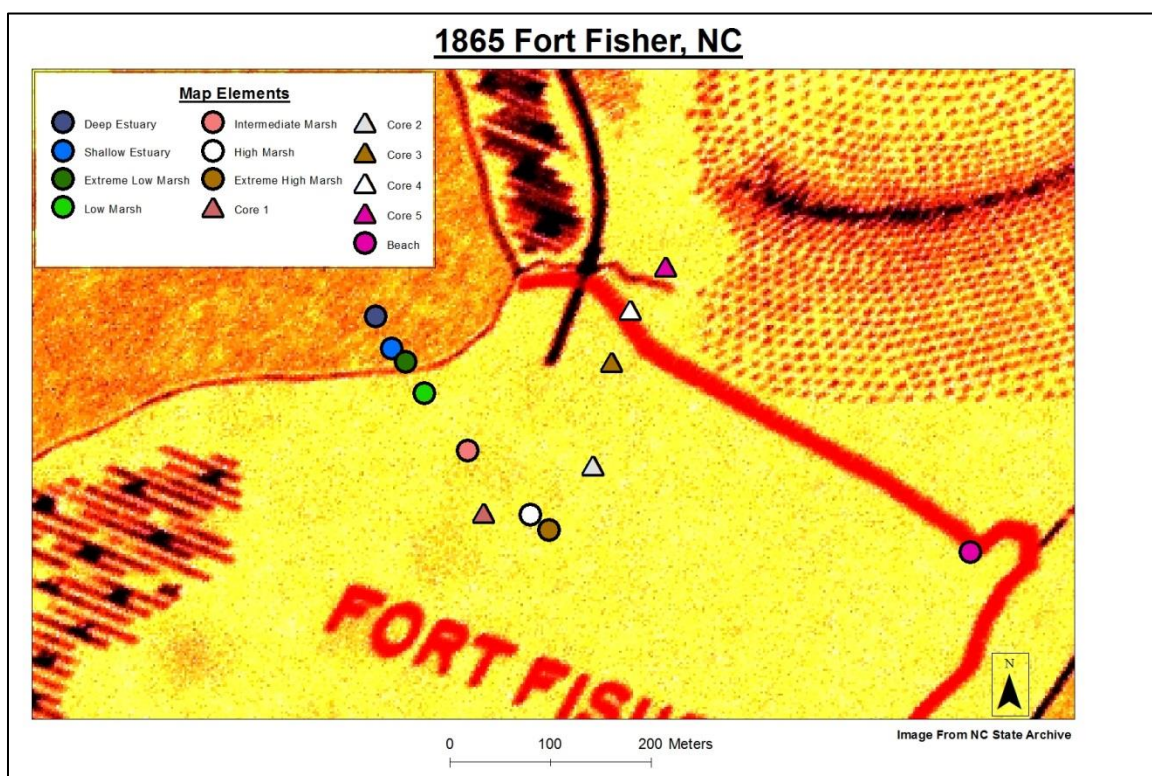


FIGURE 77: A map of 1865 showing the locations of the five core and eight surface samples that were taken adjacent to Fort Fisher. The core samples are shown by triangles and are color-coded to match the subenvironments of the surface samples that are represented by circles. Note: All samples and cores were recovered outside of the Fort Fisher Historical Site state property.

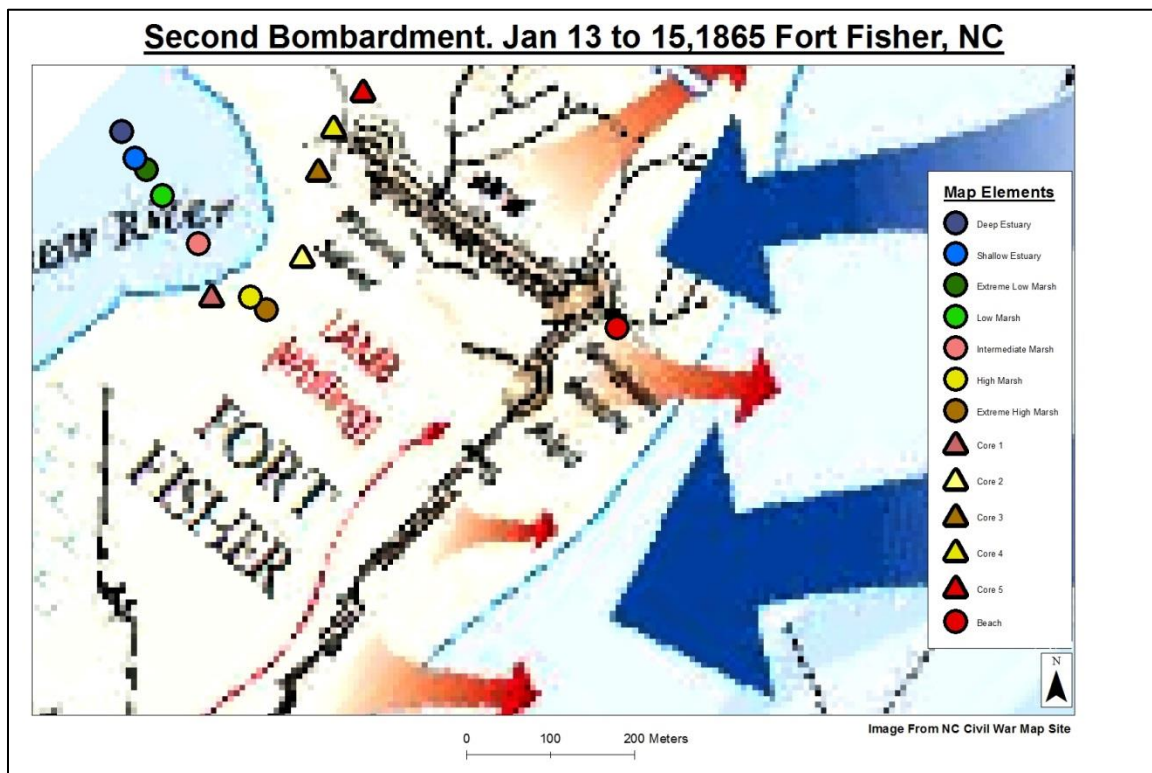


FIGURE 78: A map of 1865 showing the locations of the five core and eight surface samples that were taken adjacent to Fort Fisher. The core samples are shown by triangles and are color-coded to match the subenvironments of the surface samples that are represented by circles. Note: All samples and cores were recovered outside of the Fort Fisher Historical Site state property.

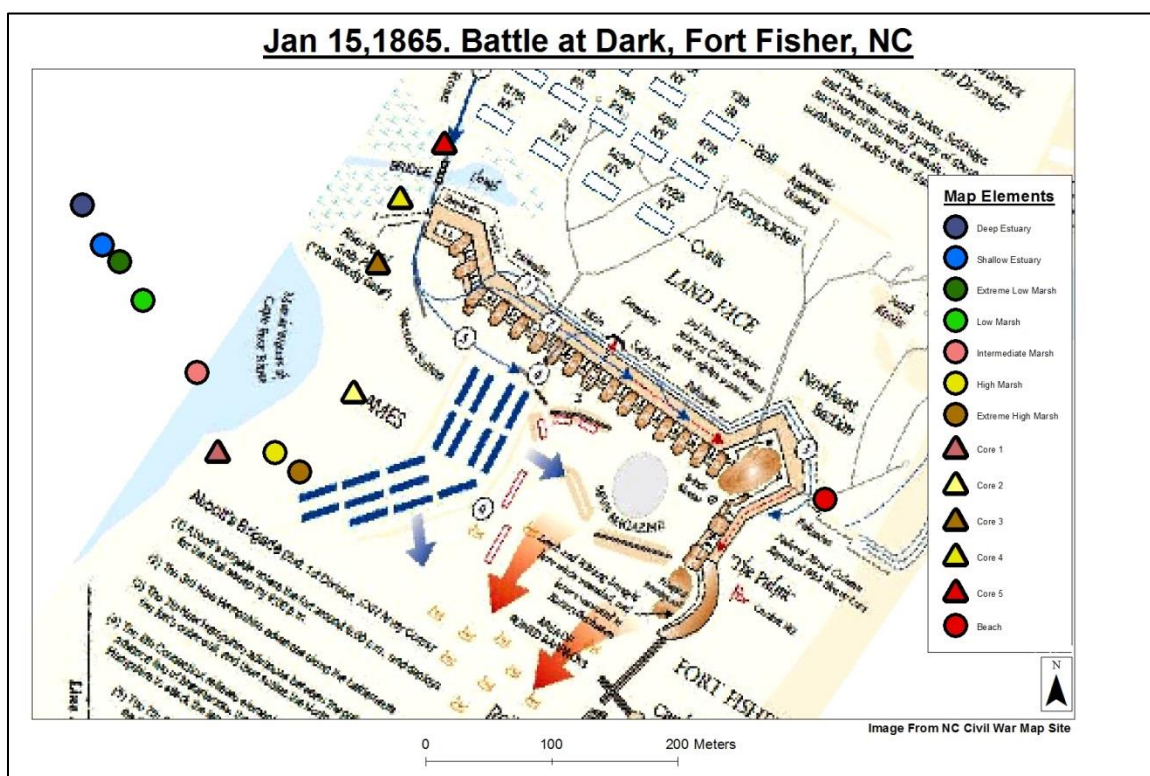


FIGURE 79: A map of 1865 showing the locations of the five core and eight surface samples that were taken adjacent to Fort Fisher. The core samples are shown by triangles and are color-coded to match the subenvironments of the surface samples that are represented by circles. Note: All samples and cores were recovered outside of the Fort Fisher Historical Site state property.

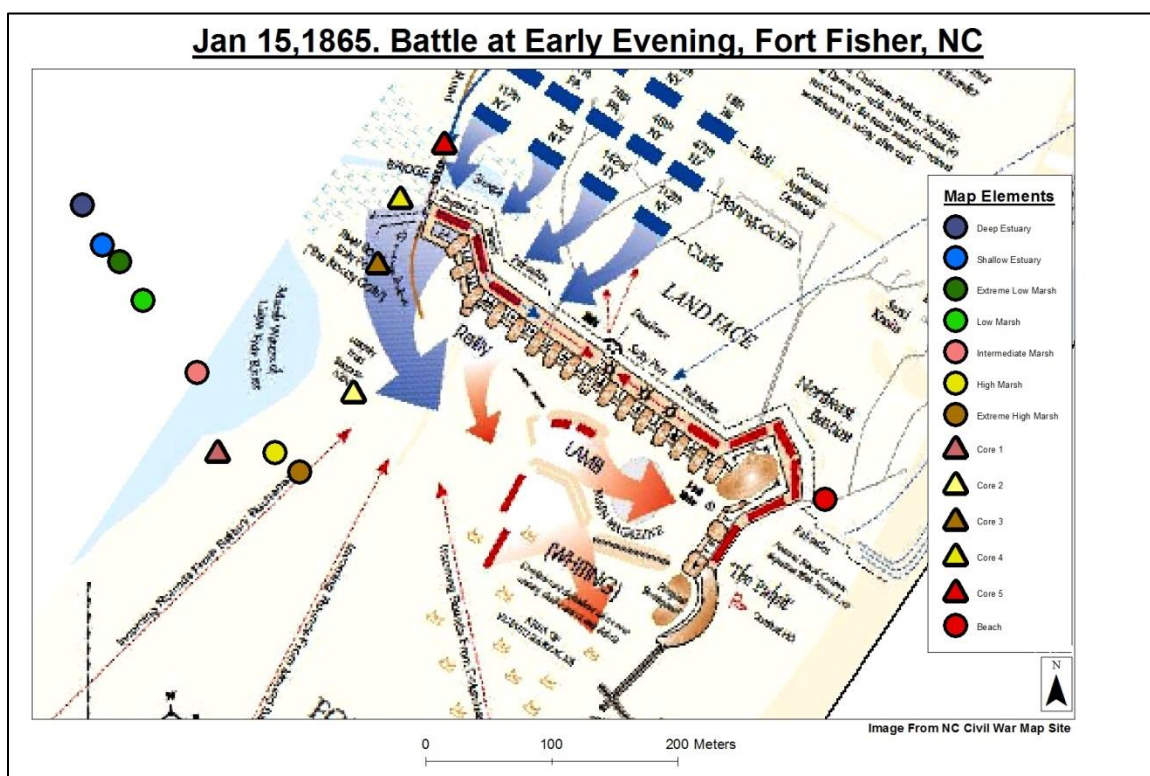


FIGURE 80: A map of 2002 showing the locations of the five core and eight surface samples that were taken adjacent to Fort Fisher. The core samples are shown by triangles and are color-coded to match the subenvironments of the surface samples that are represented by circles. Note: All samples and cores were recovered outside of the Fort Fisher Historical Site state property.

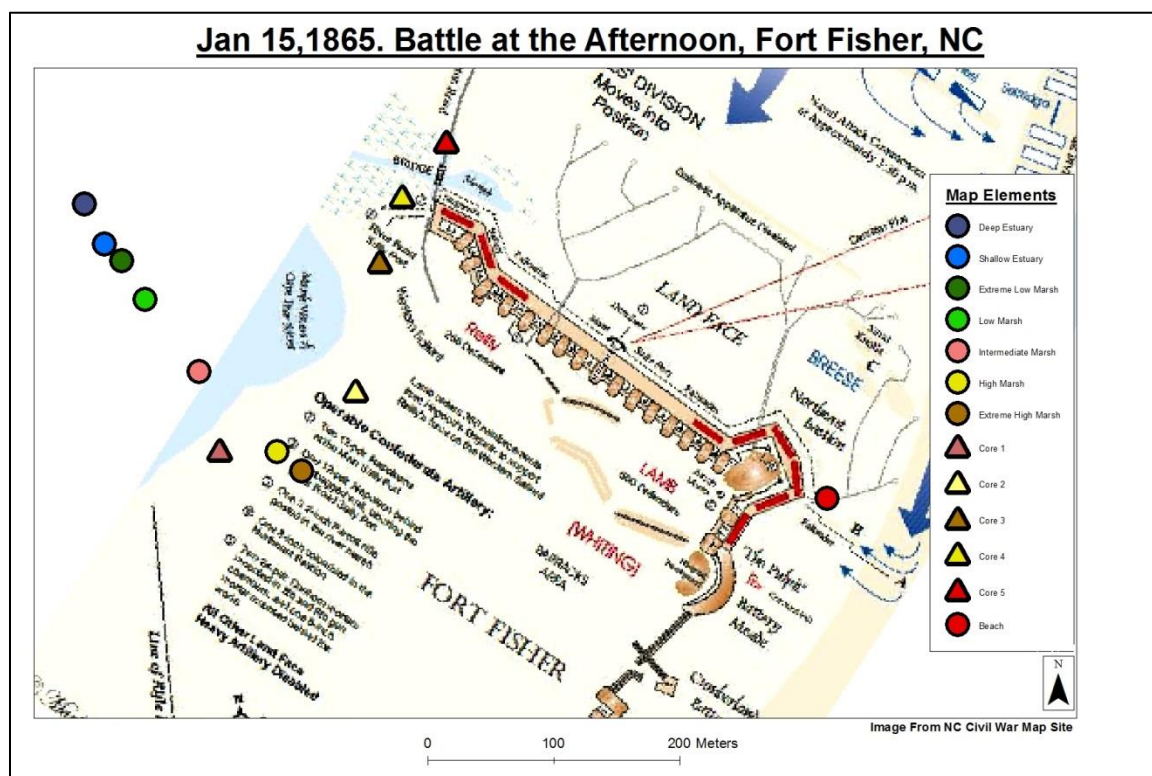


FIGURE 81: A map of 1865 showing the locations of the five core and eight surface samples that were taken adjacent to Fort Fisher. The core samples are shown by triangles and are color-coded to match the subenvironments of the surface samples that are represented by circles. Note: All samples and cores were recovered outside of the Fort Fisher Historical Site state property.

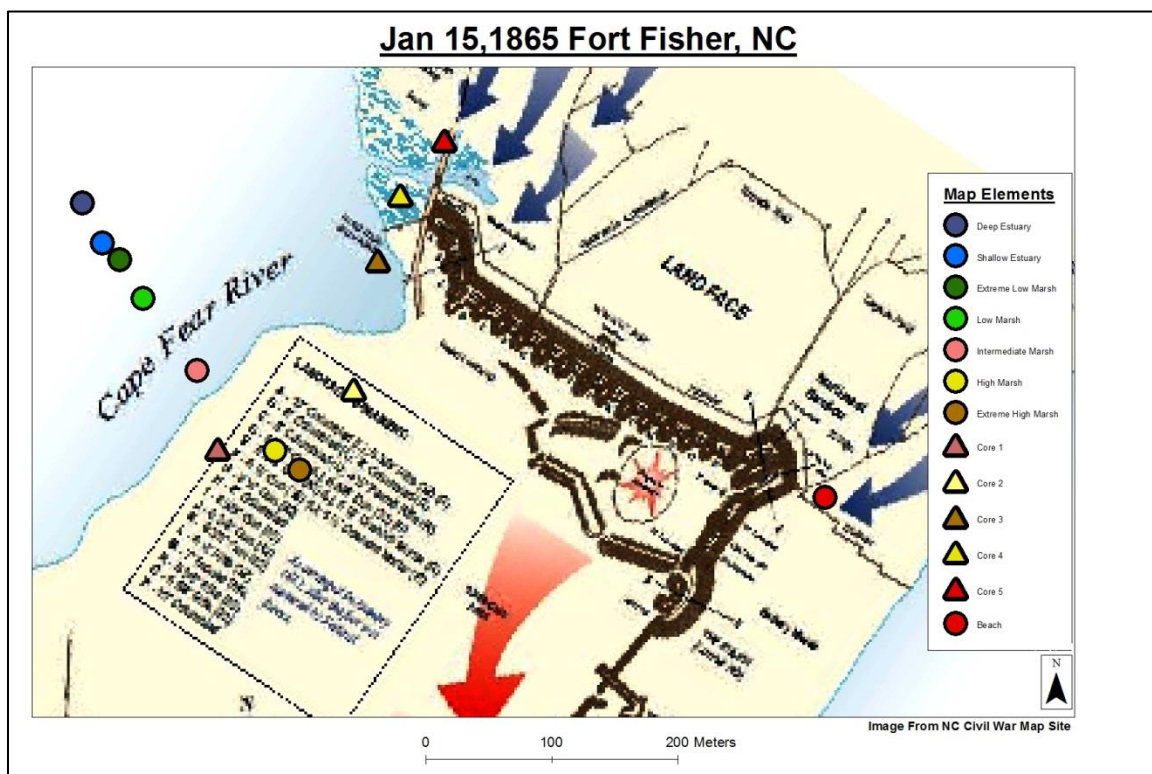


FIGURE 82: A map of 1865 showing the locations of the five core and eight surface samples that were taken adjacent to Fort Fisher. The core samples are shown by triangles and are color-coded to match the subenvironments of the surface samples that are represented by circles. Note: All samples and cores were recovered outside of the Fort Fisher Historical Site state property.

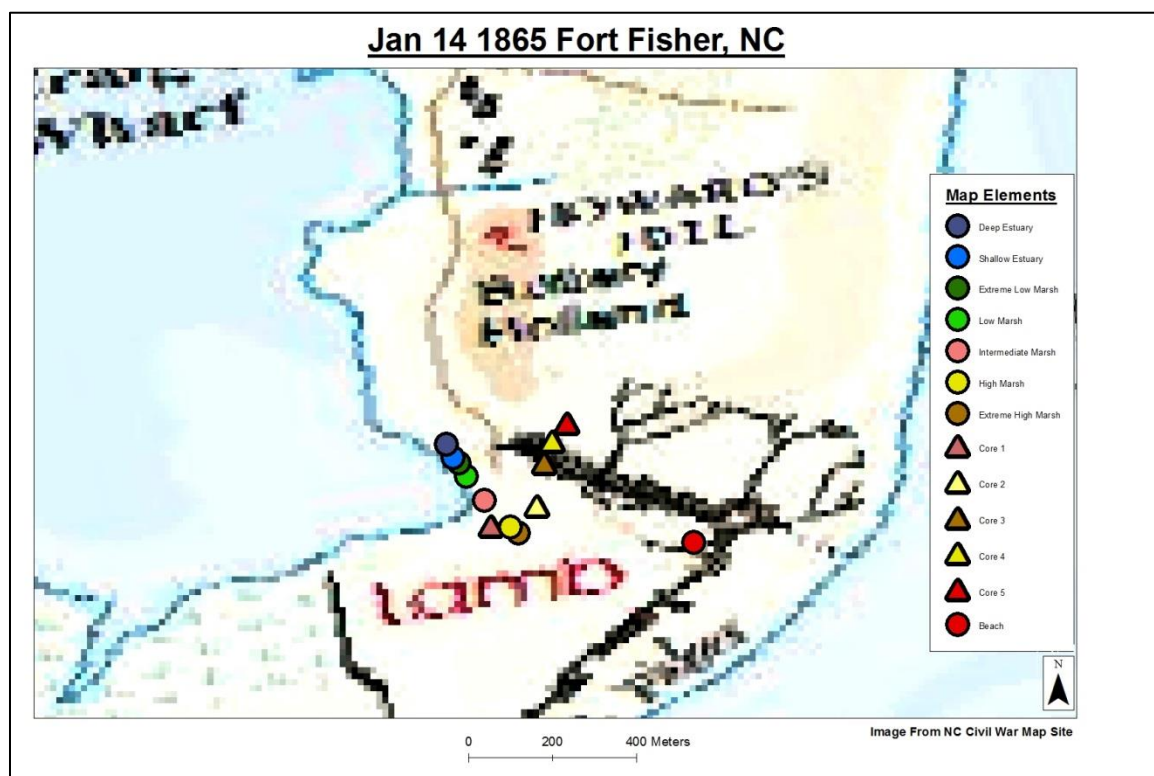


FIGURE 83: A map of 1865 showing the locations of the five core and eight surface samples that were taken adjacent to Fort Fisher. The core samples are shown by triangles and are color-coded to match the subenvironments of the surface samples that are represented by circles. Note: All samples and cores were recovered outside of the Fort Fisher Historical Site state property.

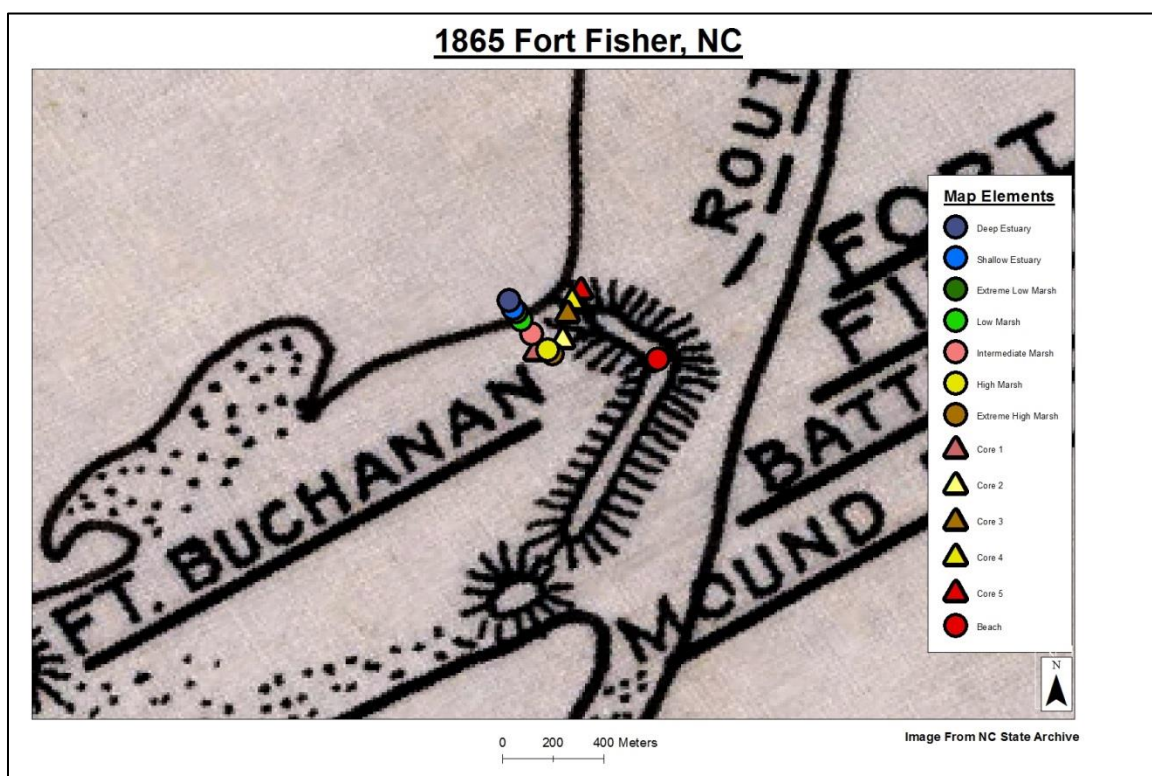


FIGURE 84: A map of 1865 showing the locations of the five core and eight surface samples that were taken adjacent to Fort Fisher. The core samples are shown by triangles and are color-coded to match the subenvironments of the surface samples that are represented by circles. Note: All samples and cores were recovered outside of the Fort Fisher Historical Site state property.

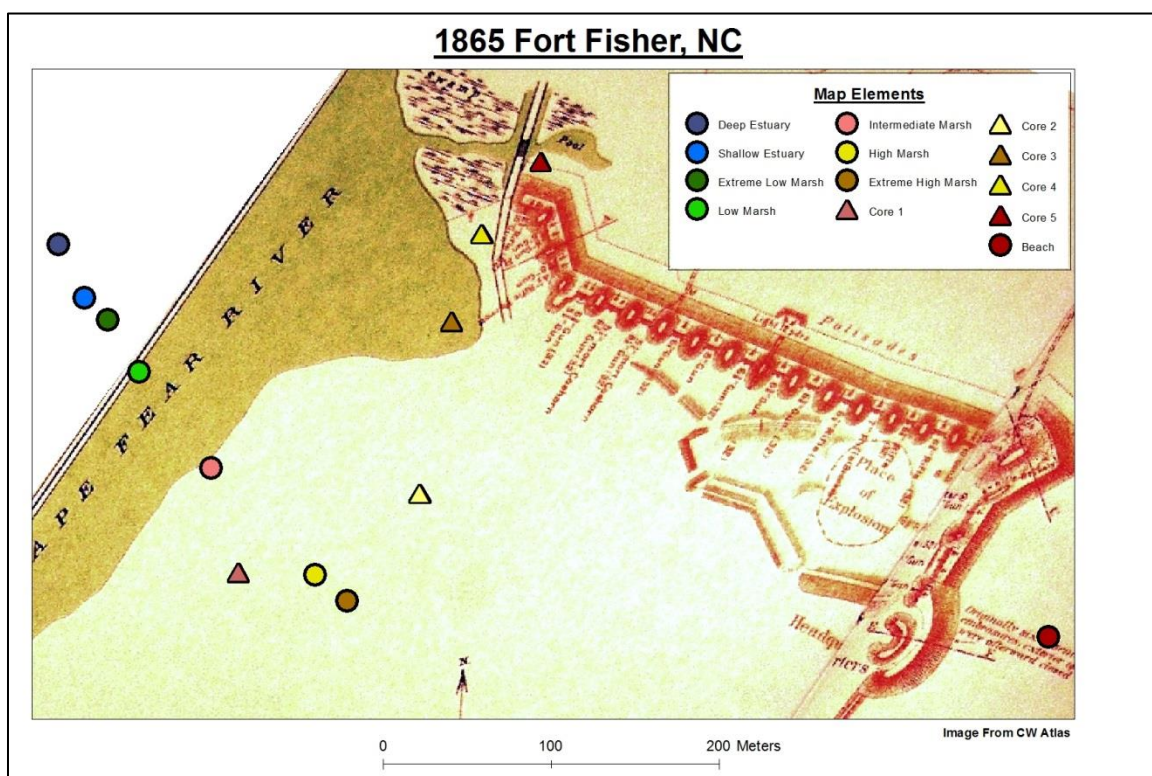


FIGURE 85: A map of 1865 showing the locations of the five core and eight surface samples that were taken adjacent to Fort Fisher. The core samples are shown by triangles and are color-coded to match the subenvironments of the surface samples that are represented by circles. Note: All samples and cores were recovered outside of the Fort Fisher Historical Site state property.

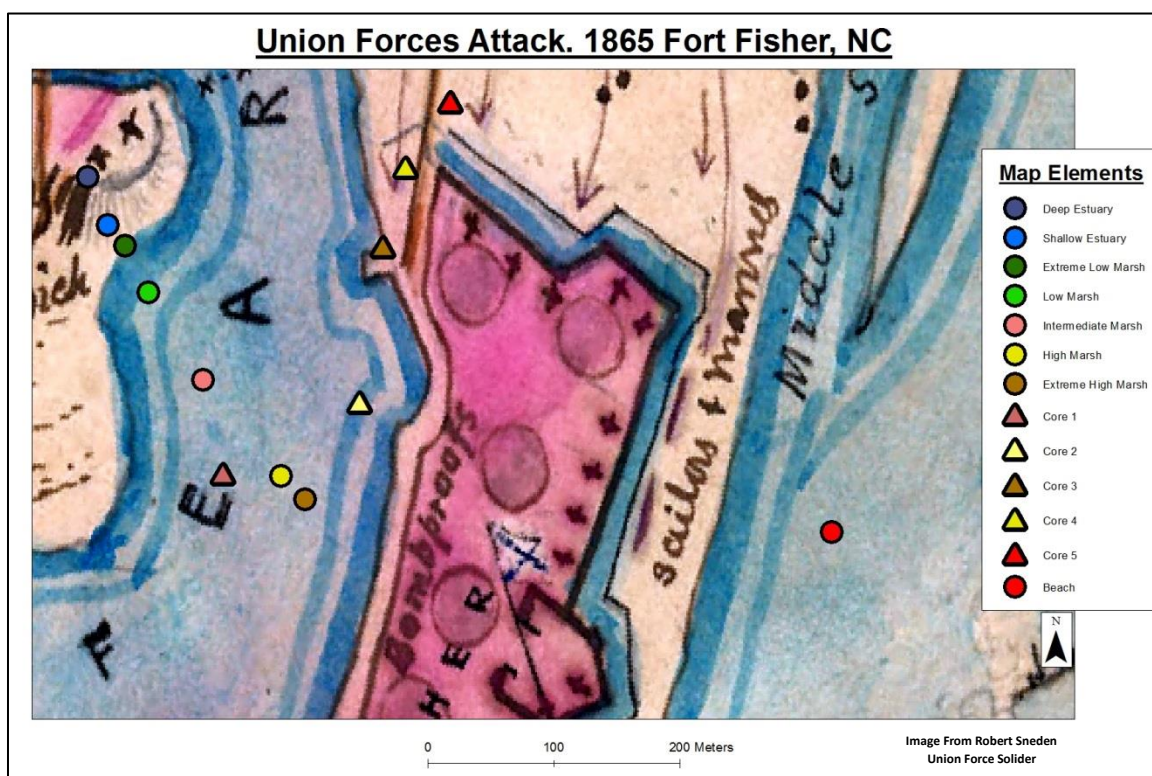


FIGURE 86: A map of 1865 showing the locations of the five core and eight surface samples that were taken adjacent to Fort Fisher. The core samples are shown by triangles and are color-coded to match the subenvironments of the surface samples that are represented by circles. Note: All samples and cores were recovered outside of the Fort Fisher Historical Site state property.

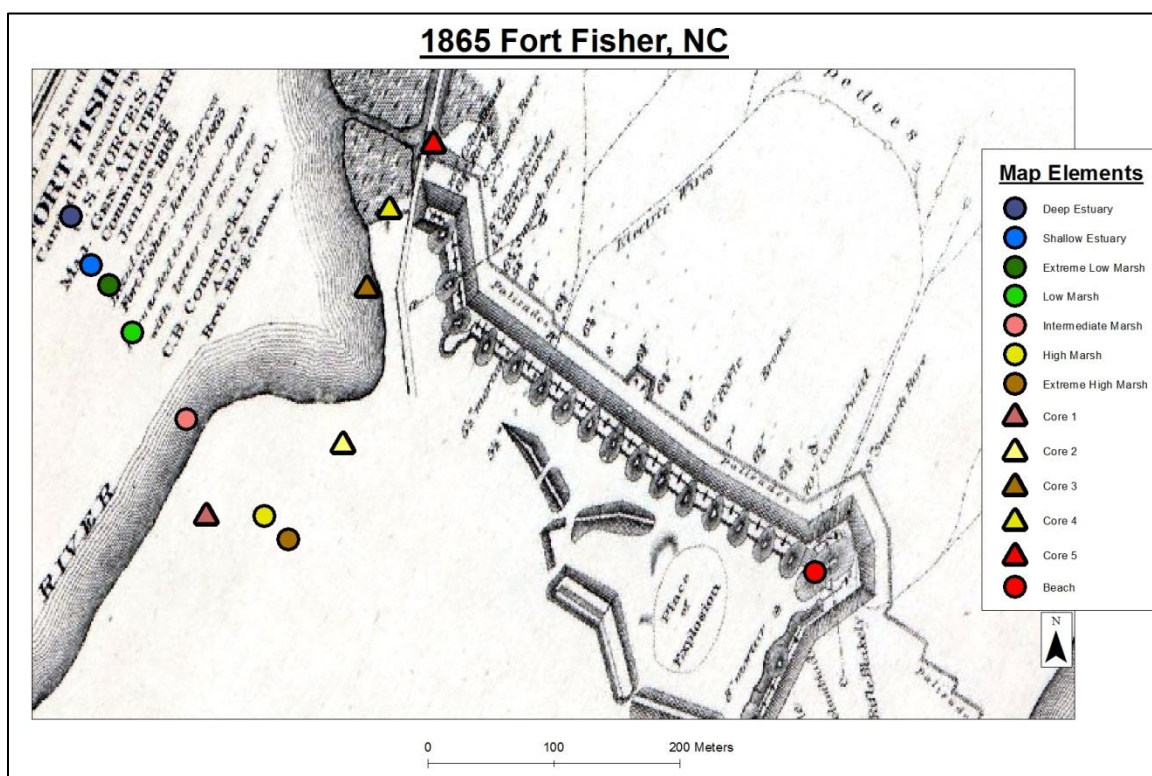


FIGURE 87: A map of 1865 showing the locations of the five core and eight surface samples that were taken adjacent to Fort Fisher. The core samples are shown by triangles and are color-coded to match the subenvironments of the surface samples that are represented by circles. Note: All samples and cores were recovered outside of the Fort Fisher Historical Site state property.

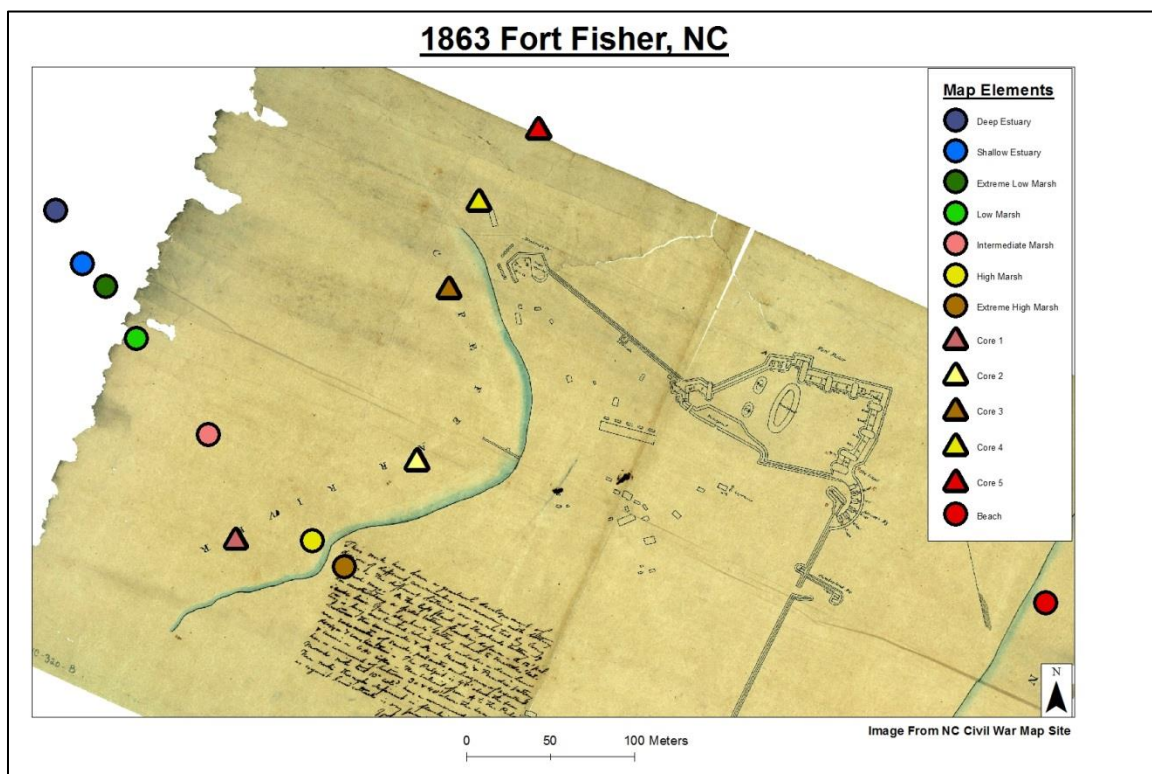


FIGURE 88: A map of 1863 showing the locations of the five core and eight surface samples that were taken adjacent to Fort Fisher. The core samples are shown by triangles and are color-coded to match the subenvironments of the surface samples that are represented by circles. Note: All samples and cores were recovered outside of the Fort Fisher Historical Site state property.

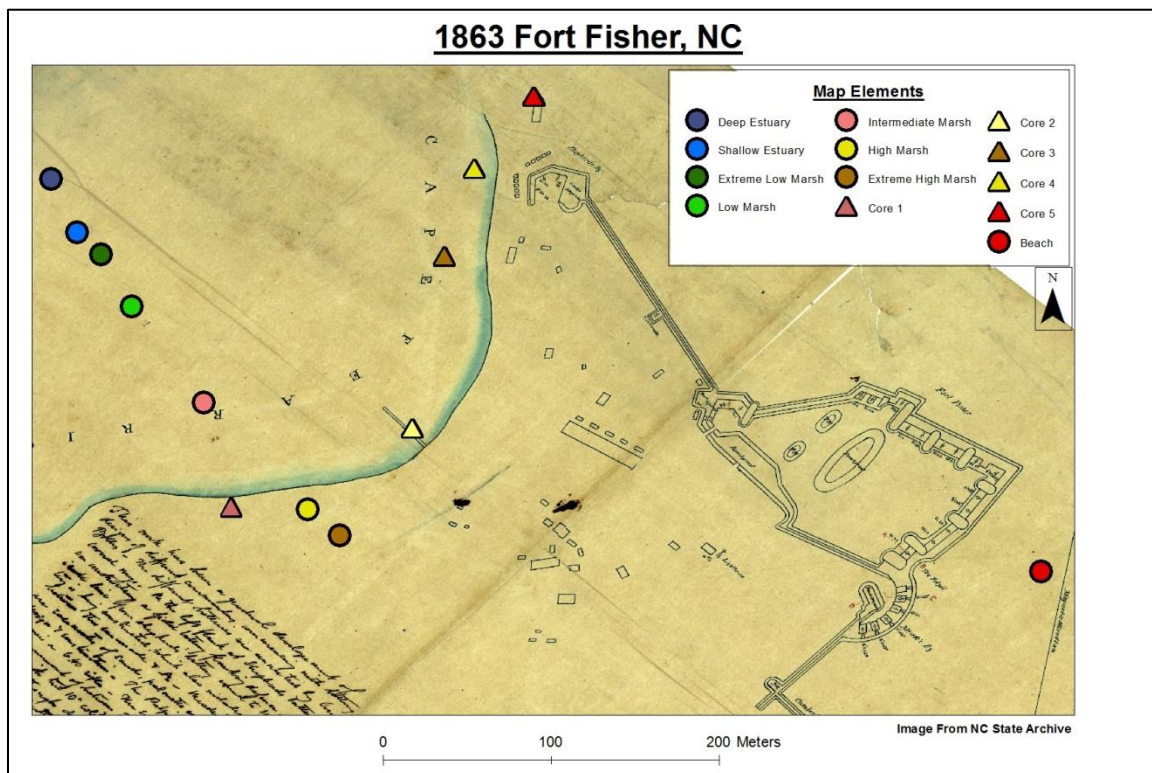


FIGURE 89: A map of 1863 showing the locations of the five core and eight surface samples that were taken adjacent to Fort Fisher. The core samples are shown by triangles and are color-coded to match the subenvironments of the surface samples that are represented by circles. Note: All samples and cores were recovered outside of the Fort Fisher Historical Site state property.

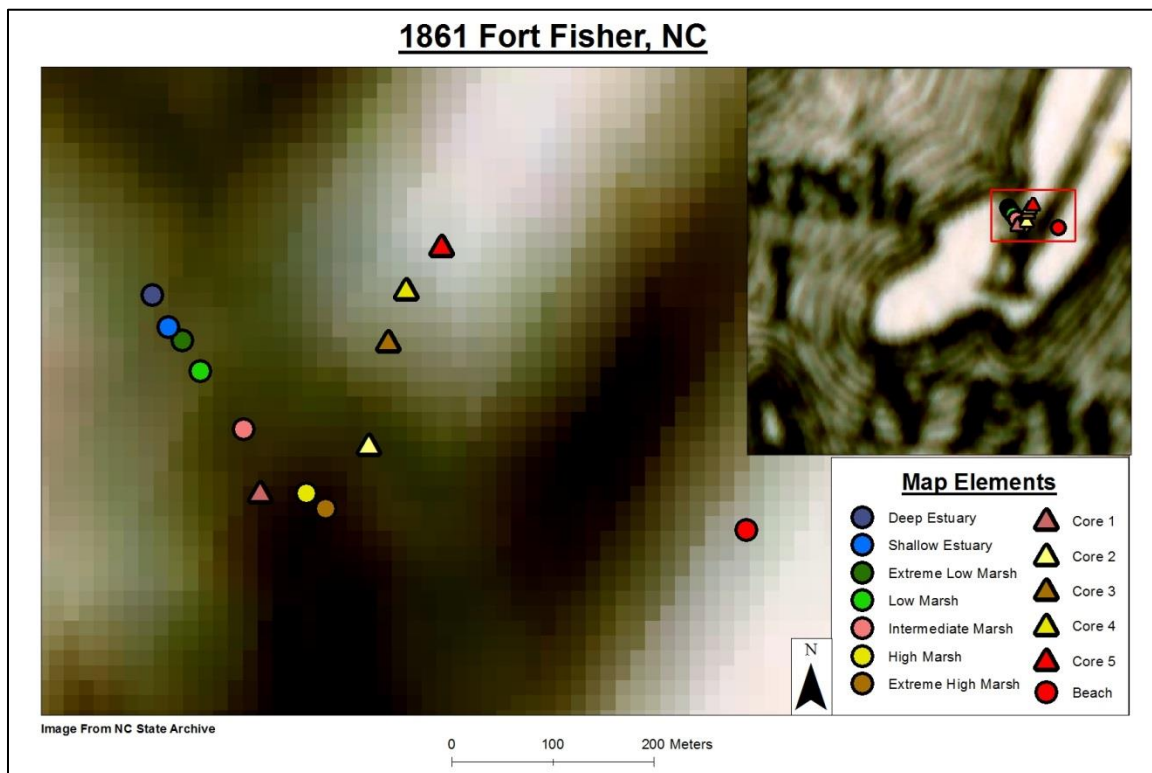


FIGURE 90: A map of 1861 showing the locations of the five core and eight surface samples that were taken adjacent to Fort Fisher. The core samples are shown by triangles and are color-coded to match the subenvironments of the surface samples that are represented by circles. Note: All samples and cores were recovered outside of the Fort Fisher Historical Site state property.

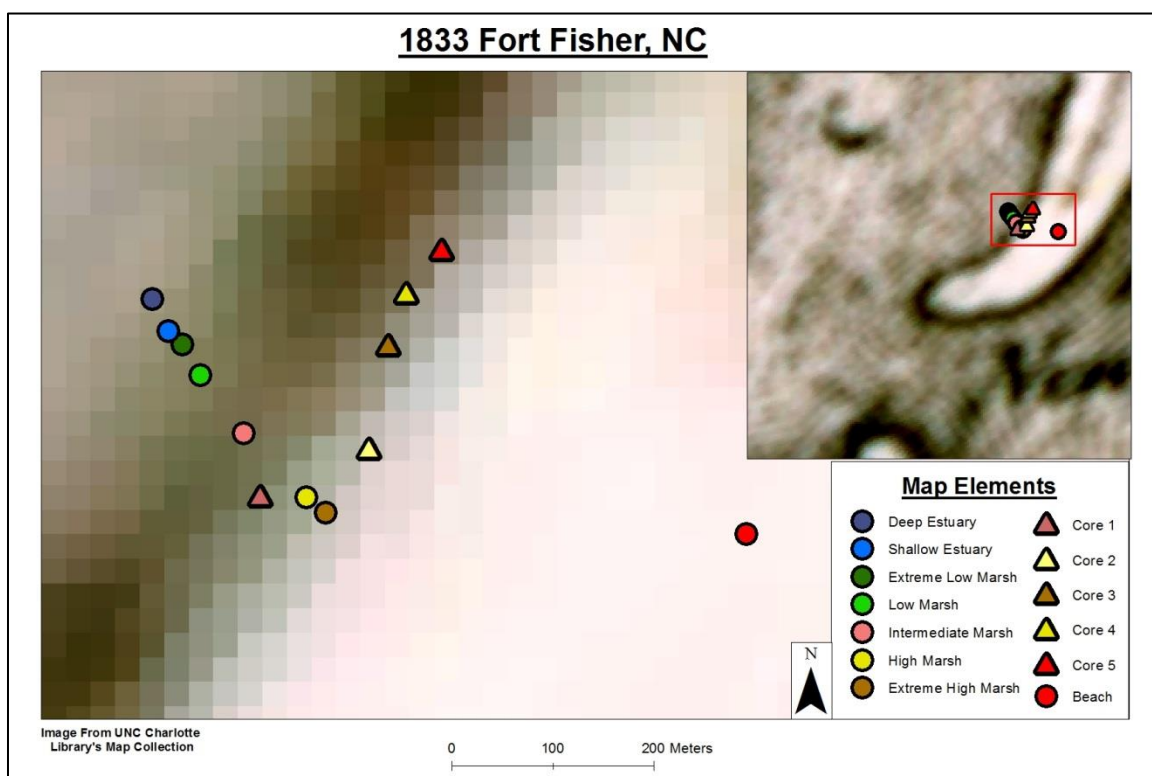


FIGURE 91: A map of 1833 showing the locations of the five core and eight surface samples that were taken adjacent to Fort Fisher. The core samples are shown by triangles and are color-coded to match the subenvironments of the surface samples that are represented by circles. Note: All samples and cores were recovered outside of the Fort Fisher Historical Site state property.

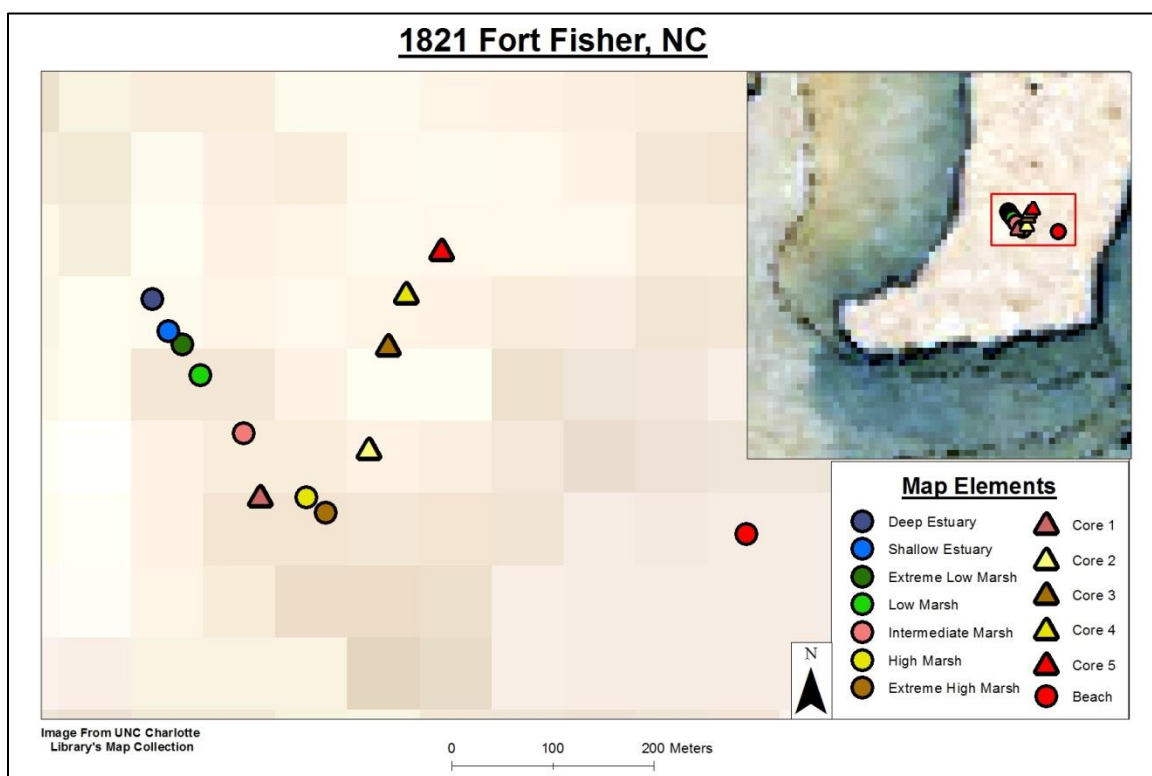


FIGURE 92: A map of 1821 showing the locations of the five core and eight surface samples that were taken adjacent to Fort Fisher. The core samples are shown by triangles and are color-coded to match the subenvironments of the surface samples that are represented by circles. Note: All samples and cores were recovered outside of the Fort Fisher Historical Site state property.

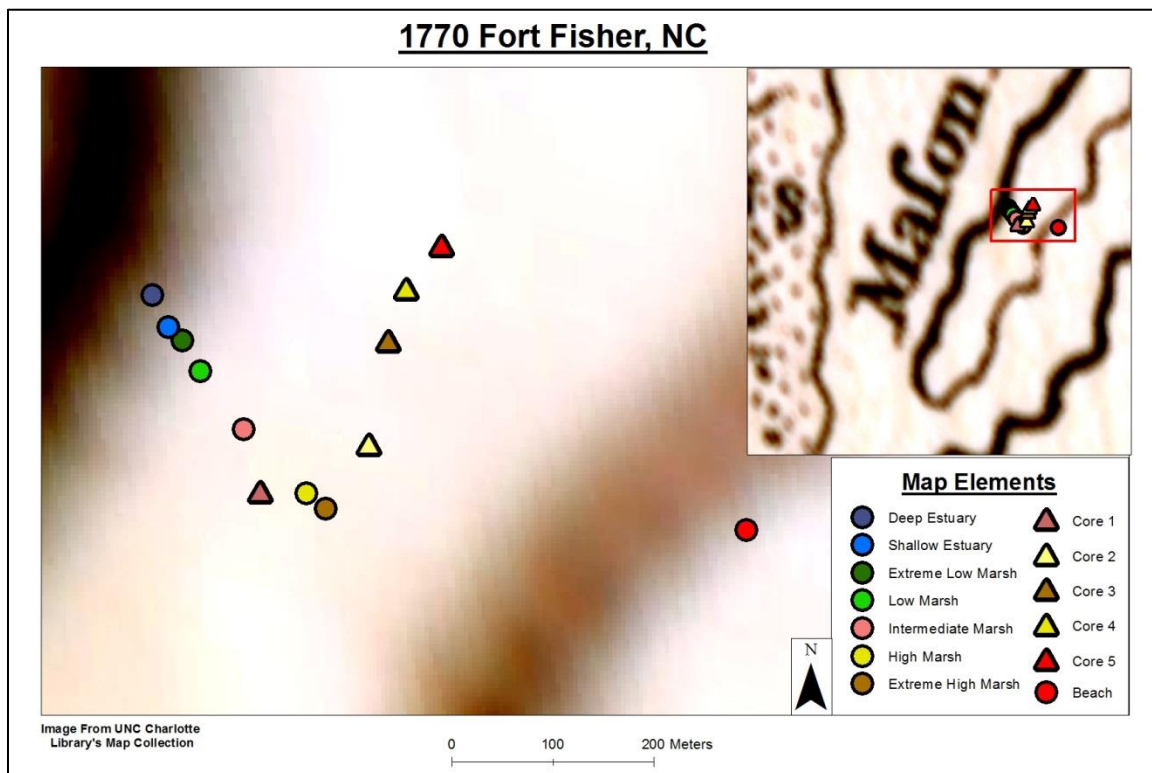


FIGURE 93: A map of 1770 showing the locations of the five core and eight surface samples that were taken adjacent to Fort Fisher. The core samples are shown by triangles and are color-coded to match the subenvironments of the surface samples that are represented by circles. Note: All samples and cores were recovered outside of the Fort Fisher Historical Site state property.

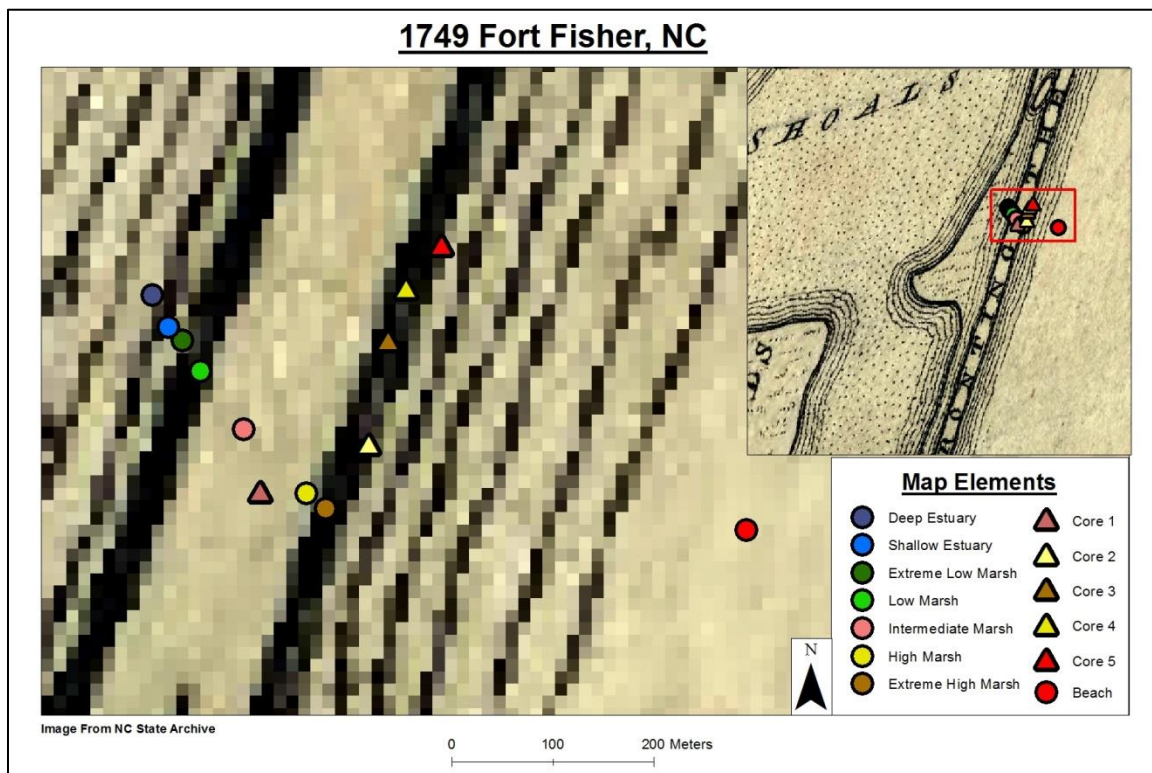


FIGURE 94: A map of 1749 showing the locations of the five core and eight surface samples that were taken adjacent to Fort Fisher. The core samples are shown by triangles and are color-coded to match the subenvironments of the surface samples that are represented by circles. Note: All samples and cores were recovered outside of the Fort Fisher Historical Site state property.

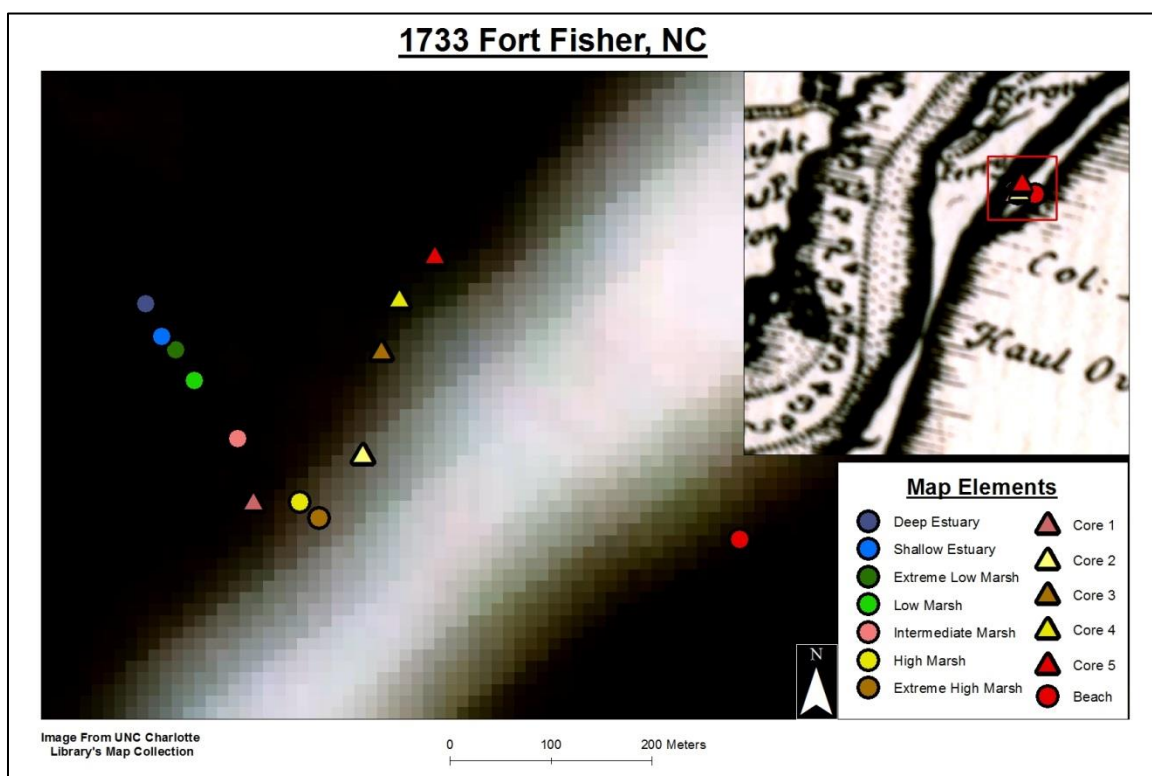


FIGURE 95: A map of 1733 showing the locations of the five core and eight surface samples that were taken adjacent to Fort Fisher. The core samples are shown by triangles and are color-coded to match the subenvironments of the surface samples that are represented by circles. Note: All samples and cores were recovered outside of the Fort Fisher Historical Site state property.

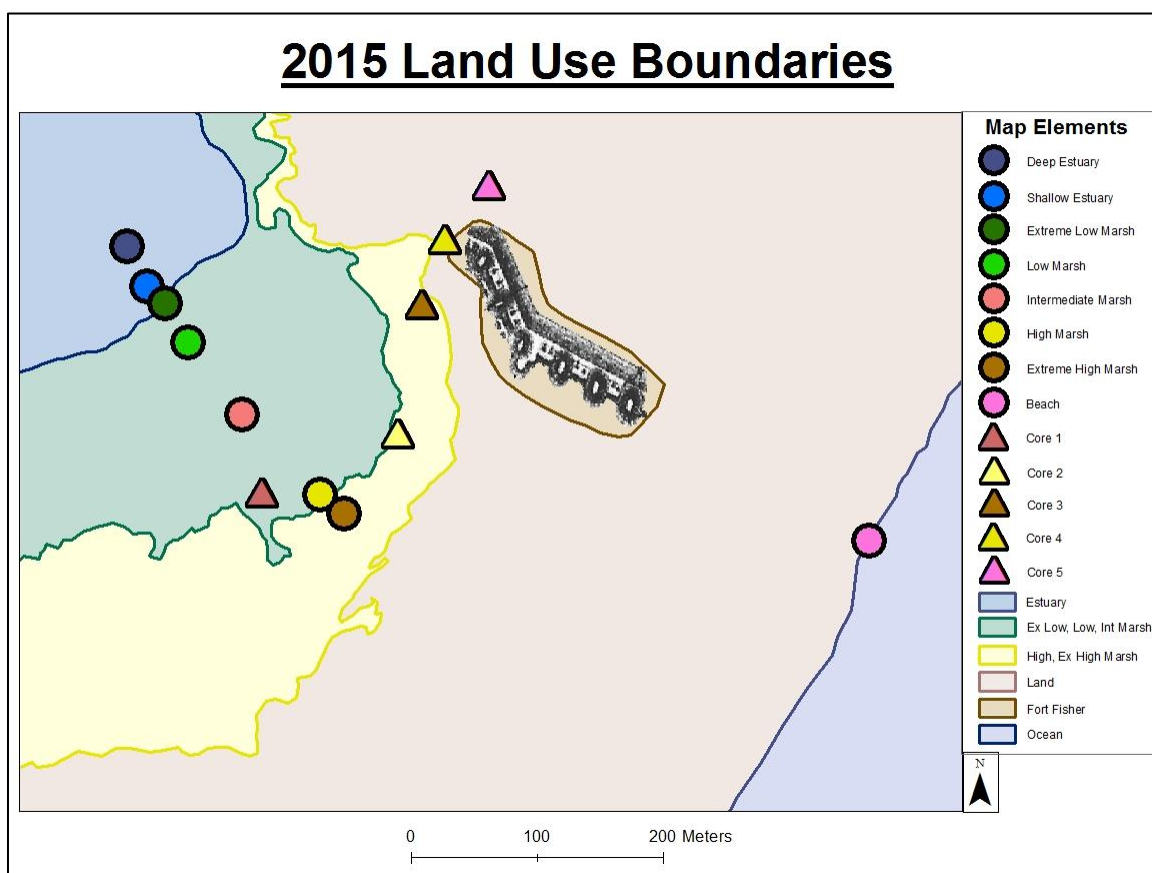


FIGURE 96: Map of 2015 depicting the boundaries between each of the distinguishable subenvironments. All five core and eight surface samples that were taken adjacent to Fort Fisher are shown, including a picture of the remaining fort. The core samples (in triangles) are color-coded to match the subenvironments of the surface samples (in circles). Additionally, each subenvironment is color-coded to distinguish it from the other subenvironments, which can be seen on the legend.

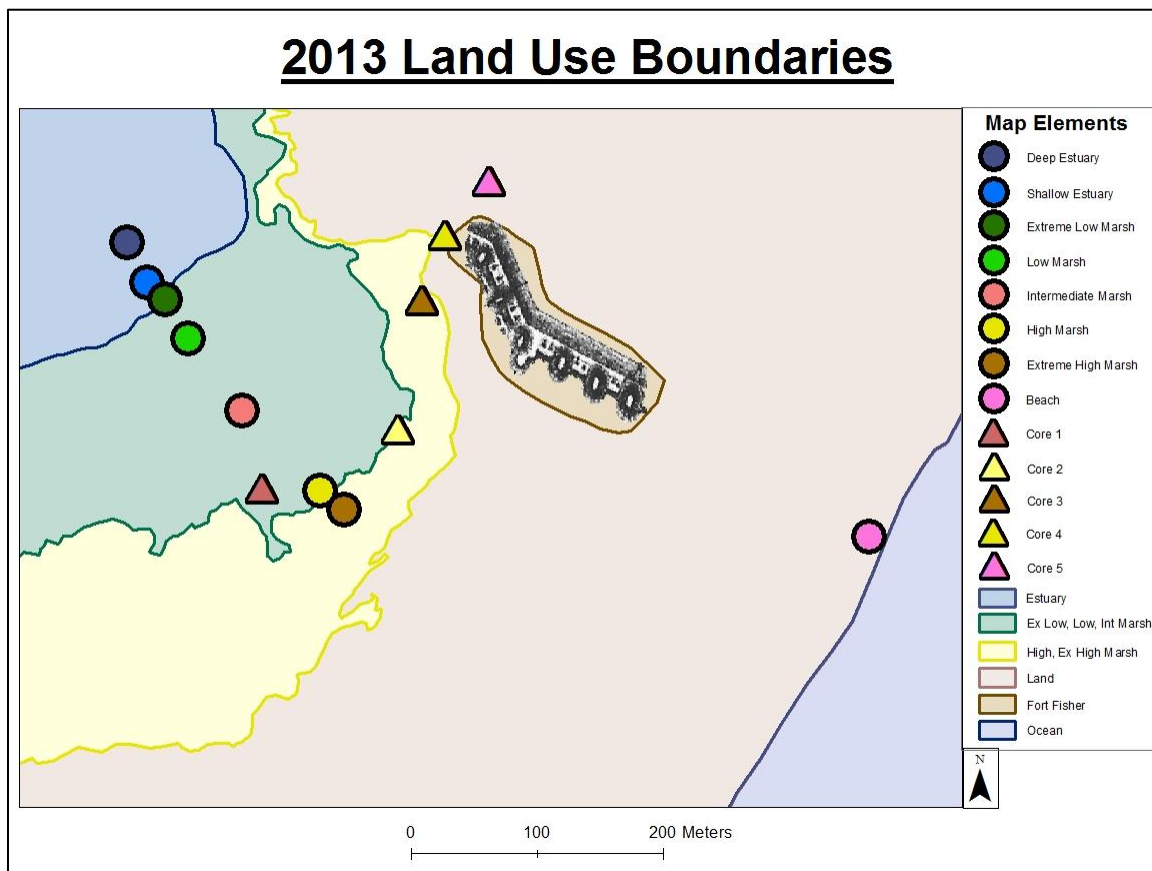


FIGURE 97: Map of 2013 depicting the boundaries between each of the distinguishable subenvironments. All five core and eight surface samples that were taken adjacent to Fort Fisher are shown, including a picture of the remaining fort. The core samples (in triangles) are color-coded to match the subenvironments of the surface samples (in circles). Additionally, each subenvironment is color-coded to distinguish it from the other subenvironments, which can be seen on the legend.

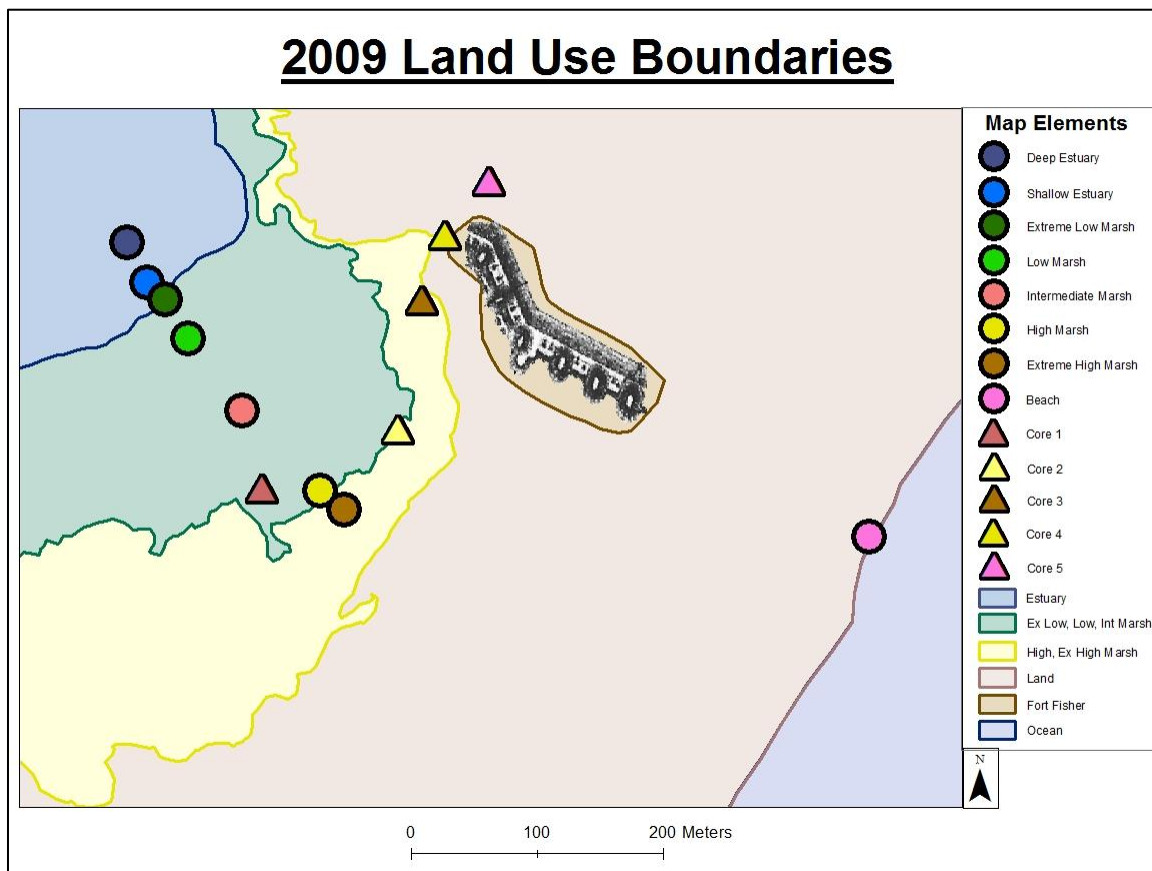


FIGURE 98: Map of 2009 depicting the boundaries between each of the distinguishable subenvironments. All five core and eight surface samples that were taken adjacent to Fort Fisher are shown, including a picture of the remaining fort. The core samples (in triangles) are color-coded to match the subenvironments of the surface samples (in circles). Additionally, each subenvironment is color-coded to distinguish it from the other subenvironments, which can be seen on the legend.

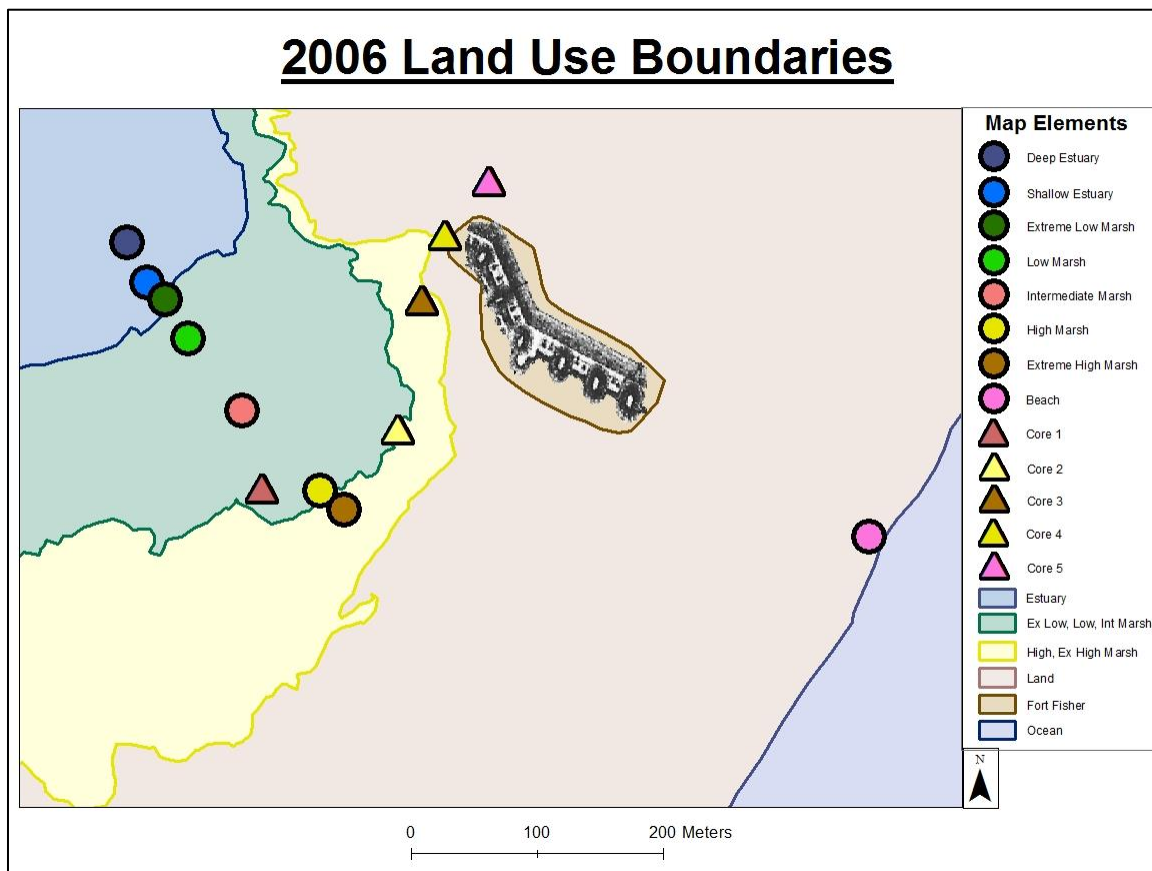


FIGURE 99: Map of 2006 depicting the boundaries between each of the distinguishable subenvironments. All five core and eight surface samples that were taken adjacent to Fort Fisher are shown, including a picture of the remaining fort. The core samples (in triangles) are color-coded to match the subenvironments of the surface samples (in circles). Additionally, each subenvironment is color-coded to distinguish it from the other subenvironments, which can be seen on the legend.

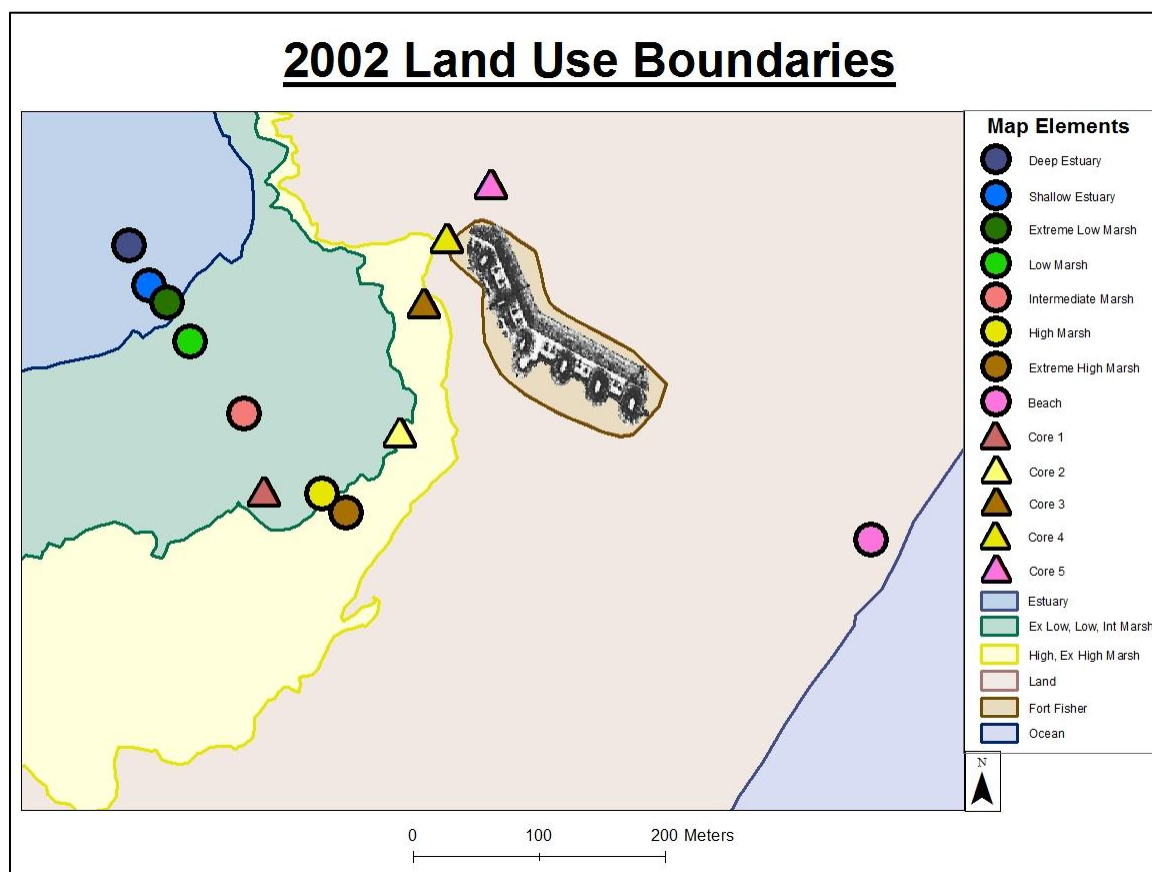


FIGURE 100: Map of 2002 depicting the boundaries between each of the distinguishable subenvironments. All five core and eight surface samples that were taken adjacent to Fort Fisher are shown, including a picture of the remaining fort. The core samples (in triangles) are color-coded to match the subenvironments of the surface samples (in circles). Additionally, each subenvironment is color-coded to distinguish it from the other subenvironments, which can be seen on the legend.

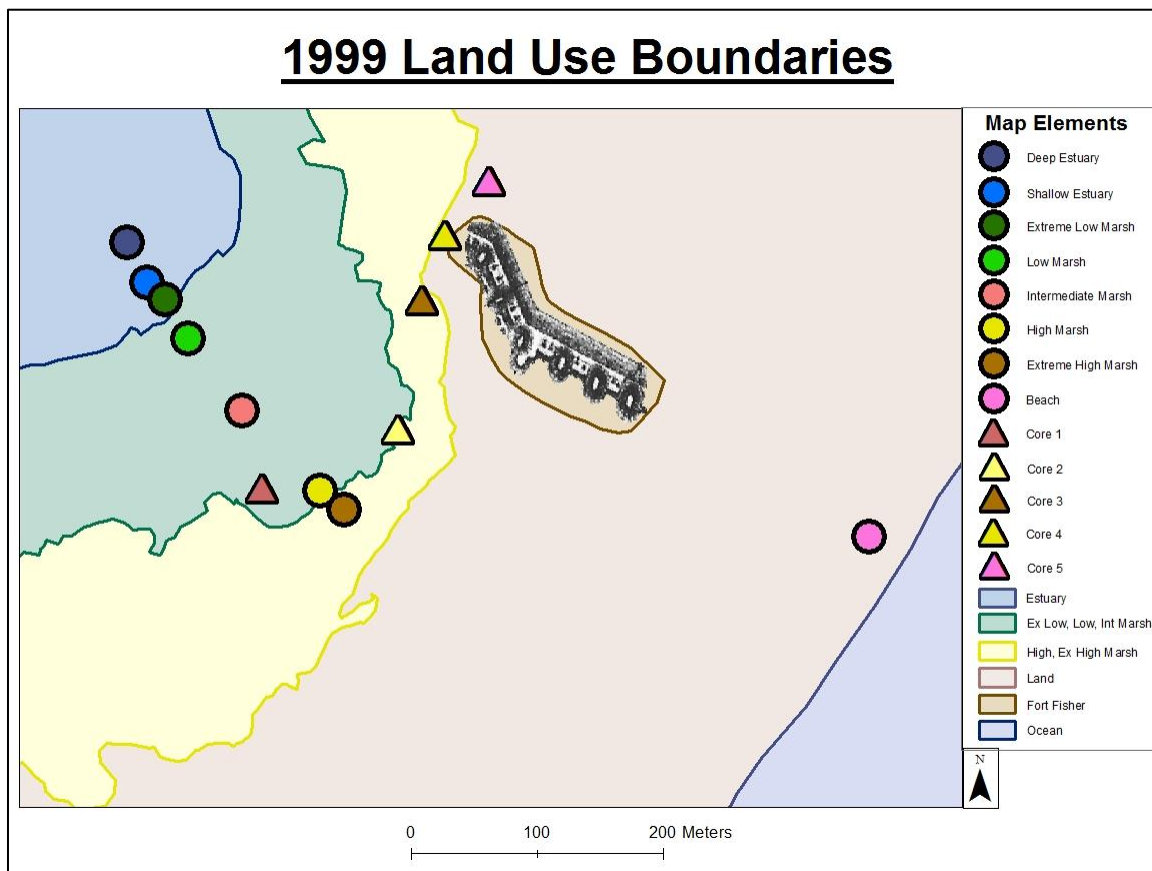


FIGURE 101: Map of 1999 depicting the boundaries between each of the distinguishable subenvironments. All five core and eight surface samples that were taken adjacent to Fort Fisher are shown, including a picture of the remaining fort. The core samples (in triangles) are color-coded to match the subenvironments of the surface samples (in circles). Additionally, each subenvironment is color-coded to distinguish it from the other subenvironments, which can be seen on the legend.

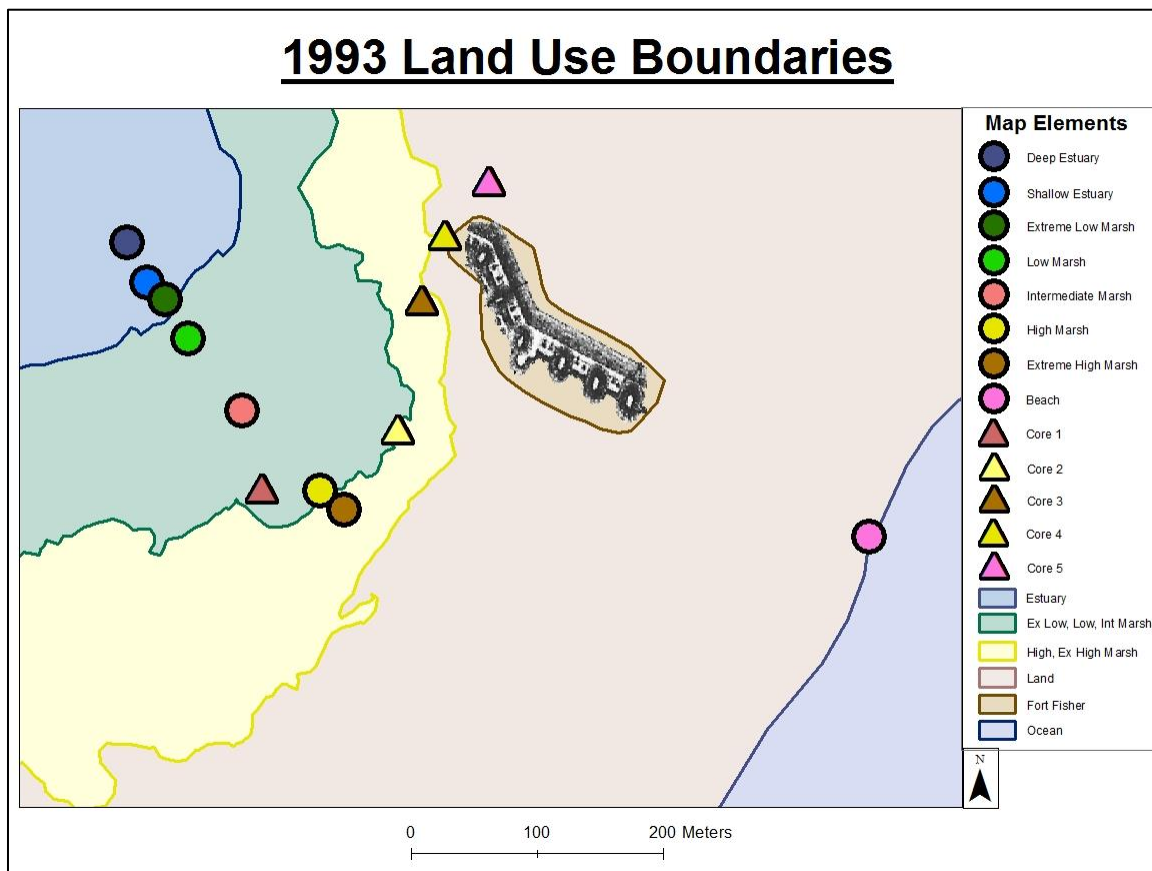


FIGURE 102: Map of 1993 depicting the boundaries between each of the distinguishable subenvironments. All five core and eight surface samples that were taken adjacent to Fort Fisher are shown, including a picture of the remaining fort. The core samples (in triangles) are color-coded to match the subenvironments of the surface samples (in circles). Additionally, each subenvironment is color-coded to distinguish it from the other subenvironments, which can be seen on the legend.

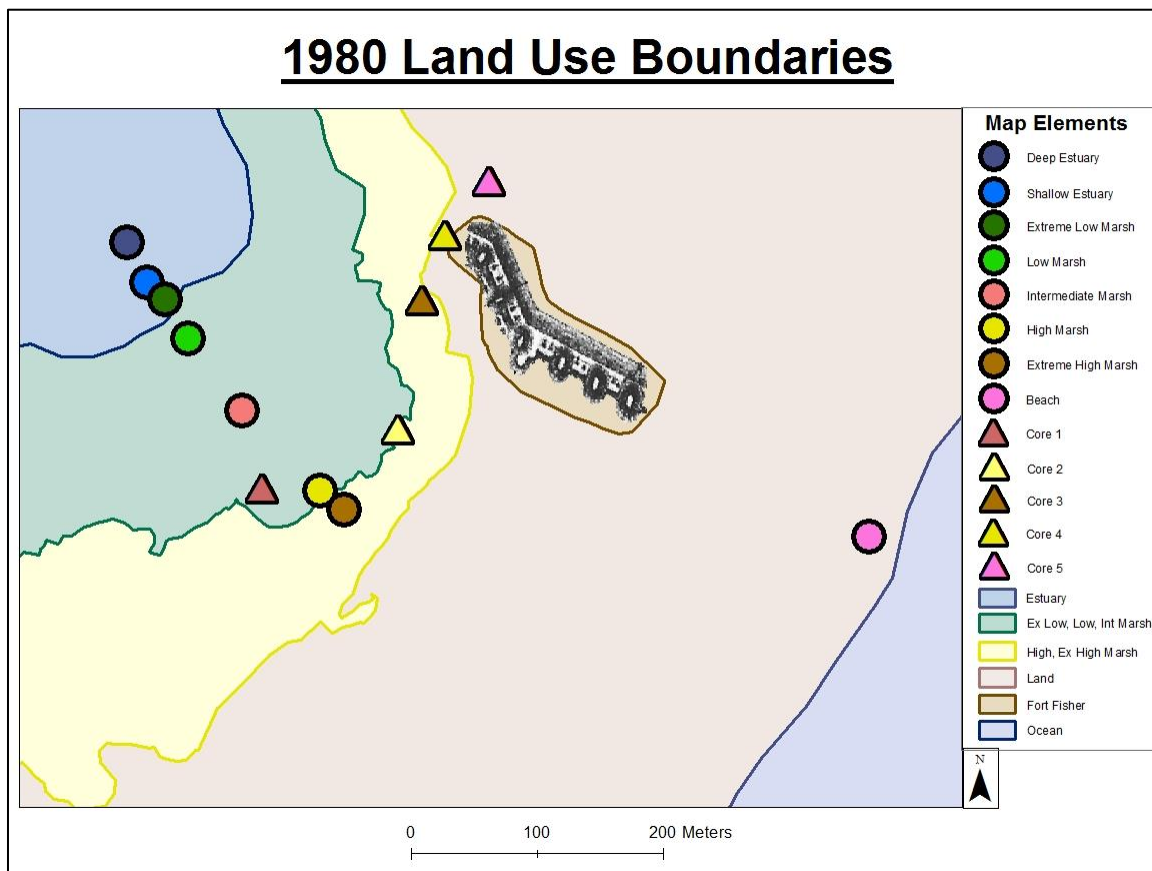


FIGURE 103: Map of 1980 depicting the boundaries between each of the distinguishable subenvironments. All five core and eight surface samples that were taken adjacent to Fort Fisher are shown, including a picture of the remaining fort. The core samples (in triangles) are color-coded to match the subenvironments of the surface samples (in circles). Additionally, each subenvironment is color-coded to distinguish it from the other subenvironments, which can be seen on the legend.

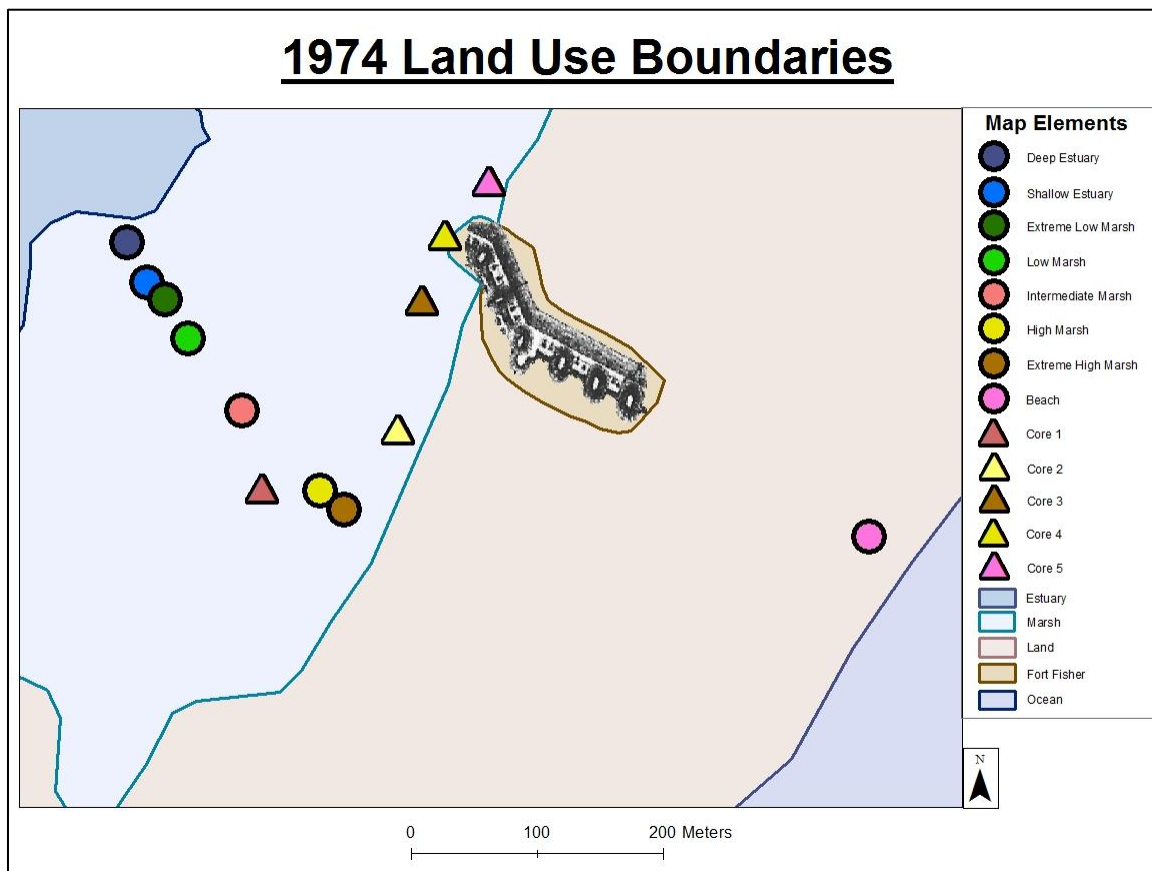


FIGURE 104: Map of 1974 depicting the boundaries between each of the distinguishable subenvironments. All five core and eight surface samples that were taken adjacent to Fort Fisher are shown, including a picture of the remaining fort. The core samples (in triangles) are color-coded to match the subenvironments of the surface samples (in circles). Additionally, each subenvironment is color-coded to distinguish it from the other subenvironments, which can be seen on the legend.

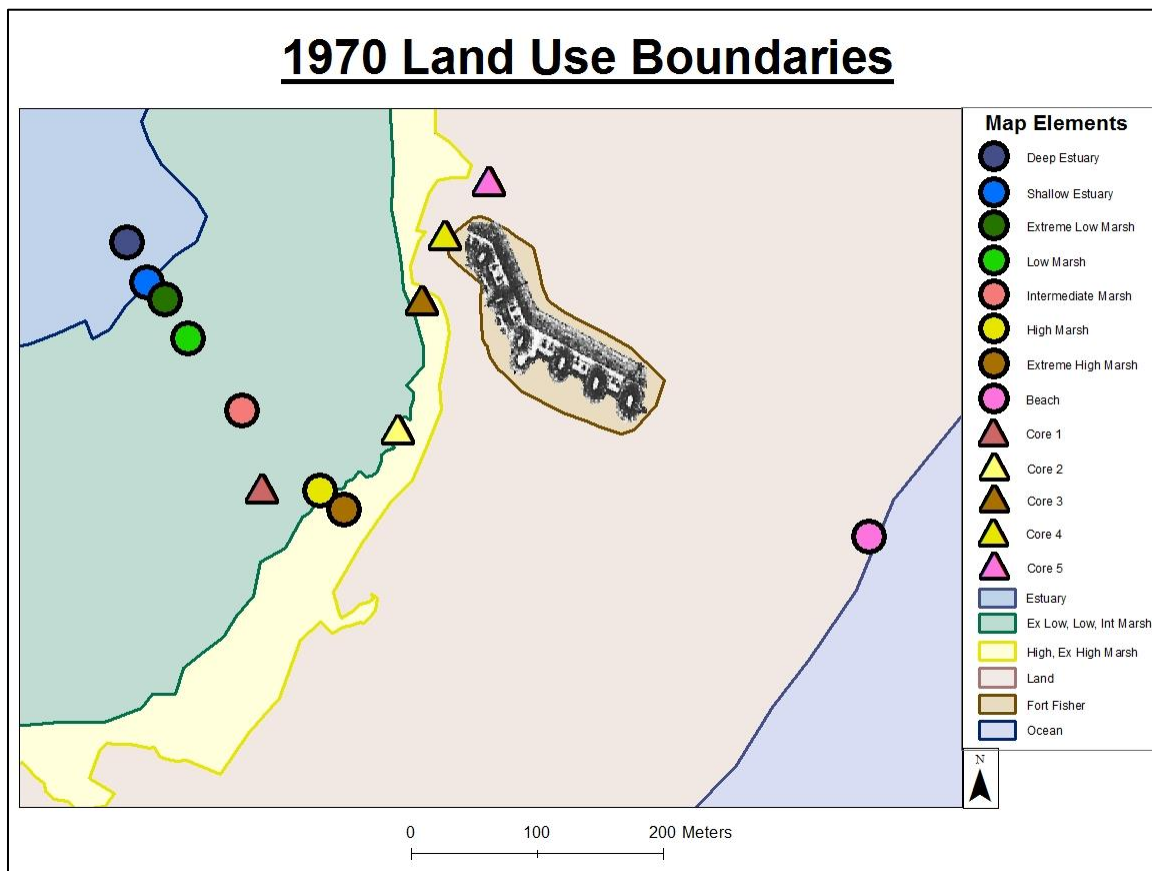


FIGURE 105: Map of 1970 depicting the boundaries between each of the distinguishable subenvironments. All five core and eight surface samples that were taken adjacent to Fort Fisher are shown, including a picture of the remaining fort. The core samples (in triangles) are color-coded to match the subenvironments of the surface samples (in circles). Additionally, each subenvironment is color-coded to distinguish it from the other subenvironments, which can be seen on the legend.

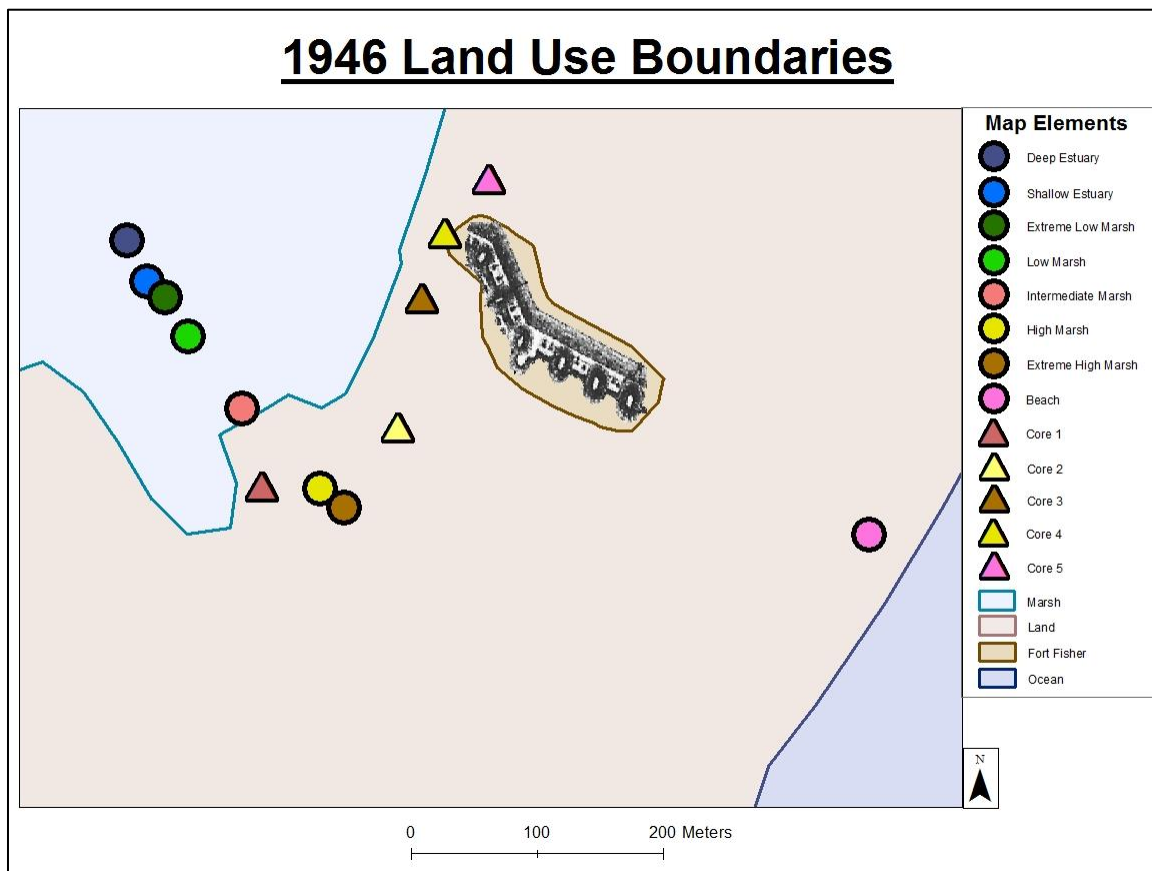


FIGURE 106: Map of 1946 depicting the boundaries between each of the distinguishable subenvironments. All five core and eight surface samples that were taken adjacent to Fort Fisher are shown, including a picture of the remaining fort. The core samples (in triangles) are color-coded to match the subenvironments of the surface samples (in circles). Additionally, each subenvironment is color-coded to distinguish it from the other subenvironments, which can be seen on the legend.

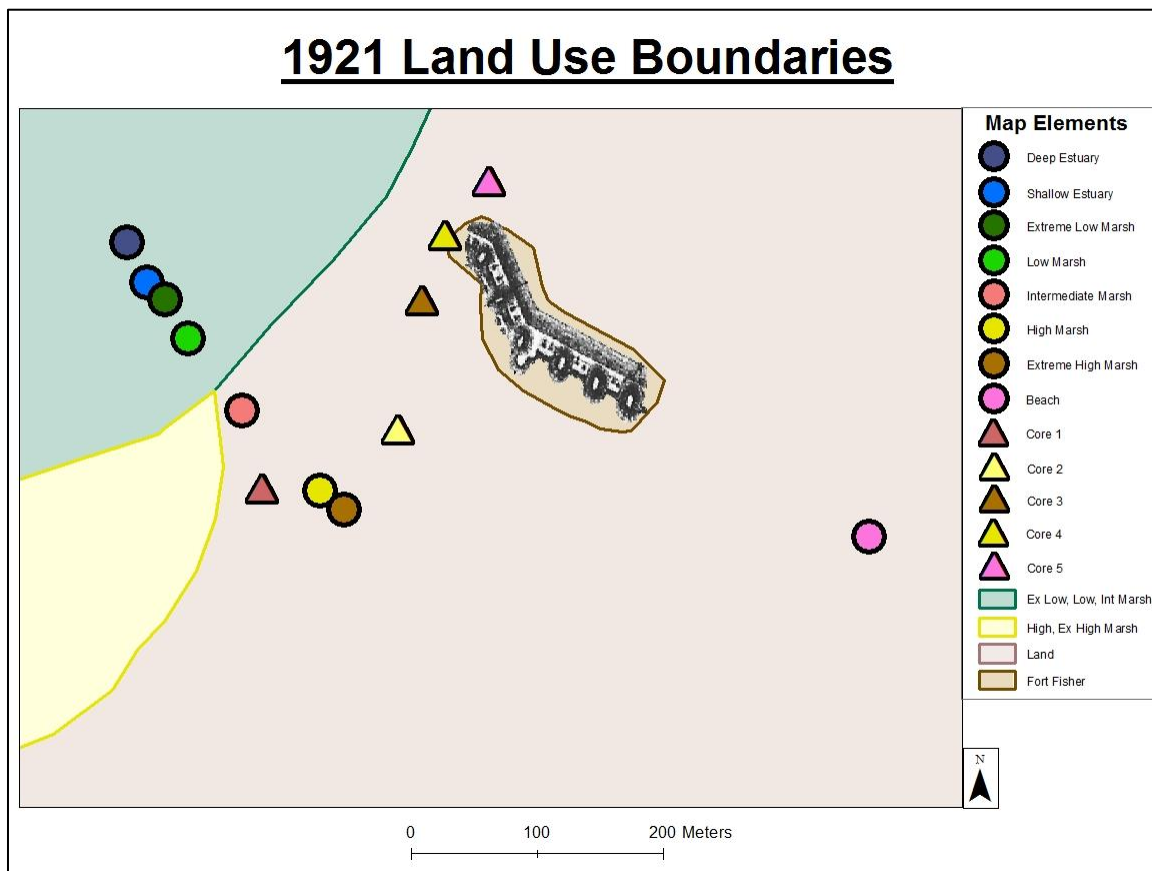


FIGURE 107: Map of 1921 depicting the boundaries between each of the distinguishable subenvironments. All five core and eight surface samples that were taken adjacent to Fort Fisher are shown, including a picture of the remaining fort. The core samples (in triangles) are color-coded to match the subenvironments of the surface samples (in circles). Additionally, each subenvironment is color-coded to distinguish it from the other subenvironments, which can be seen on the legend.

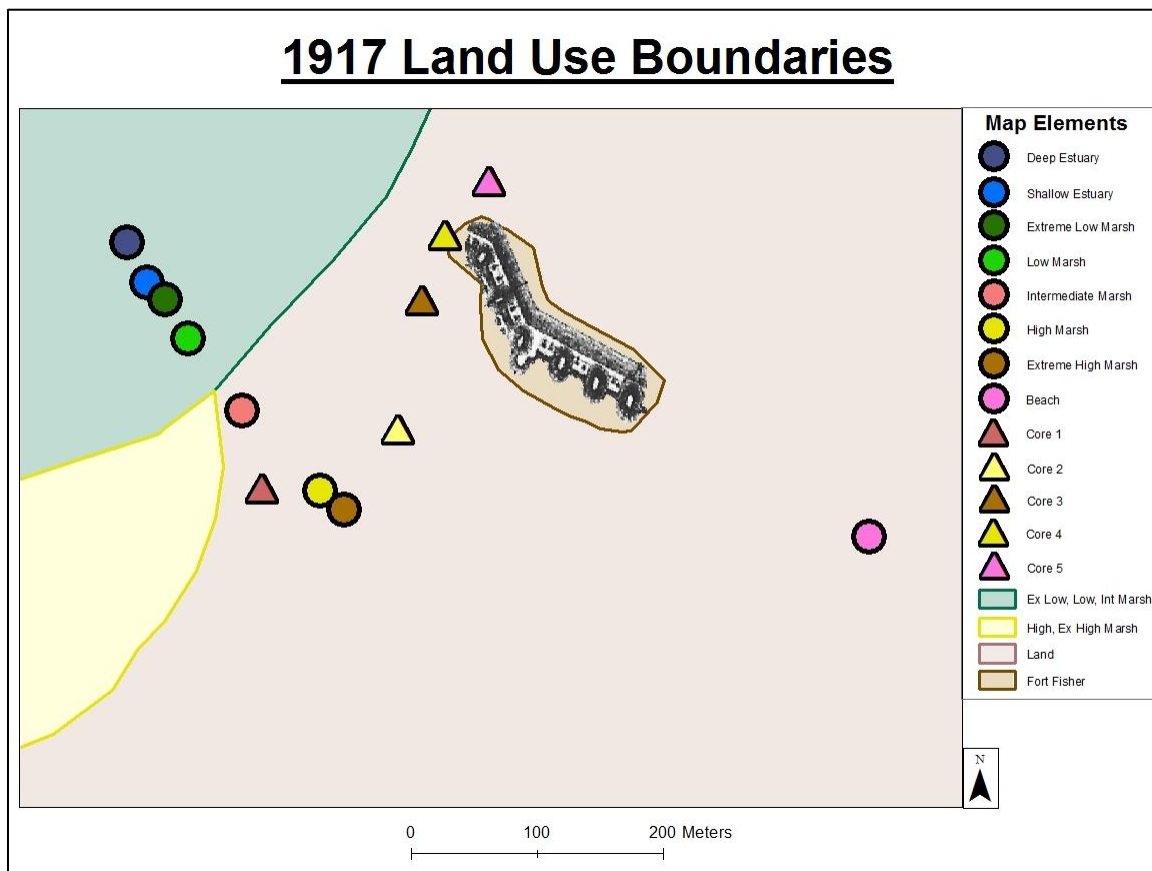


FIGURE 108: Map of 1917 depicting the boundaries between each of the distinguishable subenvironments. All five core and eight surface samples that were taken adjacent to Fort Fisher are shown, including a picture of the remaining fort. The core samples (in triangles) are color-coded to match the subenvironments of the surface samples (in circles). Additionally, each subenvironment is color-coded to distinguish it from the other subenvironments, which can be seen on the legend.

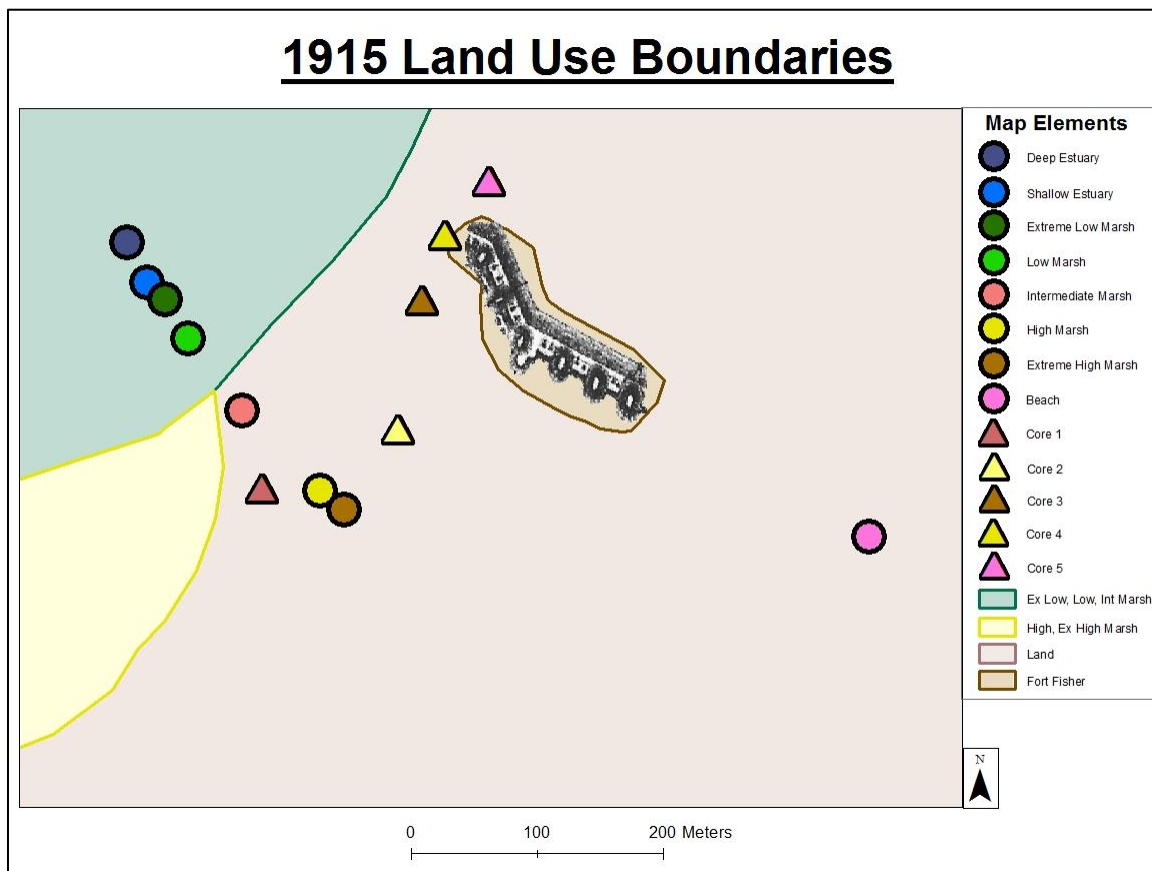


FIGURE 109: Map of 1915 depicting the boundaries between each of the distinguishable subenvironments. All five core and eight surface samples that were taken adjacent to Fort Fisher are shown, including a picture of the remaining fort. The core samples (in triangles) are color-coded to match the subenvironments of the surface samples (in circles). Additionally, each subenvironment is color-coded to distinguish it from the other subenvironments, which can be seen on the legend.

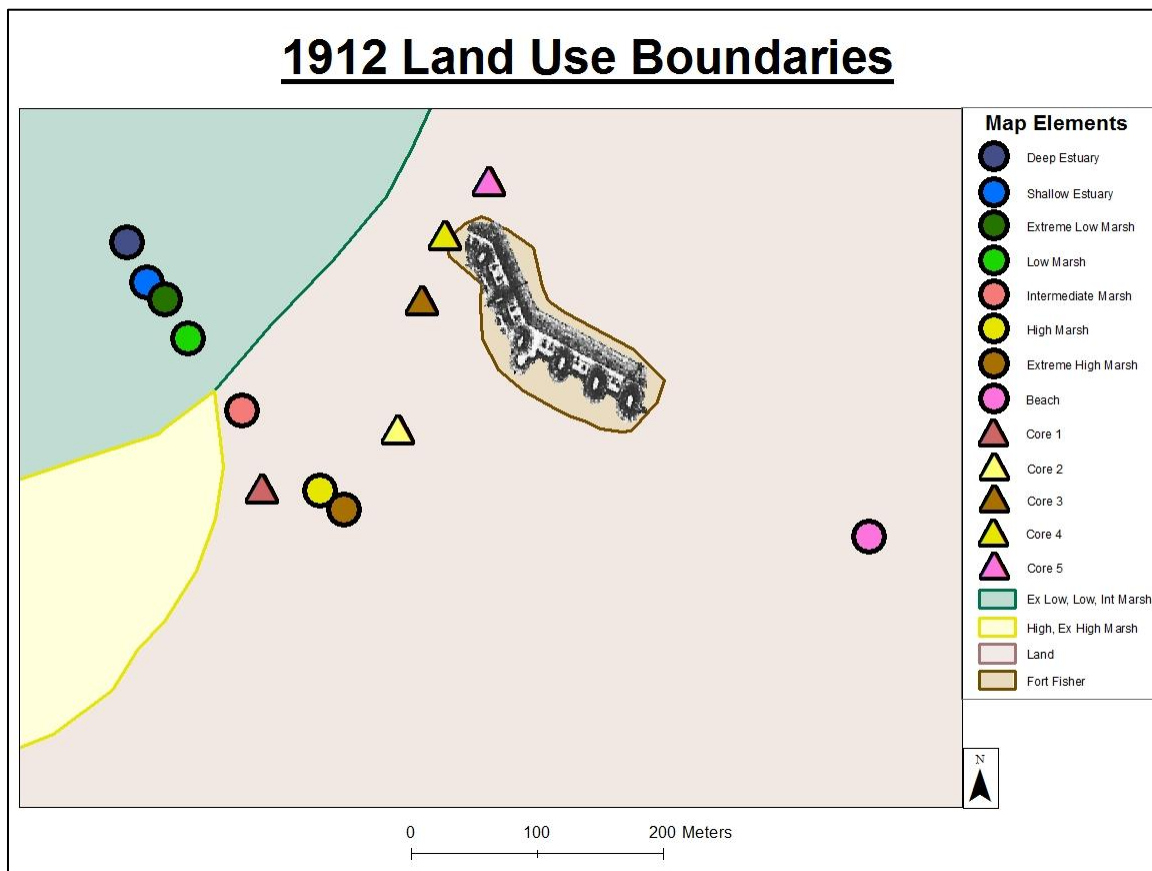


FIGURE 110: Map of 1912 depicting the boundaries between each of the distinguishable subenvironments. All five core and eight surface samples that were taken adjacent to Fort Fisher are shown, including a picture of the remaining fort. The core samples (in triangles) are color-coded to match the subenvironments of the surface samples (in circles). Additionally, each subenvironment is color-coded to distinguish it from the other subenvironments, which can be seen on the legend.

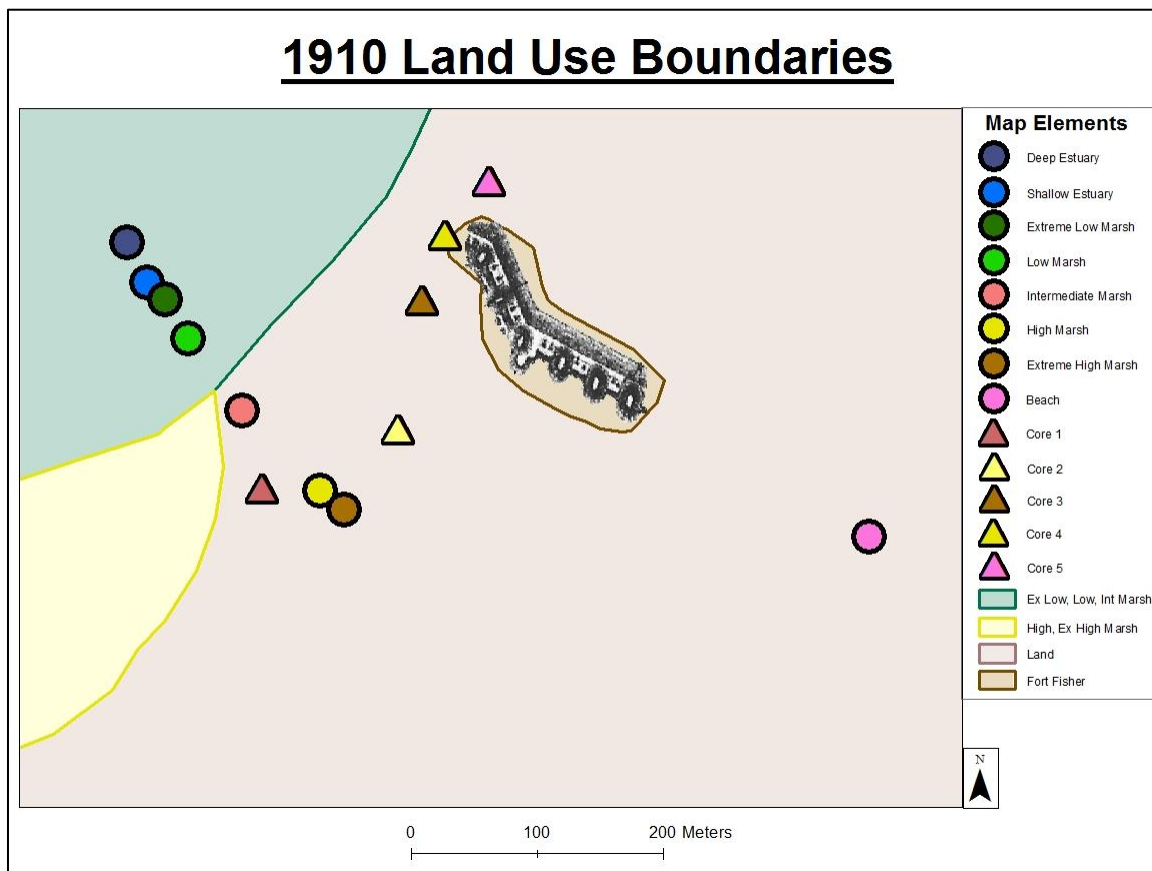


FIGURE 111: Map of 1910 depicting the boundaries between each of the distinguishable subenvironments. All five core and eight surface samples that were taken adjacent to Fort Fisher are shown, including a picture of the remaining fort. The core samples (in triangles) are color-coded to match the subenvironments of the surface samples (in circles). Additionally, each subenvironment is color-coded to distinguish it from the other subenvironments, which can be seen on the legend.

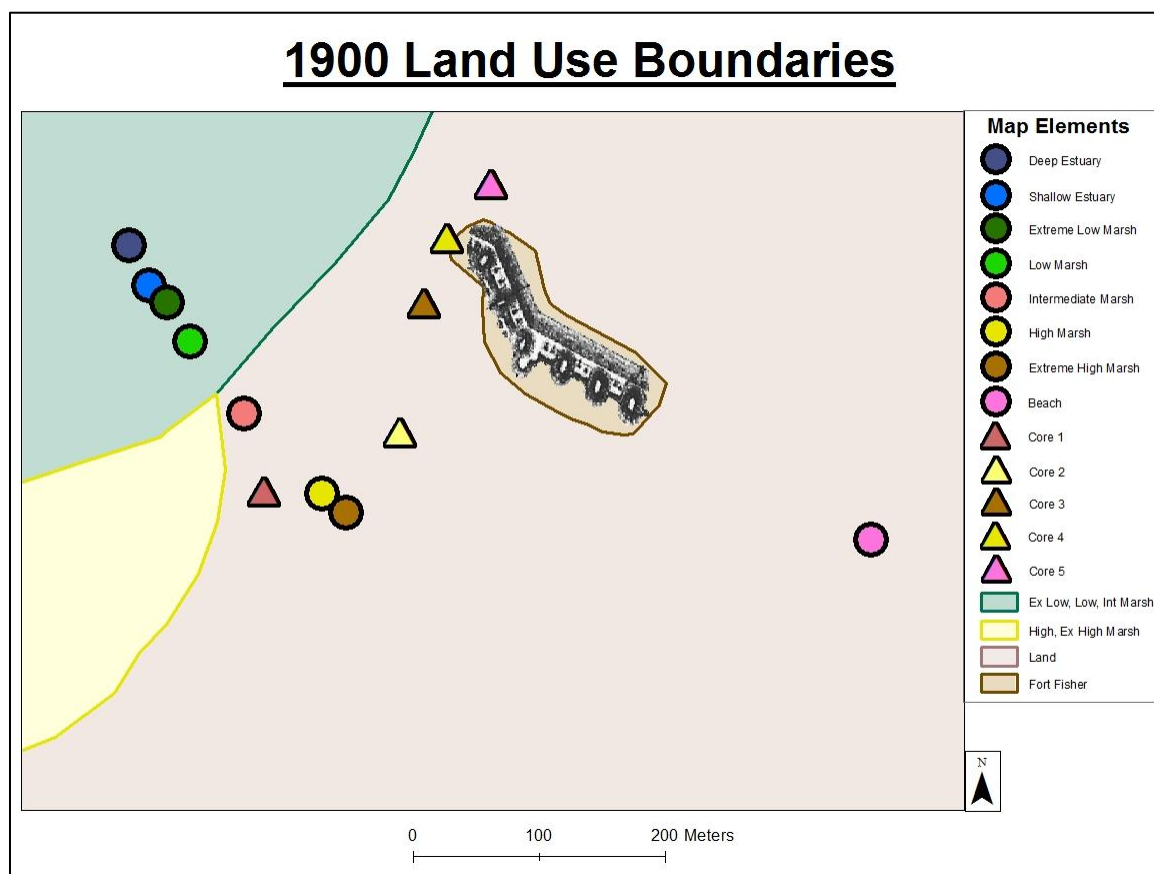


FIGURE 112: Map of 1900 depicting the boundaries between each of the distinguishable subenvironments. All five core and eight surface samples that were taken adjacent to Fort Fisher are shown, including a picture of the remaining fort. The core samples (in triangles) are color-coded to match the subenvironments of the surface samples (in circles). Additionally, each subenvironment is color-coded to distinguish it from the other subenvironments, which can be seen on the legend.

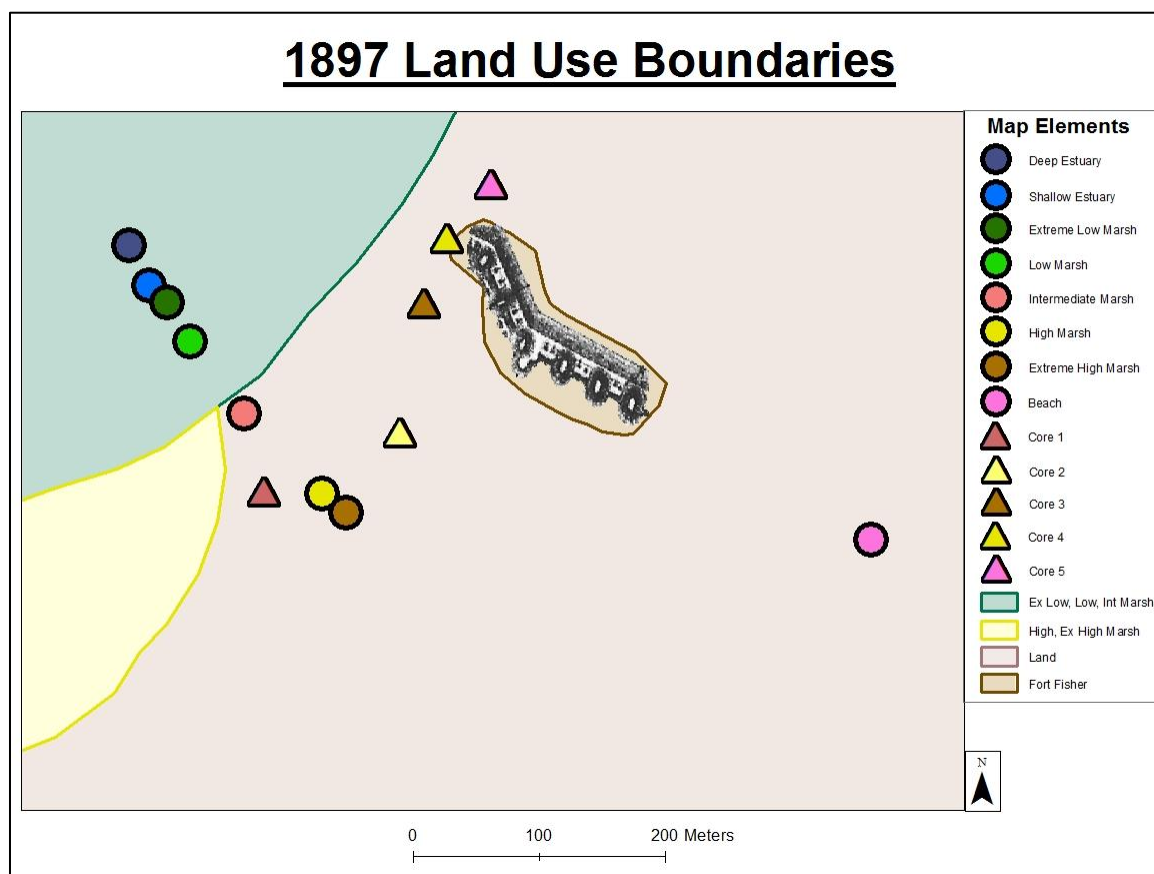


FIGURE 113: Map of 1897 depicting the boundaries between each of the distinguishable subenvironments. All five core and eight surface samples that were taken adjacent to Fort Fisher are shown, including a picture of the remaining fort. The core samples (in triangles) are color-coded to match the subenvironments of the surface samples (in circles). Additionally, each subenvironment is color-coded to distinguish it from the other subenvironments, which can be seen on the legend.

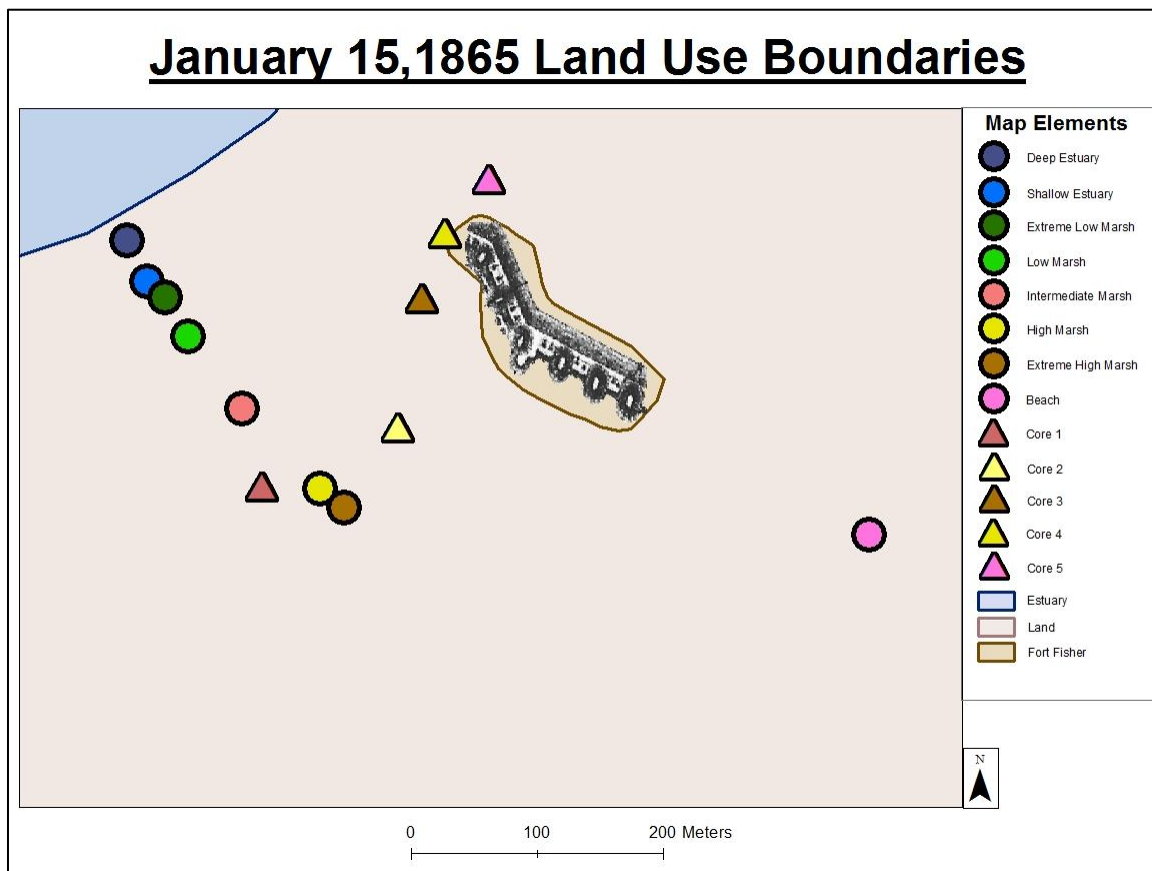


FIGURE 114: Map of 1865 depicting the boundaries between each of the distinguishable subenvironments. All five core and eight surface samples that were taken adjacent to Fort Fisher are shown, including a picture of the remaining fort. The core samples (in triangles) are color-coded to match the subenvironments of the surface samples (in circles). Additionally, each subenvironment is color-coded to distinguish it from the other subenvironments, which can be seen on the legend.

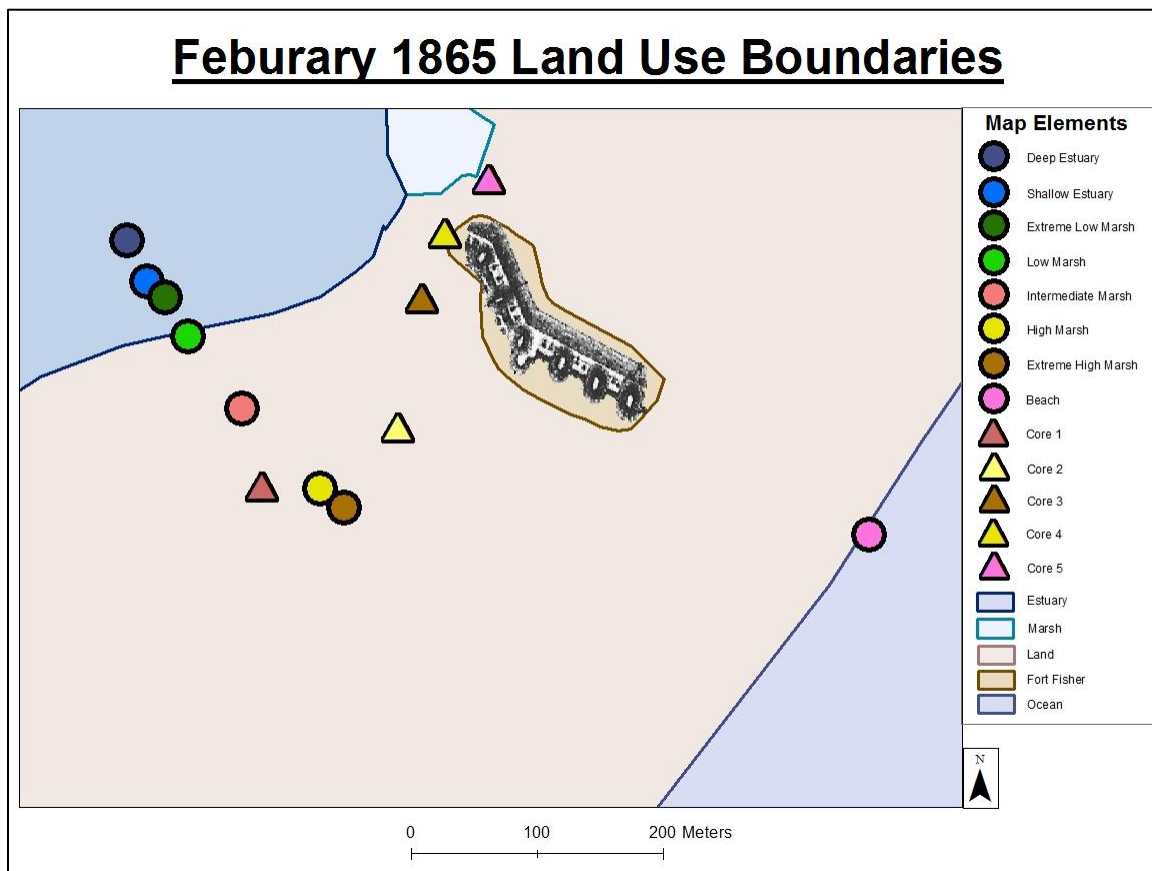


FIGURE 115: Map of 1865 depicting the boundaries between each of the distinguishable subenvironments. All five core and eight surface samples that were taken adjacent to Fort Fisher are shown, including a picture of the remaining fort. The core samples (in triangles) are color-coded to match the subenvironments of the surface samples (in circles). Additionally, each subenvironment is color-coded to distinguish it from the other subenvironments, which can be seen on the legend.

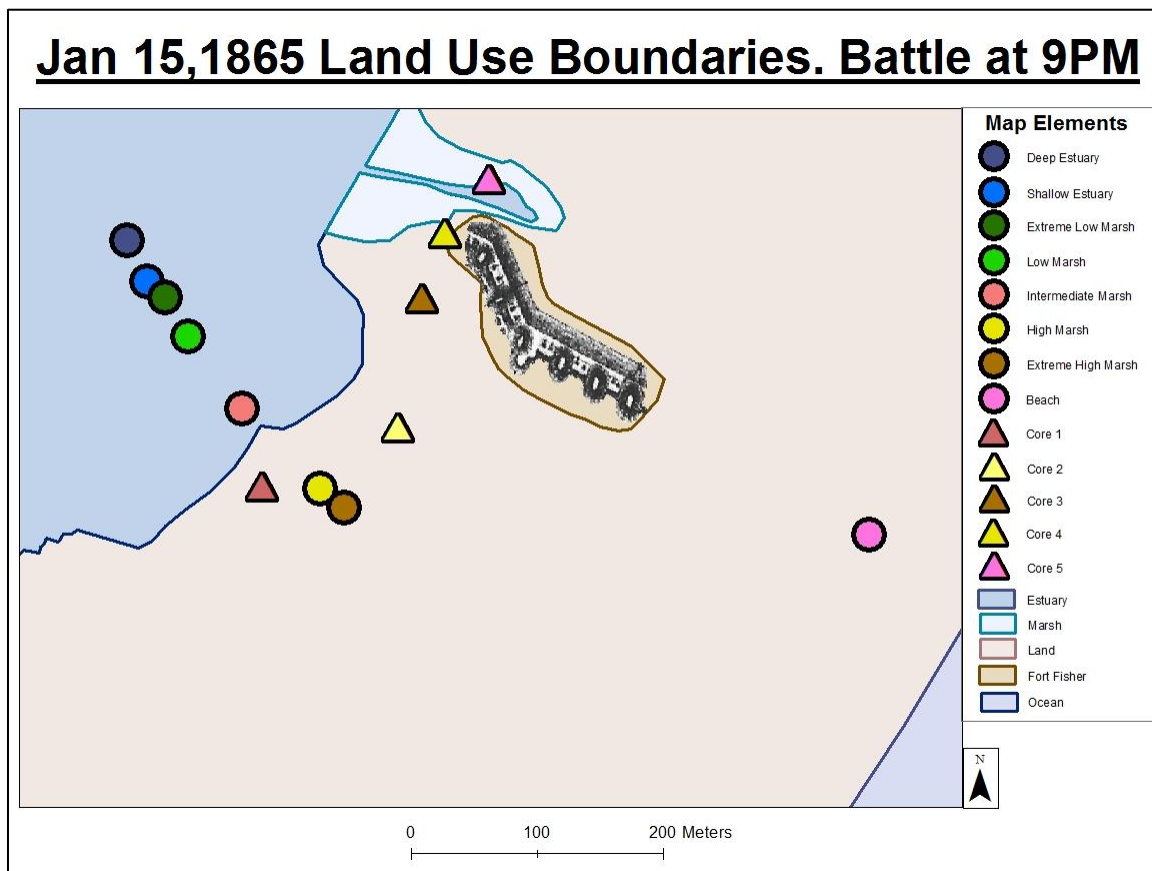


FIGURE 116: Map of 1865 depicting the boundaries between each of the distinguishable subenvironments. All five core and eight surface samples that were taken adjacent to Fort Fisher are shown, including a picture of the remaining fort. The core samples (in triangles) are color-coded to match the subenvironments of the surface samples (in circles). Additionally, each subenvironment is color-coded to distinguish it from the other subenvironments, which can be seen on the legend.

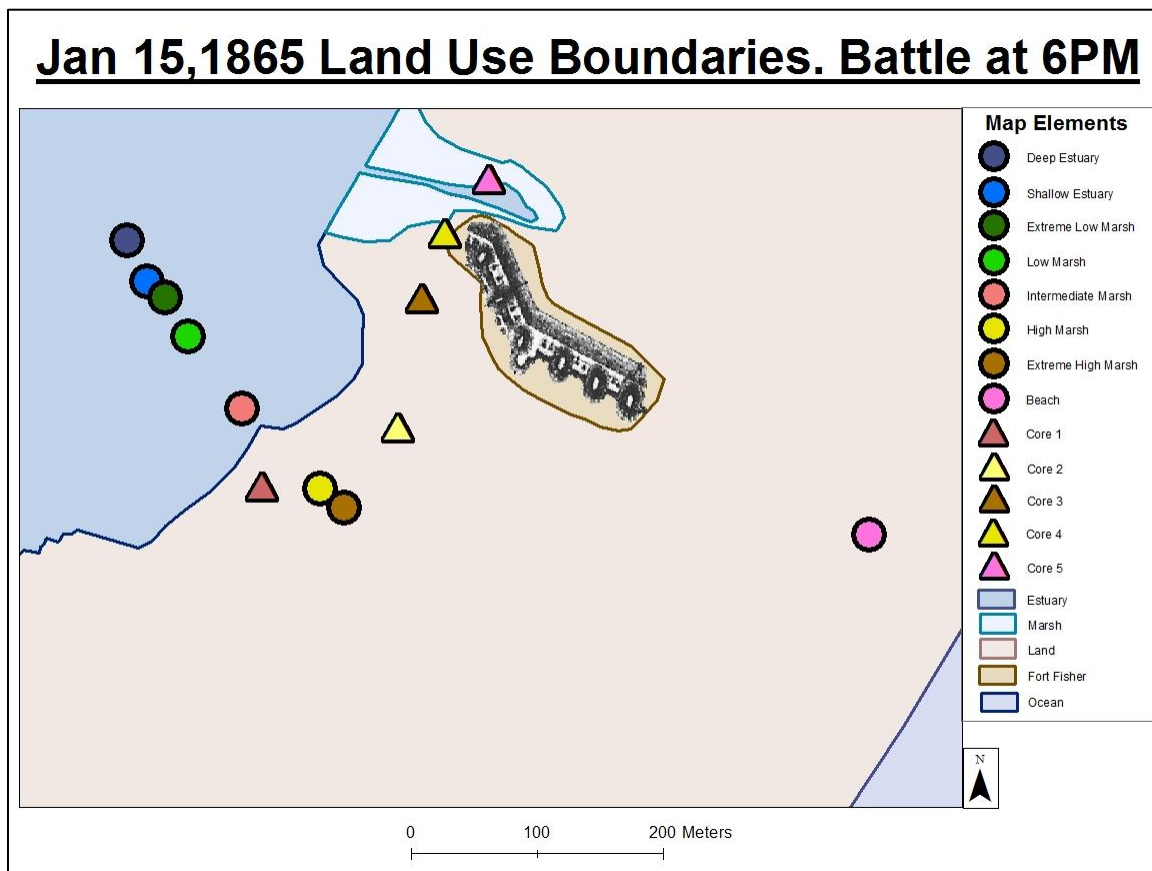


FIGURE 117: A map of 1865 showing the boundaries between each of the subenvironments that were distinguishable. All five core and eight surface samples that were taken adjacent to Fort Fisher are shown, including a picture of the remnants of the fort. The core samples are shown by triangles and are color-coded to match the subenvironments of the surface samples that are represented by circles. Additionally, each subenvironment is color-coded to distinguish it from others, as can be seen on the legend.

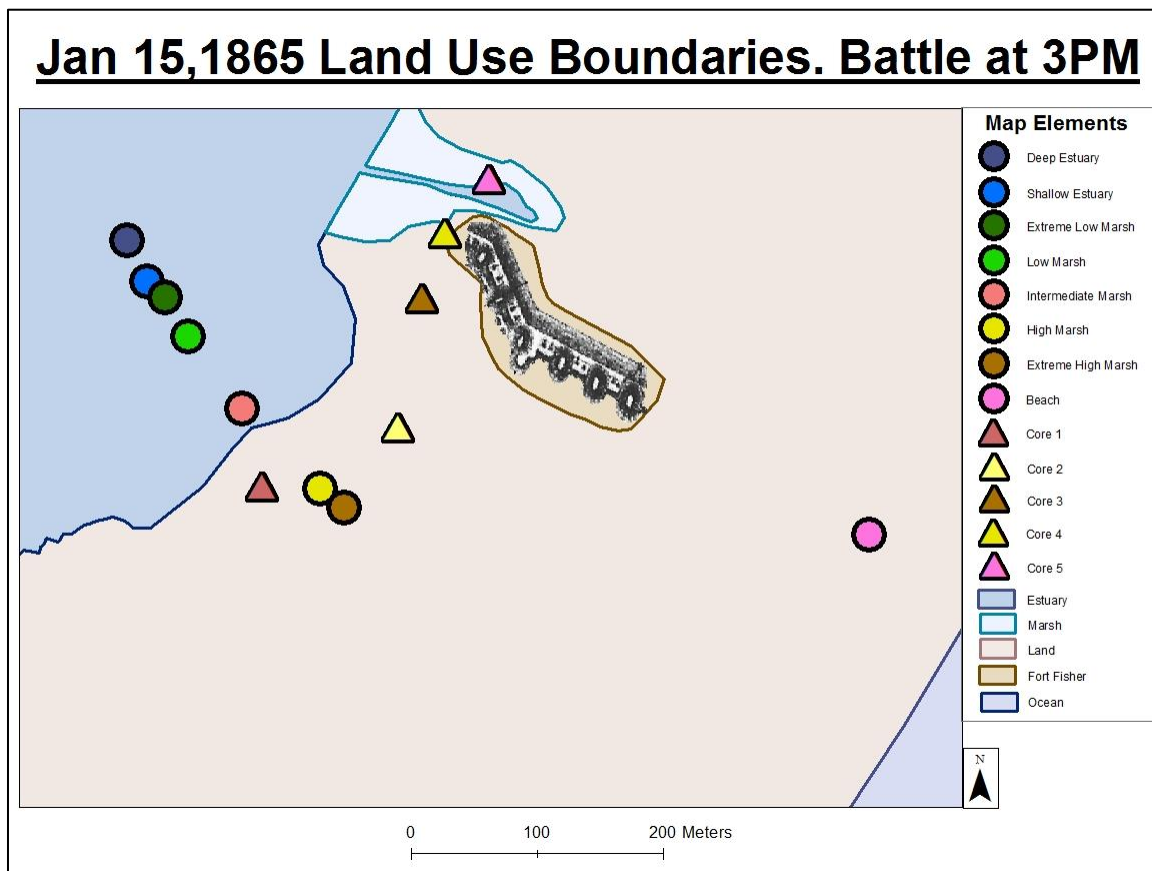


FIGURE 118: Map of 1865 depicting the boundaries between each of the distinguishable subenvironments. All five core and eight surface samples that were taken adjacent to Fort Fisher are shown, including a picture of the remaining fort. The core samples (in triangles) are color-coded to match the subenvironments of the surface samples (in circles). Additionally, each subenvironment is color-coded to distinguish it from the other subenvironments, which can be seen on the legend.

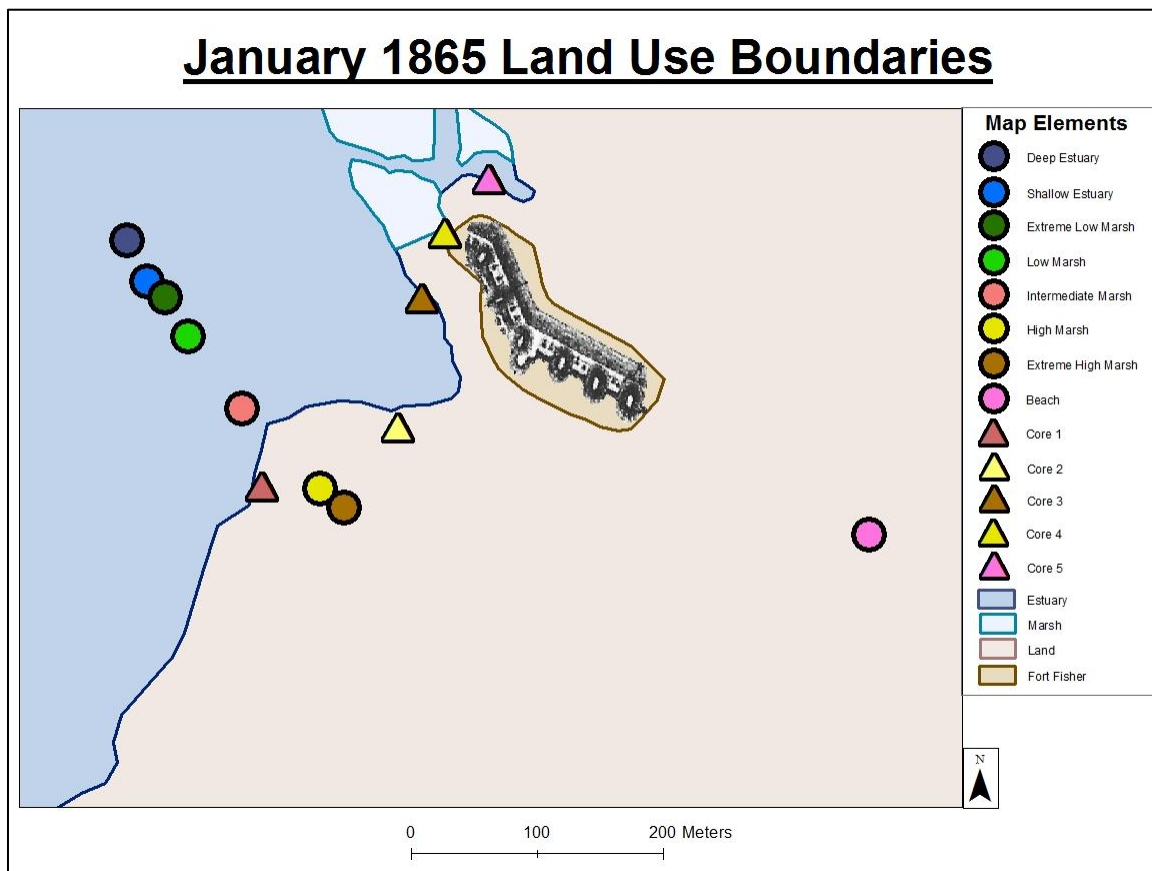


FIGURE 119: Map of 1865 depicting the boundaries between each of the distinguishable subenvironments. All five core and eight surface samples that were taken adjacent to Fort Fisher are shown, including a picture of the remaining fort. The core samples (in triangles) are color-coded to match the subenvironments of the surface samples (in circles). Additionally, each subenvironment is color-coded to distinguish it from the other subenvironments, which can be seen on the legend.

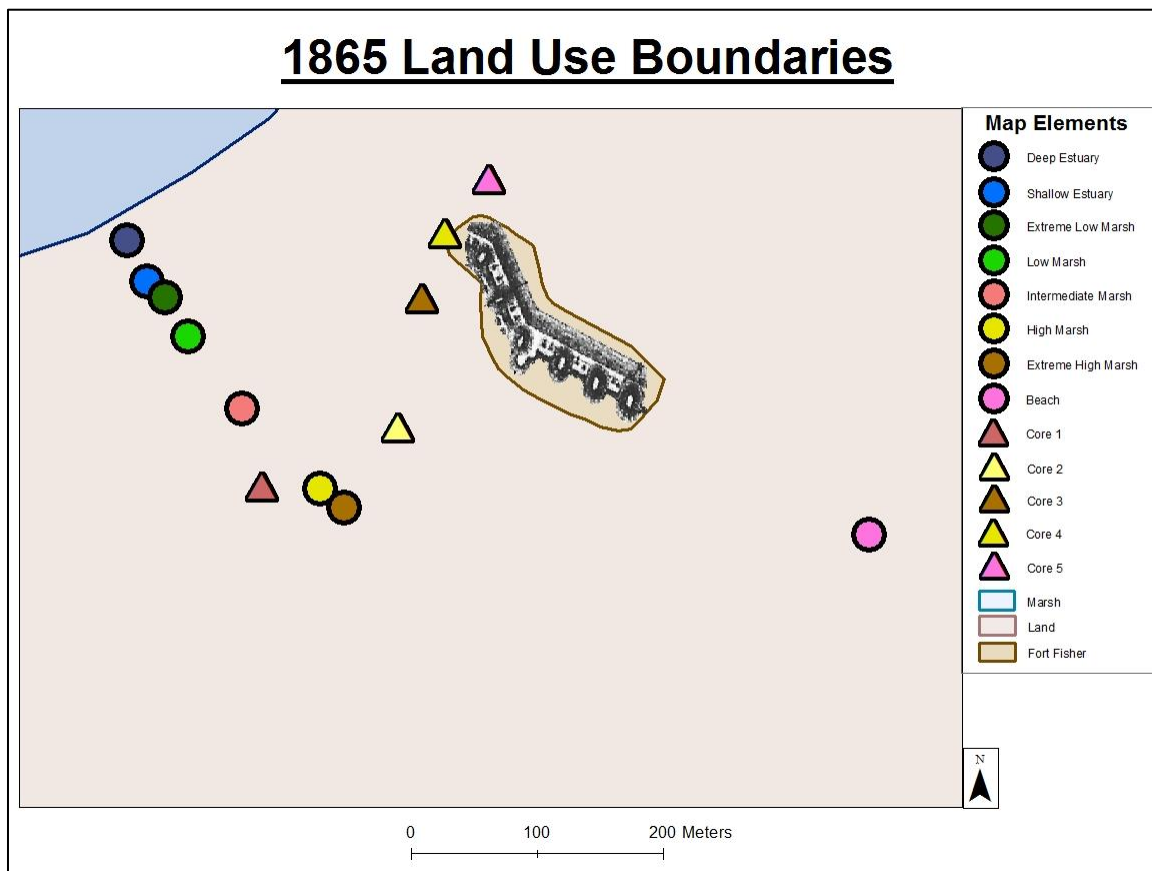


FIGURE 120: Map of 1865 depicting the boundaries between each of the distinguishable subenvironments. All five core and eight surface samples that were taken adjacent to Fort Fisher are shown, including a picture of the remaining fort. The core samples (in triangles) are color-coded to match the subenvironments of the surface samples (in circles). Additionally, each subenvironment is color-coded to distinguish it from the other subenvironments, which can be seen on the legend.

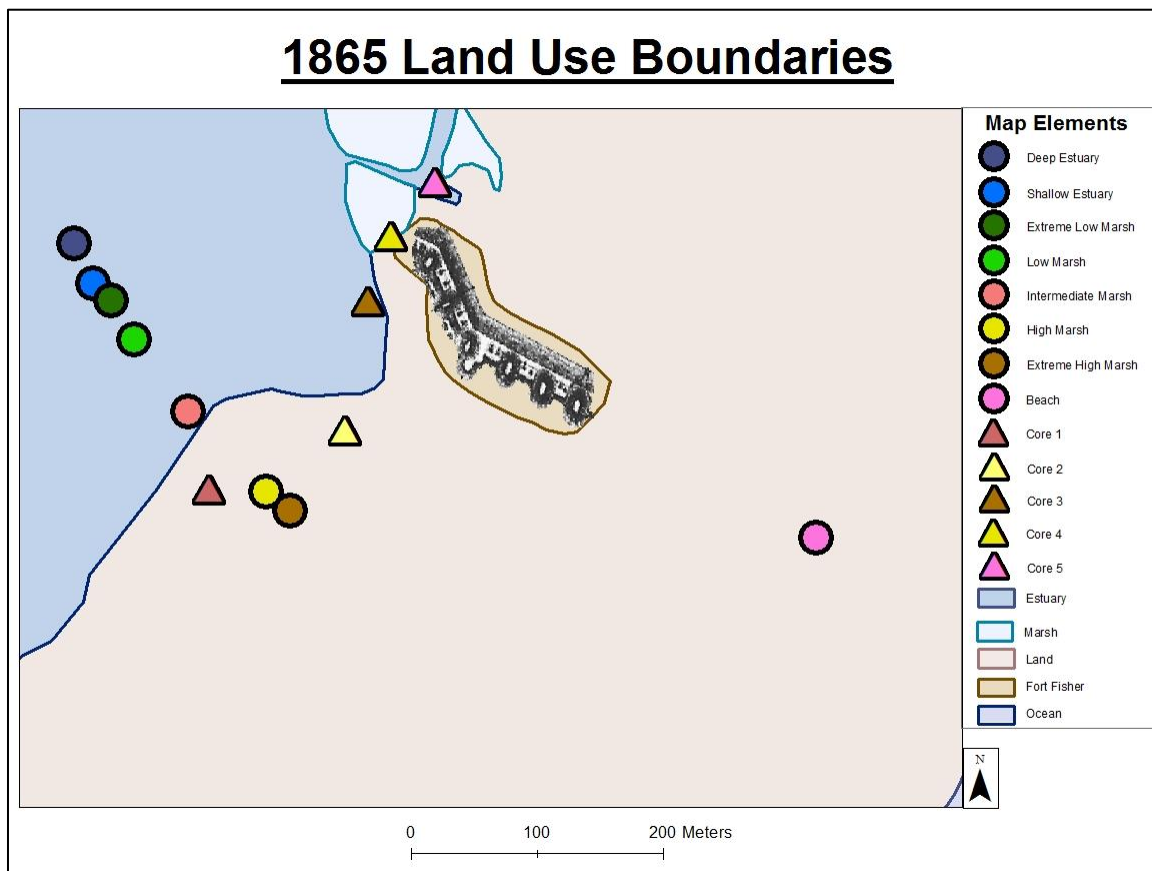


FIGURE 121: Map of 1865 depicting the boundaries between each of the distinguishable subenvironments. All five core and eight surface samples that were taken adjacent to Fort Fisher are shown, including a picture of the remaining fort. The core samples (in triangles) are color-coded to match the subenvironments of the surface samples (in circles). Additionally, each subenvironment is color-coded to distinguish it from the other subenvironments, which can be seen on the legend.

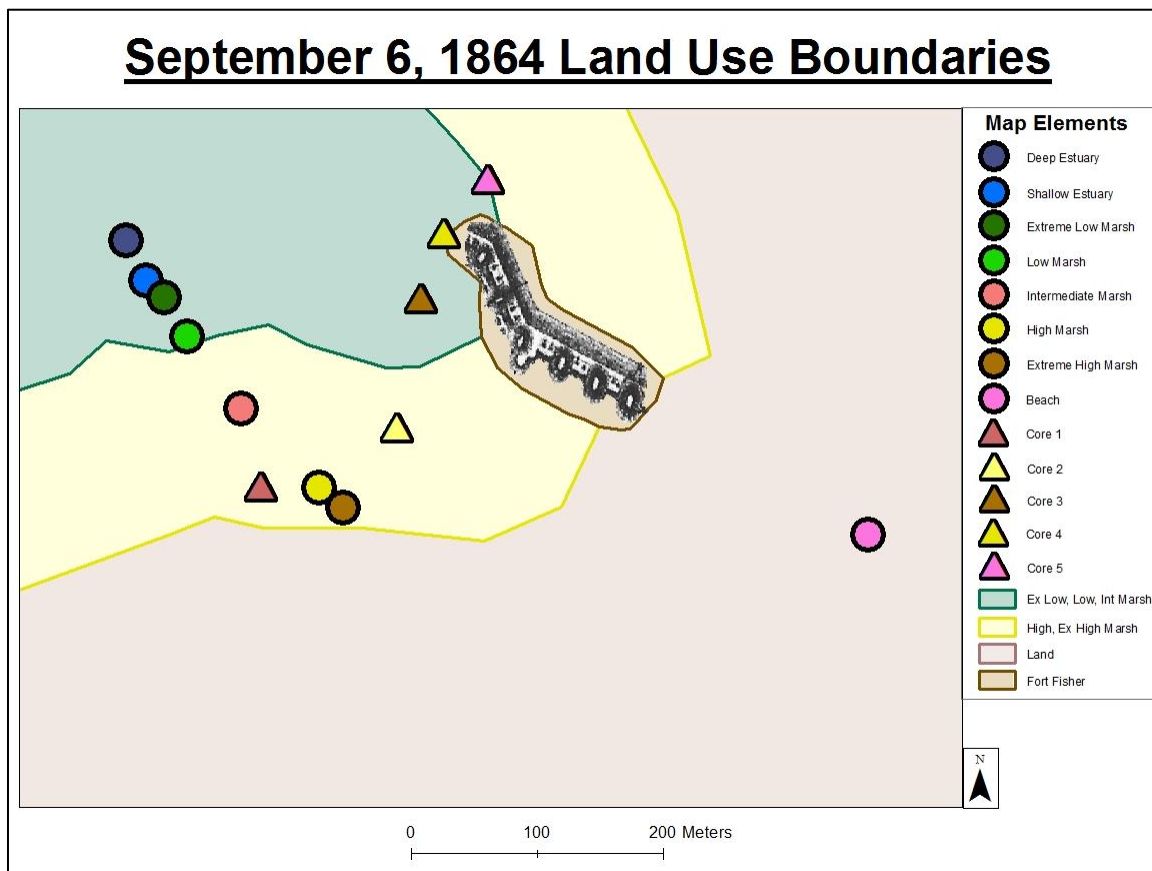


FIGURE 122: Map of 1865 depicting the boundaries between each of the distinguishable subenvironments. All five core and eight surface samples that were taken adjacent to Fort Fisher are shown, including a picture of the remaining fort. The core samples (in triangles) are color-coded to match the subenvironments of the surface samples (in circles). Additionally, each subenvironment is color-coded to distinguish it from the other subenvironments, which can be seen on the legend.

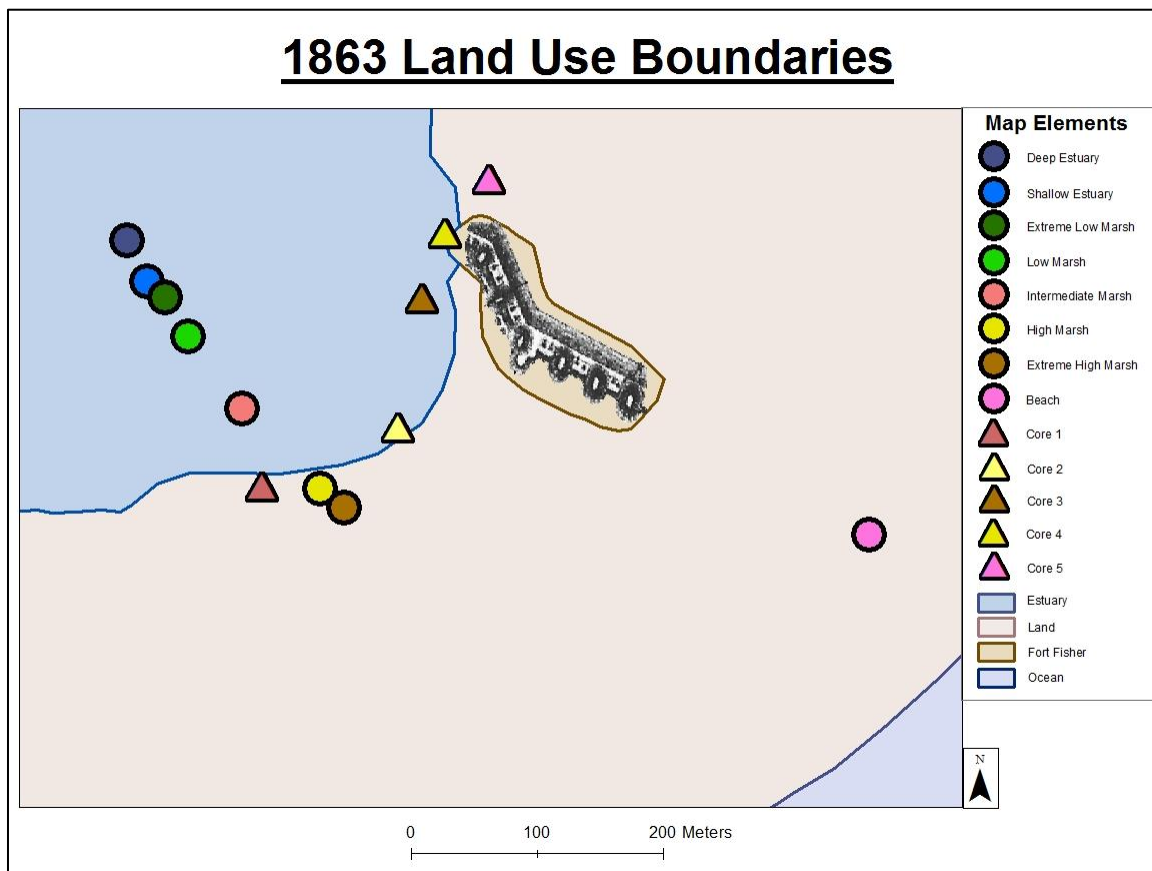


FIGURE 123: Map of 1863 depicting the boundaries between each of the distinguishable subenvironments. All five core and eight surface samples that were taken adjacent to Fort Fisher are shown, including a picture of the remaining fort. The core samples (in triangles) are color-coded to match the subenvironments of the surface samples (in circles). Additionally, each subenvironment is color-coded to distinguish it from the other subenvironments, which can be seen on the legend.

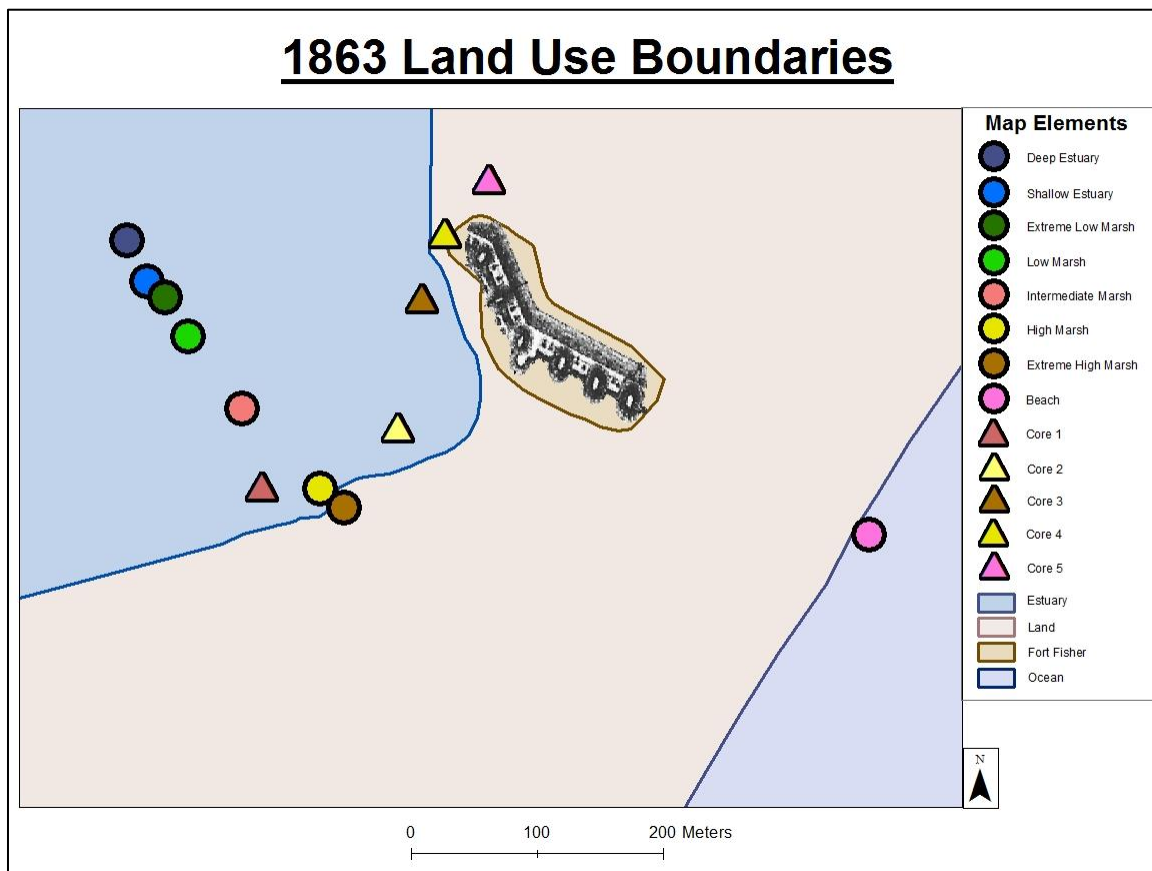


FIGURE 124: Map of 1863 depicting the boundaries between each of the distinguishable subenvironments. All five core and eight surface samples that were taken adjacent to Fort Fisher are shown, including a picture of the remaining fort. The core samples (in triangles) are color-coded to match the subenvironments of the surface samples (in circles). Additionally, each subenvironment is color-coded to distinguish it from the other subenvironments, which can be seen on the legend.

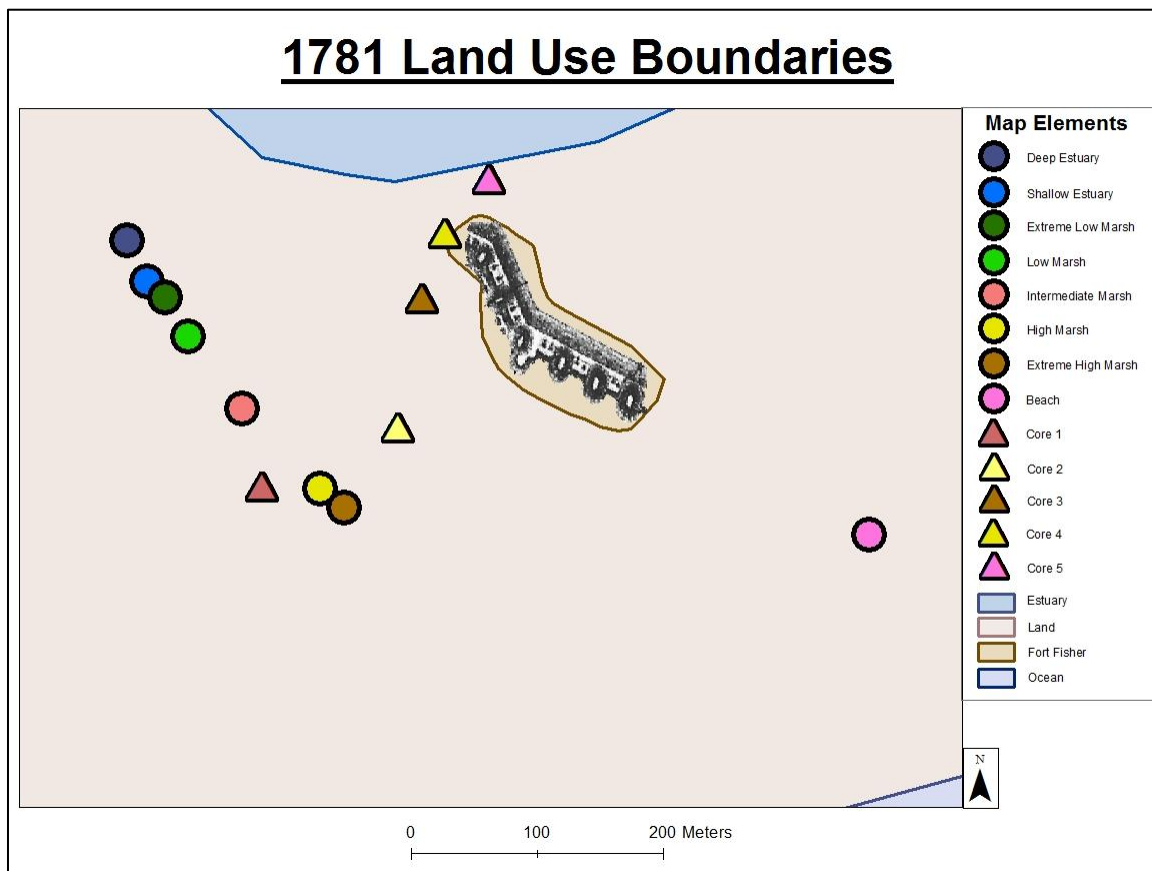


FIGURE 125: Map of 1781 depicting the boundaries between each of the distinguishable subenvironments. All five core and eight surface samples that were taken adjacent to Fort Fisher are shown, including a picture of the remaining fort. The core samples (in triangles) are color-coded to match the subenvironments of the surface samples (in circles). Additionally, each subenvironment is color-coded to distinguish it from the other subenvironments, which can be seen on the legend.